

# RADIOLOGY AND ONCOLOGY

**vol.46 no.4**

**december 2012**



# ALIMTA<sup>®</sup>

pemetreksed



## BUILD A TREATMENT STRATEGY FROM SURVIVAL

### SKRAJŠAN POVZETEK GLAVNIH ZNAČILNOSTI ZDRAVILA

**Ime zdravila** ALIMTA 100 mg prašek za koncentrat za raztopino za infundiranje in ALIMTA 500 mg prašek za koncentrat za raztopino za infundiranje. **Kakovostna in količinska sestava** ALIMTA 100 mg: vsaka viala vsebuje 100 mg pemetrekseda (v obliki dinatrijevega pemetrekseda). Po pripravi vsebuje vsaka viala 25 mg/ml pemetrekseda. Pomozne snovi: Vsaka viala vsebuje približno 11 mg natrija, manitol, klorovodikova kislina, natrijev hidroksid. ALIMTA 500 mg: vsaka viala vsebuje 500 mg pemetrekseda (v obliki dinatrijevega pemetrekseda). Po pripravi vsebuje vsaka viala 25 mg/ml pemetrekseda. Pomozne snovi: Vsaka viala vsebuje približno 54 mg natrija, manitol, klorovodikova kislina, natrijev hidroksid. **Terapevtske indikacije:** ALIMTA je v kombinaciji s cisplatinom indicirana za zdravljenje bolnikov z neresektabilnim malignim pleuralnim mezoteliomom, ki jih še nismo zdravili s kemoterapijo. ALIMTA je v kombinaciji s cisplatinom indicirana kot zdravljenje prvega izbora za bolnike z lokalno napredovalim ali metastatskim nedrobnoceličnim pljučnim rakom, ki nima pretežno ploščatocelične histologije. ALIMTA je indicirana kot monoterapija za zdravljenje lokalno napredovalga ali metastatskega nedrobnoceličnega pljučnega karcinoma, ki nima pretežno ploščatocelične histologije pri bolnikih, pri katerih bolezen ni napredovala neposredno po kemoterapiji na osnovi platine. ALIMTA je indicirana kot monoterapija za zdravljenje drugega izbora bolnikov z lokalno napredovalim ali metastatskim nedrobnoceličnim pljučnim rakom, ki nima pretežno ploščatocelične histologije. **Odmerjanje in način uporabe:** *Odmerjanje:* ALIMTA smemo dajati le pod nadzorom zdravnika, usposobljenega za uporabo kemoterapije za zdravljenje raka. ALIMTA v kombinaciji s cisplatinom. Priporočeni odmerek ALIMTE je 500 mg/m<sup>2</sup> telesne površine (TP), dan kot intravenska infuzija v 10 minutah prvi dan vsakega 21-dnevnega ciklusa. Priporočeni odmerek cisplatina je 75 mg/m<sup>2</sup> TP infundiran v dveh urah približno 30 minut po zaključku infuzije pemetrekseda prvi dan vsakega 21 dnevnega ciklusa. Bolniki morajo prejeti zadostno antiemetično zdravljenje, pred in/ali po prejemanju cisplatina jih moramo tudi ustrezno hidrirati. ALIMTA kot samostojno zdravilo. Priporočeni odmerek ALIMTE je 500 mg/m<sup>2</sup> TP, dan kot intravenska infuzija v 10 minutah prvi dan vsakega 21 dnevnega ciklusa. *Režim premedikacije:* Da zmanjšamo incidenco in resnost kožnih reakcij, dajemo kortikosteroid dan pred dajanjem pemetrekseda, na dan dajanja pemetrekseda in naslednji dan. Kortikosteroid naj ustreza 4 mg deksametazona, danega peroralno dvakrat dnevno. Za zmanjšanje toksičnosti morajo bolniki dnevno jemati tudi peroralno folno kislino ali multivitaminski pripravek, ki vsebuje (350 do 1000 mikrogramov). V sedmih dneh pred prvim odmerkom pemetrekseda morajo vzeti vsaj pet odmerkov folne kisline, odmerjanje pa morajo nadaljevati ves čas zdravljenja in še 21 dni po zadnjem odmerku pemetrekseda. Bolniki morajo prejeti tudi intramuskularno injekcijo vitamina B12 (1000 mikrogramov) v tednu pred prvim odmerkom pemetrekseda in enkrat vsake tri cikluse zatem. Kasnejše injekcije vitamina B12 lahko dajemo isti dan kot pemetreksed. **Kontraindikacije:** Preobčutljivost za zdravilno učinkovino ali katerokoli pomožno snov. Dojenje. Sočasno cepljenje proti rumeni mrzlici. **Posebna opozorila in previdnostni ukrepi:** Pemetreksed lahko zavre delovanje kostnega mozga, kar se kaže kot nevropatija, tromboticpenija in anemija (ali pancitopenija). Mielosupresija običajno predstavlja toksičnost za omejitelj odmerka. Pri bolnikih, ki pred zdravljenjem niso prejemali kortikosteroidov, so poročali o kožnih reakcijah. Uporabe pemetrekseda pri bolnikih z očistkom kreatinina < 45 ml/min ne priporočamo. Bolniki z blagim do zmernim popuščanjem delovanja ledvic naj se izogibajo jemanju nesteroidnih protivnetnih zdravil (NSAID), denimo, ibuprofena in acetilsalicilne kisline 2 dni pred dajanjem pemetrekseda, na dan dajanja in še 2 dni po dajanju pemetrekseda. Vsi bolniki, ki jih lahko zdravimo s pemetreksedom, naj se izogibajo jemanju NSAID-ov z dolgi razpolovni časi izločanja vsaj 5 dni pred dajanjem pemetrekseda, na dan dajanja in še vsaj 2 dni po dajanju pemetrekseda. Poročali so o resnih ledvičnih primerih, vključno z akutno ledvično odpovedjo, s pemetreksedom samim ali v povezavi z drugimi kemoterapevtiki. Pri bolnikih s klinično pomembno tekočino tretjega prostora moramo razmisliti o drenaži izliva pred dajanjem pemetrekseda. Kot posledico toksičnosti pemetrekseda v kombinaciji s cisplatinom za prebavila so opažali hudo dehidracijo, zato moramo bolnike pred prejemanjem terapije in/ali po njej ustrezno hidrirati, prejeti morajo zadostno antiemetično zdravljenje. Občasno so v kliničnih študijah pemetrekseda, običajno ob sočasnem dajanju z drugo citotoksično učinkovino, poročali o resnih srčnožilnih dogodkih, vključno z miokardnim infarktom in možganskožilnimi dogodki. Odsvetujemo uporabo živih oslabiljenih cepiv. Spolno zreli moški morajo v času zdravljenja in še 6 mesecev zatem, priporočamo ukrepe proti zanositvi ali vzdržnost. Zaradi možnosti, da zdravljenje s pemetreksedom povzroči trajno neplodnost, naj se moški pred začetkom zdravljenja posvetujejo o shranjevanju semen. Ženske v rodni dobi morajo v času zdravljenja s pemetreksedom uporabljati učinkovito kontracepcijo. Poročali so o primerih radiacijske pljučnice pri bolnikih, ki so jih zdravili z radiacijo pred, med ali po zdravljenju s pemetreksedom. Poročali so o radiacijskem izpuščaju pri bolnikih, ki so se zdravili z radioterapijo pred tedni ali leti. **Medsebojno delovanje z drugimi zdravili in druge oblike interakcij:** Sočasno dajanje nefrotoksičnih zdravil (denimo, aminoglikozidov, diuretikov zanke, spojin platine, ciklosporina) lahko potencialno povzroči zakasnjene očistke pemetrekseda. Sočasno dajanje snovi, ki se tudi izločajo s tubulno sekrecijo (denimo, probencid, penicilin), lahko potencialno povzroči zakasnjene očistke pemetrekseda. Pri bolnikih z normalnim delovanjem ledvic lahko visoki odmerki nesteroidnih protivnetnih zdravil (NSAID), denimo, ibuprofena in acetilsalicilne kisline v visokih odmerkih zmanjšajo eliminacijo pemetrekseda in tako lahko povečajo pojavnost neželenih učinkov pemetrekseda. Pri bolnikih z blagim do zmernim popuščanjem delovanja ledvic se moramo izogibati sočasnemu dajanju pemetrekseda z NSAID-i (denimo, ibuprofenom) ali acetilsalicilne kisline v visokih odmerkih 2 dni pred dajanjem pemetrekseda, na dan dajanja in še 2 dni po dajanju pemetrekseda. Sočasnemu dajanju NSAID-ov z daljšimi razpolovni časi s pemetreksedom se moramo izogibati vsaj 5 dni pred dajanjem pemetrekseda, na dan dajanja in še vsaj 2 dni po dajanju pemetrekseda. Velika različnost med posamezniki v koagulacijskem statusu v času bolezni ter močnost medsebojnega delovanja med peroralnimi antikoagulacijskimi učinkovinami ter kemoterapijo proti raku zahtevata povečano pogostost spremljanja INR. **Kontraindicirana sočasna uporaba:** Cepivo proti rumeni mrzlici. Tveganje za smrtno generalizirano bolezen po cepljenju. **Odsvetovana sočasna uporaba:** Živa oslabiljena cepiva (razen proti rumeni mrzlici); tveganje za sistemske, potencialno smrtno bolezni. **Neželjeni učinki** Klinične študije malignega pleuralnega mezotelioma. Zelo pogosto: znižani nevтроfilci/granulociti, znižani levkociti, znižani hemoglobin, znižani trombociti, nevropatija-senzorna, diareja, bruhanje, stomatitis/faringitis, slabost, anoreksija, zaprtje, izpuščaj, alopecija, povišan kreatinin, znižan očistek kreatinina, utrujenost. Pogosti: dehidracija, motnje okusa, konjunktivitis, dispneja. Klinične študije nedrobnoceličnega pljučnega karcinoma - ALIMTA monoterapija, zdravljenje 2. izbora: Zelo pogosti: znižani nevтроfilci/granulociti, znižani levkociti, znižan hemoglobin, diareja, bruhanje, stomatitis/faringitis, slabost, anoreksija, izpuščaj/luščenje, utrujenost. Pogosti: dehidracija, motnje okusa, konjunktivitis, dispneja. Klinične študije nedrobnoceličnega pljučnega karcinoma - ALIMTA v kombinaciji s cisplatinom, zdravljenje 1. izbora: Zelo pogosti: znižan hemoglobin, znižani nevтроfilci/granulociti, znižani levkociti, znižani trombociti, slabost, bruhanje, anoreksija, zaprtje, stomatitis/faringitis, diareja brez kolostomije, alopecija, izpuščaj/luščenje, povišan kreatinin, utrujenost. Pogosti: nevropatija-senzorična, motnje okusa, dispneja/zgaga. Klinične študije nedrobnoceličnega pljučnega karcinoma - ALIMTA monoterapija, vzdrževalno in nadaljevalno zdravljenje: Zelo pogosti: znižan hemoglobin, slabost, anoreksija, utrujenost. Pogosti: znižani levkociti, znižani nevтроfilci, nevropatija-senzorična, bruhanje, mukozitis/stomatitis, povišanje ALT (SGPT), povišanje AST (SGOT), izpuščaj/luščenje, bolečina. Občasno so v kliničnih študijah pemetrekseda poročali o primerih resnih srčnožilnih in možganskožilnih dogodkih, vključno z miokardnim infarktom, angino pektoris, cerebrovaskularnim insulantom in prehodnimi ishemičnimi atakami; primerih kolitisa ter o primerih intersticijske pljučnice z respiratorno insuficienco, primerih edema, o ezofagitisu/radiacijskem ezofagitisu in o primerih sepe. Redkeje pa o primerih potencialno resnega hepatitisa in pancitopenije. Po uvedbi zdravila na trg so poročali o primerih akutne odpovedi ledvic s pemetreksedom samim ali v povezavi z drugimi kemoterapevtiki, primerih radiacijske pljučnice pri bolnikih, ki so jih zdravili z radiacijo pred, med ali po njihovem zdravljenju s pemetreksedom, primerih radiacijske izpuščaja pri bolnikih, ki so se v preteklosti zdravili z radioterapijo, o primerih periferne ishemije, ki je včasih vodila v nekrozo okončin, redkih primerih buloznih stanj, kot sta Stevens-Johnsonov sindrom in toksična epidermalna nekroliza, ki so bila v nekaterih primerih usodna in o redkih primerih hemolitične anemije. **Imetnik dovoljenja za promet** Eli Lilly Nederland B.V., Grootslag 1 S, NL 3991 RA, Houten, Nizozemska. Datum zadnje revizije besedila 24.10.2011. **Način izdaje zdravila:** H. SAMO ZA STROKOVNO JAVNOST.

Podrobnejše informacije o zdravilu Alimta, so dostopne na spletni strani Evropske agencije za zdravila EMA <http://www.ema.europa.eu> in na lokalnem predstavništvu.

SIALM00025

Eli Lilly Farmaceutvska družba, d.o.o.

Brnčičeva 41G, 1231 Ljubljana - Črnuče, Slovenija

Telefon: +386 (0)1 5800 010

Faks: +386 (0)1 5691 705



#### Publisher

Association of Radiology and Oncology

#### Affiliated with

Slovenian Medical Association – Slovenian Association of Radiology, Nuclear Medicine Society,  
Slovenian Society for Radiotherapy and Oncology, and Slovenian Cancer Society  
Croatian Medical Association – Croatian Society of Radiology  
Societas Radiologorum Hungarorum  
Friuli-Venezia Giulia regional groups of S.I.R.M.  
Italian Society of Medical Radiology

#### Aims and scope

*Radiology and Oncology is a journal devoted to publication of original contributions in diagnostic and interventional radiology, computerized tomography, ultrasound, magnetic resonance, nuclear medicine, radiotherapy, clinical and experimental oncology, radiobiology, radiophysics and radiation protection.*

#### Editor-in-Chief

**Gregor Serša** Ljubljana, Slovenia

#### Executive Editor

**Viljem Kovač** Ljubljana, Slovenia

#### Deputy Editors

**Andrej Čör** Izola, Slovenia

**Igor Kocijancič** Ljubljana, Slovenia

**Mirjana Rajer** Ljubljana, Slovenia

**Karmen Stanič** Ljubljana, Slovenia

#### Editorial Board

Karl H. Bohuslavizki Hamburg, Germany

Maja Čemažar Ljubljana, Slovenia

Christian Dittrich Vienna, Austria

Metka Filipič Ljubljana, Slovenia

Tullio Giralardi Trieste, Italy

Maria Gódey Budapest, Hungary

Vassil Hadjidekov Sofia, Bulgaria

Nyström Håkan Uppsala, Sweden

Marko Hočevar Ljubljana, Slovenia

Miklós Kásler Budapest, Hungary

Michael Kirschfink Heidelberg, Germany

Janko Kos Ljubljana, Slovenia

Tamara Lah Turnšek Ljubljana, Slovenia

Damijan Miklavčič Ljubljana, Slovenia

Luka Milas Houston, USA

Damir Miletic Rijeka, Croatia

Maja Osmak Zagreb, Croatia

Branko Palčič Vancouver, Canada

Dušan Pavčnik Portland, USA

Geoffrey J. Pilkington Portsmouth, UK

Ervin B. Podgoršak Montreal, Canada

Primož Strojjan Ljubljana, Slovenia

Borut Štabuc Ljubljana, Slovenia

Ranka Štern-Padovan Zagreb, Croatia

Justin Teissié Toulouse, France

Gillian M. Tozer Sheffield, UK

Andrea Veronesi Aviano, Italy

Branko Zakotnik Ljubljana, Slovenia

#### Advisory Committee

Marija Auersperg Ljubljana, Slovenia

Tomaž Benulič Ljubljana, Slovenia

Božo Casar Ljubljana, Slovenia

Jure Fettich Ljubljana, Slovenia

Valentin Fidler Ljubljana, Slovenia

Berta Jereb Ljubljana, Slovenia

Vladimir Jevtič Ljubljana, Slovenia

Maksimilijan Kadivec Ljubljana, Slovenia

Stojan Plesničar Ljubljana, Slovenia

Uroš Smrdel Ljubljana, Slovenia

Živa Zupančič Ljubljana, Slovenia

Editorial office

**Radiology and Oncology**

Zaloška cesta 2

P. O. Box 2217

SI-1000 Ljubljana

Slovenia

Phone: +386 1 5879 369

Phone/Fax: +386 1 5879 434

E-mail: gsertsa@onko-i.si

Copyright © Radiology and Oncology. All rights reserved.

Reader for English

**Vida Kološa**

Secretary

**Mira Klemenčič**

**Zvezdana Vukmirović**

Design

**Monika Fink-Serša, Samo Rován, Ivana Ljubanović**

Layout

**Matjaž Lužar**

Printed by

**Tiskarna Ozimek, Slovenia**

Published quarterly in 600 copies

*Beneficiary name: DRUŠTVO RADIOLOGIJE IN ONKOLOGIJE*

*Zaloška cesta 2*

*1000 Ljubljana*

*Slovenia*

*Beneficiary bank account number: SI56 02010-0090006751*

*IBAN: SI56 0201 0009 0006 751*

*Our bank name: Nova Ljubljanska banka, d.d.,*

*Ljubljana, Trg republike 2,*

*1520 Ljubljana; Slovenia*

*SWIFT: LJBAS12X*

*Subscription fee for institutions EUR 100, individuals EUR 50*

*The publication of this journal is subsidized by the Slovenian Book Agency.*

**Indexed and abstracted by:**

*Science Citation Index Expanded (SciSearch®)*

*Journal Citation Reports/Science Edition*

*Scopus*

*PubMed*

*PubMed Central*

*EMBASE/Excerpta Medica*

*DOAJ*

*Open J-gate*

*Chemical Abstracts*

*Biomedicina Slovenica*

*Summon by Serial Solutions (ProQuest)*

*This journal is printed on acid-free paper*

On the web: ISSN 1581-3207

<http://versitaopen.com/ro>

<http://www.radioloncol.com>

<http://versita.com/science/medicine/ro/>

<http://www.onko-i.si/radioloncol/>

# contents

## *review*

- 271 **Multiple brain metastases - current management and perspectives for treatment with electrochemotherapy**  
Mette Linnert, Helle K. Iversen, Julie Gehl

## *nuclear medicine*

- 279 **Usefulness of F-18 FDG PET/CT in subcutaneous panniculitis-like T cell lymphoma: disease extent and treatment response evaluation**  
Jin-Suk Kim, Young Jin Jeong, Myung-Hee Sohn, Hwan-Jeong Jeong, Seok Tae Lim, Dong Wook Kim, Jae-Yong Kwak, Chang-Yeol Yim

## *radiology*

- 284 **Ultrasound elastography as an objective diagnostic measurement tool for lymphoedema of the treated breast in breast cancer patients following breast conserving surgery and radiotherapy**  
Nele Adriaenssens, Dries Belsack, Ronald Buyl, Leonardo Ruggiero, Catherine Breucq, Johan De Mey, Pierre Lievens, Jan Lamote
- 296 **Is rectal MRI beneficial for determining the location of rectal cancer with respect to the peritoneal reflection?**  
Eun Joo Jung, Chun Geun Ryu, Gangmi Kim, Su Ran Kim, Sang Eun Nam, Hee Sun Park, Young Jun Kim, Dae-Yong Hwang

## *experimental oncology*

- 302 **Potential of electrochemotherapy by intramuscular IL-12 gene electrotransfer in murine sarcoma and carcinoma with different immunogenicity**  
Ales Sedlar, Tanja Dolinsek, Bostjan Markelc, Lara Prosen, Simona Kranjc, Masa Bosnjak, Tanja Blagus, Maja Cemazar, Gregor Sersa
- 312 **Staurosporine induces different cell death forms in cultured rat astrocytes**  
Janez Simenc, Metoda Lipnik-Stangelj
- 321 **5-HTTLPR polymorphism and anxious preoccupation in early breast cancer patients**  
Giulia Schillani, Daniel Era, Tania Cristante, Giorgio Mustacchi, Martina Richiardi, Luigi Grassi, Tullio Giraldo

## *clinical oncology*

- 328 **Doses in organs at risk during head and neck radiotherapy using IMRT and 3D-CRT**  
Magdalena Peszynska-Piorun, Julian Malicki, Wojciech Golusinski
- 337 **Results of postoperative radiochemotherapy of the patients with resectable gastroesophageal junction adenocarcinoma in Slovenia**  
Ana Jeromen, Irena Oblak, Franc Anderluh, Vaneja Velenik, Marija Skoblar Vidmar, Ivica Ratoša
- 346 **Treatment outcomes and survival in patients with primary central nervous system lymphomas treated between 1995 and 2010 - a single centre report**  
Barbara Jezersek Novakovic
- 354 **Angiogenin and vascular endothelial growth factor expression in lungs of lung cancer patients**  
Ales Rozman, Mira Silar, Mitja Kosnik
- 360 **Interstitial lung disease in a patient treated with oxaliplatin, 5-fluorouracil and leucovorin (FOLFOX) for metastatic colorectal cancer**  
Liam M Hannan, Jaclyn Yoong, Geoffrey Chong, Christine F McDonald

## *radiophysics*

- 363 **Application of a color scanner for <sup>60</sup>Co high dose rate brachytherapy dosimetry with EBT radiochromic film**  
Mahdi Ghorbani, Mohammad Taghi Bahreyni Toossi, Ali Asghar Mowlavi, Shahram Bayani Roodi, Ali Soleimani Meigooni

## *errata*

- 370 **What sampling device is the most appropriate for vaginal vault cytology in gynaecological cancer follow up?**  
Del Pup Lino, Canzonieri Vincenzo, Serraino Diego, Campagnutta Elio

I *slovenian abstracts*

X *authors Index 2012*

XII *subject Index 2012*

RADIOLOGY AND ONCOLOGY is covered in Science Citation Index Expanded (SciSearch®), Journal Citation Reports/Science Edition, Scopus,

PubMed, PubMed Central, DOAJ, EMBASE/Excerpta Medica, Open J-gate, Chemical Abstracts, Biomedicina Slovenica, Summon by Serial Solutions (ProQuest)

# Multiple brain metastases - current management and perspectives for treatment with electrochemotherapy

Mette Linnert<sup>1</sup>, Helle K. Iversen<sup>2</sup>, Julie Gehl<sup>1</sup>

<sup>1</sup> Center for Experimental Drug and Gene Electrotransfer (C\*EDGE), Department of Oncology, Copenhagen University Hospital Herlev, Herlev, Denmark

<sup>2</sup> Department of Neurology, Copenhagen University Hospital Glostrup, Glostrup, Denmark

Radiol Oncol 2012; 46(4): 271-278.

Received 2 May 2012

Accepted 18 June 2012

Correspondence to: Dr. Julie Gehl, Center for Experimental Drug and Gene Electrotransfer (C\*EDGE), Department of Oncology, Copenhagen University Hospital Herlev, Herlev Ringvej 75, DK-2730 Herlev, Denmark. Phone: +45 38 68 29 81; Fax: +45 38 68 34 71; E-mail: Julie.Gehl@regionh.dk

Disclosure: No potential conflicts of interest were disclosed.

**Background.** Due to the advanced oncological treatments of cancer, an overall increase in cancer incidence, and better diagnostic tools, the incidence of brain metastases is on the rise. This review addresses the current treatment options for patients with multiple brain metastases, presenting electrochemotherapy (ECT) as one of the new experimental treatments for this group of patients.

**Conclusions.** Neurosurgery, stereotactic surgery, and whole-brain radiotherapy are the evidence-based treatments that can be applied for patients with multiple brain metastases. Treatment with chemotherapy and molecularly targeted agents may also be warranted. Several experimental treatments are emerging, one of which is ECT, an effective cancer treatment comprising electric pulses given by electrodes in the tumor tissue, causing electroporation of the cell membrane, and thereby augmenting uptake and the cytotoxicity of the chemotherapeutic drug bleomycin by 300 times. Preclinical data are promising and the first patient has been treated in an ongoing clinical trial for patients with brain metastases. Perspectives for ECT in the brain include treatment of primary and secondary brain tumors as well as soft tissue metastases elsewhere.

Key words: brain metastases; electroporation; bleomycin; electrochemotherapy; electrode device; blood-brain barrier

## Introduction

An increasing number of cancer patients develop brain metastases. Several factors may be responsible, including advancing age of the population, causing an overall increase in cancer incidence. Additionally, improved treatment of systemic cancer disease is leading to longer survival and thereby increasing the possibility of patients living long enough to develop brain metastases. The true incidence of brain metastases in the cancer patient population is difficult to estimate due to poor registration of this particular affliction in most countries. However, a rather precise number for the incidence of brain metastases in the Metropolitan Detroit area between 1973 and 2001 was 9.6%,

with the highest incidence in lung cancer patients (19.9%) and lowest for patients with colorectal cancer (1.8%).<sup>1</sup> In Sweden, the number of admissions due to brain metastases doubled from 1987 to 2006, with the largest increase in patients with lung and breast cancer.<sup>2</sup>

Brain metastases are developed through a long line of steps: tumor cells from the primary tumor enter the blood stream and reach the brain, attach to the endothelial cells, and extravasate into the brain parenchyma to proliferate and induce angiogenesis, see Figure 1.<sup>3</sup> Each step along this path to the development of a brain metastasis may represent targets for treatments at hand or in the future.

With modern diagnostic tools such as magnetic resonance imaging (MRI), patients can be

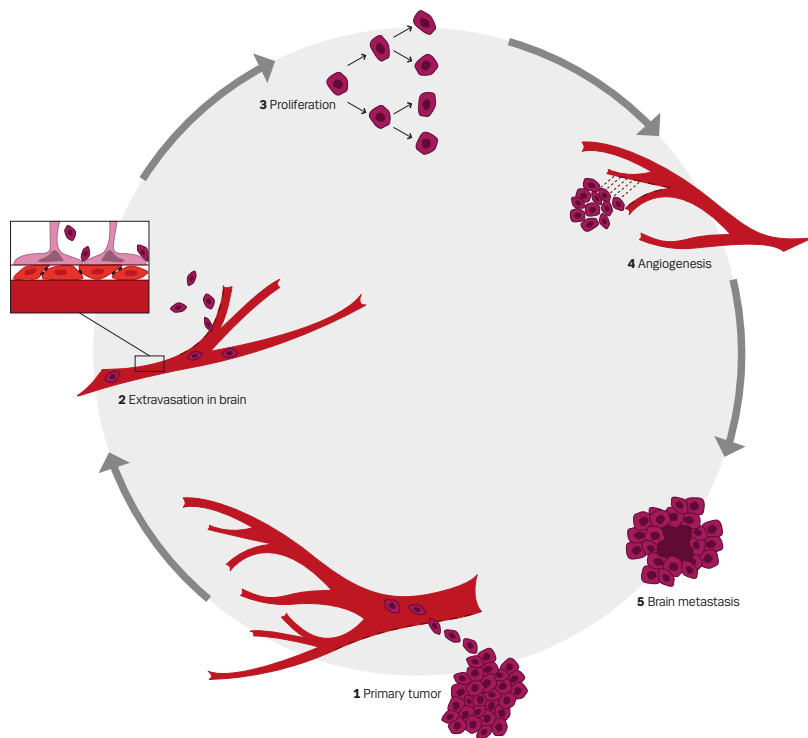


FIGURE 1. Pathogenesis of brain metastases.

diagnosed earlier in the course of the disease. Furthermore, using MRI as the diagnostic tool reveals that 80% of the patients have more than one brain metastasis and around 50% have three or more brain metastases.<sup>4</sup> Schellinger *et al.* found that CT scan failed to demonstrate multiple brain metastases in 31% of patients screened with both CT and MRI scans.<sup>5</sup>

The time of occurrence of brain metastases varies greatly within different cancer types, often occurring late with breast cancer and colorectal cancer, while lung cancer patients frequently develop brain metastases early in the disease, maybe even at the time of diagnosis.<sup>6,7</sup> Common symptoms of brain metastases are headache, paresis, and psychological changes, which are seen in about half the patients.<sup>8</sup> Many patients also suffer from symptoms of elevated intracranial pressure such as nausea, vomiting, and headache. Up to 20% of the patients have trouble walking and/or suffer from seizures.<sup>8</sup>

So far, the primary goal of most treatments of brain metastases is palliation and focuses on improvement of symptoms and the patient's quality of life. It has been shown that a reduction of tumor volume after whole brain radiation therapy is cor-

related to both improvement of the neurocognitive function and survival. Neurocognitive function is also closely related to the patient's ability to cope with activities of daily living (ADL), which again is important for the quality of life.<sup>9</sup> Therefore, reducing tumor volume is the goal of most treatments for brain metastases.

Novel molecularly targeted agents have shown activity against brain metastases, but so far nothing has revolutionized the treatment of brain metastases. Another upcoming treatment option could be electrochemotherapy (ECT), a treatment comprising of chemotherapy facilitated into the cancer cells by electric pulses that causes transient permeabilization of the cell membrane *e.g.* electroporation. The electric pulses are delivered by electrodes penetrating and covering the brain metastasis, causing electroporation of the cancer cells, and leading to a highly augmented uptake of the chemotherapeutic drug. The chemotherapeutic drug mostly used is bleomycin, which can be administered either intravenously or injected directly into the tumor. ECT has been thoroughly clinically tested as treatment for cutaneous tumors, is preclinically tested in a rat tumor model with promising results<sup>10</sup>, and a first-in-man clinical trial is now open for patients with brain metastases at our center (ClinicalTrials.gov, number NTC 01322100).

### The role of surgery

Surgery can be an excellent treatment for patients with single or few brain metastases, but is rarely an option for patients with multiple brain metastases. The key parameters used to decide whether surgery may be an option are size, number, and localization of the brain metastases, and is ultimately evaluated on a case by case basis by a neurosurgeon.<sup>11</sup> For instance, a large, surgically accessible metastasis greater than 3 cm and with complicating mass effect could be considered for surgical treatment, and need for a confirmation of a diagnosis can be an important pro for surgery.<sup>11</sup> Surgery seems to be equally as effective as stereotactic radiosurgery for the management of suitable solid metastases less than 3 cm in diameter, however, this conclusion may be subject to selection bias, as patients selected for surgery may have a better prognosis to begin with.<sup>12</sup>

### The role of radiotherapy

Radiotherapy can be applied locally, as Stereotactic Radiation Surgery (SRS) to a limited number of



TABLE 1. Re-irradiation of brain metastases

Study	Design (pts)	Radiation dose 1. treatment	Radiation dose 2. treatment	Treatment interval	MST
Shehata 1974	Retro-spective (35 pts)	10 Gy/1 fraction or 10 Gy in 2-5 daily fractions in less than a week	Not reported	Not reported	4.7 mo
Kurup 1980	Retro-spective (56 pts)	18 Gy/3 fractions, 20 Gy/5 fractions or 30 Gy/10 fractions	WBRT 1 Gy/1 fraction to 46 Gy/20 fractions / 5FW, at least 20 Gy in total dose	1-46 mo, Mean 6.3 mo Median 5 mo	3.1 mo
Hazuka 1988	Retro-spective (44 pts)	30-36 Gy/1,5-4 Gy/fraction Median 30 Gy	6-36 Gy/2-4 Gy/ fraction Median 25 Gy	Median 7.8 mo	1.7 mo
Cooper 1990	Retro-spective (52 pts)	30 Gy/10 fractions over 2 weeks	25 Gy/10 fractions over 2 weeks	At least 4 mo	4.9 mo
Wong 1996	Retro-spective (86 pts)	30 Gy/10 fractions (range 20-50.4 Gy)	WBRT 65 pt, partial brain 3 pts. Median 20 Gy/10 fractions (range 7.9-30.6 Gy)	Median 7.6 mo (range 1.5-50.6 mo)	4 mo (range 0.25-72 mo)
Abdel-Wahab 1997	Prospective (15 pts)	30-55 Gy Median 30 Gy	Partial brain 8.8 cm <sup>3</sup> Median 30 Gy (range 6-30 Gy)	Median 10 mo	3.2 mo
Sadikov 2007	Retro-spective (72 pts)	20-30 Gy/5-10 fractions Median 20 Gy	15-25 Gy/5-12 fractions Median NR	Median 9.6 mo (range 2-37.3 mo)	4 mo (range 0-17 mo)

Abbreviations: pts-patients; WBRT-whole brain radiation therapy; MST-median survival time; mo-months (weeks converted to months for the first four studies, i.e. 4.5 weeks per month).

brain metastases, or as the traditional whole brain radiation therapy (WBRT), and is sometimes combined with each other or with surgery. The combined approach is mostly used for patients initially presenting with multiple brain metastases treated with WBRT and relapsing with a single or a few brain metastases suitable for SRS. SRS treatment up front can also be followed by WBRT. Prophylactic whole brain radiation therapy is routinely applied to patients with small-cell lung cancer and limited disease, improving patient survival.<sup>13</sup>

SRS may be regarded as an option for patients with fewer than 3-4 brain metastases of less than 3-4 cm in diameter, and compared to surgery more variable locations may be treatable.<sup>14</sup> The median survival after SRS is better than for WBRT, and this is probably due to the patients being sorted using the known prognostic factors of few metastases and better performance status.

WBRT alone is most often the standard of care for patients with multiple brain metastases, leading to improvement of symptoms in about half the patients and a median survival of 4-6 months.<sup>15</sup> Approximately 50% of patients in RTOG (Radio Therapy Oncology Group) trials have disease control after 6 months with initial response rates of around 60%.<sup>4</sup> Kalkanis *et al.* found in a review of 4 studies that if surgery is combined with WBRT, both tumor control at the original site and distant control in the brain is improved, but not the overall survival.<sup>16</sup> When avoiding treatment of the whole brain, the lack of distant control in the brain can

be managed by frequent imaging surveillance, enabling salvage therapy in case of recurrence or appearance of new brain metastases.<sup>12</sup> Chang *et al.* found most patients with distant recurrences were clinically asymptomatic (18 of 21) and only detected on MRI, concluding that local treatments, such as SRS should be followed by close imaging monitoring afterwards.<sup>14</sup> Conversely, Patchell *et al.* finds that WBRT should be given up front after localized treatments, because of the generally low toxicity of WBRT, and to spare the patient of neurologic deterioration that may be irreversible when progression occurs.<sup>17</sup>

More than half the patients who are treated for brain metastases will in their lifetime eventually present with progressive disease in the brain, and more and more often as the only site of progression.<sup>18</sup> Patients present with multiple symptoms such as headache, motor deficit, impaired mentation and seizures, where headache being the most common presenting symptom at debut of brain metastases, while motor deficit is the most frequent symptom at recurrence.<sup>19</sup> At recurrence the current strategy is combining available evidence-based treatments, such as WBRT and SRS or even repeating WBRT. Event though the role of re-irradiation of the whole brain for recurrent/progressive brain metastases is controversial, mainly due to the data on the subject being retrospective, published over a large number of years while the oncological treatments have evolved somewhat. A list of these studies is shown in Table 1.

The studies on re-irradiation of the whole brain may therefore have underestimated the treatment toxicity and treated different types of patients, with respect to disease status and performance status, which is known to influence patient survival.

### The role of chemotherapy

A major concern regarding chemotherapy as a treatment for brain metastases is whether or not the antineoplastic drug crosses the blood-brain barrier (BBB). Another issue to consider is whether the patients are chemotherapy-naïve or have received several lines of chemotherapy prior to the development of brain metastases, increasing the possibility of tumor resistance.<sup>20</sup> A few cancers are responsive to treatment with chemotherapy in the brain, such as malignant melanoma, lymphoma and small cell lung cancer, but for most solid tumors, the role of chemotherapy for brain metastases remains undefined.

One chemotherapeutic agent known for years and able to penetrate the BBB in therapeutic concentrations is the oral alkylating drug temozolomide (TMZ). TMZ has demonstrated activity against both primary and secondary brain tumors, especially in patients with malignant melanoma brain metastases.<sup>21,22</sup> Agarwala *et al.* tested the efficacy and toxicity of temozolomide on 151 radiotherapy-naïve patients with malignant melanoma, showing one patient with complete response (CR), 8 patients (5%) with partial response (PR), and 40 patients (26%) with stable disease in the brain.<sup>21</sup> Significant anti-tumor effects of TMZ have also been shown in a group of patients with mixed diagnoses, when treated with TMZ plus WBRT compared to WBRT alone, although an overall survival benefit was never found.<sup>23-25</sup> The lack of ability to show a survival benefit was hypothesized by Antonadou *et al.* to be due to the fact that in their phase-II trial of 45 evaluable patients, the majority of patients in both groups progressed and died of disease progression at the primary site or developed other systemic metastases.<sup>25</sup> In a small study of 24 patients with breast cancer brain metastases, an objective response rate of 18% was observed with the treatment with TMZ and capecitabine, which is a promising result that needs further confirmation in larger trials.<sup>26</sup>

Other chemotherapeutic drugs have been tested, and one promising clinical trial is Newton *et al.*'s treatment with intra-arterial carboplatin and etoposide in patients with brain metastases from various primary cancer diagnoses, producing an objective

response rate of 38% in 24 patients with tolerable toxicity, warranting further studies.<sup>27</sup> Kiewe *et al.*'s treatment with topotecan and ifosfamide in 12 patients with brain metastases resulted in 1 patient with PR and 3 patients with stable disease (SD), but at a price of considerable hematotoxicity, discouraging further investigations into this treatment.<sup>28</sup>

### The role of molecularly targeted agents

Molecularly targeted agents are now available in the treatment of brain metastases, such as the oral tyrosine kinase inhibitor (TKI) lapatinib for HER-2-expressing breast cancer patients.<sup>29</sup> These patients have a reported high risk of brain metastases, which may be due to the poor penetration through the BBB of the otherwise effective HER-2 targeting drug trastuzumab, in addition to the possibility that HER-2-expressing breast cancer may be more biologically aggressive.<sup>29</sup>

Lapatinib is acting by binding the inactive form of the erbB2 and the epidermal growth factor receptor (EGFR), promoting cell growth inhibition and inducing apoptosis. The small molecule does penetrate the BBB and has shown efficacy in the brain in clinical trials, especially when combined with the chemotherapeutic drug capecitabine, and is now routinely used in the clinic.<sup>30,31</sup>

Sunitinib is another small molecule TKI, acting on vascular endothelial growth factor receptors (VEGFR) and platelet-derived growth factor receptors (PDGFR) among others with a direct anti-tumor and anti-angiogenic activity. The drug is playing a major role in the treatment of patients with renal cell carcinoma (RCC) in general, and it is also in this patient group the best results are found in the treatment of brain metastases. A study of 321 patients with brain metastases from RCC found an overall response rate of 12% and a clinical benefit rate of 64%.<sup>32</sup> Sunitinib has also been investigated in heavily pretreated breast cancer patients by Burstein *et al.*, resulting in 7 out of 64 patients having a partial response (PR), demonstrating activity and warranting further investigation.<sup>33</sup> Unfortunately, a phase II study of 64 patients with non-small cell lung cancer showed only marginal anti-tumor activity.<sup>34</sup>

The EGFR tyrosine kinase inhibitors, gefitinib and erlotinib, are considered active agents in a subset of patients with non small-cell lung cancer harboring EGFR-mutations and seems to be effective in the treatment of brain metastases.<sup>35,36</sup>

Bevacizumab is a monoclonal antibody that binds to and inhibits the activity of VEGF and possibly crosses the BBB, mediating a normalization

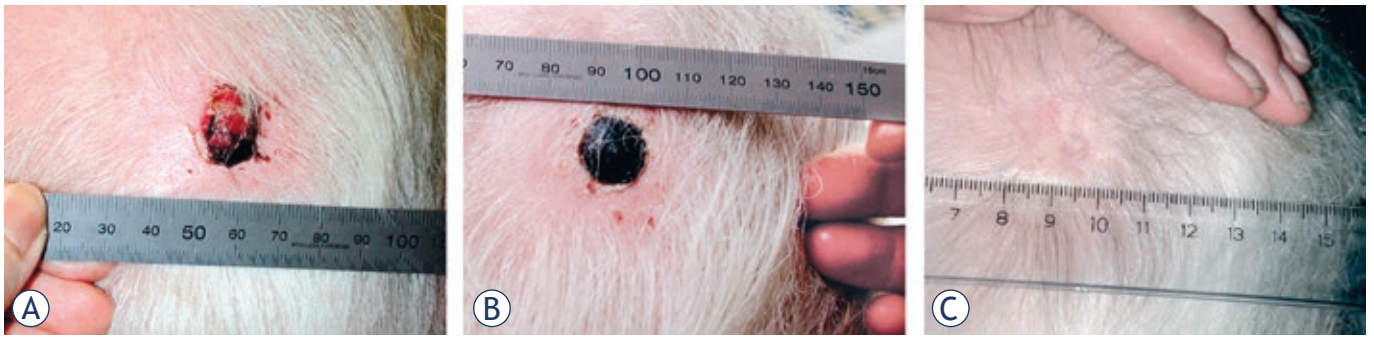


**FIGURE 2.** Treatment result of electrochemotherapy in the skin. One cutaneous metastasis from malignant melanoma treated with electrochemotherapy in general anaesthesia and intravenous injection of bleomycin. Pictures shows (a) Before treatment the metastases was ulcerated and caused haemorrhage, pain and discomfort, (b) 1 month after treatment the lesion is covered with a crust, needle marks in normal tissue are visible due to treatment of the tumor margin as well. Note that there is no necrosis of normal skin, and (c) 6 months after treatment the treated metastases is in CR (complete response) showing normal skin that had healed underneath the nodule. From Gehl, Ugeskrift for læger, 2005, with permission.

of the tumor vasculature, and thereby decreasing pressure and enhancing delivery of chemotherapy to the tumor.<sup>37</sup> In a case series of 4 patients receiving bevacizumab and paclitaxel for breast cancer brain metastases, considerable activity was demonstrated with one complete response (CR) and 3 PR's.<sup>37</sup> Normally, the chemotherapeutic drug paclitaxel does not cross the BBB, so the addition of bevacizumab seems to have made a difference, and the preliminary results are encouraging.

Molecularly targeted agents may be important in the future prevention and treatment of brain metastases, and so far lapatinib for breast cancer and sunitinib for renal cell carcinoma seem most promising. These agents should most likely be given in combination with other treatment modalities, such as chemotherapy to obtain the optimal effect.

### Electrochemotherapy in the brain

Electrochemotherapy (ECT) is a treatment where electroporation is used to facilitate the delivery and thereby augmenting the cytotoxicity of chemotherapy. Electroporation of cells is caused by application of an electric field across the cell membrane that exceeds the cell membranes' resting potential, leading to a destabilization of the membrane and formation of pores. Obtaining electroporation of cells requires insertion of electrodes into the tumor tissue and applying electric pulses, generating a sufficient electric field to cause pore formation. The pores in the cell membrane will be open for seconds to minutes before resealing, depending on the electrical parameters used (*e.g.* pulse duration and applied voltage), and in this time *e.g.* a chemotherapeutic drug can enter the cells easily and reach their intracellular target.<sup>38</sup>

The chemotherapeutic drug mostly used for ECT is bleomycin, which is highly cytotoxic once inside the cell, targeting DNA by causing double- and single strand breaks.<sup>39</sup> Bleomycin is a large, hydrophilic molecule that under normal circumstances rarely enters the cells, but when combined with electroporation, the cytotoxicity is augmented at least 300 times.<sup>40-44</sup> Bleomycin can be administered intravenously, and then the effect can be augmented in the tumor tissue by using the technique of electroporation, leading to a highly specific and localized cancer treatment. Because bleomycin is a treatment with low toxicity in single doses, this approach is readily applicable for most cancer patients.<sup>45</sup> Hence, ECT as a once-only treatment for cutaneous tumors of any histology and a diameter of less than 3 cm has been shown to produce complete response rates (CR) between 73-91%.<sup>46-48</sup> Additionally, clinical experience tells us, that the normal tissue in the tumor margins often is resistant to the effects of ECT, especially when the bleomycin is administered intravenously.<sup>47</sup> In this case only a few molecules of bleomycin enter both normal and cancer cells, causing death of cancer cells, but apparently no damage to the normal cells that are still able to repair DNA damage and restore ion homeostasis after electroporation.<sup>39</sup> For example, after once-only treatment of a cutaneous metastasis from malignant melanoma with ECT using intravenously administered bleomycin, the needle marks from the electrodes are visible, and it is evident that the healthy but treated tissue in the margins is unharmed, see Figure 2.<sup>49</sup>

Furthermore, the electric pulses cause a vascular reaction called 'the vascular lock', which is a local vasoconstriction possibly mediated by the sympathetic nervous system, resulting in hypoperfusion

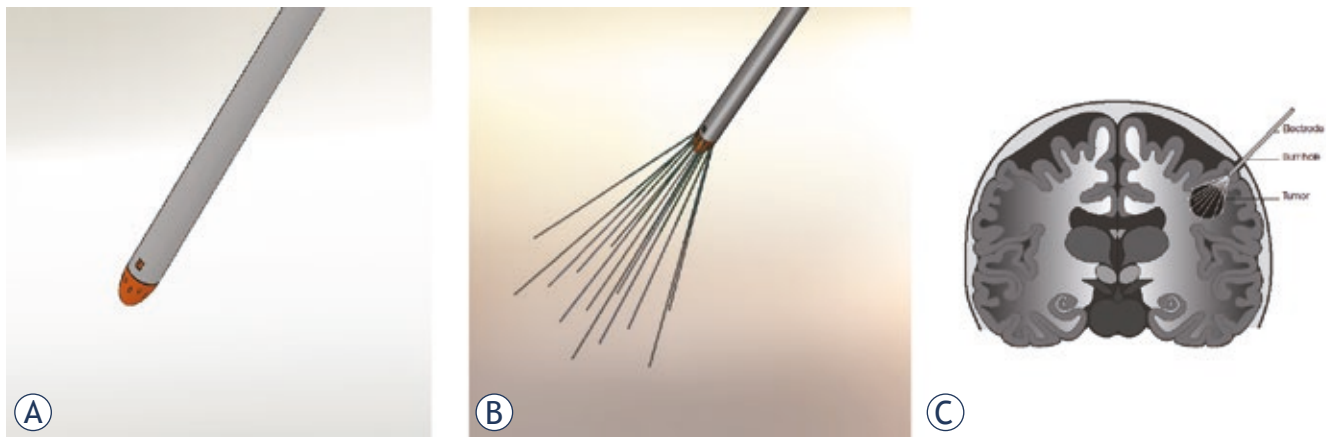


FIGURE 3. Electrochemotherapy in the human brain. Schematic drawing of the proposed electroporation procedure in the human brain

of the electroporated tissue immediately after the electric pulses, diminishing wash-out of the chemotherapeutic drug used and bleeding from the treated area.<sup>50,51</sup>

New electrode development has now made it possible to treat tumors in soft tissue inside the body, *e.g.* in the liver, gastrointestinal tract and the brain.<sup>52-54</sup> We have shown that brain tumors in a rat model can be eliminated by ECT with this novel electrode device developed for use in the brain. The first reported preclinical study of ECT as a treatment modality for brain tumors in a rat model was published in the early 90'ties, reporting an almost double survival time in the treated rats.<sup>55</sup> Acupuncture needles were then used as electrodes to treat rats inoculated with tumor cells with ECT, intravenously injected bleomycin being the chemotherapeutic drug. In our preclinical study, MRI verified tumors inoculated from glial derived tumor cells was treated with ECT, resulting in elimination of 88% of the brain tumors.<sup>56</sup>

We are currently running a phase-1 trial on ECT as a palliative treatment for brain metastases using bleomycin and the novel electrode device developed especially for treatment in soft tissue (ClinicalTrials.gov, number NCT 01322100). The expandable brain electrode device developed for the phase 1 trial is seen pictured schematically in Figure 3.

In the treatment procedure, the electrode device, with the electrodes in a retracted position (Figure 3 A), will be mounted in a stereotactic frame in a specifically developed driver unit, making it possible to slowly move it forward towards the target lesion while penetrating the brain tissue. When the tip of the expandable brain electrode device reaches the

correct coordinates, estimated from the MRI scan of the brain at baseline, the electrodes will be deployed into the brain metastasis (Figure 3 B, C). With the electrodes correctly placed and covering the entire tumor, the electric pulses can be delivered. After delivery of the electric pulses, the electrodes will be retracted back (Figure 3 A) and the expandable brain electrode device can be removed. Bleomycin is administered 15 minutes before delivery of the electric pulses, ensuring proper concentration of the drug in the brain tumor tissue.

ECT seems to be an attractive treatment to use in the brain, due to the known effectiveness on one side, and the limited toxic effects on normal tissue on the other. A review of the literature shows that bleomycin is quite tolerable when injected directly into the brain, most commonly causing adverse effects such as flue-like symptoms, fever, and nausea and vomiting.<sup>57</sup> Common adverse effects of bleomycin administered systemically are quite similar: flu-like symptoms, fever and nausea, and mostly with high cumulative dosages, serious adverse events such as pulmonary fibrosis have been observed.<sup>58,59</sup>

As only one patient has been treated in the phase I trial so far, treatment with ECT in the brain remains experimental. However, perspectives for ECT in the brain are numerous, as it may be used as a treatment for inoperable, surgically inaccessible brain metastases, maybe in combination with conventional neurosurgery. ECT may also be used for treating the tumor bed after surgical removal of primary brain tumors such as glioblastomas, treating remaining tumor cells in the margin area responsible for local recurrence.

## Conclusions

Multiple brain metastases are increasing in incidence due to factors such as overall increasing cancer incidence, better diagnostic tools, and because improved cancer treatment causes longer survival and therefore increasing possibility of patients living long enough to develop brain metastases. Treatment options today offer limited effectiveness in patients with multiple brain metastases on the long run and neurological symptoms can be the leading problem for many of these patients. One of several new experimental treatments emerging is ECT, so far showing promising preclinical data and the first patient has been treated in an ongoing clinical trial.

## Acknowledgements

The Danish Advanced Technology Foundation (HTF) has funded development of the expandable brain electrode device, preclinical validation as well as preparations for the clinical trial. Mette Linnert has a grant from The University of Copenhagen. Julie Gehl is a research fellow at the Swedish Academy of Science supported by a grant from the Acta Oncologica Foundation.

## References

- Barnholtz-Sloan JS, Sloan AE, Davis FG, Vigneaun FD, Lai P, Sawaya RE. Incidence proportions of brain metastases in patients diagnosed (1973 to 2001) in the metropolitan Detroit cancer surveillance system. *J Clin Oncol* 2004; **14**: 2865-72.
- Smedby KE, Brandt L, Backlund ML, Blomqvist P. Brain metastases admissions in Sweden between 1987 and 2006. *Br J Cancer* 2009; **111**: 1919-24.
- Fidler IJ, Yano S, Zhang RD, Fujimaki T, Bucana CD. The seed and soil hypothesis: vascularisation and brain metastases. *Lancet Oncol* 2002; **1**: 53-7.
- Khuntia D, Brown P, Li J, Mehta MP. Whole-brain radiotherapy in the management of brain metastasis. *J Clin Oncol* 2006; **8**: 1295-304.
- Schellinger PD, Meinck HM, Thron A. Diagnostic accuracy of MRI compared to CCT in patients with brain metastases. *J Neuro-Oncol* 1999; **3**: 275-81.
- Li J, Bentzen SM, Li JL, Renschler M, Mehta MP. Relationship between neurocognitive function and quality of life after whole-brain radiotherapy in patients with brain metastasis. *Int J Radiat Oncol Biol Phys* 2008; **1**: 64-70.
- Lecic M, Kovac V, Triller N, Knez L, Sadikov A, Cufer T. Outcome of small cell lung cancer (SCLC) patients with brain metastases in a routine clinical setting. *Radiol Oncol* 2012; **1**: 54-9.
- Nussbaum ES, Djalilian HR, Cho KH, Hall WA. Brain metastases - Histology, multiplicity, surgery, and survival. *Cancer* 1996; **8**: 1781-8.
- Li J, Bentzen SM, Renschler M, Mehta MP. Regression after whole-brain radiation therapy for brain metastases correlates with survival and improved neurocognitive function. *J Clin Oncol* 2007; **10**: 1260-6.
- Agerholm-Larsen B, Iversen HK, Ibsen P, Moller JM, Mahmood F, Jensen KS, et al. Preclinical validation of electrochemotherapy as an effective treatment for brain tumors. *Cancer Res* 2011; **11**: 3753-62.
- Bhangoo SS, Linskey ME, Kalkanis SN. Evidence-based guidelines for the management of brain metastases. *Neurosurg Clin N Am* 2011; **1**: 97-+.
- Jenkinson MD, Haylock B, Shenoy A, Husband D, Javadpour M. Management of cerebral metastasis: Evidence-based approach for surgery, stereotactic radiosurgery and radiotherapy. *Eur J Cancer* 2011; **5**: 649-55.
- Stanic K, Kovac V. Prophylactic cranial irradiation in patients with small-cell lung cancer: the experience at the Institute of Oncology Ljubljana. *Radiol Oncol* 2010; **3**: 180-6.
- Chang EL, Wefel JS, Hess KR, Allen PK, Lang FF, Kornguth DG, et al. Neurocognition in patients with brain metastases treated with radiosurgery or radiosurgery plus whole-brain irradiation: a randomised controlled trial. *Lancet Oncol* 2009; **11**: 1037-44.
- Videtic GM, Gaspar LE, Aref AM, Germano IM, Goldsmith BJ, Imperato JP, et al. American College of Radiology appropriateness criteria on multiple brain metastases. *Int J Radiat Oncol Biol Phys* 2009; **4**: 961-5.
- Kalkanis SN, Kondziolka D, Gaspar LE, Burri SH, Asher AL, Cobbs CS, et al. The role of surgical resection in the management of newly diagnosed brain metastases: a systematic review and evidence-based clinical practice guideline. *J Neuro-Oncol* 2010; **1**: 33-43.
- Patchell RA, Regine WF. The rationale for adjuvant whole brain radiation therapy with radiosurgery in the treatment of single brain metastases. *Technol Cancer Res Treatm* 2003; **2**: 111-5.
- Bahl A, Kumar M, Sharma DN, Basu KSJ, Jaura MS, Rath GK, et al. Reirradiation for progressive brain metastases. *J Cancer Res Ther* 2009; **3**: 161-4.
- Hazuka MB, Kinzie JJ. Brain metastases - results and effects of re-irradiation. *Int J Radiat Oncol Biol Phys* 1988; **2**: 433-7.
- Addeo R, Caraglia M, Faiola V, Capasso E, Vincenzi B, Montella L, et al. Concomitant treatment of brain metastasis with Whole Brain Radiotherapy [WBRT] and Temozolomide [TMZ] is active and improves Quality of Life. *Bmc Cancer* 2007.
- Agarwala SS, Kirkwood JM, Gore M, Dreno B, Thatcher N, Czarnetski B, et al. Temozolomide for the treatment of brain metastases associated with metastatic melanoma: A phase II study. *J Clin Oncol* 2004; **11**: 2101-7.
- Stupp R, Mason WP, van den Bent MJ, Weller M, Fisher B, Taphoorn MJB, et al. Radiotherapy plus concomitant and adjuvant temozolomide for glioblastoma. *New Engl J Med* 2005; **10**: 987-96.
- Verger E, Miguel G, Yaya R, Vinolas N, Villa S, Pujol T, et al. Temozolomide and concomitant whole brain radiotherapy in patients with brain metastases: A phase II randomized trial. *Int J Radiat Oncol Biol Phys* 2005; **1**: 185-91.
- Mehta MP, Paleologos NA, Mikkelsen T, Robinson PD, Ammirati M, Andrews DW, et al. The role of chemotherapy in the management of newly diagnosed brain metastases: a systematic review and evidence-based clinical practice guideline. *J Neuro-Oncol* 2010; **1**: 71-83.
- Antonadou D, Paraskevaidis M, Sarris G, Coliarakis N, Economou I, Karageorgis P, et al. Phase II Randomized trial of temozolomide and concurrent radiotherapy in patients with brain metastases. *J Clin Oncol* 2002; **17**: 3644-50.
- Rivera E, Meyers C, Groves M, Valero V, Francis D, Arun B, et al. Phase I study of capecitabine in combination with temozolomide in the treatment of patients with brain metastases from breast carcinoma. *Cancer* 2006; **6**: 1348-54.
- Newton HB, Slivka MA, Volpi C, Bourekas EC, Christoforidis GA, Baujan MA, et al. Intra-arterial carboplatin and intravenous etoposide for the treatment of metastatic brain tumors. *J Neuro-Oncol* 2003; **1**: 35-44.
- Kiewe P, Thiel E, Reinwald M, Korfel A. Topotecan and ifosfamide systemic chemotherapy for CNS involvement of solid tumors. *J Neuro-Oncol* 2011; **3**: 629-34.
- Addeo R, Caraglia M. The oral tyrosine kinase inhibitors lapatinib and sunitinib: new opportunities for the treatment of brain metastases from breast cancer? *Expert Review Anticancer Ther* 2011; **2**: 139-42.
- Lin NU, Carey LA, Liu MC, Younger J, Come SE, Ewend M, et al. Phase II trial of lapatinib for brain metastases in patients with human epidermal growth factor receptor 2-positive breast cancer. *J Clin Oncol* 2008; **12**: 1993-9.
- Lin NU, Dieras V, Paul D, Lossignol D, Christodoulou C, Stemmler HJ, et al. Multicenter phase II study of lapatinib in patients with brain metastases from HER2-positive breast cancer. *Clin Cancer Res* 2009; **4**: 1452-9.

32. Gore ME, Hariharan S, Porta C, Bracarda S, Hawkins R, Bjarnason GA, et al. Sunitinib in metastatic renal cell carcinoma patients with brain metastases. *Cancer* 2011; **3**: 501-9.
33. Burstein HJ, Elias AD, Rugo HS, Cobleigh MA, Wolff AC, Eisenberg PD, et al. Phase II study of sunitinib malate, an oral multitargeted tyrosine kinase inhibitor, in patients with metastatic breast cancer previously treated with an anthracycline and a taxane. *J Clin Oncol* 2008; **11**: 1810-16.
34. Novello S, Camps C, Grossi F, Mazieres J, Abrey L, Vernejoux JM, et al. Phase II study of sunitinib in patients with non-small cell lung cancer and irradiated brain metastases. *J Thorac Oncol* 2011; **7**: 1260-6.
35. Franceschi E, Brandes AA. Brain metastases from non-small-cell lung cancer: is there room for improvement? *Exp Rev Anticancer Ther* 2012; **4**: 421-3.
36. Porta R, Sanchez-Torres JM, Paz-Ares L, Massuti B, Reguart N, Mayo C, et al. Brain metastases from lung cancer responding to erlotinib: the importance of EGFR mutation. *Eur Respir J* 2011; **3**: 624-31.
37. Labidi SI, Bachelot T, Ray-Coquard I, Mosbah K, Treilleux I, Fayette J, et al. Bevacizumab and paclitaxel for breast cancer patients with central nervous system metastases: A case series. *Clin Breast Cancer* 2009; **2**: 118-21.
38. Gehl J, Sorensen TH, Nielsen K, Raskmark P, Nielsen SL, Skovsgaard T, et al. In vivo electroporation of skeletal muscle: threshold, efficacy and relation to electric field distribution. *Biochim Biophys Acta* 1999; **2-3**: 233-40.
39. Tounekti O, Kenani A, Foray N, Orłowski S, Mir LM. The ratio of single- to double-strand DNA breaks and their absolute values determine cell death pathway. *Br J Cancer* 2001; **9**: 1272-79.
40. Orłowski S, Belehradec J, Paoletti C, Mir LM. Transient electroporation of cells in culture - Increase of the cyto-toxicity of anticancer drugs. *Biochem Pharmacol* 1988; **24**: 4727-33.
41. Gothelf A, Mir LM, Gehl J. Electrochemotherapy: results of cancer treatment using enhanced delivery of bleomycin by electroporation. *Cancer Treat Rev* 2003; **5**: 371-87.
42. Mir LM, Gehl J, Sersa G, Collins CG, Garbay JR, Billard V, et al. Standard operating procedures of the electrochemotherapy: Instructions for the use of bleomycin or cisplatin administered either systemically or locally and electric pulses delivered by the Cliniporator (TM) by means of invasive or non-invasive electrodes. *EJC Suppl* 2006; **11**: 14-25.
43. Gehl J, Skovsgaard T, Mir LM. Enhancement of cytotoxicity by electroporation: an improved method for screening drugs. *Anti-Cancer Drug* 1998; **4**: 319-25.
44. Jaroszeski MJ, Dang V, Pottinger C, Hickey J, Gilbert R, Heller R. Toxicity of anticancer agents mediated by electroporation in vitro. *Anti-Cancer Drug* 2000; **3**: 201-8.
45. Matthiessen LW, Chalmers RL, Sainsbury DCG, Veeramani S, Kessell G, Humphreys AC, et al. Management of cutaneous metastases using electrochemotherapy. *Acta Oncol* 2011; **5**: 621-9.
46. Heller R, Jaroszeski MJ, Reintgen DS, Puleo CA, DeConti RC, Gilbert RA, et al. Treatment of cutaneous and subcutaneous tumors with electrochemotherapy using intralesional bleomycin. *Cancer* 1998; **1**: 148-57.
47. Marty M, Sersa G, Garbay JR, Gehl J, Collins CG, Snoj M, et al. Electrochemotherapy - An easy, highly effective and safe treatment of cutaneous and subcutaneous metastases: Results of ESOPE (European Standard Operating Procedures of Electrochemotherapy) study. *EJC Suppl* 2006; **11**: 3-13.
48. Belehradec M, Domenge C, Luboinski B, Orłowski S, Belehradec J, Mir LM. Electrochemotherapy, a new antitumor treatment - 1st clinical phase-I-II trial. *Cancer* 1993; **12**: 3694-700.
49. Gehl J. Investigational treatment of cancer using electrochemotherapy, electrochemoimmunotherapy and electro-gene transfer. *Ugeskr Laeger* 2005; **34**: 3156-9.
50. Gehl J, Skovsgaard T, Mir LM. Vascular reactions to in vivo electroporation: characterization and consequences for drug and gene delivery. *Biochim Biophys Acta* 2002; **1-3**: 51-8.
51. Sersa G, Jarm T, Kotnik T, Coer A, Podkrajsek M, Sentjurc M, et al. Vascular disrupting action of electroporation and electrochemotherapy with bleomycin in murine sarcoma. *Brit J Cancer* 2008; **2**: 388-98.
52. Soden D, Morrissey A, Collins C, Piggott J, Larkin J, Norman A, et al. Electrotherapy of tumour cells using flexible electrode arrays. *Sensor Actual B-Chem* 2004; **1-2**: 219-24.
53. Mahmood F, Gehl J. Optimizing clinical performance and geometrical robustness of a new electrode device for intracranial tumor electroporation. *Bioelectrochemistry* 2011; **1**: 10-6.
54. Edhemovic I, Gadzije EM, Breclj E, Miklavcic D, Kos B, Zupanic A, et al. Electrochemotherapy: a new technological approach in treatment of metastases in the liver. *Technol Cancer Res Treatm* 2011; **5**: 475-85.
55. Salford LG, Persson BR, Brun A, Ceberg CP, Kongstad PC, Mir LM. A new brain tumour therapy combining bleomycin with in vivo electroporation. *Biochem Biophys Res Commun* 1993; **2**: 938-43.
56. Agerholm-Larsen B, Iversen HK, Moller J, Ibsen P, Jensen KS, Linnert M, et al. Effect of electrochemotherapy with IV bleomycin on complete response in a preclinical brain tumor study. *J Clin Oncol* 2012; **30**: abstr 2069.
57. Linnert M, Gehl J. Bleomycin treatment of brain tumors: an evaluation. *Anti-Cancer Drugs* 2009; **3**: 157-64.
58. Osanto S, Bukman A, Vanhoek F, Sterk PJ, Delaat JAPM, Hermans J. Long-term effects of chemotherapy in patients with testicular cancer. *J Clin Oncol* 1992; **4**: 574-9.
59. Pliarchopoulou K, Pectasides D. Late complications of chemotherapy in testicular cancer. *Cancer Treatm Rev* 2010; **3**: 262-7.

# Usefulness of F-18 FDG PET/CT in subcutaneous panniculitis-like T cell lymphoma: disease extent and treatment response evaluation

Jin-Suk Kim<sup>1</sup>, Young Jin Jeong<sup>2</sup>, Myung-Hee Sohn<sup>3,5</sup>, Hwan-Jeong Jeong<sup>3,5</sup>, Seok Tae Lim<sup>3,5</sup>, Dong Wook Kim<sup>3,5</sup>, Jae-Yong Kwak<sup>4,5</sup>, Chang-Yeol Yim<sup>4,5</sup>

<sup>1</sup> Department of Nuclear Medicine, Konyang University Hospital, Daejeon, South Korea

<sup>2</sup> Department of Nuclear Medicine, Dong-A University Medical Center, Busan, South Korea

<sup>3</sup> Department of Nuclear Medicine, <sup>4</sup>Department of Internal Medicine and <sup>5</sup>Research Institute of Clinical Medicine, Chonbuk National University Medical School and Hospital, Jeonju, Jeonbuk, South Korea

Radiol Oncol 2012; 46(4): 279-283.

Received 30 December 2011

Accepted 21 January 2012

Correspondence to: Myung-Hee Sohn, M.D., Department of Nuclear Medicine, Chonbuk National University Medical School and Hospital, San 2-20 Geumam-dong, Deokjin-gu, Jeonju, Jeonbuk, 561-180, South Korea. Phone: +82-63-250-1174; Fax: +82-63-255-1172; E-mail: mhsohn@jbnu.ac.kr

Disclosure: The authors have no conflicts of interest to disclose.

**Background.** Subcutaneous panniculitis-like T-cell lymphoma (SPTCL) is a rare form of cutaneous lymphomas, accounting for less than 1% of cases of non-Hodgkin's lymphoma. Fluorine-18 fluorodeoxyglucose (F-18 FDG) positron-emission tomography/computed tomography (PET/CT) findings of SPTCL before and after treatment were rarely reported.

**Case report.** We report a case of SPTCL in which F-18 FDG PET/CT showed increased FDG accumulations in numerous subcutaneous nodules without extracutaneous disease. Contrast-enhanced CT during F-18 FDG PET/CT showed multiple minimally enhancing nodules with an infiltrative pattern in the subcutaneous layer throughout the body. Follow-up F-18 FDG PET/CT after three cycles of CHOP chemotherapy showed a complete metabolic remission of the lesions.

**Conclusions.** F-18 FDG PET/CT is suggested to be useful in assessing the disease activity, extent and treatment response in SPTCL.

Key words: subcutaneous panniculitis-like T-cell lymphoma; F-18 FDG; PET/CT

## Introduction

Subcutaneous panniculitis-like T-cell lymphoma (SPTCL) is a rare disorder that is often confused with panniculitis. Patients usually present with multiple subcutaneous nodules on the extremities and trunk without visceral disease. Systemic symptoms such as fever, fatigue, and weight loss may be present. The disease may be complicated by hemophagocytic syndrome, which is often associated with a rapidly progressive course.<sup>1</sup> The diagnosis of SPTCL is currently based on clinical and histological findings.<sup>2</sup> CT is a noninvasive imaging

modality that is widely used for staging in patients with lymphoma<sup>3</sup>, but it does not provide much information in cutaneous lesions.<sup>4</sup>

We report herein a patient with SPTCL in whom F-18 FDG PET/CT was valuable in assessing the extent of the disease and the treatment response.

## Case report

A 30-year-old man presented with a 10-year history of multiple subcutaneous nodules on the abdominal wall which were rubbery on palpation.

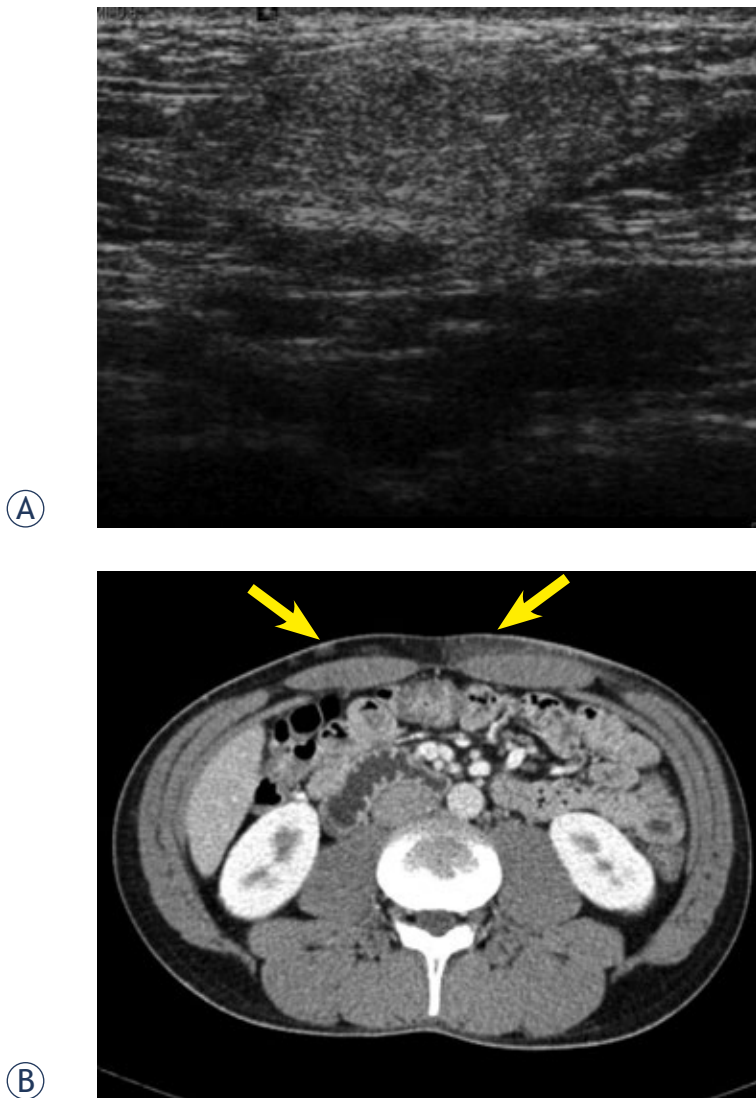


**FIGURE 1.** On gray-scale US examination of the lesion in the left abdomen shows ill-defined hyperechoic infiltration (A). Contrast enhanced CT shows multiple mild enhancing nodular and diffuse infiltrative lesions (arrows) in the subcutaneous layer of the anterior abdomen (B).

The nodules were slowly enlarging in size. He was otherwise healthy without weight loss, fever, or chill. On admission, his laboratory tests showed elevated levels of serum lactate dehydrogenase and  $\beta 2$ -microglobulin.

Ultrasonography was performed on the abdomen. The lesions revealed an ill-defined hyperechoic infiltration (Figure 1A). On abdominal and pelvic CT scanning with contrast enhancement, there were multiple slightly enhancing infiltrative nodular or non-nodular lesions in the subcutaneous layer of the abdominal wall (Figure 1B). One of subcutaneous nodules of the abdominal wall was surgically excised. On histopathologic examina-

tion of the excised tissue revealed lymphoid cells diffusely infiltrating through the subcutaneous tissue on hematoxylin & eosin staining. On immunohistochemical staining, the tumor cells were positive for CD3, CD4 and CD8, but negative for CD56. These histologic findings were consistent with SPTCL.

For systemic surveillance, F-18 FDG PET/CT was performed. Images were obtained 1 hour after an intravenous injection of F-18 FDG (440 MBq) using a PET/CT scanner (Biograph 16 LSO Hi-Res, Siemens, Germany). The patient fasted for 6 hours: the serum glucose level measured before examination was 92 mg/dl. F-18 FDG PET/CT images revealed multiple increased F-18 FDG uptakes corresponding to the infiltrative lesions in the subcutaneous adipose tissue of the chest, back, abdomen and both extremities (Figure 2A-D). However, there was no evidence of lymph node involvement.

The patient received three cycles of CHOP (Cyclophosphamide, Adriamycin, Vincristine and Prednisolone) chemotherapy. After the chemotherapy, a follow-up F-18 FDG PET/CT scan showed a complete metabolic remission of the previous lesions (Figure 3). The patient then received additional three cycles of CHOP (total 6 cycles), and maintained the complete remission with the resolution of all skin lesions. Currently, the patient has been well without recurrence for three years after the last dose of CHOP chemotherapy.

## Discussion

According to the World Health Organization (WHO) classification, lymphoid malignancies are divided largely into T- and B-cell lymphomas, and Hodgkin's disease. T-cell lymphomas are divided into precursor T-cell lymphomas and peripheral T-cell lymphomas. In the category of peripheral T-cell lymphomas, SPTCL has a very low incidence, accounting for less than 1% of cases of non-Hodgkin's lymphoma.<sup>5</sup> It was classified as a subtype of cutaneous T-cell lymphoma that preferentially infiltrates the subcutaneous tissue without overt lymph node involvement.<sup>2</sup>

SPTCL occurs in adults as well as in young children, and both sexes are equally affected. Patients present with multiple subcutaneous nodules and plaques, which progress and may ulcerate.<sup>6,7</sup> Systemic symptoms of this disease are variable, and fever, fatigue, and weight loss may be present. Dissemination to extracutaneous sites is rare. SPTCL may be preceded for years or decades



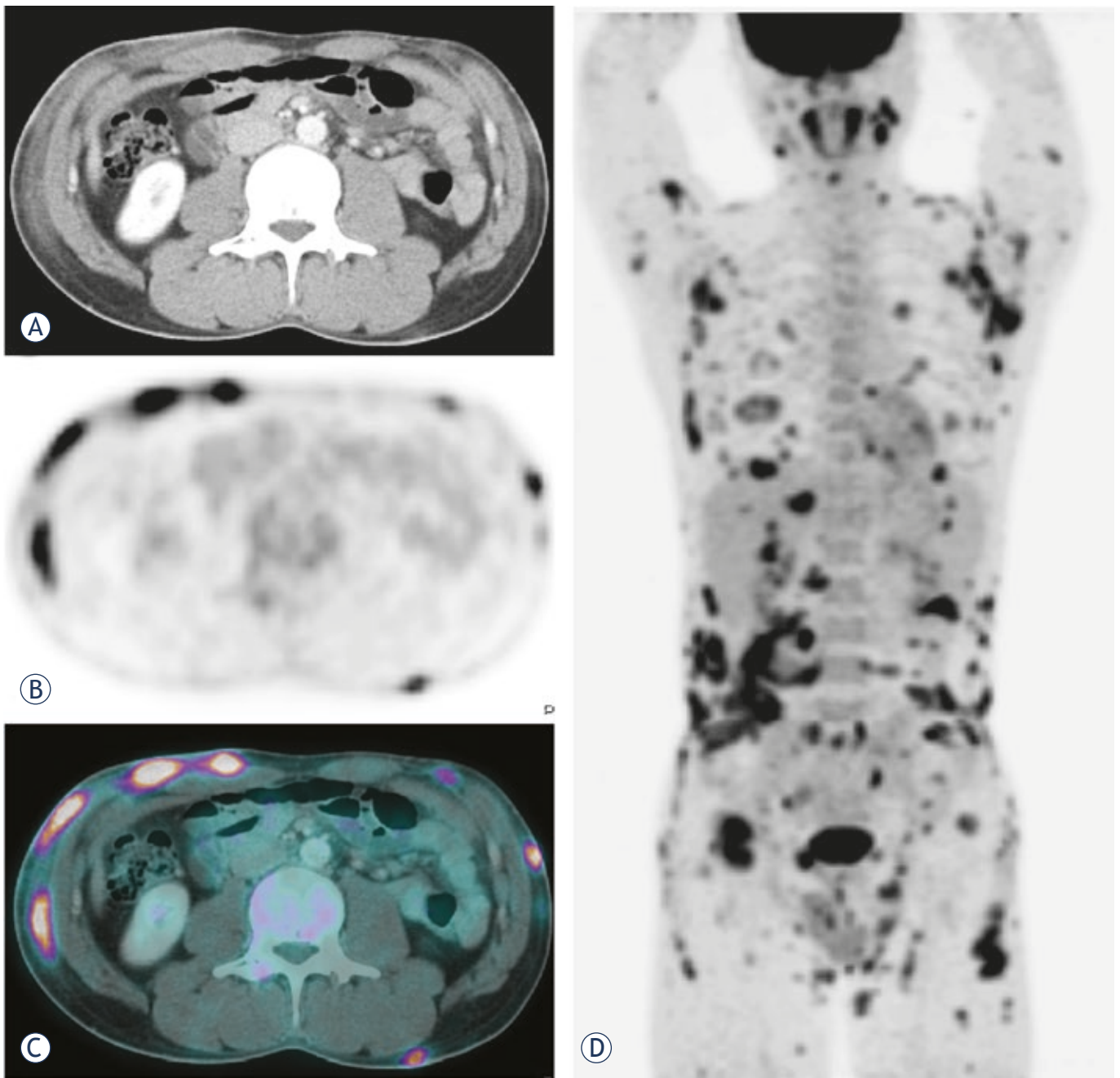


**FIGURE 2.** Axial contrast-enhanced CT (A), PET (B), and fusion PET/CT (C) images performed for initial staging demonstrated areas of abnormal increased F-18 FDG uptake corresponding to infiltrative changes in the subcutaneous adipose tissue of the anterior abdominal wall. Extensive disease involvement throughout the body with numerous subcutaneous nodules is best visualized on the maximum intensity projection (MIP) image (D).

by a seemingly benign panniculitis.<sup>8-10</sup> Two clinical courses are reported: Some patients have a protracted course of recurrent spontaneously healing subcutaneous nodules without systemic signs or symptoms; other patients have a rapidly progressive disease and very poor outcome<sup>11</sup>, which is usually due to the development of hemophagocytic syndrome or hepatic dysfunction.

Histologically, SPTCL is characterized by lymphocytic infiltrates confined primarily to the fat lobules in the subcutaneous tissue.<sup>2,4,12</sup> Rimming of individual fat cells by neoplastic T-cells is a helpful, though not completely specific, diagnostic feature.<sup>13</sup> In early stage disease, the neoplastic infiltrates may lack significant atypia and a heavy inflammatory infiltrate may predominate.<sup>8-10</sup>

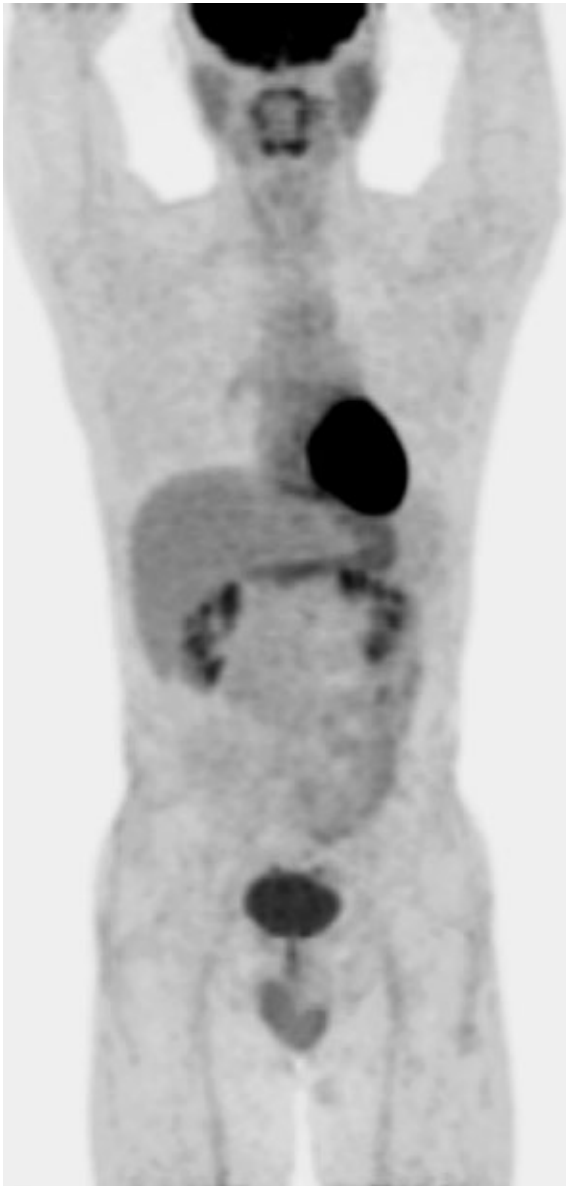


**FIGURE 3.** After three cycles of chemotherapy, the MIP image of follow-up F-18 FDG PET/CT showed complete metabolic remission of the involved lesions.

On CT examination, multiple enhancing nodules are well recognized in the subcutaneous layer of the involved body site.<sup>14</sup> However, these findings are also noted in inflammatory panniculitis associated with systemic lupus erythematosus or rheumatoid arthritis, subcutaneous metastases from malignant melanoma or breast cancer, and nodules originating from bacterial and fungal infections or from parasitic infestations.<sup>15</sup>

The F-18 FDG PET/CT has emerged as the standard of care for staging, monitoring of the response to therapy, and the detection of disease re-

currence in the majority of oncological patients as well as in patients with Hodgkin's and aggressive non-Hodgkin's lymphomas.<sup>16-18</sup> However, limited studies have been published in the literature on the value of F-18 FDG PET or PET/CT for the evaluation of cutaneous lymphoma. Moreover, only a few cases of SPTCL have been reported describing the findings of F-18 FDG PET or PET/CT. Most studies demonstrated that the subcutaneous lesions of SPTCL showed an FDG-avidity and indicated the superiority of PET/CT over CT alone in detecting nodal involvement.<sup>19-22</sup> In our case of SPTCL, F-18 FDG PET/CT detected many lesions with greater sensitivity than did physical examination or CT. These studies reported that F-18 FDG PET was valuable in monitoring the treatment response and detecting the extracutaneous lesion in SPTCL.<sup>19,23</sup>

Although further evaluations are needed, the findings in our case suggest that F-18 FDG-PET/CT is a valuable tool for diagnostic work-up, staging and response monitoring in patients with SPTCL as well as those with other FDG-avid lymphoma.

## References

1. Willemze R, Jaffe ES, Burg G, Cerroni L, Berti E, Swerdlow SH, et al. WHO-EORTC classification for cutaneous lymphomas. *Blood* 2005; **105**: 3768-85.
2. Gonzalez CL, Medeiros LJ, Brazier RM, Jaffe ES. T-cell lymphoma involving subcutaneous tissue: a clinicopathologic entity commonly associated with hemophagocytic syndrome. *Am J Surg Pathol* 1991; **15**: 17-27.
3. Horvat M, Jezersek Novakovic B. Effect of response quality and line of treatment with rituximab on overall and disease-free survival of patients with B-cell lymphoma. *Radiol Oncol* 2010; **44**: 232-8.
4. Salhany KE, Macon WR, Choi JK, Elenitsas R, Lessin SR, Felgar RE, et al. Subcutaneous panniculitis-like T-cell lymphoma: clinicopathologic, immunophenotypic, and genotypic analysis of alpha/beta and gamma/delta subtypes. *Am J Surg Pathol* 1998; **22**: 881-93.
5. Paulli M, Berti E. Cutaneous T-cell lymphomas (including rare subtypes): current concepts II. *Haematologica* 2004; **89**:1371-2.
6. Willemze R, Jansen PM, Cerroni L, Berti E, Santucci M, Assaf C, et al. Subcutaneous panniculitis-like T-cell lymphoma: definition, classification, and prognostic factors: an EORTC Cutaneous Lymphoma Group Study of 83 cases. *Blood* 2008; **111**: 838-45.
7. Kasper DL, Braunwald E, Fauci AS, Hauser SL, Longo DL, Jameson JL: Harrison's principles of internal medicine. New York: McGraw-Hill; 2005. p. 654.
8. Weenig RH, Ng CS, Pernicario C. Subcutaneous panniculitis-like T-cell lymphoma. *Am J Dermatopathol* 2001; **23**: 206-15.
9. Hoque SR, Child FJ, Whittaker SJ, Ferreira S, Orchard G, Jenner K, et al. Subcutaneous panniculitis-like T-cell lymphoma: a clinicopathological, immunophenotypic and molecular analysis of six patients. *Br J Dermatol* 2003; **148**: 516-25.
10. Marzano AV, Berti E, Paulli M, Caputo R. Cytophagocytic histiocytic panniculitis and subcutaneous panniculitis-like T-cell lymphoma. *Arch Dermatol* 2000; **136**: 889-96.
11. Pernicario C, Zalla MJ, White JW Jr, Menke DM. Subcutaneous T-cell lymphoma. Report of two additional cases and further observations. *Arch Dermatol*. 1993, **129**: 1171-6.

12. Takeshita M, Imayama S, Oshiro Y, Kurihara K, Okamoto S, Matsuki Y, et al. Clinicopathologic analysis of 22 cases of subcutaneous panniculitis-like CD56- or CD56+ lymphoma and review of 44 other reported cases. *Am J Clin Pathol* 2004; **121**: 408-16.
13. Massone C, Chott A, Metzger D, Kerl K, Citarella L, Vale E, et al. Subcutaneous, blastic natural killer (NK), NK/T-cell and other cytotoxic lymphomas of the skin: a morphologic, immunophenotypic and molecular study of 50 patients. *Am J Surg Pathol* 2004; **28**: 719-35.
14. Lee HJ, Im JG, Goo JM, Kim KW, Choi BI, Chang KH, et al. Peripheral T-Cell lymphoma: spectrum of imaging findings with clinical and pathologic features. *RadioGraphics* 2003; **23**: 7-26.
15. Kang BS, Choi SH, Cha HJ, Jung YK, Lee JH, Jeong AK, et al. Subcutaneous panniculitis-like T-cell lymphoma: US and CT findings in three patients. *Skeletal Radiol* 2007; **36**: S67-71.
16. Hodolic M. Role of 18F-choline PET/CT in evaluation of patients with prostate carcinoma. *Radiol Oncol* 2011; **45**: 17-21.
17. Huić D, Mutvar A, Kinda-Bašić S, Aurer T, Ciglar1M, Grošev D, et al. Negative predictive value of F-18-FDG coincidence PET in patients with Hodgkin's disease and a residual mass after therapy: a retrospective diagnostic test study. *Radiol Oncol* 2009; **43**: 258-63.
18. Jerusalem G, Hustinx R, Beguin Y, Fillet G. Evaluation of therapy for lymphoma. *Semin Nucl Med* 2005; **35**: 186-96.
19. Ravizzini G, Meirelles GS, Horwitz SM, Grewal RK. F-18 FDG uptake in subcutaneous panniculitis-like T-cell lymphoma. *Clin Nucl Med* 2008; **33**: 903-5.
20. Kong EJ, Cho IH, Chun KA, Bae YK, Chol JH, Hyun MS. F-18 FDG PET/CT findings of subcutaneous panniculitis-like T-cell lymphoma: a case report. *Nucl Med Mol Imaging* 2009; **43**: 240-4.
21. Tsai EY, Taur A, Espinosa L, Quon A, Johnson D, Dick S, et al. Staging accuracy in mycosis fungoides and sezary syndrome using integrated positron emission tomography and computed tomography. *Arch Dermatol* 2006; **142**: 577-84.
22. Kuo PH, McClennan BL, Carlson K, Wilson LD, Edelson RL, Heald PW, et al. FDG-PET/CT in the evaluation of cutaneous T-cell lymphoma. *Mol Imaging Biol* 2008; **10**: 74-81.
23. Rodriguez VR, Joshi A, Peng F, Rabah RM, Stockmann PT, Savaşan S. Positron emission tomography in subcutaneous panniculitis-like T-cell lymphoma. *Pediatr Blood Cancer* 2009; **52**: 406-8.

# Ultrasound elastography as an objective diagnostic measurement tool for lymphoedema of the treated breast in breast cancer patients following breast conserving surgery and radiotherapy

Nele Adriaenssens<sup>1,3</sup>, Dries Belsack<sup>2</sup>, Ronald Buyl<sup>4</sup>, Leonardo Ruggiero<sup>5</sup>, Catherine Breucq<sup>2</sup>, Johan De Mey<sup>2</sup>, Pierre Lievens<sup>3</sup>, Jan Lamote<sup>6</sup>

<sup>1</sup> Physical Therapy Department, Universitair Ziekenhuis Brussel, Belgium

<sup>2</sup> Department of Radiology, Universitair Ziekenhuis Brussel, Belgium

<sup>3</sup> Physical Therapy Department, Vrije Universiteit Brussel, Belgium

<sup>4</sup> Department of Biostatistics and Medical Informatics, Vrije Universiteit Brussel, Belgium

<sup>5</sup> Department of Engineering, Vrije Universiteit Brussel, Belgium

<sup>6</sup> Department of Oncological Surgery, Universitair Ziekenhuis Brussel, Belgium

Radiol Oncol 2012; 46(4): 284-295.

Received 1 January 2012

Accepted 14 April 2012

Correspondence to: Nele Adriaenssens, UZ Brussel - Breast Clinic, Laarbeeklaan 101, 1090 Jette, Brussels, Belgium. Phone: +32 2 477 60 15; E-mail: nmadriae@vub.ac.be

Disclosure: No potential conflicts of interest were disclosed.

**Background.** Lymphoedema of the operated and irradiated breast is a common complication following early breast cancer treatment. There is no consensus on objective diagnostic criteria and standard measurement tools. This study investigates the use of ultrasound elastography as an objective quantitative measurement tool for the diagnosis of parenchymal breast oedema.

**Patients and methods.** The elasticity ratio of the subcutis, measured with ultrasound elastography, was compared with high-frequency ultrasound parameters and subjective symptoms in twenty patients, bilaterally, prior to and following breast conserving surgery and breast irradiation.

**Results.** Elasticity ratio of the subcutis of the operated breast following radiation therapy increased in 88.9% of patients, was significantly higher than prior to surgery, unlike the non operated breast and significantly higher than the non operated breast, unlike preoperative results. These results were significantly correlated with visibility of the echogenic line, measured with high-frequency ultrasound. Big preoperative bra cup size was a significant risk factor for the development of breast oedema.

**Conclusions.** Ultrasound elastography is an objective quantitative measurement tool for the diagnosis of parenchymal breast oedema, in combination with other objective diagnostic criteria. Further research with longer follow-up and more patients is necessary to confirm our findings.

Key words: early breast cancer; breast conserving surgery; breast irradiation; lymphoedema of the breast; breast oedema; ultrasound elastography

## Introduction

The National Institutes of Health Consensus Development Conference on Treatment of Early Stage Breast Cancer indicated, 22 years ago, that

breast conserving surgery (BCS) with radiation therapy (RT) is the primary treatment for the majority of women with early stage breast cancer.<sup>1</sup> Nowadays, BCS is, after the diagnostic procedures, the most widely used surgical procedure for early breast can-

cer and in most cases it is followed by whole-breast irradiation of 55-60 Gy administered in a fractionated dose over the course of five to six weeks.<sup>2-5</sup>

An adverse side effect of this treatment is breast cancer related lymphoedema of the operated and irradiated breast (breast oedema).<sup>6</sup> Breast oedema is largely underdiagnosed in clinical practice because of lack of consensus on objective diagnostic criteria and on standard measurement tools.<sup>7,8</sup> Therefore, incidence intervals are wide and incidence is strongly influenced by follow-up time and the presence of patient and therapy related risk factors.<sup>1,3,6,7,9-14</sup> Incidences vary between 5% and 80%.<sup>3,6,7,9-12</sup>

The onset of breast oedema can occur postoperatively by disturbance of the lymphatic circulation, but it is most commonly reported following breast RT, which has been blamed for increasing the incidence following BCS.<sup>1,6,7,9,11,12</sup> RT of  $\geq 40$ Gy may lead to a significant increase in breast volume due to tissue reactions with an oedema, but breast irradiation itself does not initiate cutaneous oedema unless other predisposing or aggravating factors are present.<sup>13,14</sup> Breast irradiation does cause sclerosis of the skin, late post RT. Tissue fibrosis may obstruct lymph flow and slow down regeneration and formation of new lymph vessels.<sup>15</sup> The time course of cutaneous breast oedema during and following RT was previously described by Wratten *et al.* in 2007.<sup>14</sup> Lymph node irradiation in the breast area may decrease filter function and inhibit normal lymphatic proliferative response to inflammatory stimuli.<sup>7</sup>

Although pathophysiology of breast oedema is well known, problems with differential diagnosis occur frequently in clinical practice, because diagnosis and severity are quantified using subjective grading assessments by care takers and patients.<sup>6,9,16</sup> The clinical presentation of breast oedema becomes present in the second phase only, when the breast volume difference is obvious with symptoms of *peau d'orange*, redness, pain and positive pitting.<sup>3,9,12</sup>

Objectivities of clinical symptoms with medical imaging has shown that magnetic resonance imaging (MRI) and high-frequency ultrasound (HFUS) are feasible for some criteria of breast oedema.<sup>11,17</sup> There is a close correspondence between breast oedema demonstrated on MRI and the severity of clinical induration (palpable hardness).<sup>17</sup> Breast oedema on HFUS is presented by thickening of the skin over 2 mm with increased echogenicity, disturbance or poor visibility of the deeper echogenic line and interstitial fluid accumulation.<sup>11</sup> However, HFUS is not useful in quantifying parenchymal

breast oedema and acute inflammatory changes induced by breast irradiation.<sup>6,14</sup> Absolute HFUS echogenicity measures and visibility of the boundary of the dermis are strongly dependent on HFUS unit's gain settings and therefore unusable as a quantitative measure.<sup>6</sup> Since quantification at the onset of complications is necessary to evaluate the further evolution and treatment, a quantitative diagnostic measurement tool is necessary for breast oedema.

US elastography is a clinical application, non invasive, cost effective, safe and widely-accessible, that could give more information than HFUS on operation and radiation induced changes to the skin and subcutaneous tissue.<sup>16</sup> US elastography is a technique used for assessment of tissue elasticity, a soft tissue characterization based on the elastic properties. The principle of sono-elastography is that tissue compression results in a displacement or strain of the tissue. This strain is lower in hard tissue compared to soft tissue. By comparing the tissue during compression and decompression, information about the hardness of tissue can be assessed using a cross-correlation technique to determine the amount of displacement of each B-mode image pixel. There are several elastography techniques, the most studied in the literature being static elastography. Static elastography technique involves obtaining US signals from an axial imaging plane prior to and following a slight compression of the tissue. Typically, the pre and post compression frames are processed to generate images of local strain, commonly known as elastograms, displayed as an elasticity colour map image. On the elastogram, strain values of the different tissues viewed on the colour map image can be compared for quantification of a strain or elasticity ratio between tissues with different elasticity.<sup>18-21</sup> The breast is an application of choice for this technique, since it is readily accessible to compression with an US transducer.

Numerous groups have studied the elasticity of focal lesions in comparison with normal surrounding tissue within the breast, thyroid tissue, prostate and liver.<sup>18,22-24</sup> Also elasticity of lymph nodes has been studied and there have been studies about the applications of elastography within musculoskeletal disciplines.<sup>20,21</sup> Likewise, we assume that interstitial fluid accumulation in the breast following BCS with RT will affect the elasticity of subcutaneous breast tissue and therefore increase the tissues strain values.

Prior to embarking on a prospective study involving sequential observations in a large number of patients, we conducted a pilot study to assess the usefulness of US elastography to quantify pa-

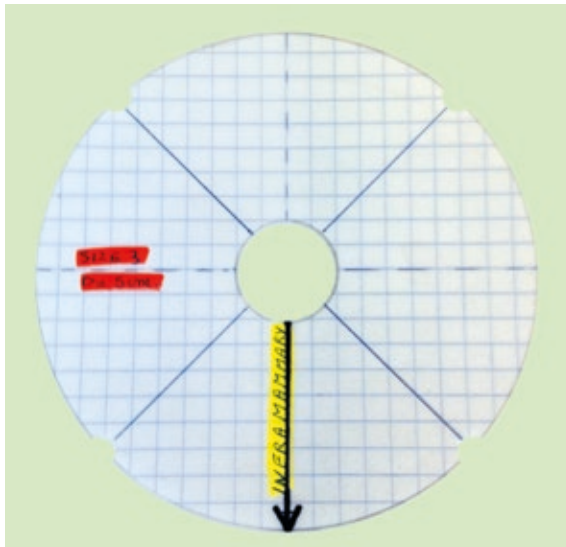


FIGURE 1. An example of a breast gauge.

renchymal breast oedema post irradiation. The aim was to determine the correlation between qualitative changes and quantitative data in the treated breast. Main research questions are: 'Is this quantitative technique able to measure early breast oedema in the operated and irradiated breast, as compared to the untreated contralateral breast and as compared to the preoperative breast?' and 'Does this quantitative technique correlate with subjective breast oedema and HFUS?'

## Patients and methods

### Patients

The study population was composed of women who were diagnosed with a primary breast cancer and scheduled for breast surgery at the University Hospital of Brussels. The trial, which was approved by the institutional ethics board, recruited women aged 18 years or older, with pathological nodal status assessed by axillary lymph node dissection (ALND) or sentinel lymph node dissection (SLND). The breast tumours have been completely resected by BCS. Enrolment into the trial took place between January 10 2011 and July 10 2011; for this report we included all evaluable patients who were measured at least twice between the trial start date and November 10 2011. The observation times were grouped to the closest planned follow-up interval. Women provided written informed consent prior to surgery. The trial was in accordance with the Helsinki Declaration of 1975, as revised in 2000.

RT was delivered as a dose of 50 Gy in 25 fractions over 5 weeks to the chest wall using tangential photon fields and to the supraclavicular, infraclavicular and axillary nodes in the case of pN1 status using an anterior field matched to the tangential fields. The majority of patients (75%) received an additional sequential boost of 16 Gy in 8 fractions over 2 weeks to the initial tumour bed using a direct electron field.<sup>25</sup> One patient participated in an experimental RT design and was delivered a dose of 42 Gy in 15 fractions over 3 weeks to the whole breast and to the supraclavicular, infraclavicular and axillary nodes because of pN1 status, using the Image Guided Radiation Therapy system Tomotherapy®. She received a simultaneous integrated boost of 9 Gy with the 15 fractions.<sup>26</sup>

### Anthropomorphic assessment

Assessments were made by a single physical therapist (NA) prior to BCS (baseline evaluation) and following completion of RT (follow-up). In this way, subjects acted as their own controls, where baseline measurements could be compared with results following RT. An assessment was also conducted prior to starting RT and is planned at six months, one year and two years post operatively, but this is not included in this report.

Baseline patient characteristics and clinical data recorded during baseline assessment were the patient's age, weight and height, the breast that is going to be operated, localization of the tumours in the breast and the dominant side. Adjuvant treatment and type of surgery were collected from the medical file.

Breast volume was calculated from anthropomorphic measurements on both breasts, with the formula of Qiao *et al.* described in 1997.<sup>27</sup> This method was proved to be adequate, most convenient and the best method for breast volume calculation by patients and doctors. The measurements have an acceptable degree of accuracy and reproducibility, but the composition of the mathematical formula is discussable.<sup>28-30</sup>

For the physical assessment of breast cancer related lymphoedema of the arm (BCRL), we measured the volume of both arms of each patient with a mobile infrared optoelectronic volumeter (Perometer® 1000M, Pero-System GmbH, Wuppertal, Germany; Peroplus Software TM). The presence of BCRL was defined as  $\geq 10\%$  inter-limb discrepancies in volume from baseline, respectively, where inter-limb discrepancy was computed as per cent volume difference (percentage volume

difference =  $100 * [\text{volume of affected arm} - \text{volume of unaffected arm}] / [\text{volume of unaffected arm}]$ .

Obesity was expressed as a body mass index (BMI) of  $\geq 30 \text{ kg/m}^2$ .<sup>7,9,11</sup> Preoperative bra cup size was calculated as the difference between the overbust circumference and the underband circumference. If the difference was  $<6.5 \text{ cm}$ ;  $6.5\text{--}13 \text{ cm}$ ;  $13\text{--}19.5$  or  $>19.5$ , the patient had, respectively an A, B, C or  $\geq D$  cup.<sup>31</sup>

### Subjective symptoms assessment

Subjective breast oedema was registered by the patient at follow-up, as an answer to a question ('Was the area of your operated breast swollen during the past week?') of the EORTC QLQ BR23 questionnaire. This questionnaire uses the 4-point categorical scale according to the modified system of Johansen *et al.*<sup>3</sup> If the patient answered 1 ('absolutely not') to this question, she had no subjective breast oedema. If she answered 2, 3 or 4, she had subjective breast oedema.

Toxicity of the breast skin was scored by an experienced breast radiotherapist following the last RT session, using Radiation Therapy Oncology Group (RTOG) acute morbidity scoring schemas.<sup>16,32</sup>

### High-frequency ultrasound assessments

HFUS evaluation of the breasts was performed using a clinical ultrasound scanner (Toshiba Aplio XG) with a High-Resolution 12-MHz linear probe (PLT 1204 BT, Toshiba) for data acquisition. The examinations were performed with patients in supine position. B-mode images were obtained focusing on the areas of interest, being the four quadrants of both breasts (SIQ, upper inner quadrant; IIQ, lower inner quadrant; IEQ, lower outer quadrant and SEQ, upper outer quadrant). To obtain the images at the same location during follow-up, plastic breast gauges of variable sizes were created and used on every patient, depending on the size of the patient's preoperative breast cup size (Figure 1).

To ensure good coupling of the probe-skin interface, a layer of ultrasound transmission gel was used in addition to a gel pad, SonarAid (Geistlich Pharma AG) size  $130 \times 120 \times 10 \text{ mm}$ . The gel pad was used as a reference tissue for elasticity measurements. The probe was held perpendicular to the breast surface, parallel with the concentric circles contouring the areola at the level indicated by the breast gauge (Figure 2). No additional compression was performed for the B-mode images. The viewing field depth was standardized at 4 cm, and the gain was not adjusted (fabric default setting, 2DG: 81).

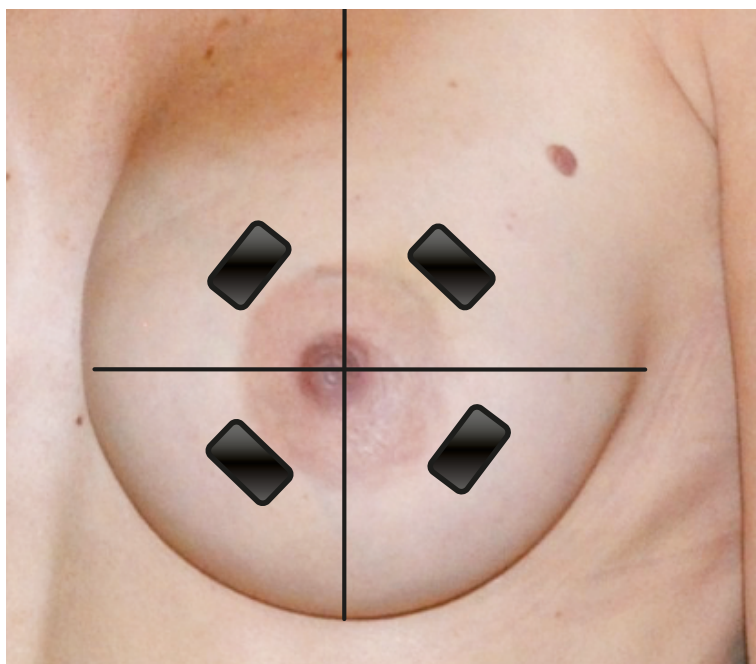


**FIGURE 2.** Position of the ultrasound probe in the four quadrants and the inframammary fold of the breast, perpendicular to the nipple.

Scans were performed at the same days as the clinical assessments. HFUS examination of the breasts was performed by an experienced breast radiologist (DB). On the B-mode HFUS images, the radiologist evaluated the visibility of the deeper echogenic line and the presence of interstitial fluid accumulation between the lobules of subcutaneous fat tissue. In addition, skin thickness was calculated at every measure location of both breasts. All images were stored for later analysis. Measurements taken from the four quadrants of the operated breast were averaged for each parameter and compared with the average value of the non operated breast of the same patient and the baseline measurements of the same breast. Although radiation dose was not uniform across the entire breast, average values were analysed to validate the viability of our technique.<sup>16</sup>

#### Skin thickness

Skin thickening is a well-known post irradiation effect, which has been researched by several groups using HFUS. Skin thickness was measured as the distance between two thin echogenic lines with the hypoechoic dermis within, as described extensively in previous studies.<sup>6,11,14,16,33</sup> Skin thickness of the four quadrants of the breast was recorded for the operated and non operated breast. Thickness of normal breast skin varies between 1 and 2 mm with a mean thickness of 1.7mm.<sup>11</sup> The underlying phys-

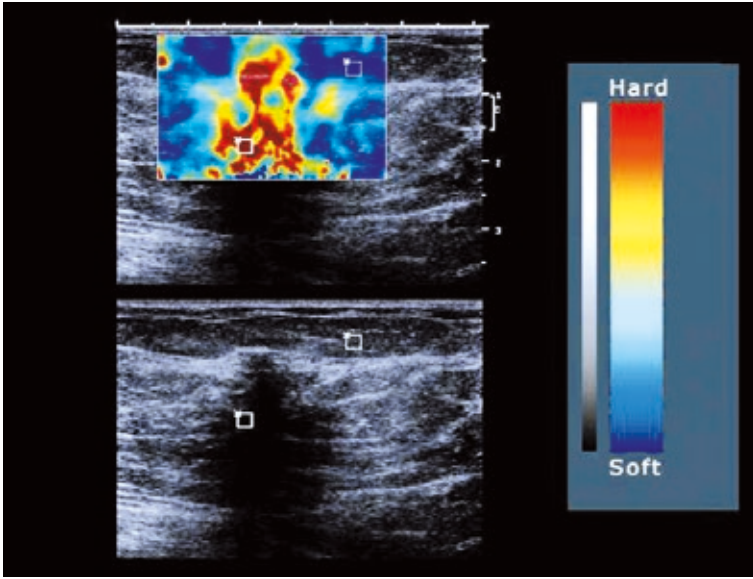


**FIGURE 3.** Elastogram with a region of interest (ROI) in two tissues with different elasticity.

ics concept behind skin thickness measurements has been described in previous reports.<sup>16</sup>

#### *Echogenicity of the subcutis*

IQ-VIEW/IQ-LITE, IMAGE Information Systems Ltd. 2008 v.2.5.0. R1 was used to measure the density of the subcutis in a selected region of interest (ROI). A rectangle is drawn over the specified area, with the tools application 'measure ROI density', and the mean, minimum, maximum and standard deviation density is given on a scale between 0 (black) and 230 (white) INT.<sup>14,33</sup>

#### *Visibility of the deeper echogenic line*

Evaluation of the deeper echogenic line as a marker for subcutaneous oedema, previously described by the Rönkä group, was performed by scoring the visibility of the subcutaneous fat interface between 0 (not visible) and 4 (clearly visible).<sup>11</sup>

#### *Interstitial fluid accumulation*

Presence of interstitial fluid accumulation was assessed on the B-mode US images as hypoechoic fluid infiltration (dark bands) between the fat lobules and scored as absent (score 0) or present (score 1).<sup>11</sup>

### Ultrasound elastography

US elastography measurements were performed following the HFUS B-mode scans at the same measurement locations in the four quadrants of both breasts as previously described, using the

same conventional linear 12-MHz transducer. In our study protocol, the static US elastography technique was applied using Toshiba ElastoQ software. Given the diffuse distribution of parenchymal breast oedema, affecting large regions or even the whole breast, comparison with normal, non affected breast tissue at the same US elastography image is impossible. Therefore a gel pad was placed on the breast skin in each patient as a reference tissue for the underlying breast tissue. The elasticity of the gel pad did not change during the term of the study, making it an excellent reference tissue. The same image settings as in the HFUS B-mode images were used. For obtaining the real-time freehand US elastography images, the transducer was compressed and released perpendicular to the skin for approximately five times along the radiation axis, in the US elastography mode.

US Elastography software measured the strain image or elastogram on which quantitative strain values were assessed. On the elastogram a strain colour scale image and strain graph are displayed. ROIs were placed on the colour scale image for comparison of strain values of tissues with different elasticity (Figure 3). In our protocol, a standardized ROI box was placed in the reference gel pad (ROI length  $10 \pm 1$  mm, depth  $4 \pm 1$  mm) and in the subcutaneous breast tissue (ROI length  $20 \pm 1$  mm, depth  $5 \pm 1$  mm). From these ROIs the average strain values were displayed as curves in a strain graph for each amount of compression force during the compression/decompression cycle. The range of strain value derived from the gel pad curve during compression/decompression varied between 0 and 0.7 on average during preliminary test exams, depending on the amount of compression given. For standardization, all measurements were obtained at  $0.4 \pm 0.1$  strain value of the reference gel pad. The strain value of the gel pad ( $0.4 \pm 0.1$ ) was divided by the strain value of the subcutaneous breast tissue at the same amount of compression, extrapolated from the gel pad value on the strain graph, giving a calculated strain ratio. These ratios were calculated in the different quadrants of each breast prior to surgery and following RT, except for the operated quadrant, because compression in this region could be painful following surgery (Figure 4).

### Statistical analysis

Data were verified on a case-by-case basis to identify inconsistencies. Descriptive statistics as frequencies, means, standard deviations and percentages were used to describe patients' characteristics. We



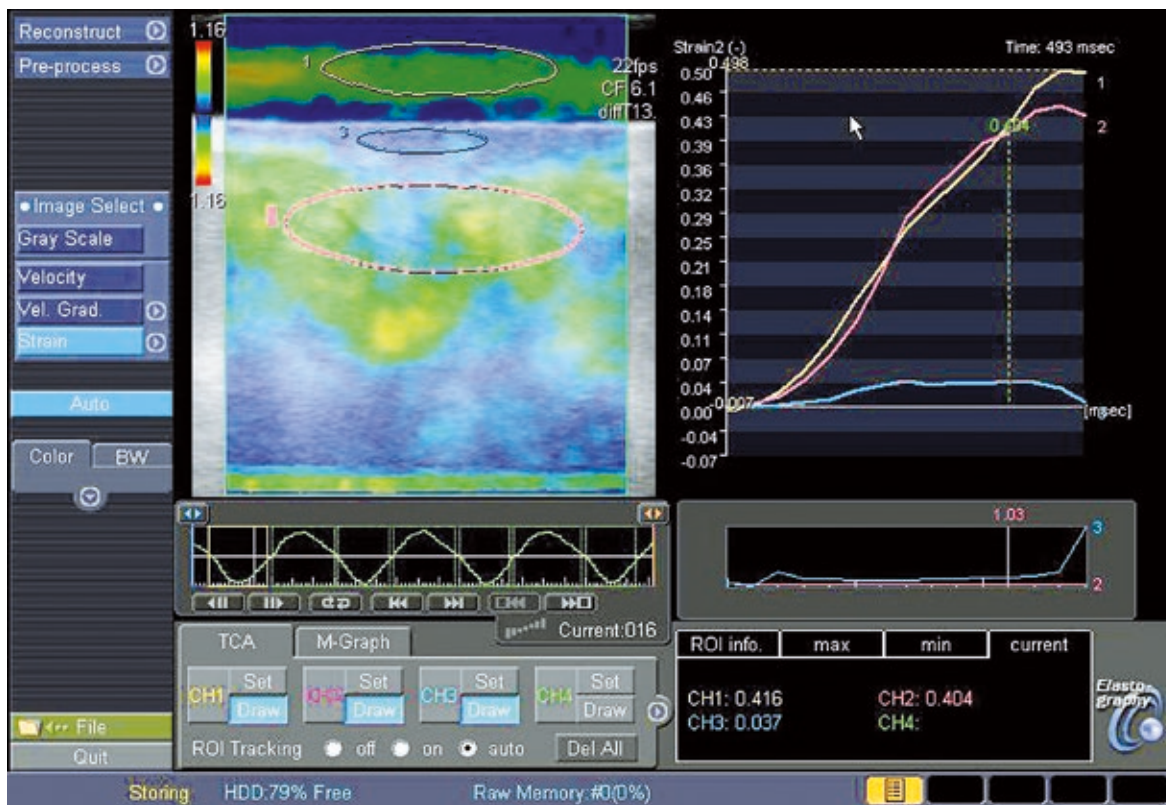


FIGURE 4. The elastogram with 3 ROI's (yellow, gel pad; blue, skin; pink, subcutis) and the strain graph with three matching curves. The strain values are displayed underneath, respectively 0.416, 0.037, 0.404. Images were taken in the IIQ of an operated breast.

have used dichotomous breast oedema criteria as well as mean continuous absolute values of the four breast quadrants and single continuous absolute values of the different breast quadrants. For univariate comparisons of baseline and follow-up measurements the matched paired t-test was used. An independent t-test was performed to examine the difference between operated and non operated breast measurements.

Correlations between the breast oedema criteria were assessed using Pearson's and Spearman Rank correlation coefficients. Pearson-Chi Square tests were used to examine the significance of the correlation between the different diagnostic criteria for breast oedema and elasticity ratio of the subcutis of the operated and non operated breast at baseline and of the operated breast following RT.

Influence of risk factors on absolute elasticity ratio of the subcutis in the operated breast following RT was assessed using a general linear model.

For all analyses, superiority was based on two-sided p values <0.05. All statistical computations used SPSS v. 20.0. (IBM Corporation, Somers, NY 10589, USA).

## Results

Of the twenty nine patients who were recruited in the trial between January 10, 2011 and September 10, 2011, twenty five received baseline evaluation and first follow-up, prior to RT (data not shown). One patient was excluded at first follow-up, because she did not have to receive RT. Four patients did not finish RT and thus second follow-up (following RT), leaving twenty patients available for analyses at November 10, 2011.

Table 1 summarizes the baseline characteristics and clinical data of the evaluable patients. The inter-limb PVD at baseline was close to zero in all patients, indicating that there were no patients with BCRL prior to and following BCS and RT (data not shown).

### Subjective swelling of the operated and irradiated breast

Subjective swelling of the operated and irradiated breast was present in 43.8% of the patients.

TABLE 1. Patient's characteristics

	mean	SD*
Age (years)	58.9	12.1
Body mass index (kg/m <sup>2</sup> )		
Preoperative	26.4	4.6
Postirradiation	26.1	4.7
Time interval (weeks)		
Preoperative – postirradiation	12.7	2.8
Time interval (weeks)		
Operation – start radiation therapy		
Volume of the operated breast (cc)		
Preoperative	961.8	695.8
Postoperative	830.6	558.3
Postirradiation	842.4	599.3

\*standard deviation

	n	Valid %
Tumours localization in the SEQ**	12	60
Operated side equals dominant side	10	50
Axillary lymph node dissection	5	25
Neoadjuvant chemotherapy	1	5
Anti-hormone therapy	13	65
Chemotherapy	6	30
Irradiation dose		
< 66 Gy	5	25
66 Gy	15	75
Skin toxicity		
Grade 1	15	83,3
Grade 2	2	11,1
Grade 3	1	5,6
Subjective swelling	7	43,8
Preoperative breast cup size		
A	3	15
B	9	45
C	7	35
≥ D	1	5
Preoperative obesity (BMI*** > 30 kg/m <sup>2</sup> )	5	25

\*\*superior external quadrant; \*\*\*body mass index

## Skin thickness

Mean skin thickness of the four quadrants following RT was over 2 mm in every patient. In the different quadrants, skin thickness over 2 mm was present in 90%, 90%, 80% and 75% of the patients in the SIQ, IIQ, IEQ and SEQ, respectively.

Absolute skin thickness significantly increased ( $p=0.000$ ) in all quadrants of the operated breast following RT, compared with baseline measurements. In the non operated breast, absolute skin thickness did not change significantly in the quadrants.

Absolute skin thickness was significantly higher ( $p=0.000$ ) in all quadrants of the operated breast following RT, compared with all quadrants of the non operated breast following RT. Baseline measurements of absolute skin thickness did not differ significantly between the operated and the non operated breast in all quadrants prior to surgery (Table 2).

## Echogenicity of the subcutis

Mean echogenicity of the subcutis in the four quadrants following RT increased in 89.5% of the patients. In the different quadrants, echogenicity of the subcutis increased in 78.9%, 70%, 80% and 61.5% of the patients in the SIQ, IIQ, IEQ and SEQ, respectively.

Absolute echogenicity of the subcutis significantly increased ( $p \leq 0.05$ ) in all quadrants, except for the SEQ, of the operated breast following RT, compared with baseline measurements. In the non operated breast, absolute echogenicity of the subcutis did not change significantly in the quadrants.

Absolute echogenicity of the subcutis was significantly higher ( $p=0.000$ ) in all quadrants of the operated breast following RT, compared with all quadrants of the non operated breast following RT. Baseline measurements of absolute echogenicity of the subcutis did not differ significantly between the operated and the non operated breast in all quadrants prior to surgery (Table 3).

## Visibility of the echogenic line

Mean visibility of the echogenic line in the four quadrants following RT decreased in every patient. In the different quadrants, visibility of the echogenic line was present in 95%, 100%, 100% and 100% of the patients in the SIQ, IIQ, IEQ and SEQ, respectively.

Mean visibility of the echogenic line significantly decreased ( $p=0.000$ ) in all quadrants of the oper-

**TABLE 2.** Skin thickness (mm) in the different quadrants of both breasts (operated and non operated) at baseline (pre) and follow-up (post)

	Operated – pre	Non operated – pre	Operated – post	Non operated – post
Mean	1.66 (.28)	1.65 (.26)	3.03 (1.28)	1.62 (.22)
SIQ	1.73 (.32)	1.72 (.28)	2.87 (1.05)	1.68 (.27)
IIQ	1.7 (.28)	1.69 (.29)	3.43 (1.9)	1.75 (.32)
IEQ	1.65 (.33)	1.64 (.29)	3.12 (1.34)	1.54 (.27)
SEQ	1.56 (.30)	1.55 (.26)	2.7 (1.10)	1.52 (.25)

SIQ, upper inner quadrant; IIQ, lower inner quadrant; IEQ, lower outer quadrant and SEQ, upper outer quadrant

**TABLE 3.** Echogenicity of the subcutis in the different quadrants of both breasts (operated and non operated) at baseline (pre) and follow-up (post)

	Operated – pre	Non operated – pre	Operated – post	Non operated – post
Mean	110.3 (18.1)	113.9 (13.5)	124.2 (19.9)	106.7 (16.6)
SIQ	110.3 (20.1)	116.9 (20.6)	127.9 (19.1)	110.1 (21.3)
IIQ	105.6 (18.4)	108.8 (21.2)	121.1 (19.9)	99.4 (17.1)
IEQ	111.3 (22.5)	114.1 (32.3)	129 (21.9)	110 (17.7)
SEQ	114 (21)	111.3 (21.5)	122.7 (28.6)	107.4 (19.3)

SIQ, upper inner quadrant; IIQ, lower inner quadrant; IEQ, lower outer quadrant and SEQ, upper outer quadrant

**TABLE 4.** US Elasticity ratio of the subcutis in the different quadrants of both breasts (operated and non operated) at baseline (pre) and follow-up (post)

	Operated - pre	Non operated - pre	Operated - post	Non operated - post
Mean	2.78 (1.66)	2.85 (1.47)	4.06 (1.31)	3.05 (1.25)
SIQ	2.77 (1.65)	3.38 (2.63)	4.08 (2.22)	3.35 (2.08)
IIQ	2.68 (1.65)	2.77 (1.76)	3.63 (1.77)	3.06 (1.87)
IEQ	3.09 (3.14)	2.44 (1.3)	3.92 (2.60)	2.92 (1.4)
SEQ	2.57 (1.18)	2.82 (2.14)	3.34 (2.46)	2.9 (1.48)

SIQ, upper inner quadrant; IIQ, lower inner quadrant; IEQ, lower outer quadrant and SEQ, upper outer quadrant

ated breast following RT, compared with baseline measurements. In the non operated breast, visibility of the echogenic line did not change significantly in the quadrants.

Mean visibility of the echogenic line was significantly lower ( $p=0.000$ ) in all quadrants of the operated breast following RT, compared with all quadrants of the non operated breast following RT. Baseline measurements of visibility of the echogenic line did not differ significantly between the operated and the non operated breast in all quadrants prior to surgery.

### Interstitial fluid accumulation

Mean interstitial fluid accumulation in the four quadrants following RT increased in 72.2% of the

patients. In the different quadrants, interstitial fluid accumulation was present in 83.3%, 77.8%, 77.8% and 88.9% of the patients in the SIQ, IIQ, IEQ and SEQ, respectively.

Mean interstitial fluid accumulation in the subcutis of the operated breast significantly increased ( $p<0.05$ ) following RT, compared with the mean baseline measurement. Although interstitial fluid accumulation of the subcutis increased in the different quadrants, they did not increase significantly for SIQ and SEQ, only for IIQ ( $p=0.042$ ) and IEQ ( $p=0.042$ ). In the non operated breast, interstitial fluid accumulation of the subcutis did not change significantly in the quadrants or as a mean interstitial fluid accumulation of the subcutis in the four quadrants. Mean interstitial fluid accumulation was significantly higher ( $p<0.05$ ) in all quadrants of

the operated breast following RT, compared with all quadrants of the non operated breast following RT, except for SIQ and SEQ. Baseline measurements of interstitial fluid accumulation did not differ significantly between the operated and the non operated breast in all quadrants prior to surgery.

### Elasticity ratio of the subcutis

Mean elasticity ratio of the subcutis in the four quadrants following RT increased in 88.9% of the patients. In the different quadrants, elasticity ratio of the subcutis increased in 63.2%, 65%, 60% and 78.6% of the patients in the SIQ, IIQ, IEQ and SEQ, respectively.

Mean absolute elasticity ratio of the subcutis significantly increased ( $p < 0.05$ ) in the operated breast following RT, compared with the mean baseline measurement. Although absolute elasticity ratio of the subcutis increased in the different quadrants, they did not increase significantly. In the non operated breast, absolute elasticity ratio of the subcutis did not change significantly in the quadrants or as a mean absolute elasticity ratio of the subcutis of the four quadrants.

Mean absolute elasticity ratio of the subcutis was significantly higher ( $p = 0.000$ ) in the operated breast following RT, compared with the non operated breast following RT. This difference was not significantly higher for all quadrants, only for IEQ ( $p = 0.032$ ). Baseline measurements of absolute elasticity ratio of the subcutis did not differ significantly between the operated and the non operated breast in all quadrants prior to surgery (Table 4).

### Correlation between elasticity ratio of the subcutis and the other breast oedema criteria

A bivariate correlation between the elasticity ratio of the subcutis and the different diagnostic criteria for breast oedema, prior to surgery, in the operated and non operated breast neither showed any correlation between the variables, nor for the operated breast following RT, except for the mean visibility of the echogenic line.

### Risk factors

ALND, tumours located in the SEQ, preoperative obesity, chemotherapy (except for IEQ; more increase in the patients with chemotherapy), RT dose of 66 Gy, operated at the dominant side, age, BMI and time between surgery and start of RT, were not

significant risk factors, neither for increase of absolute elasticity ratio of the subcutis, nor for increase of the elasticity ratio of the subcutis in the operated breast following RT. Bigger preoperative bra cup size was a significant risk factor for the increase of US elasticity ratio of the subcutis ( $p = 0.01$ ).

## Discussion

In this study, we have measured different currently used breast oedema criteria and evaluated a new objective diagnostic measurement tool for parenchymal breast oedema, prior to BCS and following RT. HFUS images and US elastography images were obtained in four quadrants of both the operated and non operated breast of 20 patients. We have compared baseline results with follow-up measurements and the operated with the non operated breast. Possible risk factors and correlations between breast oedema criteria have been investigated.

*Subjective swelling* of the operated breast, rated by the patient, was present in almost half of the patients following RT. Subjective breast oedema following RT, rated by an experienced breast radiotherapist and physical therapist (NA), resulted in respectively at least grade one skin toxicity and clinical breast oedema in all patients.<sup>3,9,12,32</sup> Subjective symptom rating by patients and clinicians are not satisfying for the diagnosis and degree of parenchymal breast oedema.

*Skin thickness* of the operated breast following RT was over 2 mm in all patients and significantly thicker than prior to surgery, unlike the non operated breast skin. Skin thickness of the operated breast following RT was significantly thicker than the non operated breast, unlike preoperative results. Skin thickness increase is caused by an increased extravascular-extracellular leakage space in the (hypo)dermis and extensive cellular fibrosis, characterized by the loss of consistent pattern in extracellular structures.<sup>16,17</sup> Mean total cutaneous thickness was 2.71 mm in an operated and irradiated breast and 1.35 mm in a non operated/irradiated breast. This difference was significant.<sup>6</sup> Mean skin thickness of the operated breast following RT in our study was 3.03 mm and 1.64 mm in the non operated/irradiated breast, which is similar to the results of Wratten *et al.* (1.36 mm increase versus 1.39 mm increase following BCS and RT).<sup>6</sup> These results show that skin thickness increase over 2 mm following BCS and RT is a reliable diagnostic criterion for cutaneous breast oedema.

*Echogenicity of the subcutis* in the operated breast following RT increased in 89.5% of the patients and was significantly higher than prior to surgery, unlike the non operated breast subcutis. Echogenicity of the subcutis of the operated breast following RT was significantly higher than the non operated breast, unlike preoperative results. Increase in echogenicity of the subcutis reflects a hypoechoic area.

Increased echogenicity of the subcutis in the operated breast following RT can be caused by an increased subcutaneous extravascular-extracellular leakage space.<sup>16,17</sup> Parenchymal breast oedema might also be the result of a manifestation of an increased number of perfused microvessels, persistent microvascular leakage, impaired drainage, and loss of architectural integrity of tissue microstructures related to radiation-induced vascular injury.<sup>16,17</sup>

Our study results could not be compared with other literature results, because echogenicity depends on the gain used on the HFUS exams, frequency of the probe, tissue characteristics, location on the breast and follow-up time. However, 85% of the patients with BCS and RT had an increase in breast tissue density in the study of Delay *et al.*; and Ronka *et al.* also observed an increased echogenicity.<sup>11,12</sup> Wratten *et al.* described a decrease in echogenicity of the subcutis following BCS and RT.

In our study HFUS settings were standardized, so we can conclude that there was a significant increase of the echogenicity of the subcutis, most likely due to the presence of oedema in the subcutis. Like skin thickness, echogenicity of the subcutis can be a valuable diagnostic criterion, when taking into account standardization of methodology as previously described.

*Visibility of the echogenic line in the subcutis* of the operated breast following RT decreased in all patients and was significantly lower than prior to surgery, unlike the non operated breast. Visibility of the echogenic line in the subcutis of the operated breast following RT was significantly lower than the non operated breast, unlike preoperative results.

These results are similar to the results of Ronka *et al.*<sup>11</sup> This criterion is subjectively scored, by only one experienced breast radiologist (DB) for all measurements in all patients. Visibility of the echogenic line in the subcutis of an operated breast following RT decreases, because of disturbance of the skin/subcutaneous fat interface due to presence of cutaneous and subcutaneous oedema. Therefore visibility of the deeper echogenic line can also be

a useful diagnostic criterion for assessing breast oedema.

*Mean interstitial fluid accumulation* of the operated breast following RT increased in 72.2% of the patients and was significantly higher than prior to surgery, unlike in the non operated breast. Interstitial fluid accumulation of the operated breast following RT was significantly higher than the non operated breast, unlike preoperative results. These results were not significantly higher in the upper quadrants of the operated and irradiated breast. This could be explained by the influence of gravity on the fluid in the breast. Presence of interstitial fluid accumulation in the operated and irradiated breast is an objective HFUS visible entity. It is a valuable diagnostic criterion for presence of interstitial oedema due to fluid leakage in the extracellular interstitial space. Our study results are similar to the results of Ronka *et al.* and Wratten *et al.* who also observed an increased interstitial fluid accumulation in the operated and irradiated breast.<sup>11,14</sup>

*Mean elasticity ratio of the subcutis* of the operated breast following RT increased in 88.9% of the patients and was significantly higher than prior to surgery, unlike the non operated breast. Mean elasticity ratio of the subcutis in the operated breast following RT was significantly higher than the non operated breast, unlike preoperative results. These results were not significantly higher for all quadrants of the operated and irradiated breast. Our group compared the strain of the subcutaneous fat tissue with the strain of an elastic gel pad giving an elasticity ratio. Increase in elasticity ratio in the operated and irradiated breast corresponds to more elastic breast tissue in comparison with the preoperative results. An increase in elasticity of the underlying breast tissue could be explained by the increase of fluid in the breast. Our study results could not be compared with other literature results, because to our knowledge, no other research group has used the same methodology.

Elasticity ratio can be a valuable diagnostic criterion, when taking into account standardization of methodology. Although elasticity ratio in the different quadrants of the operated and irradiated breast was higher than baseline measurements and the non operated breast, the difference was not significant. Further research with more patients is necessary to confirm these results.

*Correlations* between different breast oedema criteria were present between mean elasticity ratio and mean visibility of the echogenic line in the operated and irradiated breast only. Wratten *et al.*

found a correlation between subjective parenchymal breast oedema and skin thickness and between skin thickness and cutaneous echogenicity.<sup>6</sup>

The absence of other correlations with our new technique could suggest elasticity ratio to be a supplementary criterion for the diagnosis and degree of breast oedema, giving extra information on hydrated breast tissue elasticity. Additionally, making a combination of the four breast oedema criteria, measured with HFUS the incidence of breast oedema was 90.4% following RT, compared to 88.9% with increased elasticity ratio.<sup>11</sup> The breast oedema definition and our new technique result in equal incidences.

Unlike similar research, we did not find *risk factors* for the increase of parenchymal breast oedema, expressed by increased elasticity ratio in this study, except for bigger preoperative bra cup size.<sup>3,6,10,12,13</sup> All patients had an increased mean elasticity ratio in the operated and irradiated breast, except for patients with preoperative A cup.

Echogenicity and elasticity ratio were obtained from the subcutis and not cutaneous, because breast skin behaves different than the underlying breast tissue and literature showed disagreement on cutaneous measurements.<sup>6,11</sup> Measurements in the inframammary fold of the operated and irradiated breast were not discussed in this manuscript, as well as measurements of the first follow-up (postoperative but prior to RT) for the same reasons.

Our study presents several limitations. Our pilot study counts only 20 patients and a short follow-up. As part of the institution's surgical management, operated breast cancer patients receive a prescription for ambulatory physical therapy at the time of discharge. However, we did not record the compliance of patients or their receipt of manual lymphatic drainage of the breast during the study, although their beneficial effects on breast oedema could be expected.<sup>34-37</sup> Another limitation of our study is the known lack of reliability of breast oedema criteria measurements. Our study results should be interpreted with these restrictions in mind.

One strength of the study is standardization of HFUS settings, US elastography methodology and measurement protocol, like gain, gauges, etc. by a specialized breast radiologist (DB). Gain was often adjusted to become better clinical results in other studies, but this was not the case in our study.<sup>6,11</sup> Wratten *et al.* concluded that HFUS was not useful in quantifying acute inflammatory changes induced by breast irradiation, but with our standardized approach this was possible.<sup>14</sup> A second strength

of the study is the preoperative measurements to compare with immediate post irradiation measurement. To our knowledge, no other research groups have used preoperative bilateral measurements as baseline results. Another strength of our study is that the trial was conducted in a single institution. All patients were followed by the same team, which ensures that assessments were consistently performed throughout the trial. We believe that the strengths of the study outweigh its limitations and that the results are robust, at least within the current short follow-up time frame.

Because this is a pilot study, the long-term usability of this technique cannot yet be demonstrated; however, this technique seems to be an interesting quantitative objective complement to current breast oedema diagnostic criteria. A follow-up of six months and one year following surgery is scheduled as part of the study, like the time course of parenchymal breast oedema during and following RT was previously described by Wratten *et al.*<sup>6</sup> Breast oedema incidence peaks at four to six months following treatment and returns to baseline after one year. It will be interesting to see if changes, observed in this analysis are confirmed at later follow-up. Our findings suggest further investigation with more patients and longer follow-up.

We can conclude from our study results that ultrasound elastography is an objective quantitative measurement tool for the diagnosis of parenchymal breast oedema, in combination with other objective diagnostic criteria.

## Acknowledgements

The corresponding author (NA) is financed by a bursary of the IWT (Foundation for Innovation of Science and Technology); however, this study sponsor had no involvement in the study design, in the collection, analysis and interpretation of data, in the writing of the manuscript, or in the decision to submit the manuscript for publication.

## References

1. Olivetto IA, Weir LM, Kim-Sing C, Bajdik CD, Trevisan CH, Doll CM, et al. Late cosmetic results of short fractionation for breast conservation. *Radiother Oncol* 1996; **41**: 7-13.
2. Aryana K, Gholizadeh M, Momenzadeh M, Naji M, Aliakbarian M, Forghani MN, et al. Efficacy of high-energy collimator for sentinel node lymphoscintigraphy of early breast cancer patients. *Radiol Oncol* 2012; **46**: 75-80.
3. Kelemen G, Varga Z, Lázár G, Thurzó L, Kahán Z. Cosmetic outcome 1-5 years after breast conservative surgery, irradiation and systemic therapy. *Pathol Oncol Res* 2012; **18**: 421-7.

4. Feng-yan L, Zhen-yu H, Ming X, Li-xin C, San-gang W, Xun-xing G. Feasibility and acute toxicity of 3-dimensional conformal external-beam accelerated partial-breast irradiation for early-stage breast cancer after breast-conserving surgery in Chinese female patients. *Chin Med J* 2011; **124**: 1305-9.
5. Monticciolo DL, Biggs K, Gist AK, Sinclair ST, Hajdik RL, Nipper ML, et al. Breast conserving therapy with accelerated partial breast versus external beam whole breast irradiation: comparison of imaging sequela and complications in a matched population. *Breast J* 2011; **17**: 187-90.
6. Wratten C, Kilmurray J, Wright S, O'Brien PC, Back M, Hamilton CS, et al. Pilot study of High-Frequency Ultrasound to assess cutaneous oedema in the conservatively managed breast. *Int J Cancer* 2000; **90**: 295-301.
7. Meek AG. Breast radiotherapy and lymphoedema. *Cancer* 1998; **83**: 2788-97.
8. Rucigaj TP, Leskovec NK, Zunter VT. Lymphedema following cancer therapy in Slovenia: a frequently overlooked condition? *Radiol Oncol* 2010; **44**: 244-8.
9. Goffman TE, Laronga C, Wilson L, Elkins D. Lymphoedema of the arm and breast in irradiated breast cancer patients: risks in an era of dramatically changing axillary surgery. *Breast J* 2004; **10**: 405-11.
10. Pezner RD, Patterson MF, Hill LR, Desai KR, Vora N, Lipsett JA. Breast oedema in patients treated conservatively for stage I and II breast cancer. *Int J Radiat Oncol Biol Phys* 1985; **11**: 1765-8.
11. Rönkä RH, Pamiilo MS, von Smitten KAJ, Leidenius MHK. Breast lymphoedema after breast conserving treatment. *Acta Oncol* 2004; **43**: 551-7.
12. Delay E, Gosset J, Toussoun G, Delaporte T, Delbaere M. Post-treatment sequelae after breast cancer conservative surgery. *Ann Chir Plast Esth* 2008; **53**: 135-52.
13. Trog D, Garbe S, Lutterbey G, Lütter C, Barwig P, Boldt I, et al. Volumetric changes of the breast during radiotherapy. Is a replanning necessary for the electron boost? *Strahlenther Onkol* 2005; **181**: 255-9.
14. Wratten CR, O'Brien PC, Hamilton CS, ill D, Kilmurray J, Denham JW. Breast oedema in patients undergoing breast-conserving treatment for breast cancer: assessment via High Frequency Ultrasound. *Breast J* 2007; **13**: 266-73.
15. Lievens P, Pastouret F, Leduc A, Leduc O, Bougeois P. The short time effect of radiation therapy on the newly formed lymphvessels. *The European Journal of Lymphology* 2008; **19**: 25-6.
16. Liu T, Zhou J, Yoshida EJ, Woodhouse SA, Schiff PB, Wang TJC. Quantitative Ultrasonic evaluation of Radiation-induced late tissue toxicity: pilot study in breast-cancer radiotherapy. *Int J Radiat Oncol Biol Phys* 2010; **78**: 811-20.
17. Padhani AR, Yarnold J, Regan J, Husband JE. Dynamic MRI of breast hardness following radiation treatment. *J Magn Reson Im* 2003; **17**: 427-34.
18. Thomas A, Fischer T, Frey H, Ohlinger R, Grunwald S, Blohmer JU, et al. Real-time elastography—an advanced method of ultrasound: First results in 108 patients with breast lesions. *Ultrasound Obstet Gynecol* 2006; **28**: 335-40.
19. Das D, Gupta M, Kaur H, Kalucha A. Elastography: the next step. *J Oral Sci* 2011; **53**: 137-41.
20. Lalitha P, Reddy MCh, Reddy KJ. Musculoskeletal applications of elastography: a pictorial essay of our initial experience. *Korean J Radiol* 2011; **12**: 365-75.
21. Alam F, Naito K, Horiguchi J, Fukuda H, Tachikake T, Ito K. Accuracy of sonographic elastography in the differential diagnosis of enlarged cervical lymph nodes: comparison with conventional B-mode sonography. *AJR Am J Roentgenol* 2008; **191**: 604-10.
22. Kangelaris GT, Kim TB, Orloff LA. Role of ultrasound in thyroid disorders. *Otolaryngol Clin North Am* 2010; **43**: 1209-27.
23. Dudea SM, Giurgiu CR, Dumitriu D, Chiorean A, Ciurea A, Botar-Jid C, Coman I. Value of ultrasound elastography in the diagnosis and management of prostate carcinoma. *Med Ultrason* 2011; **13**: 45-53.
24. Carstensen EL, Parker KJ, Lerner RM. Elastography in the management of liver disease. *Ultrasound Med Biol* 2008; **34**: 1535-46.
25. Voordeckers M, Vinh-Hung V, Lamote J, Bretz A, Storme G. Survival benefit with radiation therapy in node-positive breast carcinoma patients. *Strahlenther Onkol* 2009; **185**: 656-62.
26. Reynders T, Tournel K, De Coninck P, Heymann S, Vinh-Hung V, Van Parijs H, et al. Dosimetric assessment of static and helical TomoTherapy in the clinical implementation of breast cancer treatments. *Radiat Ther Oncol* 2009; **93**: 71-9.
27. Qiao Q, Zhou G, Ling Y. Breast volume measurement in young Chinese women and clinical applications. *Aesth Plast Surg* 1997; **21**: 362-8.
28. Kayar R, Civelek S, Cobanoglu M, Gungor O, Catal H, Emiroglu M. Five methods of breast volume measurement: a comparative study of measurements of specimen volume in 30 mastectomy cases. *Breast Cancer* 2011; **5**: 43-52.
29. Kovacs L, Eder M, Hollweck R, Zimmermann A, Settles M, Schneider A, et al. Comparison between breast volume measurement using 3D surface imaging and classical techniques. *Breast* 2007; **16**: 137-45.
30. Bulstrode N, Bellamy E, Shrotria S. Breast volume assessment: comparing five different techniques. *Breast* 2001; **10**: 117-23.
31. Findikcioglu K, Findikcioglu F, Ozmen S, Guclu T. The impact of breast size on the vertebral column: a radiologic study. *Aesth Plast Surg* 2007; **31**: 23-7.
32. Cox JD, Stetz J, Pajak TF. Toxicity criteria of the Radiation Therapy Oncology Group (RTOG) and the European Organization for Research and Treatment of Cancer (EORTC). *Int J Radiat Oncol Biol Phys* 1995; **31**: 1341-6.
33. Wratten C, Kilmurray J, Wright S, O'Brien P, Back M, Hamilton C, et al. A study of high frequency ultrasound to assess cutaneous oedema in conservatively managed breast. *Front Radiat Ther Oncol* 2002; **37**: 121-7.
34. Olivier JB, Verhaege JL, Butarelli M, Marchal F, Houvenaeghel G. Functional anatomy of the lymphatic drainage of the breast: contribution of sentinel lymph node biopsy. *Ann Chir* 2006; **131**: 608-15.
35. Estourgie SH, Nieweg OE, Olmos RA, Rutgers EJ, Kroon BB. Lymphatic drainage patterns from the breast. *Ann Surg* 2004; **239**: 232-7.
36. Hidden G, Arvy L. Remarques sur le drainage lymphatique de la glande mammaire humaine. *Bull Assoc Anat* 1973; **57**: 879-86.
37. Leduc A, Caplan I, Leduc O. Lymphatic drainage of the upper limb. Substitution lymphatic pathways. *The European Journal of Lymphology* 1993; **13**: 11-8.

# Is rectal MRI beneficial for determining the location of rectal cancer with respect to the peritoneal reflection?

Eun Joo Jung<sup>1</sup>, Chun Geun Ryu<sup>1</sup>, Gangmi Kim<sup>1</sup>, Su Ran Kim<sup>1</sup>, Sang Eun Nam<sup>1</sup>, Hee Sun Park<sup>2</sup>, Young Jun Kim<sup>2</sup>, Dae-Yong Hwang<sup>1</sup>

<sup>1</sup> Department of Surgery, Colorectal Cancer Center, Konkuk University Medical Center, Konkuk University School of Medicine, Seoul, Republic of Korea

<sup>2</sup> Department of Radiology, Konkuk University Medical Center, Konkuk University School of Medicine, Seoul, Republic of Korea

Radiol Oncol 2012; 46(4): 296-301.

Received 24 January 2012  
Accepted 12 May 2012

Correspondence to: Professor Dae-Yong Hwang, M.D., Department of Surgery, Colorectal Cancer Center, Konkuk University Medical Center; Konkuk University School of Medicine, 4-12 Hwayang-dong, Gwangjin-gu, Seoul, 143-729, Republic of Korea. Phone: +82-2-2030-5111; Fax : +82-2-2030-5112; E-mail : hwangcrc@kuh.ac.kr

Disclosure: No potential conflicts of interest were disclosed.

**Background.** An objective method for determining the location of the cancer with respect to peritoneal reflection would be helpful to decide the treatment modality for rectal cancer. This study was designed to evaluate the accuracy and usefulness of rectal MRI to determine spatial relations between the peritoneal reflection and rectal cancer and to compare these with operative findings.

**Patients and methods.** Patients that underwent a rectal cancer operation after a rectal MRI check between November 2008 and June 2010 were considered for the study. The patients that received preoperative concurrent chemoradiation or trans-anal local excision were excluded.

**Results.** Fifty-four patients constituted the study cohort. By comparing surgical and radiologic findings, the accuracy for predicting tumour location in relation to the peritoneal reflection by rectal MRI in all patients was 90.7%. In terms of tumour location in relation to peritoneal reflection, the accuracy of rectal MRI was 93.5% in patients with a tumour located above the peritoneal reflection, 90.0% in patients with a tumour located on the peritoneal reflection, and 84.6% in patients with a tumour located below the peritoneal reflection ( $p=0.061$ ). When the cohort was subdivided by gender, body mass index (BMI), operative findings, or tumour size, no significant difference was observed among subgroups.

**Conclusions.** Rectal MRI could be a useful tool for evaluating the relation between rectal cancer and peritoneal reflection especially when tumour size is less than 8cm. Rectal MRI can provide information regarding the location of rectal cancer in relation to the peritoneal reflection for treatment planning purposes.

Key words: rectal cancer; peritoneal reflection; magnetic resonance imaging (MRI)

## Introduction

Preoperative evaluations are of considerable importance for rectal cancer management, because treatment decision making is dependent on radiologic findings. Thus, neoadjuvant therapy could be determined based on preoperative clinical staging status, but it has not been determined which parts of rectal tumours should be included in such

as staging system. Some authors have suggested that considerations of height from the anal verge might have beneficial on the radiotherapy of rectal tumors.<sup>1</sup> However, measurements of distances from the anal verge are unclear because the methods devised to date, *e.g.*, digital rectal examination or even rigid sigmoidoscopy, are rather subjective.

The peritoneal reflection is a landmark used for evaluating the rectum anteriorly, and divides the



rectum into two parts, that is, the intraperitoneal and extraperitoneal regions, which are referred to considerations of the venous and lymphatic drainage systems of the rectum.<sup>2</sup> In particular, extraperitoneal rectal tumours disseminate mainly through the systemic pelvic venous and lateral lymphatic drainage systems, whereas intraperitoneal rectal tumours disseminate mainly through the superior haemorrhoidal and inferior mesenteric venous and lymphatic drainage systems.<sup>2</sup> Furthermore, Benzoni *et al.* concluded that tumour location in relation to the peritoneal reflection is a prognostic factor in rectal cancer.<sup>2</sup> In this study, it was found that extraperitoneal rectal tumours are more aggressive than intraperitoneal tumours, even when treated by neoadjuvant chemoradiotherapy before surgery, which is common approach in the treatment of rectal cancer.<sup>2,4</sup> Thus, it appears that the peritoneal reflection might be useful for the adaptation of different treatment strategies in rectal cancer. Even though the definitions of intraperitoneal and extraperitoneal locations are ambiguous in relation to the mesorectum, it may be that the use of the peritoneal reflection as a discriminating structure in the pelvic cavity enables the differentiation of the locations of rectal tumours to the intraperitoneal and extraperitoneal regions.

Reported distances from the anal verge to the peritoneal reflection are highly variable.<sup>1,5</sup> Accordingly, measurements based on this landmark cannot be used to precisely determine the location of the peritoneal reflection. We considered that if the peritoneal reflection could be clearly visualized and localized radiologically, that a more objective localization method could be devised than those based on distances from the anal verge.

Many reports have been issued on the role of magnetic resonance imaging (MRI) in rectal cancer in terms of determining circumferential margins or perirectal nodal statuses.<sup>6-8</sup> However, few reports are available on the spatial relation between rectal cancer and the peritoneal reflection as determined by rectal MRI. Therefore, the aim of this study was to evaluate the accuracy and usefulness of rectal MRI for determining the relation between rectal cancer and the peritoneal reflection with respect to operative findings.

## Materials and methods

Of the patients that underwent surgery for rectal cancer after a preoperative work-up (including rectal MRI) at the Colorectal Cancer Center, Konkuk



FIGURE 1. Sagittal view of the peritoneal reflection (red line) by rectal MRI.

University Medical Center between November 2008 and June 2010, 54 patients that did not receive preoperative concurrent chemoradiation or trans-anal local excision were included in the present study.

Rectal MRI images were reviewed by radiologists (H.S.P., and Y.J.K), on axial, sagittal, and coronal scans of T2-weighted images without clinical information. The peritoneal reflection appears as a low-signal-intensity linear structure that extends over the surface of the bladder and can be traced posteriorly to its point of attachment onto the rectum<sup>6</sup> (Figure 1). Under the consensus decision, these two radiologists determined spatial relationships between rectal cancer and the peritoneal reflection, and allocated tumour locations to the following categories; a) a location completely proximal to the peritoneal reflection, b) a location mainly at the level of the peritoneal reflection, c) a location completely distal to the peritoneal reflection (Figure 2). In addition, tumour locations were categorized as; anterior, lateral, posterior, circumferential, anterolateral, or postero lateral.

Operative findings were recorded by a colorectal surgeon (DYH), who performed all surgeries. Intraoperative tumour levels were described by the surgeon as above, on, or below the peritoneal

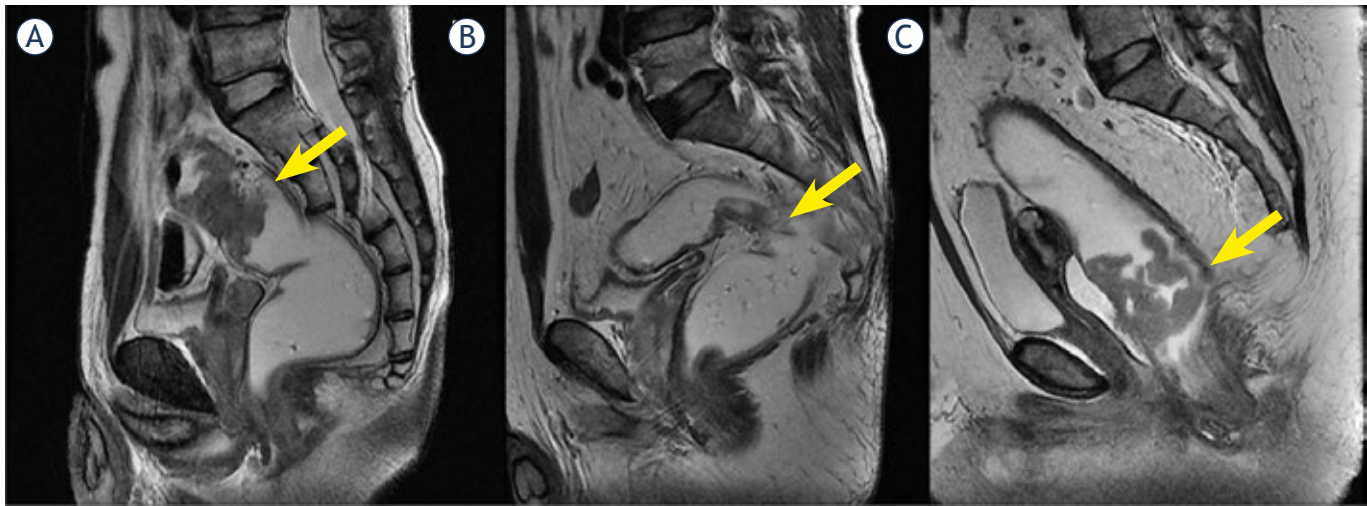


FIGURE 2. Tumour location with respect to the peritoneal reflection (PR). a. Tumour above the PR; b. tumour at the PR; c. tumour below the PR.

reflection, and as anterior, posterior, lateral, or circumferential. Tumour sizes were determined pathologically and tumours were staged according to the TNM staging system. Distances from the anal verge to lower tumour borders were determined by digital rectal examination and by sigmoidoscopy.

Body mass index (BMI) was calculated using weight (kg) divided by height (m) squared, and was divided into three groups; the low BMI group (<20 kg/m<sup>2</sup>), the normal BMI group (≥20 and <25 kg/m<sup>2</sup>), and the high BMI group (≥25 kg/m<sup>2</sup>).

Data analysis was performed using the 'Statistical Package for the Social Sciences (SPSS)' version 14.0 for Windows (SPSS, Inc. Chicago, IL). Pearson's chi-square test was used to compare locational accuracies between subgroups, and *p*-values of <0.05 were considered statistically significant.

## Results

The 54 study subjects (32 males and 22 females) had a mean age of 62.2 years. All were diagnosed with adenocarcinoma and low anterior resection was performed in 49 (90.7%) and abdominoperineal resection in 5 (9.3%). TNM tumour stage was 0 in 2 patients (3.7%), I in 11 patients (20.4%), II in 17 patients (31.5%), III in 22 patients (40.7%), and IV in 2 patients (3.7%). Mean tumour size was 4.8 cm. Patients' characteristics are summarized in Table 1.

The accuracy of predicting tumour location relative to the peritoneal reflection by rectal MRI using surgical findings as the standard in all 54 patients was 90.7% (Table 2). No significant differences

were found between gender, BMI, operative findings, and tumour size subgroups. The accuracy of predicting tumour location relative to the peritoneal reflection was 90.9% for males and 87.5% for females (*p*=0.092); for BMI, accuracies were 88.0%, 91.6%, and 86.3% in the low, normal, and high BMI subgroups, respectively (*p*=0.528).

The accuracy of rectal MRI was 93.5% in patients with a tumour located above the peritoneal reflection, 90.0% in patients with a tumour located on the peritoneal reflection, and 84.6% in patients with tumour located below the peritoneal reflection (*p*=0.061). When tumours were classified by 2 cm increments in size, accuracies were 88.9% for a tumour size of 0-1.9 cm, 91.7% for 2.0-3.9cm, 93.3% for 4.0-5.9 cm, 100% for 6.0-7.9 cm, and 57.1% for 8.0-10.0 cm (*p*=0.394), indicating that accuracy increased with tumour size until tumours exceeded 8 cm.

In terms of predicting tumour direction (anterior, lateral, and posterior), the overall accuracy of rectal MRI was 44.4%. No significant difference was observed between gender, BMI, operative findings, and tumour size subgroups. Overall, tumour directions were predicted less accurately than tumour locations (Table 3).

## Discussions

When considering treatment options for rectal cancer, preoperative evaluations are important, because decisions regarding surgery and preoperative concurrent chemoradiotherapy are dependent on tumour location, mesorectal fascia involvement,

TABLE 1. Demographics and clinical status of patients

		N=54	% (range)
Gender	M : F	32:22	59.3 : 40.7
Age(year)		62.2 ±10.8	(41-84)
Height (cm)		161.0 ± 9.6	(137 - 175)
Weight (kg)		63.4 ± 12.3	(41 - 107)
BMI (kg/m <sup>2</sup> )		23.1 ± 3.1	(17.4 – 42.3)
Proportion of high preop. CEA		18	33.3
Proportion of high preop. CA19-9		5	9.2
OP Name	LAR	49	90.7
	APR	5	9.3
Cell type (differentiation)	Well	2	3.7
	Moderately	48	88.9
	Poorly	2	3.7
	Mucinous	2	3.7
TNM stage	0	2	3.7
	I	11	20.4
	II	17	31.5
	III	22	40.7
	IV	2	3.7
Tumour size (cm)		4.8 ± 2.5	(0.9-10)
No. of retrieved LNs		24.3 ± 15.9	(3 – 87)
Distance from anal verge (cm)		8.8 ± 3.5	(1-12)

Mean ± standard deviation, BMI=body mass index, preop. = preoperative, OP=operation, LN=lymph node, LAR= low anterior resection, APR= abdomino-perineal resection.

and nodal status.<sup>6,7,9-13</sup> Rectal MRI is commonly performed preoperatively for evaluating the mesorectal fascia or adjacent organ involvement, and nodal staging.<sup>6-9</sup> However, few reports have described the clinical usefulness of rectal MRI in terms of evaluating spatial relations between rectal tumours and the peritoneal reflection.

For descriptive purposes, the rectum is divided into three parts, that is, the upper, mid, and lower thirds. The upper third is covered by peritoneum anteriorly and laterally, whereas the middle third is covered only anteriorly, and the lower third is devoid of peritoneum.<sup>9,10</sup> In Japanese classification, the rectum is also divided into three parts, designated Rs, Ra, and Rb.<sup>14</sup> The border between Ra and Rb is defined to be at the level of the peritoneal reflection, which approximately corresponds to the level of the middle Houston valve.<sup>14</sup> Thus, these classifications are based on the relation with respect to peritoneal reflection. However, it is not easy to determine the precise location of the peritoneal reflection preoperatively.

For this reason, most articles on rectal cancer define the upper rectum as 10 to 15cm from the anal verge, the mid third as 5 to 10 cm, and the lower third as < 5cm, although one author defined the upper third as 12 to 16cm from the anal verge.<sup>15</sup> However, this classification is vague and subjective, and reported distances from the anal verge based on these arbitrary divisions are not comparable.

Accordingly, we considered that the peritoneal reflection might be of use as a landmark to determine the location of the rectal subdivision for rectal cancer management. Some authors have evaluated the use of the peritoneal reflection as an anatomic landmark in rectal cancer patients. Gerdes *et al.* used trans-endorectal ultrasound (TRUS) to evaluate tumour locations with respect to the peritoneal reflection.<sup>16</sup> In this study, the indicators of an intraperitoneal location were peristalsis beyond the rectal wall or intraperitoneal fluid collection.<sup>16</sup> However, the study had two limitations, namely, that the peritoneal reflection could not be

TABLE 2. Location of rectal cancer with respect to peritoneal reflection by radiologic and operative findings

No. of case	By surgeon				
	Above PR	On PR	Below PR	Total	
By radiologists	Above PR	29	1	0	30
	On PR	2	9	2	13
	Below PR	0	0	11	11
	Total	31	10	13	54

PR = peritoneal reflection

TABLE 3. Accuracies of predicting tumour directions and locations with respect to the peritoneal reflection

	Prediction of peritoneal reflection		Prediction of tumour direction	
	Accuracy (%)	P	Accuracy (%)	P
Gender		0.092		0.561
Male (n=32)	<b>90.9</b>		43.8	
Female (n=22)	<b>87.5</b>		45.5	
BMI		0.528		0.197
Low (<20 kg/m <sup>2</sup> ) (n=7)	<b>88.0</b>		48.3	
Normal (20-25 kg/m <sup>2</sup> ) (n=36)	<b>91.6</b>		45.1	
High (> 25 kg/m <sup>2</sup> ) (n=11)	<b>86.3</b>		43.0	
Relationship with PR		0.061		0.076
Above PR (n=31)	<b>93.5</b>		38.7	
On PR (n=10)	<b>90.0</b>		66.7	
Below PR (n=13)	<b>84.6</b>		46.2	
Tumour size (cm)		0.394		0.462
0-1.9 (n=9)	<b>88.9</b>		66.7	
2.0-3.9 (n=12)	<b>91.7</b>		58.3	
4.0-5.9 (n=15)	<b>93.3</b>		46.7	
6.0-7.9 (n=11)	<b>100.0</b>		36.4	
8.0-10.0 (n=7)	<b>57.1</b>		28.6	

BMI = body mass index, PR = peritoneal reflection

found in the absence of bowel peristalsis or fluid collection, and that trans-endorectal ultrasound is a practitioner-dependent subjective procedure. Others have also evaluated the usefulness of the peritoneal reflection as a landmark in rectal cancer by comparing intraoperative rigid proctoscopy and intraoperative findings.<sup>5,17</sup> However, in these studies, data just suggested the location of peritoneal reflection or distance between the peritoneal reflection and anal verge, and in clinical practice, this data is not applicable for determining treatment plans in rectal cancer.

On rectal MR images, the peritoneal reflection appears as low-signal intensity linear structure at the junction between the rectum and the posterior aspect of the bladder in males or the vagina in females (Figure 1). In the present study, the accuracy of predicting the location of a rectal tumour with respect to the peritoneal reflection exceeded 88%. Furthermore, clinical variables examined, such as gender or BMI, had no effect on this accuracy, but when the tumour size exceeded 8 cm, accuracy fell to 57%, presumably because large tumours disrupt the normal anatomy.

In the present study, the accuracy of determining tumour direction was not high as 44.4%, probably because natural rectal folds make the interpretation of direction difficult, although near the peritoneal reflection, the accuracy of tumour direction determination was rather high. However, as tumour size increased, it became more difficult to determine tumour direction. Nevertheless, the peritoneal reflection could be used to determine directions accurately for small size tumours less than 4 cm.

In a Dutch study, it was suggested that upper third rectal cancer be treated like colon cancer<sup>18</sup>, and in a Dutch trial, no significant difference was found between a radiotherapy plus surgery group and a surgery only group in terms of local recurrence rates in upper rectal cancer.<sup>19</sup> Lopez-Kostner *et al.* suggested that treatment outcomes for rectal cancer located 10 to 15cm above the anal verge are similar to those of sigmoid colon cancer.<sup>20</sup> At this time, no complete answer can be reached regarding whether upper third rectal cancer should be treated like colon cancer or rectal cancer.<sup>15</sup> Nevertheless, recently, preoperative concurrent chemoradiotherapy has gained acceptance for the treatment of mid and lower rectal cancer.<sup>5</sup>

## Conclusions

In conclusions, we believe that subdivision of the rectum by rectal MRI based on the location of the peritoneal reflection is more objective and anatomical than previously described methods, and that the more accurate information obtained regarding anatomic relations between rectal tumours and the peritoneal reflection aids treatment planning.

## References

1. Memon S, Keating JP, Cooke HS, Dennett ER. A study into external rectal anatomy: improving patient selection for radiotherapy for rectal cancer. *Dis Colon Rectum* 2009; **52**: 87-90.
2. Benzoni E, Terrosu G, Bresadola V, Cerato F, Cojutti A, Milan E, et al. Analysis of clinical outcomes and prognostic factors of neoadjuvant chemoradiotherapy combined with surgery: intraperitoneal versus extraperitoneal rectal cancer. *Eur J Cancer Care* 2006; **15**: 286-92.
3. Lewander A, Gao J, Adell G, Zhang H, Sun XF. Expression of NF-kappa B p65 phosphorylated at serine-536 in rectal cancer with or without preoperative radiotherapy. *Radiol Oncol* 2011; **45**: 279-84.
4. Mihaylova I, Parvanova V, Velikova C, Kurteva G, Ivanova D. Degree of tumor regression after preoperative chemo-radiotherapy in locally advanced rectal cancer—Preliminary results. *Rep Pract Oncol Radiother* 2011; **16**: 237-42.
5. Yun HR, Chun HK, Lee WS, Cho YB, Yun SH, Lee WY. Intra-operative measurement of surgical lengths of the rectum and the peritoneal reflection in Korean. *J Korean Med Sci* 2008; **23**: 999-1004.
6. Brown G, Kirkham A, Williams GT, Bourne M, Radcliffe AG, Sayman J, et al. High-resolution MRI of the anatomy important in total mesorectal excision of the rectum. *AJR Am J Roentgenol* 2004; **182**: 431-9.
7. Iafrate F, Laghi A, Paolantonio P, Rengo M, Mercantini P, Ferri M, et al. Preoperative staging of rectal cancer with MR imaging: Correlation with surgical and histopathologic findings. *Radiographics* 2006; **26**: 701-14.
8. Tayler FGM, Swift RI, Blomqvist L, Brown G. A systemic approach to the interpretation of preoperative staging MRI for rectal cancer. *AJR* 2008; **191**: 1827-1835.
9. Gordon PH, Santhath Nivatvongs. *Principle and practice of surgery for the colon, rectum, and anus*. 3rd edition. New York: Informa Health Care; 2006.
10. Townsend CM, Beauchamp RD, Evers BM, Mattox K. *Textbook of surgery: The biologic basis of modern surgical practice*. 17th edition. Philadelphia: Elsevier Saunders; 2004.
11. Oblak I, Petric P, Andrejuh F, Velenik V, Fras PA. Long term outcome after combined modality treatment for anal cancer. *Radiol Oncol* 2012; **46**: 145-52.
12. Ocvirk J. Advances in the treatment of metastatic colorectal carcinoma. *Radiol Oncol* 2009; **43**: 1-8.
13. Conde S, Borrego M, Teixeira T, Teixeira R, Corbal M, Sá A, et al. Impact of neoadjuvant chemoradiation on pathologic response and survival of patients with locally advanced rectal cancer. *Rep Pract Oncol Radiother* 2010; **15**: 51-9.
14. Japanese Society for Cancer of the Colon and Rectum. *Japanese classification of colorectal carcinoma*. Tokyo: Kanehara & Co., LTD; 1997. p. 4-5.
15. Rosenberg R, Maak M, Schuster T, Becker K, Friess H, Gergler R. Does a rectal cancer of the upper third behave more like a colon or a rectal cancer? *Dis Colon Rectum* 2010; **53**: 761-70.
16. Gerdes B, Langer P, Kopp I, Bartsch D, Stinner B. Localization of the peritoneal reflection in the pelvis by endorectal ultrasound. *Surg Endosc* 1998; **12**: 1401-4.
17. Najarian MM, Belzer GE, Cogbill TH, Mathiason MA. Determination of the peritoneal reflection using intraoperative proctoscopy. *Dis Colon Rectum* 2004; **47**: 2080-5.
18. Peeters KCMJ, Marijnen CAM, Nagtegaal ID, Kranenbarg EK, Putter H, Wiggers T et al. The TME trial after a median follow-up of 6 years: increased local control but no survival benefit in irradiated patients with resectable rectal carcinoma. *Ann Surg* 2007; **246**: 693-701.
19. Kapiteijn E, Marijnen CA, Nagtegaal ID, Putter H, Steup WH, Wiggers T, et al. Preoperative radiotherapy combined with total mesorectal excision for resectable rectal cancer. *N Engl J Med* 2001; **345**: 638-46.
20. Lopez-Kostner F, Lavery IC, Hool GR, Rybicki LA, Fazio VW. Total mesorectal excision is not necessary for cancers of the upper rectum. *Surgery* 1998; **124**: 612-7.

# Potential of electrochemotherapy by intramuscular IL-12 gene electrotransfer in murine sarcoma and carcinoma with different immunogenicity

Ales Sedlar<sup>1</sup>, Tanja Dolinsek<sup>1</sup>, Bostjan Markelc<sup>1</sup>, Lara Prosen<sup>3</sup>, Simona Kranjc<sup>1</sup>, Masa Bosnjak<sup>1</sup>, Tanja Blagus<sup>1</sup>, Maja Cemazar<sup>1,2</sup>, Gregor Sersa<sup>1</sup>

<sup>1</sup> Institute of Oncology Ljubljana, Department of Experimental Oncology, Ljubljana, Slovenia

<sup>2</sup> University of Primorska, Faculty of Health Sciences, Izola, Slovenia

<sup>3</sup> Kolektor Group, Nanotesla Institute, Ljubljana, Slovenia

Radiol Oncol 2012; 46(4): 302-311.

Received 21 July 2012

Accepted 15 August 2012

Correspondence to: Prof. Gregor Serša, Institute of Oncology Ljubljana, Department of Experimental Oncology, Zaloška 2, SI-1000 Ljubljana, Slovenia. Tel./Fax: +386 1 5879 434; E-mail: gsertsa@onko-i.si

Disclosure: No potential conflicts of interest were disclosed.

**Background.** Electrochemotherapy provides good local tumor control but requires adjuvant treatment for increased local response and action on distant metastasis. In relation to this, intramuscular interleukin-12 (IL-12) gene electrotransfer, which provides systemic shedding of IL-12, was combined with local electrochemotherapy with cisplatin. Furthermore, the dependence on tumor immunogenicity and immunocompetence of the host on combined treatment response was evaluated.

**Materials and methods.** Sensitivity of SA-1 sarcoma and TS/A carcinoma cells to electrochemotherapy with cisplatin was tested *in vitro*. *In vivo*, intratumoral electrochemotherapy with cisplatin (day 1) was combined with a single (day 0) or multiple (days 0, 2, 4) intramuscular murine IL-12 (mIL-12) gene electrotransfer. The antitumor effectiveness of combined treatment was evaluated on immunogenic murine SA-1 sarcoma in A/J mice and moderately immunogenic murine TS/A carcinoma, in immunocompetent BALB/c and immunodeficient SCID mice.

**Results.** Electrochemotherapy *in vitro* resulted in a similar  $IC_{50}$  values for both sarcoma and carcinoma cell lines. However, *in vivo* electrochemotherapy was more effective in the treatment of sarcoma, the more immunogenic of the tumors, resulting in a higher log cell kill, longer specific tumor growth delay, and also 17% tumor cures compared to carcinoma where no tumor cures were observed. Adjuvant intramuscular mIL-12 gene electrotransfer increased the log cell kill in both tumor models, potentiating the specific tumor growth delay by a factor of 1.8-2 and increasing tumor cure rate by approximately 20%. In sarcoma tumors, the potentiation of the response by intramuscular mIL-12 gene electrotransfer was dose-dependent and also resulted in a faster onset of tumor cures. Comparison of the carcinoma response to the combined treatment modality in immunocompetent and immunodeficient mice demonstrated that the immune system is needed both for increased cell kill and for attaining tumor cures.

**Conclusions.** Based on the comparison of the antitumor effectiveness of electrochemotherapy to intratumoral cisplatin administration, we can conclude that the fraction of cells killed and the tumor cure rate are higher in immunogenic sarcoma tumor compared to moderately immunogenic carcinoma tumor. The tumor cell kill and cure rate depend on the immune response elicited by the destroyed tumor cells, which might depend on the tumor immunogenicity. The effect of adjuvant intramuscular mIL-12 gene electrotransfer is dependent on the amount of IL-12 in the system and the immune competence of the host, as demonstrated by the dose-dependent increase in the cure rate of SA-1 tumors after multiple intramuscular mIL-12 gene electrotransfer and in the differential cure rate of TS/A tumors growing in immunocompetent and immunodeficient mice.

Key words: IL-12; gene electrotransfer; cisplatin; electrochemotherapy; sarcoma; carcinoma; mice

## Introduction

Electrochemotherapy is an established local tumor treatment modality relying on electrically mediated transfer of drugs, such as cisplatin and bleomycin, into tumors.<sup>1,2</sup> In the clinical setting, it proved to be efficient on cutaneous and subcutaneous tumor nodules as well as on deep-seated tumors.<sup>3-6</sup> However, a major drawback of electrochemotherapy is the lack of systemic effect. With the intent of adding an efficient systemic antitumor treatment modality, adjuvant immunotherapy with different cytokines (IL-2, TNF- $\alpha$ , GM-CSF and IL-12) has already been explored.<sup>7-19</sup> Among the tested cytokines, interleukin-12 (IL-12) seems a promising one, thus it deserves further investigations on its combined use with electrochemotherapy, predominantly on its proven good local and systemic antitumor effects.<sup>19,20</sup>

Immunotherapy with IL-12 was initially investigated using recombinant proteins. However, repetitive intravenous administration resulted in toxic systemic peak concentrations.<sup>21</sup> This challenge was successfully overcome by the advent of gene therapy, enabling sustained IL-12 levels in the non-toxic range.<sup>20,22-25</sup> A safe and efficient gene transfection method is gene electrotransfer, utilizing the electric pulse application that can be performed locally on tumors, skin or in the muscle.<sup>20,26-30</sup>

IL-12 gene electrotransfer has already proved efficient in combination with electrochemotherapy.<sup>7,10,11,13</sup> The majority of studies were performed using bleomycin that was applied intratumorally together with plasmid DNA coding for IL-12, followed by electric pulse application. Synergistic antitumor effect with high tumor cure rates as well as systemic effect on metastasis were observed in murine carcinoma and melanoma, as well as in spontaneous canine tumors.<sup>7,10,11,13</sup> In the clinical setting, both bleomycin and cisplatin proved to be equally efficient for use in electrochemotherapy.<sup>6,31-33</sup> In addition, cisplatin also proved very effective in veterinary medicine, namely in the treatment of equine and canine tumors.<sup>34-36</sup> Therefore, intramuscular IL-12 gene electrotransfer was used in combination with electrochemotherapy with cisplatin and surgery for the treatment of spontaneous canine tumors, resulting in excellent tumor response.<sup>37</sup>

Based on these studies it is evident that adjuvant immunotherapy increases the antitumor response of electrochemotherapy. So far no study has indicated how the immunogenic status of the tumors affects the response rate of the tumors to electrochemotherapy with cisplatin, and our presumption

is that different immunogenicity of tumors significantly affects the cure rate of tumors.

Therefore, the aim of our study was to evaluate the antitumor effect of intratumoral electrochemotherapy with cisplatin and the potentiating effect of additional single or multiple intramuscular murine IL-12 (mIL-12) gene electrotransfer. The antitumor effectiveness was compared between immunogenic sarcoma and moderately immunogenic carcinoma tumor models, as well as the effectiveness between immunocompetent and immunodeficient mice on a carcinoma model.

## Materials and methods

### Cells, animals and tumors

Murine fibrosarcoma SA-1 (Jackson Laboratory, Bar Harbor, ME, USA) and murine mammary adenocarcinoma TS/A<sup>38</sup> cells were used for the experiments. For the *in vitro* studies, cells were grown in Advanced MEM (Gibco, Grand Island, NY, USA) supplemented with 5% fetal bovine serum (Sigma-Aldrich, St. Louis, MO, USA) in a humidified atmosphere at 37°C containing 5% CO<sub>2</sub>. The cells were routinely subcultured twice a week.

A/J and BALB/c mice were purchased from the Medical Experimental Centre, Institute of Pathology, Faculty of Medicine, University of Ljubljana (Slovenia), and SCID mice (C.B-17/IcrHanHsd-Prkdc<sup>scid</sup>) were purchased from Harlan, Italy. Mice were held in a specific pathogen-free animal colony at controlled temperature and humidity with a 12-h light/dark cycle. Food and water were provided *ad libitum*. Experiments were performed on mice of both sexes, 12-14 weeks old and weighing 20-25 g. A SA-1 fibrosarcoma tumor model (Jackson Laboratory), described in the literature as immunogenic<sup>39</sup>, was used in syngeneic A/J mice. TS/A mammary adenocarcinoma<sup>38</sup>, described in the literature as poorly, relatively or moderately immunogenic<sup>40-43</sup>, was used in syngeneic BALB/c and SCID mice. SA-1 and TS/A cell suspensions were prepared in a 0.9% NaCl solution at the final concentration of  $5 \times 10^6$  cells/ml and  $20 \times 10^6$  cells/ml, respectively. Solid subcutaneous tumors were induced in the flank of mice by subcutaneous injection of a 100  $\mu$ l suspension of tumor cells. SA-1 tumor cells were obtained from the ascitic form of the tumors in mice. When the tumors reached approximately 40-50 mm<sup>3</sup> in volume, the mice were marked and divided randomly into different experimental groups and subjected to a specific protocol. The protocols were approved by

the Ministry of Agriculture and the Environment of the Republic of Slovenia (Permission No. 34401-10/2009/6).

### Drugs

Cis-Diamminedichloroplatinum (II) (CDDP) was obtained from Pharmacia & Upjohn S.p.A. (Milan, Italy) as a crystalline powder. It was dissolved in sterile H<sub>2</sub>O at a concentration of 2 mg/ml for *in vivo* use. Further dilutions for *in vitro* experiments were performed with Advanced MEM medium.

### Plasmid DNA

Therapeutic plasmid encoding mIL-12 (pORF-mIL-12, InvivoGen, Toulouse, France) and control plasmid with the same plasmid backbone, but encoding red fluorescent protein (pORF-dsRed, constructed in our laboratory) instead of mIL-12, were prepared using the Qiagen Maxi Endo-Free Kit (Qiagen, Hilden, Germany) in accordance with the manufacturer's instructions and diluted to a concentration of 1 mg/ml.

### *In vitro* electrochemotherapy

90  $\mu$ l of cell suspension ( $22 \times 10^6$  cells/ml) was prepared in electroporation buffer (125 mmol/L saccharose, 10 mmol/L K<sub>2</sub>HPO<sub>4</sub>, 2.5 mmol/L KH<sub>2</sub>PO<sub>4</sub>, 2 mmol/L MgCl<sub>2</sub>·6H<sub>2</sub>O) at 4°C. Final cell suspension was mixed with 10  $\mu$ l of different stock concentrations of cisplatin as previously described.<sup>44</sup> While 50  $\mu$ l of the mixture served only as a control for cisplatin treatment the other 50  $\mu$ l was pipetted between two stainless-steel parallel-plate electrodes (2 mm apart) and 8 square-wave electric pulses (amplitude over distance ratio of 1300 V/cm, duration of 100  $\mu$ s and frequency of 1 Hz) were applied. These parameters were chosen because of their use in electrochemotherapy in the clinical setting.<sup>45</sup> In the present study, the same parameters were used in both *in vitro* and *in vivo* experiments, so the sensitivity of cells to cisplatin *in vitro* could be better related to the response of tumors to electrochemotherapy *in vivo*. Electric pulses were generated with the electric pulse generator GT-01 (Faculty of Electrical Engineering, University of Ljubljana, Ljubljana, Slovenia). The final cisplatin concentrations ranged from 2 to 400  $\mu$ g/ml. The cells were incubated 5 min after electroporation at room temperature, and then Advanced MEM medium was added. Subsequently, clonogenic assay was performed. The survival of cells treated with

electrochemotherapy was normalized to the survival of cells treated with electric pulses only. The experiment was performed 3-4 times for each cell line, and, in each repetition, 3 parallels were used per experimental group. From the survival curves, the IC<sub>50</sub> values were determined (cisplatin concentration required to reduce cell survival by 50%). The difference in sensitivity to cisplatin of both cell lines was calculated at the IC<sub>50</sub> level.

### *In vivo* electrochemotherapy

Mice were anesthetized with inhalation anesthesia (Isofluran, Torrex Chiesi Pharma GmbH, Viena, Austria) using an anesthesia apparatus Narkosespiromat 656 (Drägerwerk AG, Lübeck, Germany). Electrochemotherapy was performed by intratumoral injection of cisplatin (2 mg/kg), and 1 minute later 8 square-wave electric pulses (two sets of four pulses in perpendicular directions at an amplitude over distance ratio of 1300 V/cm, duration of 100  $\mu$ s and frequency of 1 Hz) were applied to the tumor.<sup>46</sup> Cisplatin dose used in the *in vivo* experiments was suboptimal to enable us an evaluation of the combined treatment effect. Pulses were delivered by Cliniporator™ (IGEA S.r.l., Carpi, Italy) using stainless-steel parallel-plate electrodes (6 mm apart). Conductive gel (Kameleon, d.o.o., Maribor, Slovenia) was used to ensure a better contact between the electrodes and the tumor.

### Gene electrotransfer

Gene electrotransfer was performed by injecting 20  $\mu$ l of plasmid DNA (20  $\mu$ g) into the muscle *tibialis cranialis* of anesthetized mice, followed immediately by an application of electric pulses to the muscle (1 pulse at an amplitude over distance ratio of 600 V/cm and duration of 100  $\mu$ s, followed by a 1-s pause and subsequent 4 pulses at an amplitude over distance ratio of 80 V/cm, duration of 100 ms and frequency of 1 Hz) using the same electrodes and conducting gel as for electrochemotherapy.<sup>47</sup>

### Treatment protocol and treatment evaluation

Based on our previous studies, intramuscular mIL-12 gene electrotransfer was performed on day 0 (right leg) for single treatment or for multiple treatments on days 0, 2 and 4 (alternating between the right and left leg).<sup>48</sup> Intratumoral electrochemotherapy with cisplatin was performed on day 1.



**TABLE 1.** IC<sub>50</sub> values for cisplatin and electrochemotherapy with cisplatin of SA-1 and TS/A cells.

GROUP	IC <sub>50</sub> (µg/ml)	
	SA-1	TS/A
Cisplatin	74.5* ± 12.1	11.8 ± 4.1
Electrochemotherapy	7.1 ± 0.4	7.5 ± 0.3

\* - Statistically significant difference ( $p < 0.001$ ) compared to all other values.

The tumor growth delay and complete response rates were used as a measure of antitumor effectiveness of the therapies. Tumors were measured in three perpendicular directions (a, b, c) every 2-4 days with a digital Vernier caliper. Tumor volume was calculated using the formula:  $V = a \times b \times c \times \pi/6$ . Tumor growth delay for each experimental group was determined as the difference in tripling time between the experimental group and the control group. Specific tumor growth delay was calculated by dividing the tumor growth delay with the tripling time of the control group. Log cell kill was calculated using the formula:  $\log_{10} \text{ cell kill} = \text{GD} / (2.096 \times \text{TT})$ , where GD is the growth delay of the experimental group, 2.096 is the number of cell triplings per log of growth and TT is the tripling time of the control group.<sup>49</sup> Response to the therapy was evaluated using the percentage of tumors that completely regressed (complete response). Mice that remained tumor-free for 100 days were termed as cured. The possible systemic side effects of single or combined therapies were determined by weighing the animals.

## Statistical analysis

SigmaPlot 12 software (Systat Software GmbH, Erkrath, Germany) was used for statistical analysis. All data were tested with the Shapiro-Wilk test for normality of distribution. The differences between mean values of experimental groups were tested using the t-test or by one-way ANOVA, followed by the Holm-Sidak test for multiple comparisons. Values of  $p < 0.05$  were considered significant.

## Results

### In vitro sensitivity to cisplatin

Sensitivity of SA-1 sarcoma and TS/A carcinoma cells to cisplatin and electrochemotherapy with cisplatin was determined *in vitro*. TS/A carcinoma cells had statistically significantly lower IC<sub>50</sub> dose

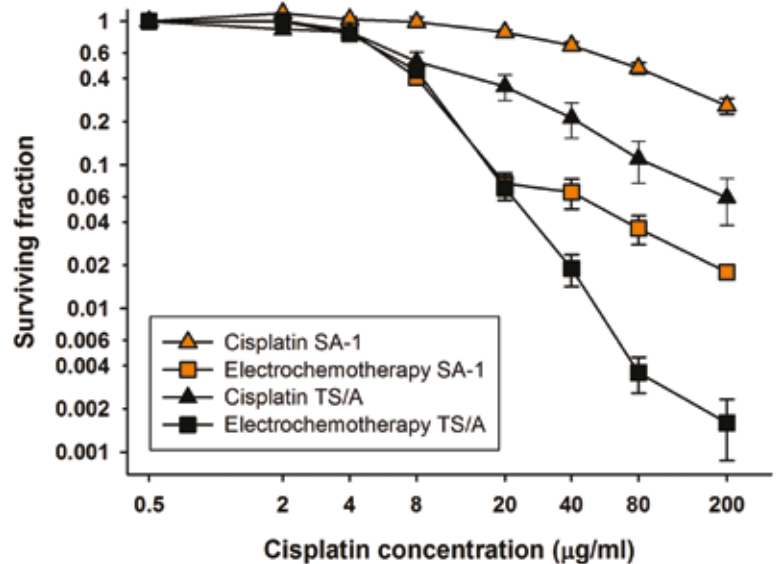


**FIGURE 1.** Cell survival of SA-1 and TS/A tumor cells after treatment with cisplatin or electrochemotherapy with cisplatin. Error bars represent standard error. Survival of cells treated with electrochemotherapy was normalized to the survival of cells treated with electric pulses alone. Survival of SA-1 and TS/A cells treated with electric pulses alone was  $0.93 \pm 0.07$  and  $0.82 \pm 0.10$  respectively.

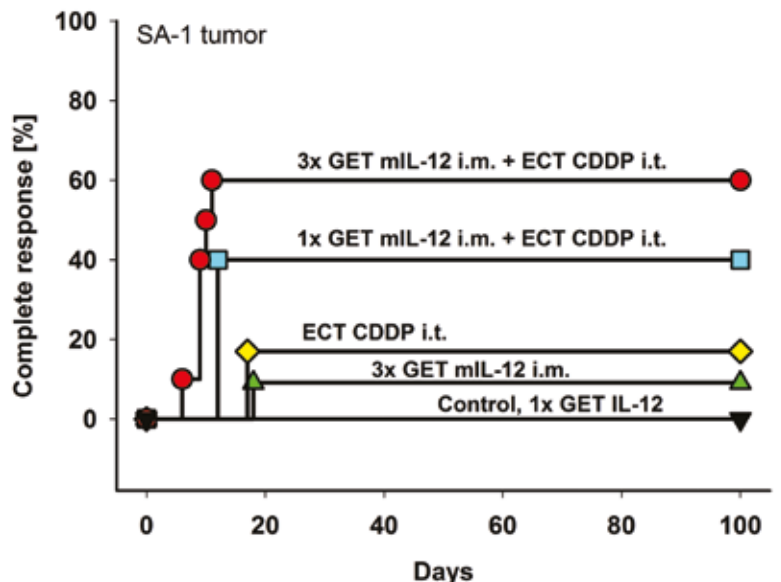


**FIGURE 2.** Complete responses of the SA-1 tumor-bearing mice after intratumoral electrochemotherapy combined with a single or multiple intramuscular mIL-12 gene electrotransfer. Gene electrotransfer was performed on day 0 for single treatment or on days 0, 2, 4 for multiple treatments. Electrochemotherapy was performed on day 1.

Abbreviations: GET mIL-12 i.m. = intramuscular mIL-12 gene electrotransfer; ECT CDDP i.t. = intratumoral electrochemotherapy with cisplatin; 1x = single therapy; 3x = multiple therapies.

**TABLE 2.** Antitumor effectiveness of electrochemotherapy combined with a single or multiple intramuscular mL-12 gene electrotransfer in murine SA-1 sarcoma.

Single gene electrotransfer					Multiple gene electrotransfer				
GROUP	TT* ± SE	SGD**	Log cell kill <sup>#</sup>	CR <sup>†</sup> (n; %)	GROUP	TT* ± SE	SGD**	Log cell kill <sup>#</sup>	CR <sup>†</sup> (n; %)
Control	3.7 ± 0.3			0					
EP	6.6 ± 0.7	0.80	0.38	0					
CDDP	10.2 ± 1.2	1.75	0.84	0					
ECT CDDP	35.5 ± 9.1	8.64	4.12	2/12 (17%)					
1x GET dsRed	4.6 ± 0.4	0.26	0.12	0	3x GET dsRed	4.7 ± 0.3	0.28	0.13	0
1x GET dsRed + ECT CDDP	38.0 ± 16.0	9.30	4.44	1/5 (20%)	3x GET dsRed + ECT CDDP	43.7 ± 11.0	10.85	5.18	2/9 (22%)
1x IL-12	4.8 ± 0.6	0.29	0.14	0	3x IL-12	4.2 ± 0.5	0.15	0.07	0
1x IL-12 + ECT CDDP	39.5 ± 14.1	9.70	4.63	1/6 (17%)	3x IL-12 + ECT CDDP	35.5 ± 9.5	8.63	4.12	1/8 (13%)
1x GET IL-12	6.8 ± 2.3	0.83	0.40	0	3x GET IL-12	16.7 ± 8.7	3.52	1.68	1/11 (9%)
1x GET IL-12 + EP	8.0 ± 1.2	1.16	0.55	0	3x GET IL-12 + EP	31.1 ± 13.5	7.43	3.55	2/12 (17%)
1x GET IL-12 + CDDP	26.7 ± 18.4	6.25	2.98	1/5 (20%)	3x GET IL-12 + CDDP	38.9 ± 13.5	9.56	4.56	3/10 (30%)
1x GET IL-12 + ECT CDDP	60.0 ± 17.3	15.28	7.29	2/5 (40%)	3x GET IL-12 + ECT CDDP	76.0 ± 8.8	19.63	9.36	6/10 (60%)

**Abbreviations:** Application of electric pulses to tumors (EP), intratumoral cisplatin injection (CDDP), intratumoral electrochemotherapy with cisplatin (ECT CDDP), intramuscular injection of plasmid DNA coding for mL-12 (IL-12), intramuscular gene electrotransfer of plasmid DNA coding for mL-12 (GET IL-12) or dsRed (GET dsRed). The combination of treatments is indicated with the "+" symbol. 1x denotes single and 3x denotes multiple therapies.

Mice per group for single therapy = 4-6; mice per group for multiple therapies = 5-11.

The first four groups were pooled from both experiments (n= 10-13).

\* Tumor tripling time - cured mice were included in the calculation with the tripling time of 100 days.

\*\* Specific tumor growth delay was calculated from tumor tripling time.

<sup>#</sup> Log cell kill was calculated from specific tumor growth delay.

<sup>†</sup> Cures were determined 100 days after treatment.

**TABLE 3.** Antitumor effectiveness of electrochemotherapy combined with intramuscular mL-12 gene electrotransfer in murine TS/A carcinoma in immunocompetent (BALB/c) and immunodeficient (SCID) mice.

Immunocompetent BALB/c mice					Immunodeficient SCID mice				
GROUP	TT* ± SE	SGD**	Log cell kill <sup>#</sup>	CR <sup>†</sup> (n; %)	GROUP	TT* ± SE	SGD**	Log cell kill <sup>#</sup>	CR <sup>†</sup> (n; %)
Control	6.1 ± 0.8			0	Control	5.3 ± 0.6			0
EP	7.1 ± 0.6	0.17	0.07	0	EP	4.7 ± 0.4	-0.12	-0.06	0
CDDP	10.7 ± 1.5	0.74	0.20	0	CDDP	7.3 ± 0.0	0.37	0.18	0
ECT CDDP	25.2 ± 2.6	3.12	1.49	0	ECT CDDP	26.9 ± 1.2	4.07	1.94	0
1x GET dsRed	6.3 ± 0.6	0.03	0.01	0	3x GET dsRed	5.1 ± 0.5	-0.04	-0.02	0
1x GET dsRed + ECT CDDP	24.1 ± 3.6	2.94	0.36	0	3x GET dsRed + ECT CDDP	31.6 ± 3.2	4.95	2.36	0
1x IL-12	7.7 ± 0.4	0.25	0.10	0	3x IL-12	5.4 ± 0.2	0.01	0.00	0
1x IL-12 + ECT CDDP	37.9 ± 8.5	5.19	2.48	1/9 (11%)	3x IL-12 + ECT CDDP	32.4 ± 5.2	5.09	2.43	0
1x GET IL-12	7.3 ± 0.6	0.20	0.08	0	3x GET IL-12	7.9 ± 1.2	0.49	0.24	0
1x GET IL-12 + EP	8.5 ± 1.0	0.40	0.14	0	3x GET IL-12 + EP	6.5 ± 1.4	0.22	0.10	0
1x GET IL-12 + CDDP	10.4 ± 1.2	0.70	0.20	0	3x GET IL-12 + CDDP	11.5 ± 2.5	1.16	0.55	0
1x GET IL-12 + ECT CDDP	45.1 ± 10.5	6.37	3.04	2/9 (22%)	3x GET IL-12 + ECT CDDP	25.5 ± 2.3	3.82	1.82	0

**Abbreviations:** Application of electric pulses to tumors (EP), intratumoral cisplatin injection (CDDP), intratumoral electrochemotherapy with cisplatin (ECT CDDP), intramuscular injection of plasmid DNA coding for mL-12 (IL-12), intramuscular gene electrotransfer of plasmid DNA coding for mL-12 (GET IL-12) or dsRed (GET dsRed).

The combination of treatments is indicated with the "+" symbol. 1x denotes single and 3x denotes multiple therapies.

BALB/c mice per group; n = 6-9

SCID mice per group; n = 2-5

\* Tumor tripling time - cured mice were included in the calculation with the tripling time of 100 days.

\*\* Specific tumor growth delay was calculated from tumor tripling time.

<sup>#</sup> Log cell kill was calculated from specific tumor growth delay.

<sup>†</sup> Cures were determined 100 days after treatment.

and were more sensitive to treatment with cisplatin alone compared to SA-1 sarcoma cells ( $p < 0.001$ ). Electrochemotherapy with cisplatin resulted in similar  $IC_{50}$  doses for both cell lines, but the survival of TS/A cells was more reduced at concentrations higher than 20  $\mu\text{g}/\text{ml}$ , indicating an effective permeabilization of a larger number of TS/A carcinoma cells (Figure 1, Table 1).

### Response to the combined treatment (electrochemotherapy and intramuscular mIL-12 gene electrotransfer) of sarcoma tumors *in vivo*

The antitumor effect of intratumoral electrochemotherapy combined with a single or multiple intramuscular mIL-12 gene electrotransfer was determined in immunogenic murine SA-1 sarcoma tumors. Single intramuscular mIL-12 gene electrotransfer potentiated the cell kill by electrochemotherapy by 3.2 log, resulting in a 23% increase in tumor cures as well as prolonged specific tumor growth delay of the remaining tumors (Figures 2,3). The potentiation of cell kill by electrochemotherapy was even more pronounced with multiple intramuscular mIL-12 gene electrotransfer, by 5.3 log, resulting in a 43% increase in tumor cures as well as statistically significant prolongation of specific tumor growth delay (Figures 2,3). Moreover, the combined treatment resulted in an earlier onset of complete responses of sarcoma tumors compared to either of the single treatments (Figure 2). Multiple intramuscular mIL-12 gene electrotransfer resulted in an earlier onset of complete responses ( $9.0 \pm 0.7$  days) than a single intramuscular mIL-12 gene electrotransfer ( $12.0 \pm 0.0$  days). The tumor response results of pertinent control groups are listed in Table 2.

### Response to the combined treatment (electrochemotherapy and intramuscular mIL-12 gene electrotransfer) of carcinoma tumors *in vivo*

The combined treatment effect was determined also for moderately immunogenic murine TS/A carcinoma tumors in immunocompetent BALB/c mice and immunodeficient SCID mice. Electrochemotherapy resulted in a cell kill of 1.5 and 1.9 log in immunocompetent and immunodeficient SCID mice, respectively (Figure 3, Table 3). Tumor cures were observed in neither immunocompetent nor immunodeficient mice and there was also no difference in the specific tumor growth

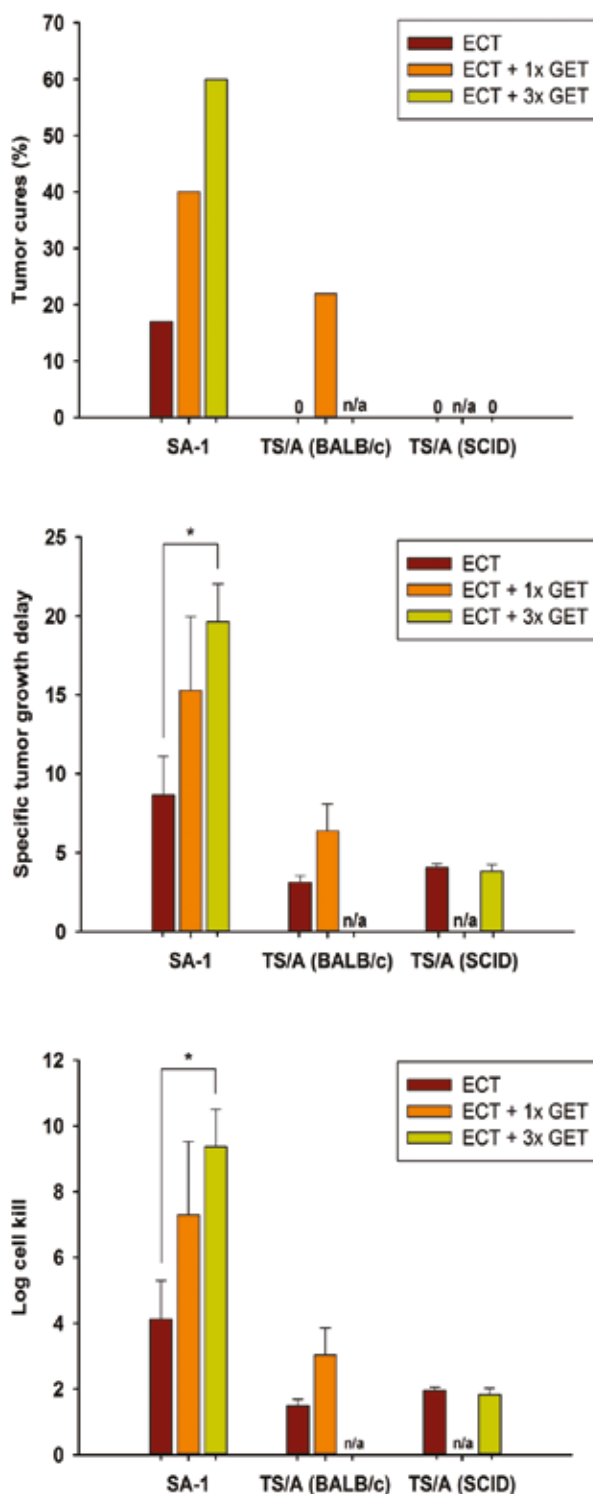


**FIGURE 3.** Tumor cures (A), specific tumor growth delay (B) and log cell kill (C) after electrochemotherapy alone or combined with a single or multiple intramuscular mIL-12 gene electrotransfer.

**Abbreviations:** ECT = intratumoral electrochemotherapy with cisplatin; GET = intramuscular mIL-12 gene electrotransfer; 1x = single therapy; 3x = multiple therapy; SA-1 = murine sarcoma; TS/A (BALB/c) = murine carcinoma transplanted on BALB/c mice; TS/A (SCID) = murine carcinoma transplanted in SCID mice; n/a = not tested; \* = statistically significant difference ( $p < 0.05$ ).

delay. In immunocompetent mice, single intramuscular mIL-12 gene electrotransfer increased the cell kill by 1.5 log, resulting in 22% of tumor cures and a prolongation of a specific tumor growth delay. In SCID mice, the log cell kill by electrochemotherapy was not increased even after multiple intramuscular mIL-12 gene electrotransfer, resulting also in zero cure rate and having no effect on the specific tumor growth delay. The tumor response results of pertinent control groups are listed in Table 3.

## Discussion

Electrochemotherapy *in vitro* resulted in similar  $IC_{50}$  values for both sarcoma and carcinoma cell lines. However, *in vivo* electrochemotherapy was more effective in the treatment of sarcoma, the more immunogenic of the tumors, resulting in a higher log cell kill, specific tumor growth delay, and also 17% tumor cures compared to carcinoma where no tumor cures were observed. Adjuvant intramuscular mIL-12 gene electrotransfer increased the tumor response of both tumor models growing in immunocompetent mice to approximately the same degree: the log cell kill by 3.2 and 1.5, the specific tumor growth delay by a factor of 1.8-2, and the tumor cure rate by approximately 20% in SA-1 and TS/A, respectively. In sarcoma tumors, the potentiation of response by intramuscular mIL-12 gene electrotransfer was dose-dependent. Comparison of the carcinoma response to the combined treatment modality in immunocompetent and immunodeficient mice demonstrates that the adaptive immune system is needed both for increased cell kill and for attaining tumor cures.

Electrochemotherapy is becoming a standard treatment in human and veterinary oncology for local tumor treatment. In human oncology, the success rate of electrochemotherapy is approximately 70% complete responses and 80% objective responses, and it is used predominantly in palliative intent for treatment of cutaneous metastasis of melanoma. Moreover, it is effective also on cutaneous metastasis of other tumor types and deep-seated tumors.<sup>1,45,50</sup> The response rate is the same in veterinary oncology, but most of the tumors are primary and of different histology.<sup>34,35</sup> Until recently, there has been no evidence-based analysis of the variability of the tumor response to electrochemotherapy, depending on the histological properties of the tumor. The study of Marty and Sersa *et al.*<sup>45</sup> has already indicated a differential response between the melanoma tumors and other tumor

types that could be more responsive. There are also some preclinical data indicating that there must be a differential response between the tumor types, but so far the underlying mechanism has not yet been determined.<sup>51,52</sup> However, a recent systematic analysis of the clinical data has indicated that the non-melanoma tumors respond better to electrochemotherapy with either bleomycin or cisplatin than melanoma tumors.<sup>53</sup> The differential response was not analyzed, but for electrochemotherapy it is presumed that the variable response could be due to different immunogenicity of the tumors, which contributes to the cure rate of the tumors.<sup>54,55</sup> So far, no study has indicated how the immunogenic status of tumors affects their response rate to electrochemotherapy with cisplatin. Our study, however, implies that the cure rate depends on the immunogenicity of the tumors; highly immunogenic sarcomas<sup>39</sup> had a 17% complete response rate, whereas the moderately immunogenic carcinoma model<sup>40-43</sup> had none. To continue, the specific tumor growth delay was longer in the sarcoma tumor model, resulting in 4.12 log cell kill, which was by 2.5 log higher compared to the carcinoma tumor with 1.5 log cell kill. The tumors received the same treatment and had the same tumor volume at the treatment time. Since there is no significant difference in the  $IC_{50}$  doses after electrochemotherapy with cisplatin between the SA-1 sarcoma and TS/A carcinoma cell lines *in vitro*, the cure rate and log cell kill should depend on the immunogenicity of the tumors. Besides tumor immunogenicity, the success of electrochemotherapy depends also on the immunocompetence of the host. A previous preclinical study has compared the effectiveness of electrochemotherapy in immunocompetent and immunodeficient mice, clearly demonstrating that, considering the complete response of the tumors, the immune response contributes to the overall response of the tumors to electrochemotherapy.<sup>56</sup>

However, besides the immune status of the organisms and tumor immunogenicity, other factors may also contribute to antitumor effectiveness. As indicated by the *in vitro* results, it is evident that the *in vitro* chemosensitivity of cells to cisplatin does not predict the tumor response to electrochemotherapy *in vivo*. Furthermore, electroporation of cells increases the cytotoxicity of the drug, in our case cisplatin, and may result in a similar cell kill *in vitro* of two differently chemosensitive cell lines, indicating that the SA-1 cells are resistant to cisplatin mainly due to the membrane-related mechanism.<sup>57</sup> Furthermore, cells have different "electrosensitivity", *i.e.*, the degree of cell

permeabilization. From cell survival curves, it can be observed that less SA-1 cells were electropermeabilized, as demonstrated by the flattening of the curve<sup>58</sup>, compared to TS/A cells, which get electropermeabilized in a much greater fraction. The *in vitro* data on tumor cells do not predict the result of *in vivo* electrochemotherapy because of its dependence on other factors; first being the degree of tumor perfusion, which may influence drug delivery to the tumors, and electrochemotherapy might also result in a vascular-disrupting effect,<sup>59</sup> and the second being controlled by physical factors, *e.g.*, electric field distribution and electrical properties of the tissue for electropermeabilization of cells in the tumors, namely tumor and stromal cells.<sup>5, 60</sup> Some reports have indicated that the disruption of tumor cells by electrochemotherapy can induce the immune response of the organism, which was demonstrated after electrochemotherapy with bleomycin on the SA-1 tumor model, the same model as used in the present study.<sup>54</sup> The importance of the immune system was demonstrated in a clinical study, where the high number of infiltrating CD8<sup>+</sup> lymphocytes assessed in the cutaneous melanoma metastasis before treatment was associated with a higher probability of a response to electrochemotherapy with bleomycin.<sup>61</sup>

Some studies have indicated that boosting the immune response of the organism with cytokines (GM-CSF, IL-2, IL-12, TNF- $\alpha$ ) can increase the response rate of the tumors to electrochemotherapy.<sup>8-14,16-18,62</sup> In our study, we have observed that the intramuscular mIL-12 gene electrotransfer successfully increases the response rate of the tumors by approximately 20% tumor cures, both in the immunogenic sarcoma and moderately immunogenic carcinoma models. The specific tumor growth delay increased by a factor of 1.8-2, indicating that the adjuvant intramuscular mIL-12 gene electrotransfer increases direct tumor cell kill achieved by electrochemotherapy, in addition to increasing the tumor cure rate. After electrochemotherapy, the effect must be exerted on the remaining tumor cells that need to be eradicated by immune surveillance. As evident in sarcoma tumors, the effect was dose-dependent; multiple intramuscular mIL-12 gene electrotransfer was more effective than a single one. This notion is supported by the results in immunodeficient mice, where the specific tumor growth delay was the same in spite of adjuvant intramuscular mIL-12 gene electrotransfer immunotherapy. In addition, the cure rate also did not increase.

Based on the comparison of the antitumor effectiveness of electrochemotherapy with intratumoral cisplatin administration, we can conclude that the fraction of killed cells and the cure rate are higher in the immunogenic sarcoma tumor, compared to the moderately immunogenic carcinoma tumor. The tumor cell kill and cure rate depend on the immune response elicited by destroyed tumor cells which, as indicated in the present study, might depend on tumor immunogenicity. The effect of the adjuvant intramuscular mIL-12 gene electrotransfer is dependent on the amount of IL-12 in the system and the immune competence of the host, as demonstrated by the dose-dependent increase in the cure rate of SA-1 tumors after multiple intramuscular mIL-12 gene electrotransfer and the differential cure rate of TS/A tumors growing in immunocompetent and immunodeficient mice.

## Acknowledgements

The authors acknowledge the financial support of the State Budget through the Slovenian Research Agency (Program No. P3-0003, Projects Nos. J3-2277 and J3-4259). Research was conducted in the scope of LEA EBAM (French-Slovenian European Associated Laboratory: Pulsed Electric Fields Applications in Biology and Medicine) and COST Action TD1104.

## References

1. Sersa G, Miklavcic D, Cemazar M, Rudolf Z, Pucihar G, Snoj M. Electrochemotherapy in treatment of tumours. *EJSO* 2008; **34**: 232-40.
2. Kranjc S, Tevz G, Kamensek U, Vidic S, Cemazar M, Sersa G. Radiosensitizing effect of electrochemotherapy in a fractionated radiation regimen in radiosensitive murine sarcoma and radioresistant adenocarcinoma tumor model. *Radiat Res* 2009; **172**: 677-85.
3. Edhemovic I, Gadzijevec EM, Breclj E, Miklavcic D, Kos B, Zupanic A, et al. Electrochemotherapy: a new technological approach in treatment of metastases in the liver. *Technol Cancer Res Treat* 2011; **10**: 475-85.
4. Heller R, Gilbert R, Jaroszeski MJ. Clinical trials for solid tumors using electrochemotherapy. *Methods Mol Med* 2000; **37**: 137-56.
5. Miklavcic D, Snoj M, Zupanic A, Kos B, Cemazar M, Kropivnik M, et al. Towards treatment planning and treatment of deep-seated solid tumors by electrochemotherapy. *Biomed Eng Online* 9: 10.
6. Sersa G, Stabuc B, Cemazar M, Miklavcic D, Rudolf Z. Electrochemotherapy with cisplatin: clinical experience in malignant melanoma patients. *Clin Cancer Res* 2000; **6**: 863-7.
7. Cutrera J, Torrero M, Shiomitsu K, Mauldin N, Li S. Intratumoral bleomycin and IL-12 electrochemogenotherapy for treating head and neck tumors in dogs. *Methods Mol Biol* 2008; **423**: 319-25.
8. Heller L, Pottinger C, Jaroszeski MJ, Gilbert R, Heller R. In vivo electroporation of plasmids encoding GM-CSF or interleukin-2 into existing B16 melanomas combined with electrochemotherapy induces long-term antitumor immunity. *Melanoma Res* 2000; **10**: 577-83.

9. Sersa G, Cemazar M, Menart V, Gaberc-Porekar V, Miklavcic D. Anti-tumor effectiveness of electrochemotherapy with bleomycin is increased by TNF-alpha on SA-1 tumors in mice. *Cancer Lett* 1997; **116**: 85-92.
10. Torrero M, Li S. Treatment of SCCVII tumors with systemic chemotherapy and Interleukin-12 gene therapy combination. *Methods Mol Biol* 2008; **423**: 339-49.
11. Torrero MN, Henk WG, Li S. Regression of high-grade malignancy in mice by bleomycin and interleukin-12 electrochemogenetherapy. *Clin Cancer Res* 2006; **12**: 257-63.
12. Mir LM, Roth C, Orlowski S, Quintin-Colonna F, Fradelizi D, Belehradec J, Jr, et al. Systemic antitumor effects of electrochemotherapy combined with histoincompatible cells secreting interleukin-2. *J Immunother Emphasis Tumor Immunol* 1995; **17**: 30-8.
13. Kishida T, Asada H, Itokawa Y, Yasutomi K, Shin-Ya M, Gojo S, et al. Electrochemo-gene therapy of cancer: intratumoral delivery of interleukin-12 gene and bleomycin synergistically induced therapeutic immunity and suppressed subcutaneous and metastatic melanomas in mice. *Mol Ther* 2003; **8**: 738-45.
14. Orlowski S, An D, Belehradec J, Jr, Mir LM. Antimetastatic effects of electrochemotherapy and of histoincompatible interleukin-2-secreting cells in the murine Lewis lung tumor. *Anticancer Drugs* 1998; **9**: 551-6.
15. Ramirez LH, Orlowski S, An D, Bindoula G, Dzodic R, Ardouin P, et al. Electrochemotherapy on liver tumours in rabbits. *Br J Cancer* 1998; **77**: 2104-11.
16. Andersen MH, Gehl J, Reker S, Geertsen P, Becker JC, thor Stratem P. Concomitant administration of interleukin-2 during therapeutic vaccinations against cancer: the good, the bad, or the evil? *J Clin Oncol* 2005; **23**: 5265-7.
17. Mir LM, Orlowski S, Poddevin B, Belehradec J, Jr. Electrochemotherapy tumor treatment is improved by interleukin-2 stimulation of the host's defenses. *Eur Cytokine Netw* 1992; **3**: 331-4.
18. Andersen MH, Gehl J, Reker S, Pedersen LO, Becker JC, Geertsen P, et al. Dynamic changes of specific T cell responses to melanoma correlate with IL-2 administration. *Semin Cancer Biol* 2003; **13**: 449-59.
19. Cemazar M, Sersa G, Pavlin D, Tozon N. Intramuscular IL-12 Electrogene Therapy for Treatment of Spontaneous Canine Tumors. In: You Y, editor. *Targets in Gene Therapy*. InTech; 2011. p. 299 - 320.
20. Cemazar M, Jarm T, Sersa G. Cancer electrogene therapy with interleukin-12. *Curr Gene Ther* 2010; **10**: 300-11.
21. Leonard JP, Sherman ML, Fisher GL, Buchanan LJ, Larsen G, Atkins MB, et al. Effects of single-dose interleukin-12 exposure on interleukin-12-associated toxicity and interferon-gamma production. *Blood* 1997; **90**: 2541-8.
22. Kang WK, Park C, Yoon HL, Kim WS, Yoon SS, Lee MH, et al. Interleukin 12 gene therapy of cancer by peritumoral injection of transduced autologous fibroblasts: outcome of a phase I study. *Hum Gene Ther* 2001; **12**: 671-84.
23. Mazzolini G, Prieto J, Melero I. Gene therapy of cancer with interleukin-12. *Curr Pharm Des* 2003; **9**: 1981-91.
24. Prijic S, Prosen L, Cemazar M, Scancar J, Romih R, Lavrencak J, et al. Surface modified magnetic nanoparticles for immuno-gene therapy of murine mammary adenocarcinoma. *Biomaterials* 2012; **33**: 4379-91.
25. Sangro B, Melero I, Qian C, Prieto J. Gene therapy of cancer based on interleukin 12. *Curr Gene Ther* 2005; **5**: 573-81.
26. Daud AI, DeConti RC, Andrews S, Urbas P, Riker AI, Sondak VK, et al. Phase I trial of interleukin-12 plasmid electroporation in patients with metastatic melanoma. *J Clin Oncol* 2008; **26**: 5896-903.
27. Heller LC, Heller R. Electroporation gene therapy preclinical and clinical trials for melanoma. *Curr Gene Ther* 2010; **10**: 312-7.
28. Teissie J, Escoffre JM, Paganin A, Chabot S, Bellard E, Wasungu L, et al. Drug delivery by electropulsation: Recent developments in oncology. *Int J Pharm* 2012; **423**: 3-6.
29. Pavlin D, Cemazar M, Coer A, Sersa G, Pogacnik A, Tozon N. Electrogene therapy with interleukin-12 in canine mast cell tumors. *Radiol Oncol* 2011; **45**: 31-9.
30. Markelc B, Bellard E, Sersa G, Pelofy S, Teissie J, Coer A, et al. In vivo molecular imaging and histological analysis of changes induced by electric pulses used for plasmid DNA electrotransfer to the skin: A study in a dorsal window chamber in mice. *J Membr Biol* 2012; **245**: 545-54.
31. Rebersek M, Cufer T, Cemazar M, Kranjc S, Sersa G. Electrochemotherapy with cisplatin of cutaneous tumor lesions in breast cancer. *Anticancer Drugs* 2004; **15**: 593-7.
32. Sersa G, Stabuc B, Cemazar M, Jancar B, Miklavcic D, Rudolf Z. Electrochemotherapy with cisplatin: potentiation of local cisplatin antitumor effectiveness by application of electric pulses in cancer patients. *Eur J Cancer* 1998; **34**: 1213-8.
33. Sersa G, Stabuc B, Cemazar M, Miklavcic D, Rudolf Z. Electrochemotherapy with cisplatin: the systemic antitumor effectiveness of cisplatin can be potentiated locally by the application of electric pulses in the treatment of malignant melanoma skin metastases. *Melanoma Res* 2000; **10**: 381-5.
34. Tamzali Y, Borde L, Rols MP, Golzio M, Lyazrhi F, Teissie J. Successful treatment of equine sarcoids with cisplatin electrochemotherapy: a retrospective study of 48 cases. *Equine Vet J* 2012; **44**: 214-20.
35. Spugnini EP, Vincenzi B, Citro G, Dotsinsky I, Mudrov T, Baldi A. Evaluation of Cisplatin as an electrochemotherapy agent for the treatment of incompletely excised mast cell tumors in dogs. *J Vet Intern Med* 2011; **25**: 407-11.
36. Tozon N, Sersa G, Cemazar M. Electrochemotherapy: potentiation of local antitumor effectiveness of cisplatin in dogs and cats. *Anticancer Res* 2001; **21**: 2483-8.
37. Cemazar M, Pavlin D, Sersa G, Tozon N. *Electrogene therapy in veterinary oncology*. In: Proceedings of the Fundamental & Applied Bioelectrics, 23-27<sup>th</sup> 2012 Norfolk, USA: an international scientific workshop. Norfolk: Old Dominion University, 2012, 94-9.
38. Nanni P, de Giovanni C, Lollini PL, Nicoletti G, Prodi G. TS/A: a new metastasizing cell line from a BALB/c spontaneous mammary adenocarcinoma. *Clin Exp Metastasis* 1983; **1**: 373-80.
39. North RJ, Neubauer RH, Huang JJ, Newton RC, Loveless SE. Interleukin 1-induced, T cell-mediated regression of immunogenic murine tumors. Requirement for an adequate level of already acquired host concomitant immunity. *J Exp Med* 1988; **168**: 2031-43.
40. Rakhmievich AL, Janssen K, Hao ZL, Sondel PM, Yang NS. Interleukin-12 gene therapy of a weakly immunogenic mouse mammary carcinoma results in reduction of spontaneous lung metastases via a T-cell-independent mechanism. *Cancer Gene Ther* 2000; **7**: 826-38.
41. Oshikawa K, Shi FS, Rakhmievich AL, Sondel PM, Mahvi DM, Yang NS. Synergistic inhibition of tumor growth in a murine mammary adenocarcinoma model by combinational gene therapy using IL-12, pro-IL-18, and IL-1 beta converting enzyme cDNA. *Proc Natl Acad Sci U S A* 1999; **96**: 13351-6.
42. Di Carlo E, Cappello P, Sorrentino C, D'Antuono T, Pellicciotta A, Giovarelli M, et al. Immunological mechanisms elicited at the tumour site by lymphocyte activation gene-3 (LAG-3) versus IL-12: sharing a common Th1 anti-tumour immune pathway. *J Pathol* 2005; **205**: 82-91.
43. Allione A, Consalvo M, Nanni P, Lollini PL, Cavallo F, Giovarelli M, et al. Immunizing and curative potential of replicating and nonreplicating murine mammary adenocarcinoma cells engineered with interleukin (IL)-2, IL-4, IL-6, IL-7, IL-10, tumor necrosis factor alpha, granulocyte-macrophage colony-stimulating factor, and gamma-interferon gene or admixed with conventional adjuvants. *Cancer Res* 1994; **54**: 6022-6.
44. Sersa G, Krzic M, Sentjurc M, Ivanusa T, Beravs K, Kotnik V, et al. Reduced blood flow and oxygenation in SA-1 tumours after electrochemotherapy with cisplatin. *Br J Cancer* 2002; **87**: 1047-54.
45. Marty M, Sersa G, Garbay J, Gehl J, Collins C, Snoj M, et al. Electrochemotherapy – An easy, highly effective and safe treatment of cutaneous and subcutaneous metastases: Results of ESOPÉ (European Standard Operating Procedures of Electrochemotherapy) study. *Eur J Cancer Suppl* 2006; **4**: 3-13.
46. Cemazar M, Milacic R, Miklavcic D, Dolzan V, Sersa G. Intratumoral cisplatin administration in electrochemotherapy: antitumor effectiveness, sequence dependence and platinum content. *Anticancer Drugs* 1998; **9**: 525-30.
47. Tevz G, Pavlin D, Kamensek U, Kranjc S, Mesojednik S, Coer A, et al. Gene electrotransfer into murine skeletal muscle: a systematic analysis of parameters for long-term gene expression. *Technol Cancer Res Treat* 2008; **7**: 91-101.

48. Tevz G, Kranjc S, Cemazar M, Kamensek U, Coer A, Krzan M, et al. Controlled systemic release of interleukin-12 after gene electrotransfer to muscle for cancer gene therapy alone or in combination with ionizing radiation in murine sarcomas. *J Gene Med* 2009; **11**: 1125-37.
49. Corbett TH, Valeriote FA. Rodent models in experimental chemotherapy. In: Kallman RF, editor. *Rodent Tumour Models in Experimental Cancer Therapy*. New York: Pergamon Press; 1987. p. 233-47.
50. Sersa G, Cufer T, Paulin SM, Cemazar M, Snoj M. Electrochemotherapy of chest wall breast cancer recurrence. *Cancer Treat Rev* 2012; **38**: 379-86.
51. Cemazar M, Miklavcic D, Sersa G. Intrinsic sensitivity of tumor cells to bleomycin as an indicator of tumor response to electrochemotherapy. *Jpn J Cancer Res* 1998; **89**: 328-33.
52. Sersa G, Cemazar M, Miklavcic D. Antitumor effectiveness of electrochemotherapy with cis-diamminedichloroplatinum(II) in mice. *Cancer Res* 1995; **55**: 3450-5.
53. Mali B, Jarm T, Snoj M, Sersa G, Miklavcic D. Antitumor effectiveness of electrochemotherapy: a systematic review and meta-analysis. *Eur J Surg Oncol* 2012, <http://dx.doi.org/10.1016/j.ejso.2012.08.016>;
54. Sersa G, Kotnik V, Cemazar M, Miklavcic D, Kotnik A. Electrochemotherapy with bleomycin in SA-1 tumor-bearing mice—natural resistance and immune responsiveness. *Anticancer Drugs* 1996; **7**: 785-91.
55. Sersa G, Cemazar M, Miklavcic D, Mir LM. Electrochemotherapy: variable anti-tumor effect on different tumor models. *Bioelectrochem Bioener* 1994; **36**: 83-7.
56. Sersa G, Miklavcic D, Cemazar M, Belehradec J, Jr., Jarm T, Mir LM. Electrochemotherapy with CDDP on LPB sarcoma: comparison of the anti-tumor effectiveness in immunocompetent and immunodeficient mice. *Bioelectrochem Bioener* 1997; **43**: 279-83.
57. Cemazar M, Miklavcic D, Mir LM, Belehradec J, Jr., Bonnay M, Fourcault D, et al. Electrochemotherapy of tumours resistant to cisplatin: a study in a murine tumour model. *Eur J Cancer* 2001; **37**: 1166-72.
58. Orłowski S, Belehradec J, Jr., Paoletti C, Mir LM. Transient electroporation of cells in culture. Increase of the cytotoxicity of anticancer drugs. *Biochem Pharmacol* 1988; **37**: 4727-33.
59. Sersa G, Jarm T, Kotnik T, Coer A, Podkrajsek M, Sentjurc M, et al. Vascular disrupting action of electroporation and electrochemotherapy with bleomycin in murine sarcoma. *Br J Cancer* 2008; **98**: 388-98.
60. Corovic S, Mir LM, Miklavcic D. In vivo muscle electroporation threshold determination: realistic numerical models and in vivo experiments. *J Membr Biol* 2012; **245**: 509-20.
61. Quaglino P, Osella-Abate S, Marengo F, Nardo T, Gado C, Novelli M, et al. FoxP3 expression on melanoma cells is related to early visceral spreading in melanoma patients treated by electrochemotherapy. *Pigm Cell Melanoma R* 2011; **24**: 734-6.
62. Mir LM, Roth C, Orłowski S, Belehradec J, Jr., Fradelizi D, Paoletti C, et al. [Potentiation of the antitumoral effect of electrochemotherapy by immunotherapy with allogeneic cells producing interleukin 2]. *C R Acad Sci III* 1992; **314**: 539-44.

# Staurosporine induces different cell death forms in cultured rat astrocytes

Janez Simenc<sup>1,2</sup>, Metoda Lipnik-Stangelj<sup>1</sup>

<sup>1</sup> University of Ljubljana, Faculty of Medicine, Ljubljana, Slovenia

<sup>2</sup> University of Maribor, Faculty of Medicine, Maribor, Slovenia

Radiol Oncol 2012; 46(4): 312-320.

Received 22 March 2012

Accepted 18 May 2012

Correspondence to: Prof. Metoda Lipnik-Štangelj, PhD, University of Ljubljana, Faculty of Medicine, Institute of Pharmacology and Experimental Toxicology, Korytkova ulica 2, SI-1000 Ljubljana, Slovenia. Phone: +386 1 543 37 70; Fax: + 386 1 543 37 71; E-mail: metoda.lipnik-stangelj@mf.uni-lj.si

Disclosure: No potential conflicts of interest were disclosed.

**Background.** Astroglial cells are frequently involved in malignant transformation. Besides apoptosis, necroptosis, a different form of regulated cell death, seems to be related with glioblastoma genesis, proliferation, angiogenesis and invasion. In the present work we elucidated mechanisms of necroptosis in cultured astrocytes, and compared them with apoptosis, caused by staurosporine.

**Materials and methods.** Cultured rat cortical astrocytes were used for a cell death studies. Cell death was induced by different concentrations of staurosporine, and modified by inhibitors of apoptosis (z-vad-fmk) and necroptosis (nec-1). Different forms of a cell death were detected using flow cytometry.

**Results.** We showed that staurosporine, depending on concentration, induces both, apoptosis as well as necroptosis. Treatment with  $10^{-7}$  M staurosporine increased apoptosis of astrocytes after the regeneration in a staurosporine free medium. When caspases were inhibited, apoptosis was attenuated, while necroptosis was slightly increased. Treatment with  $10^{-6}$  M staurosporine induced necroptosis that occurred after the regeneration of astrocytes in a staurosporine free medium, as well as without regeneration period. Necroptosis was significantly attenuated by nec-1 which inhibits RIP1 kinase. On the other hand, the inhibition of caspases had no effect on necroptosis. Furthermore, staurosporine activated RIP1 kinase increased the production of reactive oxygen species, while an antioxidant BHA significantly attenuated necroptosis.

**Conclusion.** Staurosporine can induce apoptosis and/or necroptosis in cultured astrocytes via different signalling pathways. Distinction between different forms of cell death is crucial in the studies of therapy-induced necroptosis.

Key words: astrocytes; staurosporine; necroptosis; apoptosis; reactive oxygen species; flow cytometry

## Introduction

In the central nerve system (CNS), astroglial cells are frequently involved in malignant transformation. It is believed that dysfunction of apoptosis underlies glioblastoma genesis, proliferation and resistance to chemotherapy and radiotherapy. Besides, necrosis seems to be related with glioblastoma proliferation, angiogenesis and invasion. Induction of apoptosis has not made sufficient achievements in the treatment of glioblastoma, mainly because the tumour cells are often resistant to apoptosis. Better result in this case may be

achieved by modulating the necroptosis, thus circumvent the apoptosis resistance.<sup>1</sup> The knowledge of molecular pathways, involved in different forms of cell death is therefore crucial.

Apoptosis is a well-studied form of programmed cell death, with morphological characteristics such as cell shrinkage, fragmentation of cellular organelles and nucleus. In early apoptosis plasma membrane remains largely intact however it redistributes phosphatidylserine from the cytoplasmic to the outer surface prior to any morphological changes. In late apoptosis, plasma membrane often becomes permeable, causing sec-



ondary necrosis.<sup>2,3</sup> Described changes are mostly due to the activated intracellular cysteine-proteases caspases.<sup>4</sup> In contrast, primary necrosis is morphologically characterized by swelling of the cytoplasm and cell organelles, followed by early plasma membrane ruptures. The release of intracellular content outside of the cell may induce an inflammatory response and additional cell loss. Contrary to apoptosis, primary necrosis does not involve caspases.<sup>3</sup> For long time, primary necrosis has only been considered as an unregulated, passive cell death caused by the devastating stress. However, at least a part of necrotic cells may die by necroptosis, a highly regulated form of primary necrosis.<sup>5</sup>

Apoptosis and necroptosis are rather interconnected and not entirely separated events. In different susceptible cell lines, Fas ligand or TNF- $\alpha$ , which normally activates apoptosis through the death receptors, can induce necroptosis when caspases are inhibited or deficient.<sup>6</sup> While the mechanisms of apoptosis are well known, necroptosis is not fully understood. One critical molecular regulator, mediating different cellular responses upon activation through the death receptors, is a multifunctional receptor interacting protein (RIP) which is essential for the activation of necroptosis, when caspases are inhibited.<sup>6</sup> Recent reports revealed several details of necroptotic death signalling pathway and have confirmed a critical role of RIP1 kinase in necroptosis.<sup>7,8</sup>

In the central nerve system, astroglial cells in the brain may die by apoptosis or necroptosis in different pathologies.<sup>9-11</sup> Distinction of the mechanisms of astrocytes apoptosis and necroptosis is necessary to improve our understanding of pathophysiology of neurological disorders, cancer or trauma and provide new therapy opportunities. Astroglial cell cultures have proven an appropriate *in vitro* model for studying cellular and molecular functions of astrocytes, including cell death.<sup>12</sup> Recently we have reported, that staurosporine is able to induce necroptosis in cultured astrocytes.<sup>13</sup> So far, the signalling pathways of staurosporine induced necroptosis have not been elucidated. Therefore in the present study we clarified the molecular mechanisms of necroptosis, induced by staurosporine, and compared them with apoptosis. We showed that necroptosis is caspases independent and occurs through the activation of RIP1 kinase. Furthermore, we demonstrated that the reactive oxygen species (ROS) production is increased through RIP1 kinase activity, while increased ROS is associated with necroptosis.

## Materials and methods

### Materials

L-15 Leibowitz medium, foetal bovine serum (FBS), Dulbecco's modified Eagle medium and Ham's nutrient mixture F-12 (DMEM/F12), Penicillin (10,000 IU/ml), Streptomycin (10,000 mg/ml; P/S), Dulbecco's phosphate buffered saline (PBS) were purchased from Gibco BRL, Life Technologies, Scotland. Staurosporine, 2-7-dichlorodihydrofluorescein diacetate (DCFH-DA) probe, Necrostatin-1(nec-1), and Butylated hydroxyanisole (BHA) were obtained from Sigma Chemicals, USA. The pan-caspase inhibitor (z-vad-fmk) was purchased from R&D systems, USA. Petri plates were purchased from Nunc, Germany, and tissue culture flasks were obtained from TPP, Switzerland. Annexin V-fluorescein isothiocyanate (Annexin V-FITC) and 7-Aminoactinomycin D (7-AAD) staining kit for a flow cytometry was obtained from Beckman-Coulter, USA. All flow cytometry experiments were carried out on the Quanta SC MPL flow cytometer (Beckman Coulter, USA).

### Animals

New-born Wistar rats (1-2 days old) were obtained from our own breeding colony. All animal studies were approved by the Veterinary Authority of the Republic of Slovenia (License number: 34401-80/2008/4), and performed in accordance with the EU Directive 2010/63/EU and the European Convention for the protection of vertebrate animals used for experimental and other scientific purposes (ETS 123).

### Cell cultures

Cultures of rat cortical astrocytes were prepared from the brain of new-born rats in DMEM/F12 (1:1), 10% FBS, 1% Penicillin-Streptomycin culture medium as described previously.<sup>13</sup> Cells were grown at 37°C in a humidified environment containing 10% CO<sub>2</sub> until they became confluent. When they reached confluence, the cells were used for the treatment.

### Induction of cell death and production of ROS by staurosporine

The astrocytes were treated with 10<sup>-7</sup> M staurosporine for 6 hours to induce apoptosis. After the treatment, the cells were allowed to regenerate for 22 hours in a staurosporine free medium, or

were analysed without regeneration. Similarly, the astrocytes were treated with  $10^{-6}$  M staurosporine for 3 hours to induce the production of ROS and/or necroptosis. After the treatment, the cells were allowed to regenerate for 22 hours in a staurosporine free medium, or were analysed without regeneration. The cells were trypsinized and stained for an analysis with a flow cytometer. The control cells were not exposed to staurosporine.

### Attenuation of apoptosis

The astrocytes were pre-treated with z-vad-fmk, an irreversible pan-caspase inhibitor, at  $4 \times 10^{-5}$  M concentration, for one hour. Then  $10^{-7}$  M staurosporine was added into the culture medium, and the cells were incubated for an additional 6 hours. During 22 hours regeneration, the cells were incubated in z-vad-fmk containing medium without staurosporine. The cells were also exposed only to  $4 \times 10^{-5}$  M z-vad-fmk for 24 hours.

### Attenuation of necroptosis and ROS production

The astrocytes were pre-treated with  $10^{-4}$  M nec-1, a specific RIP1 kinase inhibitor, or with  $4 \times 10^{-5}$  M z-vad-fmk, one hour before  $10^{-6}$  M staurosporine was added. Then the cells were incubated for an additional 3 hours. For the regeneration, the cells were incubated in the presence of nec-1 or z-vad-fmk for 22 hours. The cells were exposed only to  $10^{-4}$  M nec-1 for 24 hours as well. For the attenuation of ROS production, the cells were pre-treated with  $10^{-4}$  M nec-1, one hour before  $10^{-6}$  M staurosporine was added. Then the cells were incubated for additional 3 hours. For the regeneration, the cells were incubated in the presence of nec-1 for 22 hours. Additionally, to attenuate the ROS associated necroptosis, the cells were treated one hour with  $10^{-4}$  M BHA, a ROS scavenger, before  $10^{-6}$  M staurosporine was added. Then the cells were incubated for an additional 3 hours. For the regeneration, the cells were incubated in the presence of BHA for 22 hours. The cells were exposed only to  $10^{-4}$  M BHA for 24 hours as well.

### Flow cytometric analysis of a cell death and ROS production

The cells were stained simultaneously with Annexin V-FITC and 7-AAD dye according to the modified manufacturer's instructions (for details see Šimenc&Lipnik-Štangelj<sup>13</sup>). Data acquisition

was carried out using a flow cytometer. The differentiation of early apoptotic, secondary necrotic, necroptotic and viable cells was made according to their phenotype: Annexin V<sup>+</sup>/7-AAD<sup>-</sup> were considered early apoptotic, Annexin V<sup>+</sup>/7-AAD<sup>+</sup>, necroptotic, Annexin V<sup>+</sup>/7-AAD<sup>+</sup> secondary necrotic, and Annexin V<sup>-</sup>/7-AAD<sup>-</sup> viable cells. In each sample, 10.000 cells were analysed.

For the detection of ROS production, the cells were prepared according to the modified protocol.<sup>14</sup>

### Statistical analyses

Statistical analyses were made with SPSS 19 software (SPSS, Inc, USA). For each treatment and controls, ten samples from two independent groups of animals were analysed. For inhibitors toxicity (z-vad-fmk or nec-1), five samples were analysed. In the cell death experiments, data (means  $\pm$  SEM) were expressed as the percentage of cell death. For statistical comparisons, only the proportions of early apoptotic and necroptotic cells were considered. For the ROS production, data (means  $\pm$  SEM) were expressed as the percentage of DCF fluorescence. The differences between various groups were examined for a significance using the non-parametric Mann-Whitney U test. In all cases a p value of  $< 0.01$  was considered statistically significant.

## Results

### Determination of apoptosis and necroptosis

Apoptosis and necroptosis were detected by the flow cytometry dot plots (Figures 1, 2). The proportions of apoptotic and necroptotic cells were simultaneously detected with the binding of Annexin V-FITC and uptake of 7-AAD dye. The binding of Annexin V is considered independent of a cell death stimulus and specific marker of apoptosis. It precedes the loss of ability to exclude viability dyes, membrane ruptures, or occurrence of any morphological changes associated with apoptosis.<sup>15,16</sup> On the other hand, the uptake of 7-AAD dye is a specific marker of necroptosis.<sup>17</sup> However, it has been reported for the Jurkat cells with necrotic morphology, that the binding of Annexin V<sup>+</sup> precedes the formation of membrane ruptures and necrosis.<sup>6</sup> This observation suggests that secondary necrotic cells (Annexin V<sup>+</sup>/7-AAD<sup>+</sup>) may not necessarily die by apoptosis. Therefore, to avoid potential bias, secondary necrotic cells were omitted from the analyses, and only early apoptotic cells

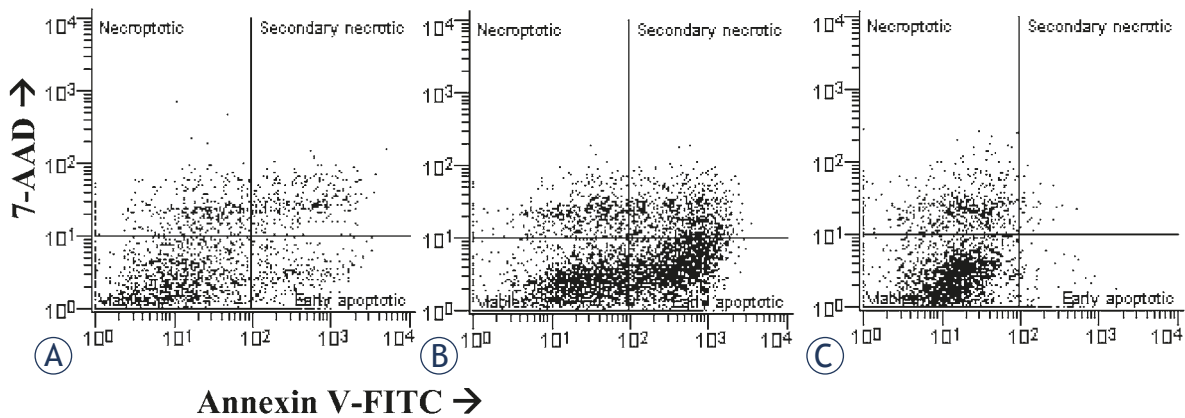


**FIGURE 1.** Examples of two-parameter flow cytometry dot plots showing simultaneous binding of Annexin V and 7-AAD uptake by cultured rat astrocytes after the induction of apoptosis. For each treatment, ten samples from two independent groups of animals were analysed. (A) Cells were not exposed to staurosporine (controls). (B) Cells were exposed to  $10^{-7}$  M staurosporine for 6 hours, and regenerated for 22 hours in a staurosporine free medium. (C) Cells were exposed to  $10^{-7}$  M staurosporine for 6 hours, and analysed without regeneration.

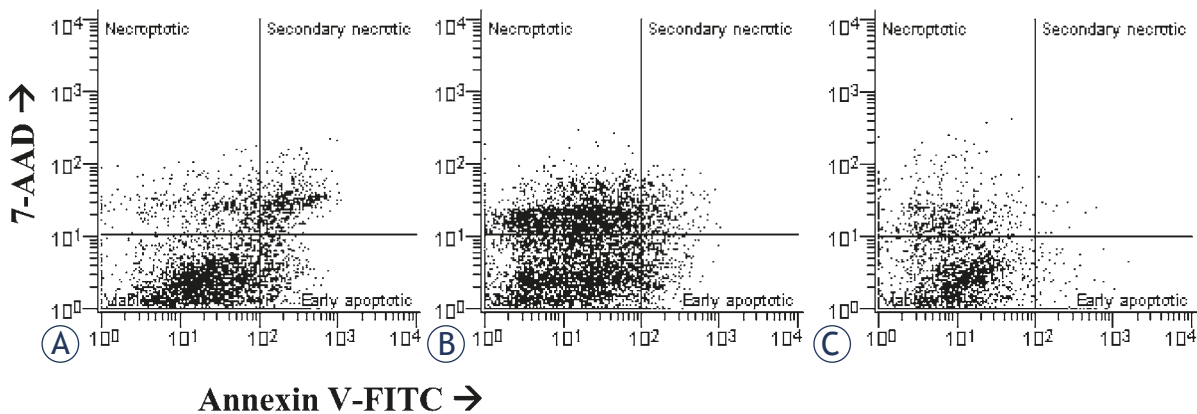


**FIGURE 2.** Examples of two-parameter flow cytometry dot plots, showing the simultaneous binding of Annexin V and 7-AAD uptake by cultured rat astrocytes after the induction of necroptosis. For each treatment, ten samples from two independent groups of animals were analysed. (A) Cells were not exposed to staurosporine (controls). (B) Cells were exposed to  $10^{-6}$  M staurosporine for 3 hours, and regenerated for 22 hours in a staurosporine free medium. (C) Cells were exposed to  $10^{-6}$  M staurosporine for 3 hours, and analysed without regeneration.

(Annexin-V<sup>+</sup> / 7-aad<sup>+</sup>) were considered apoptotic. Accordingly, only the cells with Annexin V/7-AAD<sup>+</sup> phenotype were considered as necroptotic cells, while secondary necrotic cells were omitted from the analyses.

### Induction and attenuation of apoptosis and necroptosis

For the induction of apoptosis, the cells were exposed to  $10^{-7}$  M of staurosporine for 6 hours, and regenerated for 22 hours in a staurosporine free medium. As shown in Figure 3, staurosporine increased early apoptosis approximately 5-fold in comparison to control cells, while necroptosis was not influenced. In order to confirm the induction

of apoptosis, inhibition experiments with z-vad-fmk were carried out. The results showed that inhibition of caspases by z-vad-fmk strongly reduced early apoptosis, induced by staurosporine. On the contrary, the number of necroptotic cells was slightly increased, suggesting that the cells were switched from one form of a cell death (apoptosis) to another (necroptosis) (Figure 3).

To induce necroptosis, cell cultures were exposed to  $10^{-6}$  M staurosporine for 3 hours, and regenerated as described previously. The results showed that a higher concentration of staurosporine increased the extent of necroptosis (staurosporine  $29.01 \pm 1.03\%$  vs control cells  $5.76 \pm 0.54\%$ ), whereas early apoptosis was not affected. To confirm the RIP1 kinase involvement in the transduction of the signal,

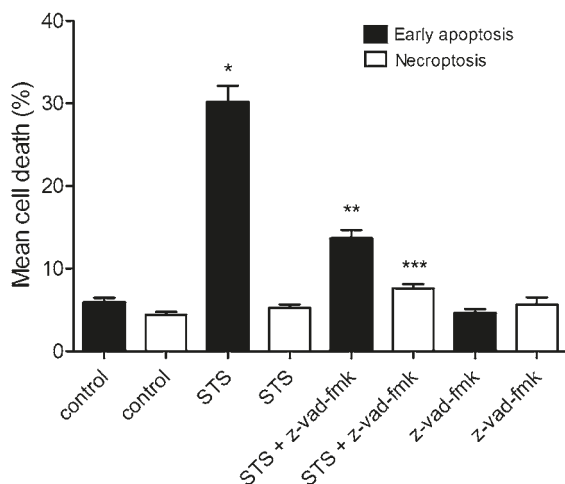


**FIGURE 3.** Percentages of a cell death in cultured rat astrocytes after the exposure to  $10^{-7}$  M staurosporine. Early apoptosis and necroptosis were determined by the binding of Annexin V-FITC and 7-AAD uptake, using a flow cytometry. Data are the means  $\pm$  SEM of ten samples from two independent groups of animals. For the z-vad-fmk treatment, only five samples were analysed. (Control) Control cells were not exposed to staurosporine or z-vad-fmk. (STS) Cells were exposed to  $10^{-7}$  M staurosporine for 6 hours, and regenerated for 22 hours in a staurosporine free medium. (STS+z-vad-fmk) Cells were exposed to staurosporine and  $4 \times 10^{-5}$  M z-vad-fmk for 6 hours, and regenerated for 22 hours in a staurosporine free medium with z-vad-fmk. (z-vad-fmk) Cells were exposed to  $4 \times 10^{-5}$  M z-vad-fmk for 24 hours. Data were analysed using the non-parametric Mann-Whitney U test; \*  $p < 0.00$  vs Control-early apoptosis, \*\*  $p < 0.00$  vs STS-early apoptosis and \*\*\*  $p = 0.002$  vs STS-necroptosis indicate significance.

we inhibited necroptosis with nec-1. The results showed that nec-1 reduced staurosporine induced necroptosis to half, while early apoptosis remained unaffected. Furthermore, z-vad-fmk did not influence necroptosis which indicating that necroptosis, induced by staurosporine, was caspases independent (Figure 4).

### Induction and attenuation of ROS production and ROS associated necroptosis

In the cultures, exposed to  $10^{-6}$  M staurosporine, the ROS accumulation was detected by DCF fluorescence. Linear amplification of the signal was observed in the staurosporine treated cells. Analyses were made by the logarithmically versus linear amplified DCF fluorescence cytometry dot plots (Figure 5). As shown in Figure 6, staurosporine increased the ROS production approx. 3-fold in comparison to control cells. Nec-1 reduced the ROS production, induced by staurosporine, to half.

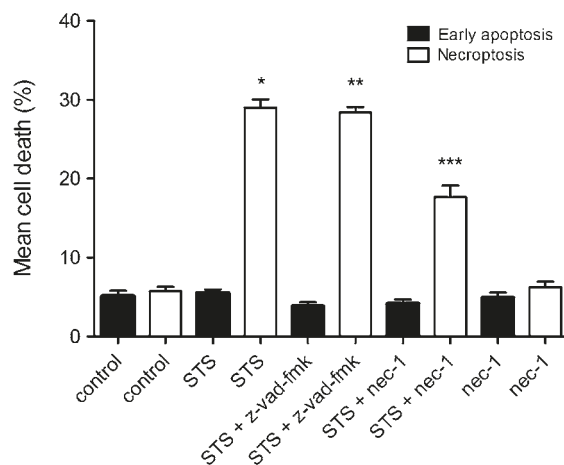


**FIGURE 4.** Percentages of a cell death in cultured rat astrocytes after the exposure to  $10^{-6}$  M staurosporine and the regeneration period. Early apoptosis and necroptosis were determined by the binding of Annexin V-FITC and 7-AAD uptake, using a flow cytometry. Data are the means  $\pm$  SEM of ten samples from two independent groups of animals. For the nec-1 treatment, only five samples were analysed. (Control) Control cells were not exposed to staurosporine or inhibitors. (STS) Cells were exposed to  $10^{-6}$  M staurosporine for 3 hours, and regenerated for 22 hours in a staurosporine free medium. (STS+z-vad-fmk) Cells were exposed to staurosporine and  $4 \times 10^{-5}$  M z-vad-fmk for 3 hours, and regenerated for 22 hours in a staurosporine free medium with the z-vad-fmk. (STS+nec-1) Cells were exposed to staurosporine and  $10^{-4}$  M nec-1 for 3 hours, and regenerated for 22 hours in a staurosporine free medium with nec-1. (nec-1) Cells were exposed to  $10^{-6}$  M nec-1 for 24 hours. Data were analysed using the non-parametric Mann-Whitney U test; \*  $p < 0.00$  vs Control-necroptosis, \*\*  $p < 0.00$  vs Control-necroptosis and \*\*\*  $p < 0.00$  vs STS-necroptosis indicate significance.

In order to show that increased ROS is associated with necroptosis, the cells were treated with  $10^{-6}$  M staurosporine in the presence of  $10^{-4}$  M BHA. As shown in Figure 7, BHA strongly reduced necroptosis, while early apoptosis was not influenced.

### Induction of a cell death without regeneration

To assess the impact of regeneration period on a cell death, the experiments without regeneration were carried out. As shown in Figure 8, in the cultures treated with  $10^{-7}$  M staurosporine for 6 hours, early apoptosis was significantly decreased, while necroptosis was increased. Similarly, in the cultures, treated with  $10^{-6}$  M staurosporine for 3 hours, early apoptosis was significantly decreased, while necroptosis was increased (Figure 8). These results indicated that regeneration of the cells is crucial for apoptosis, while it is not necessary for necroptosis.

## Discussion

Death is an important issue in cell biology. Cells may die as a part of normal development or tissue homeostasis. On the other hand, they may die when they are damaged or infected. Cell death failure may underlay tumour genesis and resistance to chemotherapy or radiotherapy.

There are various cell death forms, which are differentiated by several morphological and functional criteria.<sup>3</sup> The knowledge of the cell death mechanisms and tumorigenic properties of the cells, and development of advanced therapies is therefore a key to successful treatment.<sup>18,19</sup>

In our study we showed that staurosporine, depending on concentration, induces at least two different forms of a regulated cell death. When cultured astrocytes were exposed to  $10^{-7}$  M staurosporine, a significant proportion of early apoptotic cells was observed in comparison to the control cells, while necroptosis was not influenced (Figure 1A,B). To confirm the induction of apoptosis, inhibition experiments with z-vad-fmk, an irreversible pan-caspase inhibitor, were carried out. In the cultures, co-treated with z-vad-fmk, apoptosis was significantly attenuated. Importantly, as shown in Figure 3, necroptosis was slightly, yet significantly increased as compared to necroptosis in the staurosporine treated or control cultures. This observation suggests that staurosporine induced apoptosis and necroptosis are rather interconnected events in cultured rat astrocytes. Our results are in agreement with previously described induction of necroptosis instead of apoptosis, through the death receptors signalling, if caspases were inhibited.<sup>6</sup>

Staurosporine is widely used as a potent inducer of apoptosis. The mechanisms of apoptosis induction are diverse and may depend on the cell type.<sup>20</sup> In mouse acute lymphoid leukaemia cells L1210, various human melanoma cell types, and human breast carcinoma cells MCF-7 have been shown that staurosporine induces apoptosis through both, rapid caspases dependent, and slow, caspase independent pathway.<sup>21-23</sup> In cultured rat astrocytes, the exposure to  $10^{-7}$  M staurosporine for 3 hours has induced delayed, caspase-3 dependent apoptosis.<sup>24</sup> Our study expands these observations, as in addition to apoptosis, we induced necroptosis as well (Figure 2B). As shown in Figure 4, in the cultures exposed to a higher concentration of staurosporine, necroptosis was increased, while apoptosis was not.

Necroptosis is induced through RIP1 kinase activity.<sup>6-8</sup> In order to confirm this hypothesis, RIP1

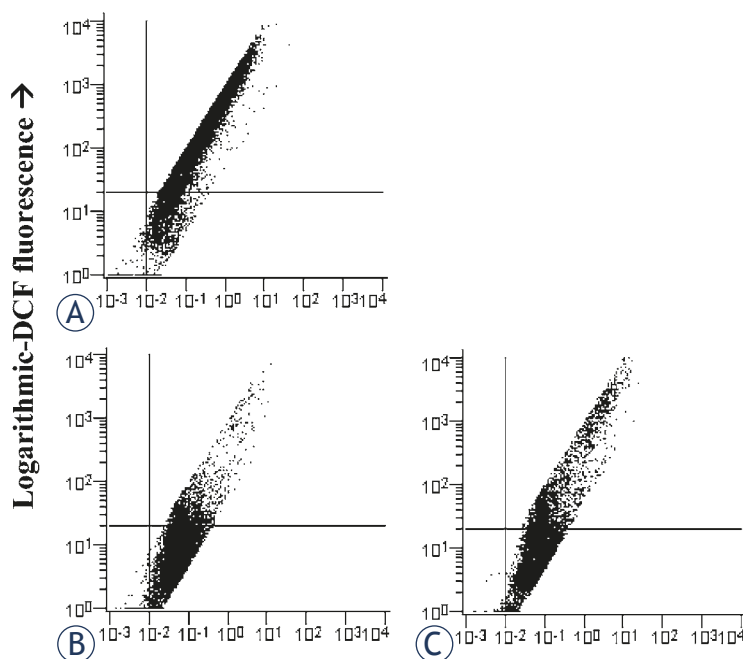


**FIGURE 5.** Detection of ROS production in cultured rat astrocytes by a flow cytometry. Examples of the forward scatter dot plots of the logarithmic versus linear amplified DCF fluorescence. Percentages of the cells from lower right quadrants were compared for the ROS production. For each treatment, ten samples from two independent groups of animals were analysed. (A) Cells were not exposed to staurosporine. (B) Cells were exposed to  $10^{-6}$  M staurosporine for 3 hours, and regenerated for 22 hours in a staurosporine free medium. (C) Cells were exposed to  $10^{-6}$  M staurosporine and  $10^{-4}$  M nec-1 for 3 hours, and regenerated for 22 hours in a staurosporine free medium with nec-1.

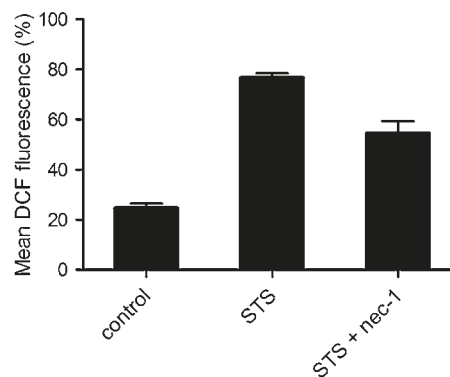


**FIGURE 6.** Production of ROS, detected as the percentage of DCF fluorescent cells. Data are the means  $\pm$  SEM of ten samples from two independent groups of animals. (Control) Cells were not exposed to staurosporine. (STS) Cells were exposed to  $10^{-6}$  M staurosporine for 3 hours, and regenerated for 22 hours in a staurosporine free medium. (STS+nec-1) Cells were exposed to  $10^{-6}$  M staurosporine and  $10^{-4}$  M nec-1, for 3 hours, and regenerated for 22 hours in a staurosporine free medium with nec-1. Data were analysed using the non-parametric Mann-Whitney U test; \*  $p < 0.00$  vs Control, \*\*  $p = 0.001$  vs STS indicate significance.

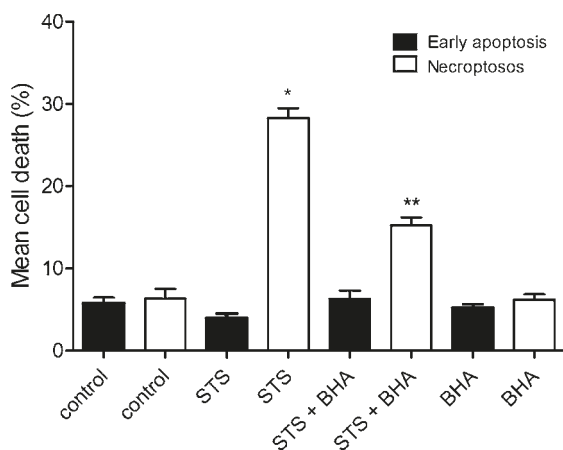


**FIGURE 7.** Percentages of a cell death in cultured rat astrocytes after the exposure to  $10^{-6}$  M staurosporine and the regeneration period. Early apoptosis and necroptosis were determined by the binding of Annexin V-FITC and 7-AAD uptake, using a flow cytometry. Data are the means  $\pm$  SEM of ten samples from two independent groups of animals. For the BHA treatment, only five samples were analysed. (Control) Control cells were not exposed to staurosporine or inhibitor. (STS) Cells were exposed to  $10^{-6}$  M staurosporine for 3 hours, and regenerated for 22 hours in a staurosporine free medium. (STS+BHA) Cells were exposed to staurosporine and  $10^{-4}$  M BHA for 3 hours, and regenerated for 22 hours in a staurosporine free medium with the BHA. (BHA) Cells were exposed to  $10^{-4}$  M BHA for 24 hours. Data were analysed using the non-parametric Mann-Whitney U test; \*  $p < 0.00$  vs CON-necroptosis, \*\*  $p < 0.00$  vs STS-necroptosis indicate significance.

kinase was inhibited by its specific inhibitor, nec-1. Indeed, in the samples, co-treated with nec-1, necroptosis was significantly attenuated, as depicted in Figure 4. Necroptosis has also been shown as caspases-independent cell death<sup>5</sup> which is in accordance with our results, where z-vad-fmk had no attenuating effect on necroptosis (Figure 4). We clearly show that the mechanism of necroptosis in cultured rat astrocytes, induced by staurosporine, is RIP1 kinase dependent and caspases independent. Apparently, at a higher concentration of staurosporine caspases play no role and astrocytes die by necroptosis. Similar results were obtained in mouse astrocytes, where necroptosis, induced by hemin, was shown RIP1 kinase dependent and caspases independent.<sup>11</sup> Taken together; necroptosis is an important form of astrocyte death, regardless of an initial stimulus.

In several cell types the reactive oxygen species (ROS) production has shown to be RIP1 kinase dependent.<sup>24,25</sup> Similarly, we found that ROS were increased in the staurosporine treated astrocytes through the RIP1 kinase activity (Figure 5), while the production of ROS was attenuated, when

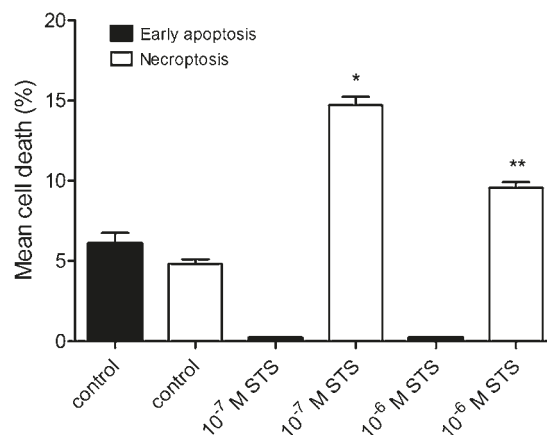


**FIGURE 8.** Percentages of a cell death in cultured rat astrocytes, induced by staurosporine, without the regeneration period. Cells were exposed either to  $10^{-7}$  M staurosporine for 6 hours, or  $10^{-6}$  M staurosporine for 3 hours, and analysed immediately. Early apoptosis and necroptosis were determined by the binding of Annexin V-FITC and 7-AAD uptake, using a flow cytometry. Data are the means  $\pm$  SEM of ten samples from two independent groups of animals. (Control) Control cells were not exposed to staurosporine. ( $10^{-7}$  M STS) Cells were exposed to  $10^{-7}$  M staurosporine. ( $10^{-6}$  M STS) Cells were exposed to  $10^{-6}$  M staurosporine. Data were analysed using the non-parametric Mann-Whitney U test; \*  $p < 0.00$  vs Control-necroptosis, \*\*  $p < 0.00$  vs Control-necroptosis indicate significance.

the cells were co-treated with nec-1 (Figure 6). Furthermore, as shown in Figure 7, necroptosis was significantly reduced, when cells were co-treated with staurosporine and an antioxidant BHA. These observations clearly indicate that increased ROS contributes to necroptosis in a staurosporine treated rat astrocytes. Similarly, necroptosis, associated with ROS, was observed in hemin treated mouse astrocytes.<sup>11</sup> It is conceivable that increased ROS production play an important role in astrocyte necroptosis.

Notably, apoptosis and necroptosis were significantly increased after a regeneration period in a staurosporine free medium. We elucidated therefore, whether regeneration is absolutely necessary. The astrocytes were exposed to different concentrations of staurosporine, and analysed without regeneration (Figures 1C, 2C). On the contrary to the experiments with regeneration, almost no apoptosis was detected, regardless of treatment, while necroptosis was already increased at  $10^{-6}$  M as well as at  $10^{-7}$  M staurosporine exposure (Figure 8). Whereas the regeneration seems not to be necessary for necroptosis, it is crucial for apoptosis. This observation indicates that the occurrence of necroptosis is much faster than of apoptosis. The later observation is in agreement with the reports

of delayed apoptosis induced by staurosporine in various cell types including astrocytes.<sup>21-23</sup> The delay in apoptosis may reflect a high resistance of astrocytes to apoptosis, which is in line with previously reported resistance of human fetal astrocytes to apoptosis, induced via cell death receptors.<sup>26</sup>

Reduced expression of different death receptors is also one of the crucial mechanisms of the resistance of glioblastoma to apoptosis.<sup>28</sup> It can occur via mutated p53 pathway, which is the most commonly mutated pathway in tumorigenesis, and is strongly connected to apoptosis and necroptosis as well.<sup>28,29</sup> Furthermore, mutation of human rat sarcoma (RAS) genes is also frequently associated with glioblastoma tumorigenesis. RAS regulates downstream mitogen-activated protein kinase (MAPK) signalling pathway and aberrant expression or defects in the RAS/MAPK pathway causes abnormal cellular activities such as invasion and cell death. Both, p53 and MAPK signalling pathways are associated with RIP1 kinase activity and necroptosis, and could be therefore important targets for glioma therapy.

In conclusion, staurosporine is able to induce two different forms of a cell death, apoptosis and necroptosis, in cultured astrocytes. Necroptosis is RIP1 kinase dependent and involves ROS production. Both cell death forms were significantly increased after the regeneration period; however increased necroptosis was already detected without regeneration. It seems that cultured astrocytes are more prone to necroptosis than apoptosis. Whether this is a general property of cultured astrocytes or it is confined to staurosporine only, requires further studies. As the demise of astrocytes is still ill understood, revealing the forms of their death may improve our understanding of the pathophysiology of various neurological disorders, malignant transformation, brain infections or traumatic brain injury. Moreover, our results may be useful in the studies of therapy-induced necroptosis in malignant transform cells. In this respect, the study provides a simple *in vitro* approach for the induction and detection of apoptosis and necroptosis in astroglial cells.

## Acknowledgement

The authors thank Mrs Cvetka Blažek for excellent technical assistance. The work was founded by the research grant P3-0067 from the Slovenian Research Agency.

## References

- Jiang YG, Peng Y, Koussougbo KS. Necroptosis: a novel therapeutic target for glioblastoma. *Med Hypotheses* 2011; **76**: 350-2.
- Taylor RC, Cullen SP, Martin SJ. Apoptosis: controlled demolition at the cellular level. *Nat Rev Cell Mol Biol* 2008; **9**: 231-41.
- Kroemer G, Galluzzi L, Vandenabeele P, Abrams J, Alnemri ES, Baehrecke EH, et al. Classification of cell death: recommendations of the Nomenclature Committee on Cell Death. *Cell Death Differ* 2009; **16**: 3-11.
- Kumar S. Caspase function in programmed cell death. *Cell Death Differ* 2007; **14**: 32-43.
- Degterev A, Huang Z, Boyce M, Li Y, Jagtap P, Mizushima N, et al. Chemical inhibitor of nonapoptotic cell death with therapeutic potential for ischemic brain injury. *Nat Chem Biol* 2005; **2**: 112-9.
- Holle N, Zaru R, Micheau O, Thome M, Attinger A, Valitutti S, et al. Fas triggers an alternative, caspase-8-independent cell death pathway using the kinase RIP as effector molecule. *Nat Immunol* 2000; **6**: 489-95.
- Cho YS, Challa S, Moquin D, Genga R, Ray TD, Guildford M, et al. Phosphorylation driven assembly of the RIP1 RIP3 complex regulates programmed necrosis and virus induced inflammation. *Cell* 2009; **137**: 1112-23.
- Zhang DW, Shao J, Lin J, Zhang N, Lu BJ, Lin SC, et al. RIP3, an energy metabolism regulator that switches TNF-induced cell death from apoptosis to necrosis. *Science* 2009; **325**: 332-6.
- Rollins S, Perkins E, Mandybur G, Zhang JH. Oxyhemoglobin produces necrosis, not apoptosis in astrocytes. *Brain Res* 2002; **945**: 41-9.
- Takuma K, Baba A, Matsuda T. Astrocyte apoptosis: implications for neuroprotection. *Prog. Neurobiol* 2004; **72**: 111-27.
- Laird MD, Wakade C, Alleyne CH, Dhandapani KM. Hemin induced necroptosis involves glutathione depletion in mouse astrocytes. *Free Radic Biol Med* 2008; **45**: 1103-14.
- Falsig J, Latta M, Leist M. Defined inflammatory states in astrocyte cultures: correlation with susceptibility towards CD95-driven apoptosis. *J Neurochem* 2004; **1**: 181-93.
- Šimenc J, Lipnik-Stangelj M. Staurosporine induces apoptosis and necroptosis in cultured rat astrocytes. *Drug Chem Toxicol* 2012; **35**: 399-405.
- Eruslanov E, Kusmartsev S. Identification of ROS using oxidized DCFDA and flow cytometry. In: Armstrong D, editor. *Advanced protocols in oxidative stress II, Methods in Molecular Biology*. New York: Humana Press; 2010. p. 57-72.
- Martin SJ, Reutelingsperger CEM, McGahon AJ, Rader JA, van Schie RCAA, LaFace DM, et al. Early redistribution of plasma membrane phosphatidylserine is a general feature of apoptosis regardless of the initiating stimulus: inhibition by overexpression of Bcl-2 and Abl. *J Exp Med* 1995; **182**: 1545-56.
- Vermes I, Haanen C, Steffens-Nakken H, Reutelingsperger C. A novel assay for apoptosis. Flow cytometric detection of phosphatidylserine expression on early apoptotic cells using fluorescein labelled Annexin V. *J Immunol Methods* 1995; **184**: 39-51.
- Schmid I, Uittenbogaart CH, Keld B, Giorgi JV. A rapid method for measuring apoptosis and dual-color immunofluorescence by single laser flow cytometry. *J Immunol Methods* 1994; **170**: 145-57.
- Todorovic V, Sersa G, Mlakar V, Glavac D, Cemazar M. Assessment of the tumorigenic and metastatic properties of SK-MEL28 melanoma cells surviving electrochemotherapy with bleomycin. *Radiol Oncol* 2012; **46**: 32-45.
- Vranic A. New developments in surgery of malignant gliomas. *Radiol Oncol* 2011; **45**: 159-65.
- Stepczynska A, Lauber K, Engels IH, Janssen O, Kabelitz D, Wesselborg S, et al. Staurosporine and conventional anticancer drugs induce overlapping, yet distinct pathways of apoptosis and caspase activation. *Oncogene* 2001; **20**: 1193-202.
- Belmokhtar CA, Hillion J, Ségal-Bendirdjian E. Staurosporine induces apoptosis through both caspase-dependent and caspase-independent mechanisms. *Oncogene* 2001; **20**: 3354-62.

22. Xue LY, Chiu SM, Oleinick NL. Staurosporine-induced death of MCF-7 human breast cancer cells: a distinction between caspase-3 dependent steps of apoptosis and the critical lethal lesions. *Exp Cell Res* 2003; **283**: 135-45.
23. Zhang XD, Gillespie SK, Hersey P. Staurosporine induces apoptosis of melanoma by both caspase dependent and independent apoptotic pathways. *Mol Cancer Ther* 2004; **3**: 187-97.
24. D'Alimonte I, Ballerini P, Nargi E, Buccella S, Giuliani P, Di Iorio P, et al. Staurosporine-induced apoptosis in astrocytes is prevented by A1 adenosine receptor activation. *Neurosci Lett* 2007; **418**: 66-71.
25. Kim SY, Morgan MJ, Choksi S, Liu ZG. TNF induced activation of the Nox 1 NADPH oxidase and its role in the induction of necrotic cell death. *Mol Cell* 2007; **26**: 675-87.
26. Song JH, Bellail A, Tse MCL, Wee Yong V, Hao C. Human astrocytes are resistant to Fas ligand and tumor necrosis factor-related apoptosis inducing ligand induced apoptosis. *J Neurosci* 2006; **26**: 3299-308.
27. Sharon Biton S, Ashkenazi A. NEMO and RIP1 control cell fate in Response to extensive DNA damage via TNF- $\alpha$  feedforward signaling. *Cell* 2011; **145**: 92-103.
28. Mao H, Lebrun DG, Yang J, Zhu VF, Li M. Deregulated signaling pathways in glioblastoma multiforme: molecular mechanisms and therapeutic targets. *Cancer Invest* 2012, **30**: 48-56.



# 5-HTTLPR polymorphism and anxious preoccupation in early breast cancer patients

Giulia Schillani<sup>1</sup>, Daniel Era<sup>1</sup>, Tania Cristante<sup>2</sup>, Giorgio Mustacchi<sup>2</sup>,  
Martina Richiardi<sup>1</sup>, Luigi Grassi<sup>3</sup>, Tullio Giraldi<sup>1</sup>

<sup>1</sup> Department of Life Sciences, University of Trieste, Trieste, Italy

<sup>2</sup> University of Trieste and Centro Sociale Oncologico, ASS1, Trieste, Italy

<sup>3</sup> Section of Psychiatry, Department of Behavior and Communication, University of Ferrara, Ferrara, Italy

Radiol Oncol 2012; 46(4): 321-327.

Received 15 October 2011

Accepted 2 February 2012

Correspondence to: Giulia Schillani, Research Assistant, Department of Life Sciences, University of Trieste, Via L. Giorgieri 7, 34127 Trieste, Italy. Phone: +39 040 558 7947 ; Fax: +39 040 577435; E-mail: gschillani@units.it

Disclosure: No potential conflicts of interest were disclosed.

**Background.** Difficulties in coping with cancer, and the accompanying anxious and depressive symptoms, have been shown to affect the mood and the quality of life in breast cancer patients. 5-Hydroxytryptamine Transporter Gene-linked Polymorphic Region (5-HTTLPR) functional polymorphism of serotonin transporter has been shown to influence the adaptation to stressful life events. The aim of this prospective study was therefore to examine the association of 5-HTTLPR with the mental adaptation to cancer diagnosis and treatment.

**Patients and methods.** Forty eight consecutive patients with early mammary carcinoma were evaluated at enrolment and at follow up after one and three months. The patients were characterized psychometrically using the Hospital Anxiety and Depression Scale (HADS) and the Mini-Mental Adjustment to Cancer Scale (Mini-MAC); 5-HTTLPR allelic variants were determined using PCR-based techniques.

**Results.** In women with early breast cancer, the mental adaptation to the disease was associated with high scores of avoidance and anxious preoccupation of Mini-MAC, which decreased with time at follow up. Anxious preoccupation decreased with time less in patients with the S/S and S/L genetic variant of 5-HTTLPR as compared with the L/L carriers ( $p=0.023$ ), indicating gene - environment interactions.

**Conclusions.** These results indicate that the characterization of 5-HTTLPR allows the identification of breast cancer patients in greater risk of mental suffering, for which specific intervention may be focused; in case of drug therapy, they provide indications for the choice of most appropriate agent in a pharmacogenetic perspective.

Key words: breast cancer; mental adjustment to cancer; depression; anxiety; 5-HTTLPR polymorphism.

## Introduction

A large literature indicates that facing a neoplastic disease is a challenging experience which deeply involves cognitive and emotional aspects of the individual.<sup>1-12</sup> Coping with cancer requires a mental adaptation to the communication of diagnosis, to the choice between the alternatives for the subsequent adjuvant treatment, and to the follow-up. Specific modalities of mental adaptation to cancer, namely hopelessness-helplessness, fighting spirit, fatalism, avoidance and anxious preoccupation,

have been shown by Greer *et al.* and Watson *et al.* to characterize the individual modalities of coping with the disease.<sup>13,14</sup> While these modalities have evident implications for the quality of life of the patients, these investigators also reported an increased risk of death in women with high scores on the hopelessness-helplessness category of the Mental Adjustment to Cancer (MAC) Scale, and also on the Hospital Anxiety and Depression Scale (HADS) category of depression.<sup>13,14</sup>

The role of the genetic polymorphism in the response to treatment and survival for oncological

patients is well known.<sup>15,16</sup> However, the genetic polymorphism of serotonin transporter (SERT) in causing an increased risk of depression in subjects who experienced stressful life events is also known and it has been initially reported by Caspi *et al.*<sup>17</sup> In the prospective-longitudinal study of a representative birth cohort, the authors tested why stressful experiences lead to depression only in some subjects. A functional polymorphism, consisting in one or two copies of the short (S) allele of the 5-HTTLPR (5-Hydroxytryptamine Transporter Gene-linked Polymorphic Region) in the promoter region of the SERT gene, was found to increase the influence of stressful life events on the development of depression, representing gene - environment interactions.<sup>17</sup> A large number of investigations have subsequently examined the associations of the development of mental disorders in a variety of psychological and psychiatric conditions with SERT polymorphism, evaluating the role played by the allelic variants of 5-HTTLPR, which are endowed with high (L/L) or low (S/S, S/L) functional activity and have a high penetrance in the populations examined.<sup>18</sup>

The most frequent oncological disease in women is breast cancer<sup>19,20</sup> and the communication of breast cancer diagnosis, as well as the treatments subsequently performed, has been shown to be a constellation of significant stressful events, requiring adequate psychological adaptation by patients.<sup>1-5</sup> Different modalities of mental adaptation to cancer have been identified<sup>6</sup>, and may affect the quality of life<sup>7-12</sup> and even the prognosis of the disease.<sup>21</sup> The mental adjustment to cancer has been extensively investigated by Greer *et al.* in terms of the coping strategies adopted by patients.<sup>13</sup> An initial prospective study of subjects with early breast cancer showed that the disease free survival at five years was significantly more frequent among those women who initially reacted by denial or fighting spirit, rather than by stoic acceptance or feelings of helplessness and hopelessness.<sup>13</sup> In a larger cohort subsequently examined, helplessness-hopelessness identified using the MAC scale, and depression measured by the HADS scale, were shown to be significant prognostic factors for the decreased survival.<sup>14</sup>

The aim of the present prospective study has been therefore to examine in women with early breast cancer the role of 5-HTTLPR polymorphism in relation to mental adaptation to cancer, and to depression and anxiety. A group of women who had received the diagnosis of mammary carcinoma, and had been treated with surgery and adjuvant therapy, has been genotypically characterized for 5-HTTLPR. The presence of the functional A>G

variation within the L allele of SERT polymorphism, which has been reported to modulate the role of 5-HTTLPR for depression<sup>22,23</sup>, has been also examined. At the time of recruitment and at follow-up one and three months later, these patients were psychometrically characterized using Mini-MAC for evaluating their mental adaptation to cancer, and HADS for assessing depression and anxiety. The data obtained have been analyzed in order to identify the occurrence of associations between the psychometric variables obtained and the patients' 5-HTTLPR genotypic characteristics of the patients; the results obtained are hereafter reported.

## Patients and methods

The study population consisted of women who received a diagnosis of mammary carcinoma, and who were referred to the Centro Sociale Oncologico, Azienda Servizi Sanitari 1, Trieste, Italy, between February 2008 and August 2009. The patients were recruited after the communication of the cancer diagnosis and surgery and before the beginning of adjuvant treatment (average time 135±9.7 days), and were evaluated at enrolment into the study (T0), and at follow up one (T1) and three (T2) months later.

The study was carried out in accordance with the Declaration of Helsinki and Good Clinical Practice Guidelines, after having been approved by the relevant institutional Ethical Committee, and having received the informed consent by each participant. Conflicts of interest do not appear to exist according to the statements of the authors.

The subjects were characterized psychometrically by a trained psychologist using the Hospital Anxiety and Depression Scale (HADS)<sup>24</sup>, and the Mini Mental Adjustment to Cancer Scale (Mini-MAC)<sup>10</sup> to examine the mechanisms of psychological adaptation to the disease. HADS is a 14-item questionnaire measuring anxiety (7 items) and depression (7 items), and is designed for the use in medical outpatients. HADS has been used in general psychiatry<sup>25</sup> and in cancer settings indicating its usefulness, reliability and validity. The Mini-MAC is a 29-item questionnaire measuring patients' coping with cancer (fighting spirit, avoidance, hopelessness, anxious preoccupation and fatalism) The Mini-MAC was chosen as the primary outcome measure and the validated Italian version of mini-MAC was employed in this study.<sup>10,11</sup>

The patients were also characterized for the 5-HTTLPR polymorphism as described below.

Subjects older than 75 years, and those with a previous history of psychopathology such as psychotic or endogenous major depressive disorder, were not included in the study. For each patient, the demographic, as well as the previous and current medical history, were recorded for the later analysis.

Genomic DNA was obtained from whole blood or buccal cells, using standard procedures (MasterAmp™ buccal swab brushes, Epicentre Technologies; GenElute™ blood Genomic DNA Kit, Sigma).

Polymerase chain reaction (PCR) amplification of the DNA region of 5-HTTLPR was performed using the primers described by Gelernter *et al.*<sup>26</sup>, and with the GC-Rich PCR System (Roche Molecular Biomedicals) in a 50- $\mu$ L reaction containing 20-100 ng of DNA; 100  $\mu$ m deoxyribonucleoside triphosphate (dNTPs), 20 pmol for each primer, and 1.5 mM MgCl<sub>2</sub>. DNA was denatured at 95°C for 10 min and subjected to 40 cycles of 40s denaturation at 94°C, 45s annealing at 56°C, 40s extension at 72°C, and 10 min final extension at 72°C. The products of PCR amplification were separated on a 2% agarose gel, and were visualised in ultraviolet light after ethidium bromide staining.

The presence of the functional A>G variation in the long (L) allele identified by Hu *et al.*<sup>23</sup> as the La and Lg alleles, was also evaluated by digestion of the PCR products with the Hpa II enzyme. The digested mixture was size-fractionated on agarose gel and visualised in ultraviolet light after ethidium bromide staining.

A statistical analysis was carried out using descriptive statistic, Pearson correlation and Analysis of Variance (ANOVA) to characterize the sample and to evaluate the relationships of the psychometric scales scores as a function of follow-up time and of 5-HTTLPR genotypic variants, using the SPSS 13.0 package (SPSS Inc. Chicago, IL, USA), as indicated in the Tables. Statistical significance was set at the  $p < 0.05$  level.

## Results

The patients' socio-demographic data and clinical characteristics are illustrated in Table 1. The patients considered were initially subjected at recruitment to psychometrical evaluation (T0: N=48), and were re-tested psychometrically at follow up one month after recruitment (T1: N=48); a third evaluation (T2: N=35) three months after T0 could be performed on 35 (72.9%) of the initial 48 patients.

The allelic variants of 5-HTTLPR polymorphism of the subjects considered are shown in Table 2.

TABLE 1. Socio-demographic and clinical characteristics of the patients

	Patients N = 48
<b>SOCIO-DEMOGRAPHIC CHARACTERISTICS</b>	
Age (mean $\pm$ S.E.)	60.2 $\pm$ 1.33
Min-max	37 - 73
30-39	1 (2.1%)
40-49	8 (16.7%)
40-59	7 (14.6%)
60-69	27 (56.3%)
70-79	5 (10.4%)
<b>Employment status</b>	
Employed	16 (33.3%)
Unemployed	9 (18.8%)
Retired	23 (47.9%)
<b>Marital status</b>	
Married	34 (70.8%)
Single	2 (4.2%)
Divorced/Separated	3 (15.8%)
Widowed	8 (16.7%)
<b>Education completed</b>	
Primary school	7 (14.6%)
Secondary school	12 (25.0%)
Professional school	9 (18.8%)
High school	20 (41.7%)
<b>CLINICAL CHARACTERISTICS</b>	
<b>Grading</b>	
1	7 (14.6%)
2	31 (64.6%)
3	10 (20.8%)
<b>Disease stage</b>	
-	1 (2.1%)
I	23 (47.9%)
II	20 (41.7%)
III	4 (8.3%)
<b>Surgery</b>	
No surgery	2 (4.2%)
Tumorectomy	1 (2.1%)
Quadrantectomy	34 (70.8%)
Mastectomy	11 (22.9%)
<b>Treatment</b>	
Chemotherapy	16 (33.3%)
Radiation therapy	36 (75%)
Hormonal therapy	34 (70.8%)
Biological therapy	0

TABLE 2. 5-HTTLPR allelic variants of the patients

	Allelic variant	Functionality*	N	%
5-HTTLPR	"short" (S)	Low	3	6.3
	"short-long" (S/L)	Low	26	54.2
	"long" (L/L)	High	19	39.6

\*The functional activity is classified as indicated by Lesch (Lesch et al., 1996)

None of the patients had an Lg allele; the genotypic distribution for 5-HTTLPR did not significantly differ from the Hardy-Weinberg equilibrium ( $\chi^2=2.30$ ;  $p=0.13$ ).

The psychometric measures performed were initially analyzed to determine the possible existence of difference attributable to the socio-demographic and clinical characteristics of the patients. When the scores of subscale employed were stratified for age, employment and marital status, education, disease stage and treatment, no significant differences were observed at recruitment (T0). Six out of 48 patients were receiving at recruitment an antidepressant treatment which had been prescribed before recruitment into this study, and 12 patients were treated with benzodiazepines. These groups displayed at T0 and T1 scores for depression (HADS) higher than the untreated ones; in both cases, the difference was not significant also when examined at follow up. Any reduction with time of anxiety and depression observed during the present study cannot consequently be ascribed to differences existing at recruitment, and to the drug treatments performed.

The data obtained using Mini-MAC are reported in Table 3. The scores of Mini-MAC sub-scale for anxious preoccupation displayed a decrease with time of follow up, and the analysis with ANOVA showed a significant effect of time ( $F=5.646$ ,  $df=2.128$ ,  $p=0.004$ ) and genotype ( $F=5.296$ ,  $df=2.128$ ,  $p=0.023$ ). For Mini-MAC avoidance scores, ANOVA showed a significant effect of time only ( $F=3.107$ ,  $df=2.128$ ,  $p=0.048$ ).

The psychometric scores obtained using HADS at T0, T1 and T2 are illustrated in Table 4. For both HADS subscales, no statistically significant effects of time and genotype were observed.

## Discussion

The initial findings of Caspi *et al.* on the role played by the 5-HTTLPR genetic polymorphism of serotonin transporter in modulating the appear-

ance of depression after stressful life-events was initially not supported by the results of the meta-analysis performed in 2009 by Riesch *et al.*<sup>27</sup>, and by Munafò *et al.*<sup>28</sup> Moreover, Middeldorp *et al.*, in a study conducted on series of twins, were unable to demonstrate any significant interaction between 5-HTTLPR polymorphism and the number of life events experienced across the life span or the year preceding the depressive episode.<sup>29</sup> A subsequent meta-analysis, where the small number of studies previously considered was increased has been recently published, provided support, in contrast to the results of the these earlier studies, for the hypothesis that 5-HTTLPR influences the relationship between stress and depression.<sup>30</sup>

The aim of the present study was that to examine in cancer patients the role of 5-HTTLPR in the mental adaptation to the disease, where diagnosis and treatment were considered to be the stressful life events requiring adequate coping by the patients. When the role of 5-HTTLPR in relation to mental adaptation to cancer has been examined by us in a recent previous occasion previously, the baseline HADS and mini-MAC scores measured at recruitment in a different sample of women with early breast cancer were found not to depend on the genetic polymorphism of serotonin transporter.<sup>31</sup>

The evaluation of the patients' conditions at first assessment (T0) indicates no significant difference in the score of any of the psychometric scales employed when the patients are grouped according to their SERT genotypic variant. An improvement with time, not dependent on 5-HTTLPR, appeared for the avoidance scores of Mini-Mac. The results presented here also indicate that the scores of anxious preoccupation, as identified using Mini-MAC, significantly depended on the genotype of SERT. Moreover, a gene - environment interaction appears for the anxious preoccupation scores, which significantly decreased with the time of follow up, in a way more pronounced in the group of patients carriers of the L/L genetic variant as compared with the carriers of at least one S allele ( $r^2=0.17$  *v.s.*  $r^2=0.04$ ,  $p=0.002$ ). The enrolled women were further characterized for the L and S variants of 5-HTTLPR genetic polymorphism, also considering the triallelic 5-HTTLPR classification; none of the patients presently investigated had an Lg allele, which is not further considered.

These results support the view that anxious preoccupation plays a significant role in patients with non advanced breast cancer during the early phase of the treatment of the disease. In this connection, several studies showed that an increased anxious

TABLE 3. Subscale scores of MINI-MAC in relation to time and 5-HTTLPR genotype

	Allelic variants	T0 mean±SEM	T1 mean±SEM	T2 mean±SEM	Effect of Time p <sup>a</sup>	Effect of genotype p <sup>b</sup>
<b>Hopelessness- Helplessness</b>	S/S-S/L-L/L	11.94±0.58 (N=48)	11.67±0.53 (N=48)	11.06±0.64 (N=35)	.581	.692
	S/S-S/L	11.86±0.71 (N=29)	11.62±0.72 (N=29)	11.63±1.06 (N=19)	.969	
	L/L	12.05±1.01 (N=19)	11.74±0.78 (N=19)	10.38±0.61 (N=16)	.353	
<b>Fighting spirit</b>	S/S-S/L-L/L	14.17±0.37 (N=48)	14.25±0.28 (N=48)	14.20±0.47 (N=35)	.986	.455
	S/S-S/L	14.17±0.40 (N=29)	14.28±0.32 (N=29)	14.68±0.57 (N=19)	.698	
	L/L	14.16±0.71 (N=19)	14.21±0.52 (N=19)	13.63±0.78 (N=16)	.803	
<b>Fatalism</b>	S/S-S/L-L/L	9.35±0.35 (N=48)	9.04±0.32 (N=48)	8.94±0.31 (N=35)	.663	.520
	S/S-S/L	9.14±0.43 (N=29)	8.97±0.43 (N=29)	8.95±0.44 (N=19)	.942	
	L/L	9.68±0.61 (N=19)	9.16±0.49 (N=19)	8.94±0.44 (N=16)	.595	
<b>Anxious preoc- cupation</b>	S/S-S/L-L/L	15.71±0.70 (N=48)	13.50±0.65 (N=48)	12.51±0.67 (N=35)	.004	.023
	S/S-S/L	16.31±0.96 (N=29)	13.72±0.86 (N=29)	14.21±0.96 (N=19)	.102	
	L/L	14.79±0.99 (N=19)	13.16±1.00 (N=19)	10.50±0.66 (N=16)	.008	
<b>Avoidance</b>	S/S-S/L-L/L	10.79±0.47 (N=48)	9.50±0.41 (N=48)	9.43±0.44 (N=35)	.048	.698
	S/S-S/L	11.00±0.65 (N=29)	9.31±0.53 (N=29)	9.68±0.65 (N=19)	.105	
	L/L	10.47±0.65 (N=19)	9.79±0.66 (N=19)	9.13±0.60 (N=16)	.352	

The data reported are the mean±SEM of the psychometric scores at recruitment (T0), after one month (T1) and three months (T2)

The data were analyzed with the analysis of variance (ANOVA), testing the effect of time<sup>a</sup> and of genetic polymorphism<sup>b</sup> as independent variables; statistical significance was set at p<0.05 level

preoccupation, as determined with the Mini-MAC scale, was significantly associated with evidence of psychological stress symptoms, and appeared to be the most significant indicator of patients' difficulties in mental adjustment to cancer.<sup>10,32-34</sup> These findings are also in agreement with a feasibility study of psychosocial intervention in women with early breast cancer, which indicated high baseline values of anxious preoccupation HADS scores, which could be reduced by a psycho-educational intervention<sup>35</sup> based on the approach originally devised by Fawzy and Fawzy for melanoma patients.<sup>36</sup>

The data reported so far indicate that the scores of anxious preoccupation decrease spontaneously with time at follow up, indicating that coping and mental adaptation to the initial diagnosis and to the adjuvant therapy were occurring. The significance of the reduction of avoidance scores appears less clear, since this style of coping has been identified as a risk factor for the poor general mental adjustment and disease progression<sup>37-39</sup>, and has been suggested to be adaptive in the short run, but maladaptive for the long-term adjustment.<sup>40</sup>

The decrease with time of anxious preoccupation significantly depended on SERT polymorphism, and was less pronounced in women carrying one or two S alleles; these patients appeared to be those

in greater need of intervention. The available literature indicates that psycho-social or psycho-educational interventions<sup>36,41-44</sup>, or drug treatment<sup>45-47</sup> might be indicated. The data presently reported suggest that the individual molecular-genetic information concerning 5-HTTLPR polymorphism can be usefully considered for identifying the patients at greater risk of anxious preoccupation, and may be considered for the choice of the agent in case of drug treatment on the basis of the pharmacogenetic evidence available. The implications for the choice of the possible treatment of the patients with anxiolytic or antidepressant drugs, which are indicated also for conditions involving an anxious component<sup>48</sup> as an alternative to psycho-educational intervention, are interesting. The review of the pharmacogenetic of selective serotonin reuptake inhibitor (SSRI) antidepressants indicates that a greater incidence of adverse effects, and presumably a lesser therapeutic response, is likely to occur in carriers of S alleles of 5-HTTLPR variants of serotonin transporter.<sup>45,48</sup> When the drug treatment is the choice of intervention for treating difficulties of mental adaptation to cancer, benzodiazepines or antidepressant agents with a mechanism of action different from that of SSRIs<sup>49,50</sup> should be considered in the perspective of a personalized

TABLE 4. Subscale scores of HADS in relation to time and 5-HTTLPR genotype

	Allelic variants	T0 mean±SEM	T1 mean±SEM	T2 mean±SEM	Effect of Time p <sup>a</sup>	Effect of genotype p <sup>b</sup>
Depression	S/S-S/L-L/L	4.15±0.46 (N=48)	3.10±0.38 (N=48)	2.97±0.50 (N=35)	.124	.429
	S/S-S/L	4.31±0.60 (N=29)	3.14±0.51 (N=29)	3.32±0.77 (N=19)	.318	
	L/L	3.89±0.75 (N=19)	3.05±0.59 (N=19)	2.56±0.62 (N=16)	.365	
Anxiety	S/S-S/L-L/L	4.56±0.59 (N=48)	3.60±0.49 (N=48)	3.37±0.62 (N=35)	.288	.170
	S/S-S/L	5.41±0.83 (N=29)	3.90±0.60 (N=29)	4.21±0.97 (N=19)	.325	
	L/L	3.26±0.69 (N=19)	3.16±0.85 (N=19)	2.38±0.69 (N=16)	.681	

The data reported are the mean±SEM of the psychometric scores at recruitment (T0), after one month (T1) and three months (T2)

The data were analyzed with the analysis of variance (ANOVA), testing the effect of time<sup>a</sup> and of genetic polymorphism<sup>b</sup> as independent variables; statistical significance was set at p<0.05 level

and more effective treatment. A focussed attention thus might be given to pharmacogenetics, together with consideration to possible pharmacokinetic or pharmacodynamic interactions between the drugs received by the patients<sup>51</sup>, such as those already reported for SSRIs and tamoxifen.<sup>52,53</sup>

The further research extended to include a larger cohort of patients, appears to be encouraged by the results reported and is currently being performed by the authors in the perspective of a further investigation of mental adaptation to cancer in relation to the genetic and cultural ethnic milieu of the patients, including the goal of a personalized and more effective intervention.

## Acknowledgements

This work was made possible by the generous contribution of Fondazione Benefica Alberto & Kathleen Foreman Casali and of Beneficentia Stiftung Lichtenstein, was supported by the "Programma di Ricerca Scientifica di Interesse Nazionale of Italian Ministero dell'Istruzione, dell'Università e della Ricerca" entitled "Phenotypic and genotypic characterization of mental adaptation to cancer and of the response to the treatment with antidepressant drugs in oncology (Anno 2007 - prot. 20074XMRSE) "and by Azienda per I Servizi Sanitari N° 1, Trieste, Italy.

## References

1. Stanton AL, Danoff-Burg S, Huggins M. The first year after breast cancer diagnosis: hope and coping strategies as predictors of adjustment. *Psychooncology* 2002; **11**: 93-102.
2. Ozalp E, Soygu H, Cankurtaran E, Turhan L, Akbyk D, Geyik P. Psychiatric morbidity and its screening in Turkish women with breast cancer: a comparison between the HADS and SCID tests. *Psychooncology* 2008; **17**: 668-75.
3. Lueboonthavatchai P. Prevalence and psychosocial factors of anxiety and depression in breast cancer patients. *J Med Assoc Thai* 2007; **90**: 2164-74.
4. Boehmke MM, Dickerson SS. The diagnosis of breast cancer: transition from health to illness. *Oncol Nurs Forum* 2006; **33**: 1121-7.
5. Fertig DL. Depression in patients with breast cancer: prevalence, diagnosis, and treatment. *Breast J* 1997; **5**: 292-302.
6. Holland JC, Mastrovito R. Psychologic adaptation to breast cancer. *Cancer* 1980; **46(4 Suppl)**: 1045-52.
7. Akechi T, Okuyama T, Imoto S, Yamawaki S, Uchitomi Y. Biomedical and psychosocial determinants of psychiatric morbidity among postoperative ambulatory breast cancer patients. *Breast Cancer Res Treat* 2001; **65**: 195-202.
8. Matsuoka Y, Nakano T, Inagaki M, Sugawara Y, Akechi T, Imoto S, et al. Cancer-related intrusive thoughts as an indicator of poor psychological adjustment at 3 or more years after breast surgery: a preliminary study. *Breast Cancer Res Treat* 2002; **76**: 117-24.
9. Cordova MJ, Giese-Davis J, Golant M, Kronnenwetter C, Chang V, Mc Farlin S, et al. Mood disturbance in community cancer support groups. The role of emotional suppression and fighting spirit. *J Psychosomatic Res* 2003; **55**: 461-7.
10. Grassi L, Buda P, Cavana L, Annunziata MA, Torta R, Varetto A. Styles of coping with cancer: The Italian version of the Mini-Mental Adjustment to Cancer (Mini-Mac) scale. *Psychooncology* 2005; **14**: 115-24.
11. Grassi L, Travado L, Moncayo FLG, Sabato S, Rossi E and the SEPOS group. Psychosocial morbidity and its correlates in cancer patients of the Mediterranean area: findings from the Southern European Psycho-Oncology Study. *J Affect Disord* 2004; **83**: 243-8.
12. Bloom JR, Stewart SL, Johnston M, Banks P, Fobair P. Sources of support and the physical and mental well being of young women with breast cancer. *Soc Sci Med* 2001; **53**: 1513-24.
13. Greer S, Morris T, Pettingale KW. Psychological response to breast cancer: effect on outcome. *Lancet* 1979; **2**: 785-7.
14. Watson M, Haviland JS, Greer S, Davidson J, Bliss JM. Influence of psychological response on survival in breast cancer: a population-based cohort study. *Lancet* 1999; **354**: 1331-6.
15. Erčulj N, Kovac V, Hmeljak J, Dolzan V. The influence of platinum pathway polymorphisms on the outcome in patients with malignant mesothelioma. *Ann Oncol* 2012; **23**: 461-7.
16. Erčulj N, Kovač V, Hmeljak J, Franko A, Dodič-Fikfak M, Dolžan V. The influence of gemcitabine pathway polymorphisms on treatment outcome in patients with malignant mesothelioma. *Pharmacogenet Genomics* 2012; **22**: 58-68.
17. Caspi A, Sugden K, Moffitt TE, Taylor A, Craig IW, Harrington H, et al. Influence of life stress on depression: moderation by a polymorphism in the 5-HTT gene. *Science* 2003; **301**: 386-9.
18. Lesch KP, Bengel D, Heils A, Sabol SZ, Greenberg BD, Petri S, et al. Association of anxiety-related traits with a polymorphism in the serotonin transporter gene regulatory region. *Science* 1996; **274**: 1527-31.
19. Plesnicar A, Golcnik M, Fazarinc IK, Kralj B, Kovac V, Plesnicar BK. Attitudes of midwifery students towards teaching breast-self examination. *Radiol Oncol* 2010; **44**: 52-6.

19. Ovcaricek T, Frkovic SG, Matos E, Mozina B, Borstnar S. Triple negative breast cancer - prognostic factors and survival. *Radial Oncol* 2011; **45**: 46-52.
20. Andersen B, William B, Farrar WB, Golden-Kreutz D, Kutz LA, Courtney ME, et al. Stress and immune responses after surgical treatment for regional breast cancer. *J Natl Cancer Inst* 1998; **90**: 30-6.
21. Zalsman G, Huang Y, Oquendo MA, Burke AK, Hu X, Brent DA, et al. Association of a triallelic serotonin transporter gene promoter region (5-HTTLPR) polymorphism with stressful life events and severity of depression. *Am J Psychiatry* 2006; **163**: 1588-93.
22. Hu XZ, Lipsky RH, Zhu G, Akhtar LA, Taubman J, Greenberg BD, et al. Serotonin transporter promoter gain-of-function genotypes are linked to obsessive-compulsive disorder. *Am J Hum Genet* 2006; **78**: 815-26.
23. Zigmond AS, Snaith RP. The Hospital Anxiety and Depression Scale. *Acta Psychiatr Scand* 1983; **67**: 361-70.
24. Garcia-Cebrian A, Bauer M, Montejo AL, Dantchev N, Demyttenaere K, Gandhi P, et al. Factors influencing depression endpoints research (FINDER): Study design and population characteristics. *European Psychiatry* 2008; **23**: 57-65.
25. Gelernter J, Kranzler H, Cubbels JF. Serotonin transporter protein (SLC6A4) allele and haplotype frequencies and linkage disequilibria in African and European-American and Japanese populations and in alcohol-dependent subjects. *Hum Genet* 1997; **101**: 243-6.
26. Risch N, Herrell R, Lehner T, Liang KY, Eaves L, Hoh J, et al. Interaction between the serotonin transporter gene (5-HTTLPR), stressful life events, and risk of depression: a meta-analysis. *JAMA* 2010; **301**: 2462-71.
27. Munafò MR, Freimer NB, Ng W, Ophoff R, Veijola J, Miettunen J, et al. 5-HTTLPR genotype and anxiety-related personality traits: a meta-analysis and new data. *Am J Med Genet B* 2009; **150**: 271-81.
28. Middeldorp CM, de Geus EJ, Willemsen G, Hottenga JJ, Slagboom PE, Boomsma DI. The serotonin transporter gene length polymorphism (5-HTTLPR) and life events: no evidence for an interaction effect on neuroticism and anxious depressive symptoms. *Twin Res Hum Gen* 2010; **13**: 544-9.
29. Karg K, Burmeister M, Shedden K, Sen S. The Serotonin Transporter Promoter Variant (5-HTTLPR), Stress, and Depression Meta-analysis Revisited: Evidence of Genetic Moderation. *Arch Gen Psychiat* 2011; **68**: 444-54.
30. Grassi L, Rossi E, Cobiainchi M, Aguiari L, Capozzo MA, et al. Depression and serotonin transporter (5-HTTLPR) polymorphism in breast cancer patients. *J Affect Disord* 2010; **124**: 346-50.
31. Kash KM, Mago R, Kunkel E. Psychosocial oncology: supportive care for the cancer patients. *Semin Oncol* 2004; **32**: 211-8.
32. Ho SM, Fung WK, Chan CL, Watson M, Tsui YK. Psychometric properties of the Chinese version of the Mini-Mental Adjustment to Cancer (MINIMAC) scale. *Psychooncology* 2003; **12**: 547-56.
33. Anagnostopoulos F, Kolokotroni P, Spanea E, Chrysochoou M. The mini-mental adjustment to cancer (mini-MAC) scale: construct validation with a Greek sample of breast cancer patients. *Psychooncology* 2006; **15**: 79-89.
34. Capozzo MA, Martinis E, Pellis G, Giraldi T. An early structured psychoeducational intervention in breast cancer patients: results from a feasibility study. *Cancer Nurs* 2010; **33**: 228-34.
35. Fawzy FI, Fawzy NW. A structured psychoeducational intervention for cancer patients. *Gen Hosp Psychiatry* 1994; **16**: 149-52.
36. Carver CS, Pozo C, Harris SD. How coping mediates the effect of optimism on distress: A study of women with early stage breast cancer. *J Pers Soc Psychol* 1993; **65**: 375-90.
37. Osowiecki D, Compas BE. Psychological adjustment to cancer: Control beliefs and coping in adult cancer patients. *Cog Ther Res* 1998; **22**: 483-99.
38. Stanton AL, Danoff-Burg S, Cameron CL. Emotionally expressive coping predicts psychological and physical adjustment to breast cancer. *J Consul Clin Psychol* 2000; **68**: 875-82.
39. Roth S, Cohen LJ. Approach, avoidance, and coping with stress. *Am Psychol* 1986; **41**: 813-9.
40. Fukui S, Kugaya A, Okamura H, Kamiya M, Koike M, Nakanishi T, et al. A psychosocial group intervention for Japanese women with primary breast cancer: a randomized controlled trial. *Cancer* 2000; **89**: 1026-36.
41. Weis J. Support groups for cancer patients. *Support Care Cancer* 2003; **11**: 763-8.
42. Kissane D, Bloch S, Smith GC, Miach P. Cognitive-existential group psychotherapy for women with primary breast cancer: a randomised controlled trial. *Psychooncology* 2003; **12**: 532-46.
43. Maeda T, Kurihara H, Morishima I, Munakata T. The effect of psychological intervention on personality change, coping, and psychological distress of Japanese primary breast cancer patients. *Cancer Nurs* 2008; **31**: 27-35.
44. Smits K, Smits L, Peeters F, Schouten J, Janssen R, Smeets H, et al. Serotonin transporter polymorphisms and the occurrence of adverse events during treatment with selective serotonin reuptake inhibitors. *Int Clin Psychopharm* 2007; **22**: 137-43.
45. Schillani G, Capozzo MA, Aguglia E, De Vanna M, Grassi L, Conte MA, et al. 5-HTTLPR polymorphism of serotonin transporter and effects of sertraline in terminally ill cancer patients: report of eleven cases. *Tumori* 2008; **94**: 563-7.
46. Capozzo MA, Schillani G, Aguglia E, De Vanna M, Grassi L, Conte MA, et al. Serotonin transporter 5-HTTLPR polymorphism and response to citalopram in terminally ill cancer patients: report of twenty-one cases. *Tumori* 2009; **95**: 479-83.
47. Kato M, Serretti A. Review and meta-analysis of antidepressant pharmacogenetic findings in major depressive disorder. *Mol Psychiatr* 2010; **15**: 473-500.
48. Bandelow B, Andersen HF, Dolberg OT. Escitalopram in the treatment of anxiety symptoms associated with depression. *Depress Anxiety* 2007; **24**: 53-6.
49. Cankurtaran ES, Ozalp E, Soygur H, Akbiyik DI, Turhan L, Alkis N. Mirtazapine improves sleep and lowers anxiety and depression in cancer patients: superiority over imipramine. *Support Care Cancer* 2008; **16**: 1291-8.
50. Caraci F, Crupi R, Drago F, Spina E. Metabolic drug interactions between antidepressants and anticancer drugs: focus on selective serotonin reuptake inhibitors and hypericum extract. *Curr Drug Metab* 2011; **12**: 570-7.
51. Kelly CM, Juurlink DN, Gomes T, Duong-Hua M, Pritchard KI, Austin PC, et al. Selective serotonin reuptake inhibitors and breast cancer mortality in women receiving tamoxifen: a population based cohort study. *BMJ* 2010; **340**: c693.
52. In brief: Tamoxifen and SSRI interaction. *Med Lett Drugs Ther.* 2009; **51(1314)**: 45.

# Doses in organs at risk during head and neck radiotherapy using IMRT and 3D-CRT

Magdalena Peszynska-Piorun<sup>1</sup>, Julian Malicki<sup>2,3,4</sup>, Wojciech Golusinski<sup>5,6</sup>

<sup>1</sup> Medical Physics Department, Mikolaj Kopernik Memorial Regional Specialized Hospital, Lodz, Poland

<sup>2</sup> Medical Physics Department, Greater Poland Cancer Centre, Poznan, Poland

<sup>3</sup> Electroradiology Department, University of Medical Sciences, Poznan, Poland

<sup>4</sup> Medical Physics Department, Adam Mickiewicz University, Poznan, Poland

<sup>5</sup> Head and Neck Surgery Department, Greater Poland Cancer Centre, Poznan, Poland

<sup>6</sup> Maxillofacial Surgery Department, University of Medical Sciences, Poznan, Poland

Radiol Oncol 2012; 46(4): 328-336.

Received 17 June 2012

Accepted 17 September 2012

Correspondence to: Dr Magdalena Peszynska-Piorun, Medical Physics Department, Mikolaj Kopernik Memorial Regional Specialized Hospital, Lodz, Poland. Phone: +48664196245; E-mail: m-peszynska@o2.pl

Disclosure: No potential conflicts of interest were disclosed.

**Background.** Treatment planning for head and neck (H&N) cancer is complex due to the number of organs at risk (OAR) located near the planning treatment volume (PTV). Distant OAR must also be taken into consideration. Intensity-modulated radiotherapy (IMRT) and three-dimensional conformal radiotherapy (3D-CRT) are both common H&N treatment techniques with very different planning approaches. Although IMRT allows a better dose conformity in PTV, there is much less evidence as to which technique less dose to OAR is delivered. Therefore, the aim of the study was to compare IMRT to 3D-CRT treatment in terms of dose distribution to OAR in H&N cancer.

**Patients and methods.** This was a prospective study of a series of 25 patients diagnosed with stage cT<sub>3-4</sub>N<sub>0-2</sub> laryngeal cancer. All patients underwent total laryngectomy and bilateral selective neck dissections. In all cases, patients were treated with IMRT, although a 3D-CRT treatment plan was also developed for the comparative analysis. To compare doses to specific OAR, we developed a new comparative index based on sub-volumes.

**Results.** In general, IMRT appears to deliver comparable or greater doses to OAR, although the only significant differences were found in the cerebellum, in which 3D-CRT was found to better spare the organ.

**Conclusions.** Organs located outside of the IMRT beam (*i.e.*, distant organs) are generally thought to be well-spared. However, the results of this study show that, in the case of the cerebellum, this was not true. This finding suggests that larger studies should be performed to understand the effects of IMRT on distant tissues. Anthropomorphic phantom studies could also confirm these results.

Key words: radiotherapy; IMRT; 3D-CRT; head and neck cancer

## Introduction

The global incidence of head and neck cancer is about 650000 cases per year, which represents about 6% cancer incidence (skin cancer excluded). Radiotherapy plays an important role in the treatment of head & neck (H&N) cancers.<sup>1,2</sup> However, patients, who undergo irradiation, require a comprehensive pre-treatment evaluation.<sup>3</sup> In recent decades, the treatment for H&N cancer has moved from two-dimensional radiotherapy to three-dimensional

conformal radiotherapy (3D-CRT) and recently also to intensity-modulated radiotherapy (IMRT). Both 3D-CRT and IMRT represent a significant advance over the conventional radiotherapy because they increase dose delivery accuracy while sparing surrounding normal tissues and organs at risk (OAR). The dose-modulating ability of IMRT gives a theoretical advantage over 3D-CRT, which recently has been also supported in the clinical trial.<sup>4,5</sup>

IMRT is still a relatively new technique and although its superiority over 3D-CRT in term of tu-



mor dose coverage is clear, there is still some concerns about doses in OAR.<sup>5-8</sup> Nevertheless, IMRT has become the primary treatment technique in H&N cancers due to its better dose conformity, demonstrated very well in the treatment of lesions with complex anatomy which are adjacent to vital structures such as the spinal cord or brain stem.<sup>7,9-11</sup> However, this improved the conformity to the target which may have an undesirable drawback as the large number of fields used in IMRT can potentially lead to higher doses outside the planning treatment volume (PTV).<sup>9,12,13</sup> IMRT also requires more complex quality assurance procedures.<sup>2,14-17</sup>

Few studies have compared IMRT to 3D-CRT in H&N radiotherapy to evaluate doses to OARs located outside of the PTV.<sup>18,19</sup> The present study was aimed to compare differences in calculated dose distributions to OAR for IMRT *vs.* 3D-CRT in a series of 25 patients with H&N cancer. In the article we focused on organs that had not been previously analyzed *i.e.*: thyroid gland, mandible, brain stem, brain and the cerebellum.

## Patients and methods

This was a prospective study of a series of 25 patients diagnosed with stage cT<sub>3-4</sub>N<sub>0-2</sub> laryngeal cancer. All patients underwent total laryngectomy and bilateral selective neck dissections. In all cases, patients were treated with IMRT, although a 3D-CRT treatment plan was also developed for the comparative analysis.

The IMRT treatment plan had prescription of 54 Gy delivered in fractions of 1.8 Gy (30 fractions) for the PTV1 with a simultaneous integrated boost (SIB) of 60 Gy at 2 Gy/fraction to the PTV2. A set of 6 non-coplanar 6 MV photon beams was used for 15 patients that entered the study first and a set of 7 non-coplanar 6 MV photon beams for 10 patients who followed the first group. Originally, 6-field IMRT plan was considered as a standard setup. Afterwards, as a result of a thorough comparison of the 7-field and the 6-field technique, the latter one was used. The gantry angles used for the 6-field technique were as follows: 35° (collimator 0°, table 0°), 110° (collimator 10°, table 15°), 180° (collimator 0°, 0°), 250° (collimator 350°, table 345°), 325° (collimator 0°, table 0°), 340° (collimator 0°, table 0°). Respectively, for the 7-field technique gantry angles were: 0° (collimator 0°, table 0°), 40° (collimator 0°, table 0°), 110° (collimator 108.9°, table 10°), 150° (collimator 5°, table 0°), 210°

(collimator 352.7°, table 0°), 250° (collimator 265°, table 350°), 320° (collimator 90°, table 0°).

The 3D-CRT treatment plans included two separate phases, one for the primary treatment and the second plan for the boost. Fifty Gy (2 Gy/fraction) were prescribed to the PTV1. The second phase was a boost of 10 Gy at 2 Gy/fraction to the PTV2, for a total of 30 fractions (the same as for IMRT). Both plans were mainly based on 6 MV photons, except for fields with small weights (only in phase 1), in which case 15 MV photons were used. The first phase called for 10 to 12 fields with extra 2–3 fields was used for the boost phase. All fields were coplanar, in some cases opposed: (90° and 270°, 0° and 180° but also 60°, 300°, 100°, 260°). In 2–4 fields the collimator angle was ± 18° (first phase) and ± 5° (second phase). Many field wedges (mostly 45°) had to be used due to contouring irregularity inherent in H&N treatments. In some cases, the irradiated regions could not be completely covered by a homogenous dose and wedged fields, so half-beams were also used.

Treatment plans for both techniques were calculated and optimized using the Eclipse Treatment Planning System (Varian, Medical System, Palo Alto, CA, USA) with AAA algorithm. The IMRT used a dynamic sliding window technique. The CT images acquired included the whole head and the neck to the level of T<sub>3</sub>-T<sub>4</sub> (thoracic vertebra). The clinical target volume (CTV), PTV1, PTV2/boost and OAR volumes were delineated by the same radiation oncologist for all patients and techniques. The following OARs were chosen for the dose comparison: thyroid gland, mandible, brain stem, cerebellum, brain. For 3D-CRT doses in all structures were optimized manually while for IMRT the automated optimization was performed for the following structures: PTVs, CTVs, salivary glands, spinal cord and the area above the PTV, which often overlapped with the mandible and the back side of the head/occipital bone and the neck at shallow depth under the skin, to spare the hair.

Treatment planning was performed in accordance with the International Commission on Radiation Units and Measurements (ICRU) reports on H&N cancer and IMRT (#50, #62 and #83)<sup>10,14,20-23</sup>, which recommend a homogenous dose distribution (range, 95% - 107% of the prescribed dose) to the PTV. Values for the constraints used in the process of dose optimization have been as follows: dose fractionation 1.8-2.0 Gy. Following: Brain, D(33%) ≤ 60 Gy, D(66%) ≤ 50 Gy, D(100%) ≤ 45 Gy with priority from 40 to 80; Brain stem, Dmax=54 Gy with priority circa 80, Spinal cord, Dmax=48 Gy

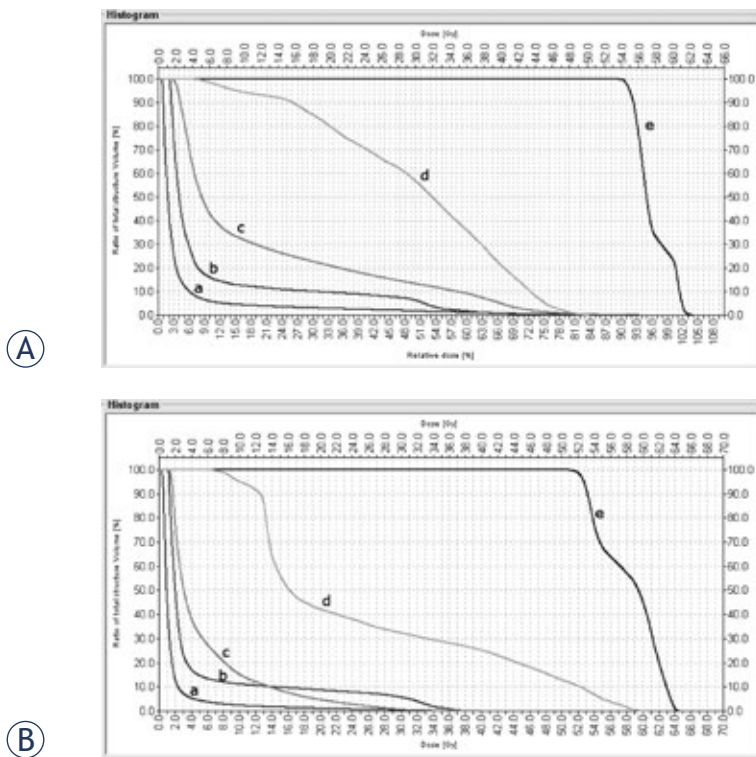


**FIGURE 1.** Dose volume histogram for the IMRT (A) and 3D-CRT (B) plans. The organs at risk are: cerebellum (c), brain stem (b), mandible (d), thyroid gland (e) and brain (a).

with priority circa 110, Salivary gland,  $D_{\text{mean}} \leq 30$  Gy, Mandible which is a part of area above the PTV,  $D_{\text{max}} \leq 70$  Gy with priority circa 90.<sup>24,25</sup>

For particular patients, additional constraints have been used, *i.e.* for salivary glands  $D(70\%) \leq 5$  Gy,  $D(50\%) \leq 18$  Gy,  $D(30\%) \leq 25$  Gy,  $D(15\%) \leq 35$  Gy with priority from 50 to 90. Function “normal tissue objective” with priority 100 was used to the further lower dose in all OARs. The modification of constraints and priorities is a part of treatment planning. It makes the optimization process slightly subjective which, however, is inevitable as a patient anatomy differs from one to another, and parameters have to be modified in order to obtain the uniform dose in PTV and the low dose in the optimized OARs

Standard parameters produced by the treatment planning software (TPS) were not sufficient to an effectively and quantitatively assess the differences between IMRT and 3D-CRT plans. Doses were very inhomogeneous and often low in OARs, making it difficult to identify small deviations. To more precisely evaluate a dose distribution to the OARs, we realized that we needed more detailed information aside from the standard maximum, minimum, and mean values. Doses at 0% volume, 30% volume, 60% volume, 90% volume (notation

$D(0\%)$ ,  $D(30\%)$ ,  $D(60\%)$ ,  $D(90\%)$ ) are considered to be representative in normal tissue complication probability (NTCP) models.<sup>21,26</sup> For this reason, we evaluated doses for each OAR in 4 sub-volumes (0%, 30%, 60%, 90% of the relative volume) and wherever more complex information was desired we evaluated doses in 10 sub-volumes (with each sub-volume representing from 0% to 90% of the volume, with a step of 10% of a relative volume). For each of the sub-volumes, maximal doses were read from the cumulative histogram for both IMRT and 3D-CRT, and then the differences and mean values for all sub-volumes were calculated.

In this paper, we present all 10 sub-volume doses in the cerebellum and brain. For other organs evaluated, we present doses only for 4 sub-volumes (90%, 60%, 30%, 0%).

### Statistical analysis and ethical consideration

After calculating the dose received by the various sub-volumes according to the treatment technique (IMRT or 3D-CRT), we used the Shapiro-Wilk test to assess the distribution of the data, which was found to be non-Gaussian. Therefore, the nonparametric U Mann-Whitney rank sum test was applied, with a significance level of 0.05. We used the software programs Statistica 8.0 and Origin 8.0 (OriginLab, Northampton) to perform the statistical analysis.

The prospective study was carried out according to the Declaration of Helsinki.

### Results

As discussed above, the primary analysis for this study was based on an index of sub-volumes for the OARs. However, prior to evaluating these sub-volumes, we calculated the dose-volume histogram (DVH) for all 25 patients and OARs evaluated in this study. The histograms for both IMRT and 3D-CRT presented similar trends for the dose-volume dependence of the OAR, although it was not possible to detect significant differences. As a result, we concluded that conventional histograms were not sufficient to perform a dose distribution comparison. The histogram of a patient in Figure 1 was taken to demonstrate the similarity between the two techniques.

Table 1 shows the doses received by the OARs for all patients. The only positive values are found for the cerebellum while the other OAR' show a range of positive and negative values (-10 Gy to +14.5 Gy),

**TABLE 1.** The authors' index of the mean dose difference ( $D_{IMRT} - D_{3DCRT}$ ) for the organs at risk and sub-volumes evaluated for this series of 25 patients. The index value was the mean dose difference ( $D_{IMRT} - D_{3DCRT}$ ) for the doses in 10 sub-volumes for cerebellum and brain and of 4 sub-volumes for thyroid gland, brain stem, and mandible. A positive value indicated that the mean dose for intensity-modulated radiotherapy (IMRT) was greater than the mean three-dimensional conformal radiotherapy (3D-CRT) dose.

Patient Number	Cerebellum Dose [Gy]	Thyroid gland Dose [Gy]	Brain stem Dose [Gy]	Mandible Dose [Gy]	Brain Dose [Gy]
1	5.75	3.09	-2.82	1.92	-0.66
2	9.82	11.83	1.15	-9.68	0.70
3	13.13	0.01	2.43	-2.06	1.16
4	12.08	8.28	6.69	1.04	2.45
5	12.81	-1.70	2.28	0.32	1.80
6	8.58	3.53	0.67	5.03	6.59
7	6.43	1.51	2.30	-10.11	1.92
8	9.06	1.88	1.49	4.09	1.59
9	8.58	3.53	0.67	5.53	2.08
10	6.74	0.48	3.49	5.59	0.74
11	7.25	2.49	-3.83	1.52	1.03
12	5.54	-0.93	0.27	5.65	0.71
13	10.05	-1.55	2.22	7.13	0.39
14	5.02	2.98	1.03	-4.18	0.86
15	8.89	-1.26	-3.64	1.22	0.73
16	8.85	0.75	0.59	0.93	2.05
17	10.72	1.83	-1.83	11.97	1.57
18	8.53	-0.57	-1.20	7.09	1.57
19	5.43	-1.34	-1.22	7.74	0.20
20	14.50	-0.25	2.59	3.26	1.70
21	1.60	0.98	-0.97	3.28	-0.65
22	8.84	-1.98	1.66	8.66	1.74
23	11.61	1.79	-0.39	-1.71	2.20
24	6.91	-2.17	2.57	6.17	0.88
25	8.33	2.16	-1.07	6.54	0.54

with less dispersion for the brain stem. The brain shows a consistent trend with minimal deviation between techniques, with many values near 0.

Dose differences between the two treatment techniques can be more clearly seen in the sub-volumes. In Figure 2, dose plots for chosen OARs are shown for all 25 patients. Dose differences ( $IMRT_{dose} - 3D-CRT_{dose}$ ) for cerebellum (a), mandible (b), thyroid gland (c), brain stem (d) and brain (e) are shown.

Figures 3 to 7 show the mean dose, maximal and minimal doses, and standard deviation in sub-volumes for the study group, for each OAR at IMRT and 3D-CRT.

Table 2 shows the mean radiation doses to the cerebellum for the group (25 patients) by the treatment technique (IMRT, 3D-CRT). The differential dose is also shown.

IMRT = intensity-modulated radiotherapy; 3D-CRT = three-dimensional conformal radiotherapy

The statistical analysis for the mandible showed significant differences in doses for 3 sub-volumes (90%, 60% and 0%;  $P= 0.04, 0.00$  and  $0.001$ , respectively). The upper-tailed Mann Whitney test showed that doses in sub-volume of 90% ( $p=0.02$ ) and sub-volume of 60% ( $p=0.0006$ ) were greater for IMRT than for 3D-CRT. The lower-tailed Mann Whitney test showed that maximal doses (which correspond to the dose at 0% of the volume) were lower for IMRT ( $p=0.00003$ ) than for 3D-CRT. The only sub-volume for which no significant difference was detected was for 30% ( $p= 0.91$ ) (Figure 3).

In the thyroid gland, we found significant differences for 90% of volume ( $p= 0.01$ ) and 0% ( $p=0.01$ ),

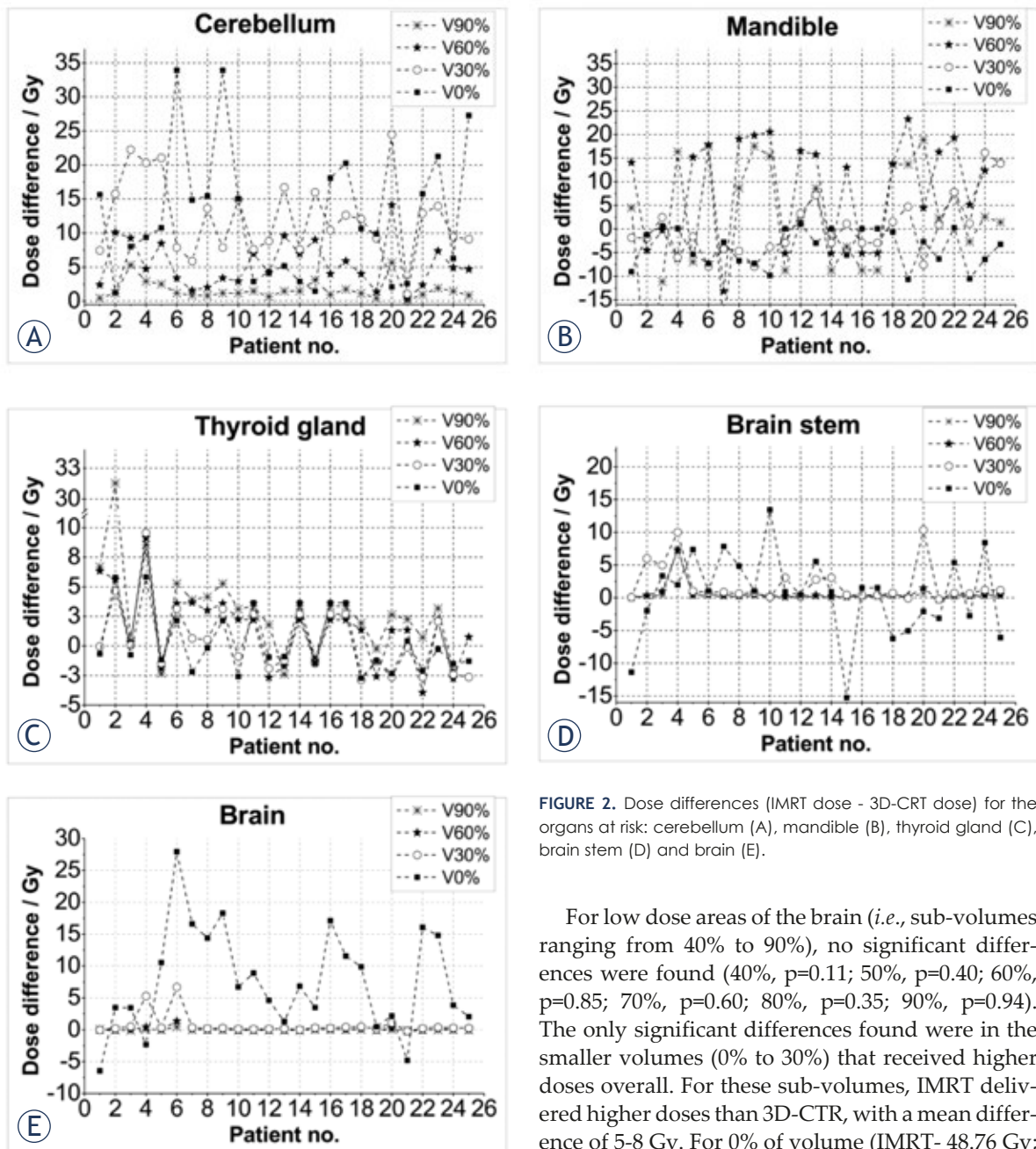


FIGURE 2. Dose differences (IMRT dose - 3D-CRT dose) for the organs at risk: cerebellum (A), mandible (B), thyroid gland (C), brain stem (D) and brain (E).

but no significant differences in sub-volume of 60% ( $p=0.09$ ) or 30% ( $p=0.66$ ). At the  $p$ -level of 0.005 for the upper-tailed test, the IMRT doses in sub-volume of 90% were significantly higher than those of 3D-CRT while the lower-tailed test revealed that maximum doses were lower with IMRT than 3D-CRT (Figure 4).

The dose differences in the brain stem were not statistically significant (90% of volume,  $p=0.06$ ; 30%,  $p=0.07$ ; 0%,  $p=0.55$ ) except for 60% of volume ( $p=0.034$ ) (Figure 5).

For low dose areas of the brain (*i.e.*, sub-volumes ranging from 40% to 90%), no significant differences were found (40%,  $p=0.11$ ; 50%,  $p=0.40$ ; 60%,  $p=0.85$ ; 70%,  $p=0.60$ ; 80%,  $p=0.35$ ; 90%,  $p=0.94$ ). The only significant differences found were in the smaller volumes (0% to 30%) that received higher doses overall. For these sub-volumes, IMRT delivered higher doses than 3D-CRT, with a mean difference of 5-8 Gy. For 0% of volume (IMRT- 48.76 Gy; 3D-CRT- 41.20 Gy),  $p=0.0001$ ; for 10% (IMRT- 6.18 Gy; 3D-CRT- 2.99 Gy),  $p=0.00$ ; for 20% (IMRT- 2.96 Gy; 3D-CRT- 1.82 Gy),  $p=0.0005$ ; for 30% (IMRT- 2.09 Gy; 3D-CRT- 1.38 Gy),  $p=0.01$ . The IMRT techniques delivered higher doses to these volumes, with a higher maximum dose (30%,  $p=0.003$ ; 20%,  $p=0.0003$ ; 10%,  $p=0.0005$ ; 0%,  $p=0.0001$ ).

## Discussion

Of all the organs at risk evaluated, the cerebellum was the only OAR in our study with a positive

**TABLE 2.** Mean radiation doses (Gy) to the cerebellum for the group (25 patients) by the treatment technique (IMRT, 3D-CRT). The differential dose for all sub-volumes (from 0% to 90%, step of 10%) is also shown.

Sub-volume	Mean dose (IMRT)	Mean dose (3D-CRT)	Dose differential (IMRT – 3D-CRT)
90% of V	4.10	2.13	1.98
80% of V	5.49	2.50	2.99
70% of V	7.11	2.87	4.24
60% of V	9.18	3.33	5.85
50% of V	11.86	3.98	7.88
40% of V	15.35	4.87	10.48
30% of V	19.57	6.37	13.21
20% of V	24.77	9.23	15.50
10% of V	31.49	15.10	16.39
0% of V	47.50	34.91	12.59

mean dose differential ( $D_{IMRT} - D_{3D-CRT}$ ), meaning that 3D-CRT delivered lower doses to the cerebellum than IMRT. Moreover, we found that the bigger the volume measured the smaller and more constant the differential dose was.

**Brain**

Dose distributions in the whole brain, including the cerebellum, were dependent on the volume evaluated. For volumes ranging from 40% to 90%, IMRT doses were lower than 3D-CRT while volumes from 0% to 30% the 3D-CRT doses were lower.

**Mandible and thyroid**

No consistent trends were observed for the mandible and thyroid gland. For some patients, IMRT doses were higher than 3D-CRT while for others it was exactly the reverse. However, it is interesting to note that the maximum dose for the mandible was, in most cases, lower for IMRT. Much bigger deviations in doses were observed in the volume of 60% and 90%, because the differences in low dose regions were larger. IMRT was superior to 3D-CRT in sparing the mandible in 6 patients while the reverse was true in 3 patients. Similarly, doses to the thyroid gland were lower (better sparing) with IMRT for 5 patients and by 3D-CRT for 8 patients.

**Brain stem**

No significant differences were observed in the brain stem as the dose distributions in this organ were similar for both techniques. The detected differences were very small and could have been due

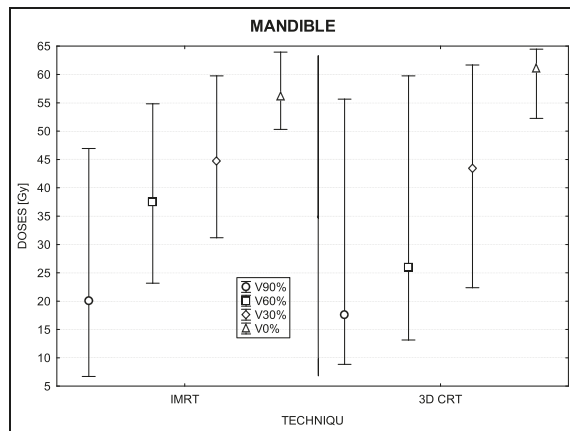


**FIGURE 3.** A box plot of the mandible for 4 volumes: V90%, V60%, V30% and V0%. Middle point is the mean value; the box, standard deviation; and whisker, Min – Max value.

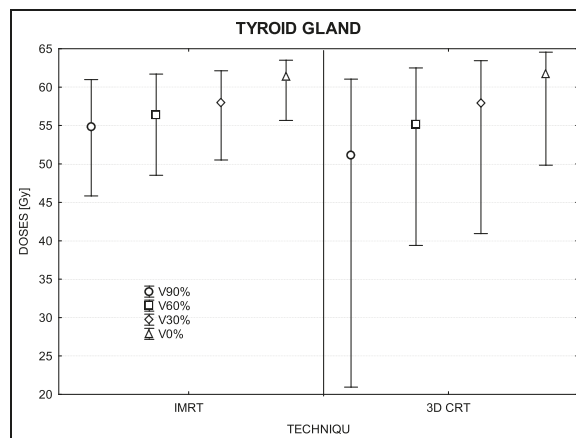


**FIGURE 4.** A box plot of thyroid gland for 4 volumes: V90%, V60%, V30% and V0%. Middle point is the mean value; the box, standard deviation; and whisker, Min – Max value.

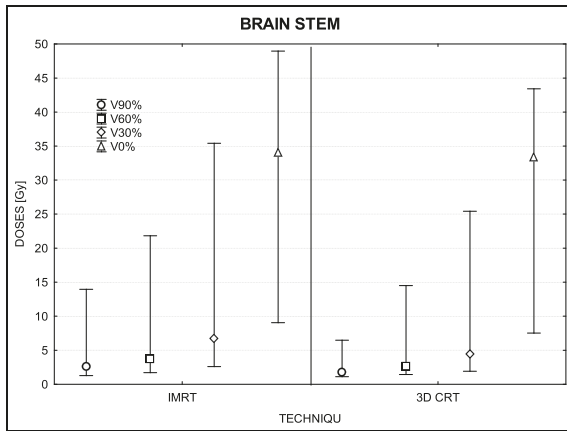


FIGURE 5. A box plot of brain stem for 4 volumes: V90%, V60%, V30% and V0%. Middle point is the mean value; the box, standard deviation; and whisker, Min – Max value.

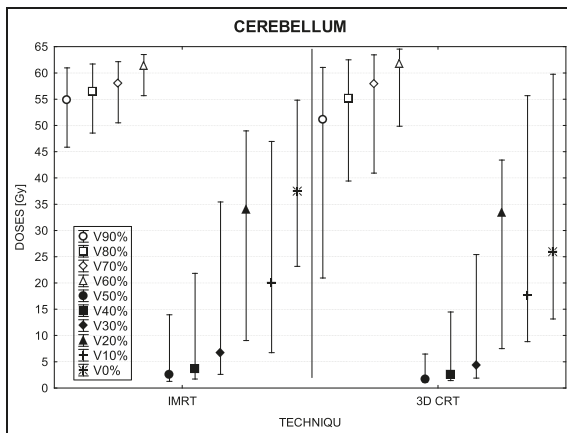


FIGURE 6. A box plot of cerebellum for 10 volumes: from V90% to V0%. Middle point is the mean value; the box, standard deviation; and whisker, Min – Max value.

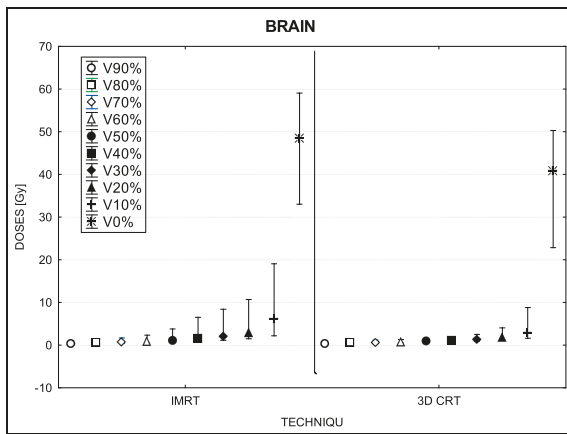


FIGURE 7. A box plot of brain for 10 volumes: from V90% to V0%. Middle point is the mean value; the box, standard deviation; and whisker, Min – Max value.

to chance. The maximum dose varied in a few patients, but this could be caused by the small volume of this organ leading to a point dose, pixel or voxel, in which the maximum dose was found.

### Cerebellum

Relative to the PTV, the cerebellum was considered a distant organ and unlike the other organs, IMRT resulted in significantly higher doses to the cerebellum in all sub-volumes. The reason for this difference is evident: not all of the 3D-CRT treatment fields covered the cerebellum whereas in IMRT, a greater number of fields passed through the cerebellum. So, even though the IMRT doses were lower, the overall accumulated dose was greater with IMRT. These differences were especially notable in small sub-volumes. In general, we found that 3D-CRT produced more homogenous doses to the brain (Figures 2A, 6) than IMRT, even though the mean dose of 3D-CRT was higher.

Our results are interesting in that they show that both techniques are largely similar in terms of OAR irradiation, with the only notable exception being the cerebellum, which receives more radiation with IMRT than 3D-CRT. These results do not contradict advantages of IMRT—that because dose distribution is more conformal than 3D-CRT, it is also less toxic to adjacent healthy tissues. However, we should keep in mind that data and follow up for IMRT are still relatively limited.<sup>7,10,27</sup>

A review of the literature shows varying data, with in principle IMRT superior for some OARs, however the concern of potentially higher doses in distant organs is noted.<sup>4,5,7,14,18,28</sup> In this work, we confirmed that IMRT allowed on better reduction of doses in OARs however in particular situation the 3D-CRT may allow on better sparing the cerebellum, thus the attention is required in such situation.

A recent study by Chen *et al.* compared dose-volume characteristics of the brachial plexus for IMRT and CRT and found out that a dose to the brachial plexus was significantly increased among patients undergoing IMRT compared with CRT.<sup>28</sup> However, a different study comparing 3D-CRT and IMRT for thyroid cancer found out that the dose to the spinal cord was 12 Gy less with IMRT and the coverage of the target volume was also better, with a smaller standard deviation (4.65% for 3D-CRT *vs.* 1.81% for IMRT). Longobardi *et al.* found out that IMRT dose planed provide more uniform coverage of the PTV than 3D-CRT and IMRT resulted in a significant reduction of mean and/or maximum doses to OAR; of particular note, these authors re-

ported that the mean dose to the parotid glands decreased by a mean of 13.5 Gy with the use of IMRT vs. 3D-CRT.<sup>29</sup> The revealed differences in dose parameters between evaluated techniques were small due to the improvement in optimization applied in all radiotherapy techniques, thus detection tools and methods that allowed to trace the differences had to be appropriately accurate.<sup>12,30,31</sup>

Both techniques present advantages and disadvantages. Using the 3D CRT does not allow for simultaneously integrated boost and in consequence two separate courses of radiotherapy are necessary, with the risk of the field overlap that may cause hot spots and some inhomogeneity in dose distributions. These drawbacks are not insignificant and may, therefore, limit the number of indications for 3D-CRT.<sup>5,32,33</sup>

IMRT, in contrast, although more complex<sup>2,13,16,34</sup>, allows for more homogenous dose deposition in the target while sparing surrounding normal tissues. Moreover, IMRT allows for integration of the boost dose (SIB) in one course of the treatment, thus resulting in a higher fraction dose (hypofractionation, *i.e.* dose fraction greater than 2 Gy) while the PTV receives a dose from range of 1.8 Gy to 2.0 Gy at the same time.

Both 3D-CRT and IMRT have their advantages, and should be selected on a case by case basis. Although IMRT is technically more sophisticated, 3D-CRT is perfectly capable of delivering the appropriate dose to the target.<sup>1,5,14,35</sup> However, the primary disadvantage with 3D-CRT is a dose distribution, which is often uneven. The main benefit of IMRT over 3D-CRT is the ability to optimize the treatment in the planning stage to deliver the appropriate dose to the target while optimizing the plan to adhere to the OAR constraints. Particularly, the IMRT is useful in the regions where the tumor is located close to OARs. The OARs, which lay outside but very near the PTV may be better spared, when using IMRT than 3D-CRT technique. In fact, this is why most experts prefer IMRT for H&N cancers. The main drawback of IMRT seems to be that the dose is not optimized for distant OARs, *i.e.*, those that are not located in the path of the beam and, thus, not considered crucial during planning.<sup>36</sup>

## Conclusions

This study has shown the feasibility of using an index of sub-volumes to better evaluate a dose distribution to OARs located outside of the PTV. We believe that this new approach allows for an effective

dose comparison of the dose distributions at locations with a steep dose gradient.

The findings of our study show that IMRT allowed the better reduction of doses in OARs, however, in particular situations the 3D-CRT may allow better sparing the cerebellum and this is an important factor to consider when planning treatments in H&N cancers. Particularly, the OAR for which dose was not optimized, might receive a higher dose (jello effect). It could occur because during IMRT larger body part is usually irradiated with a small dose and not all OARs can be taken into an optimization process.

## Acknowledgments

This study was supported by a grant from the Polish Ministry of Science and Higher Education, No NN 402458637.

## References

- Gabrys D, Wesolowska I, Suwinski R. The evaluation of 3DRT and IMRT techniques in postoperative radiotherapy for thyroid medullary carcinoma. *Rep Pract Oncol Radiother* 2008; **13**: 126-9.
- Miften MM, Das SK, Su M, Marks LB. A dose-volume-based tool for evaluating and ranking IMRT treatment plans. *J Appl Clin Med Phys* 2004; **5**: 1-14.
- Trojanowska A. Squamous cell carcinoma of the head and neck-The role of diffusion and perfusion imaging in tumor recurrence and follow-up. *Rep Pract Oncol Radiother* 2011; **16**: 203-8.
- Buettner F, Miah AB, Gulliford SL, Hall E, Harrington KJ, Webb S, et al. Novel approaches to improve the therapeutic index of head and neck radiotherapy: An analysis of data from the PARSPORT randomised phase III trial. *Radiother Oncol* 2012; **103**: 82-7.
- Nutting CM, Morden JP, Harrington KJ, Urbano TG, Bhide SA, Clark C, et al. PARSPORT trial management group. Parotid-sparing intensity modulated versus conventional radiotherapy in head and neck cancer (PARSPORT): a phase 3 multicentre randomised controlled trial. *Lancet Oncol* 2011; **12**: 127-36.
- Binhu J, Supe S, Pawar Y. Intensity modulated radiotherapy (IMRT) the white, black and grey: a clinical perspective. *Rep Pract Oncol Radiother* 2009; **14**: 95-103.
- Rosenthal DI, Chambers MS, Fuller CD, Rebuena NCS, Garcia J, Kies MS, et al. Beam path toxicities to non-target structures during intensity-modulated radiation therapy for head and neck cancer. *Int J Radiat Oncol Biol Phys* 2008; **72**: 747-55.
- Sas-Korczyńska B, Śladowska A, Rozwadowska-Bogusz B, Dyczek S, Lesiak J, Kokoszka A, et al. Comparison between intensity modulated radiotherapy (IMRT) and 3D tangential beams technique used in patients with early-stage breast cancer who received breast-conserving therapy. *Rep Pract Oncol Radiother* 2010; **15**: 79-86.
- Lee N, Puri DR, Blanco AI, Chao KSC. Intensity modulated radiation therapy in head and neck cancers: An update. *Head Neck* 2007; **29**: 387-400.
- Bhide SA, Nutting CM. Advances in radiotherapy for head and neck cancer. *Oral Oncology* 2010; **46**: 439-41.
- Clark CH, Hansen VN, Chantler H, Edwards C, James HV, Webster G, et al. Dosimetry audit for a multi-centre IMRT head and neck trial. *Radiother Oncol* 2009; **93**: 102-8.
- Tribius S, Bergelt C. Intensity-modulated radiotherapy versus conventional and 3D conformal radiotherapy in patients with head and neck cancer: Is there a worthwhile quality of life gain? *Cancer Treat Rev* 2011; **37**: 511-9.

13. Piotrowski T, Martenka P, De Patoul N, Jodda A, Coevoet M, Malicki J, et al. The new two-component conformity index formula (TCCI) and dose-volume comparisons of the pituitary gland and tonsil cancer IMRT plans using a linear accelerator and helical tomotherapy. *Rep Pract Oncol Radiother* 2009; **14**: 133-45.
14. Grzadziel A, Grosu A, Kneschaurek P. Three-dimensional conformal versus intensity-modulated radiotherapy dose planning in stereotactic radiotherapy: Application of standard quality parameters for plan evaluation. *Int J Rad Oncol Biol Phys* 2006; **66**: S87-94.
15. Peszynak C, Polgar I, Weisz C, Kiraly R, Zarand P. Verification of quality parameters for portal image in radiotherapy. *Radiol Oncol* 2011; **45**: 66-74.
16. Bailey DW, Kumaraswamy L, Podgorsak MB. A Fully electronic intensity-modulated radiation therapy quality assurance (IMRT QA) process implemented in a network comprised of independent treatment planning, record and verify, and delivery systems. *Radiol Oncol* 2010; **44**: 124-30.
17. Mendenhall W, Mancuso A. Radiotherapy for head and neck cancer – is the “next level” down? *Int J Radiat Oncol Biol Phys* 2009; **73**: 645-6.
18. Kry SF, Salehpour M, Followill DS, Stovall M, Kuban DA, Rosen II. The calculated risk of fatal secondary malignancies from intensity-modulated radiation therapy. *Int J Radiat Oncol Biol Phys* 2005; **62**: 1195-203.
19. Howell RM, Scarboro SB, Kry SF, Yaldo DZ. Accuracy of out-of-field dose calculations by a commercial treatment planning system. *Phys Med Biol* 2010; **55**: 6999-7008.
20. Prescribing, Recording, and Reporting Photon Beam Therapy (Report 50), ICRU Report No. 50; 1993.
21. Prescribing, Recording and Reporting Photon Beam Therapy (Report 62), (Supplement to ICRU Report 50), ICRU Report 62; 1999.
22. Reference Data for the Validation of Doses from Cosmic-Radiation Exposure of Aircraft Crew (ICRU 84), ICRU Report 84. *Journal of the ICRU* 2012; **10(2)**.
23. Hall E, Wu C. Radiation-induced second cancers: the impact of 3D-CRT and IMRT1. *Int J Radiat Oncol Biol Phys* 2003; **56**: 83-8.
24. Dorr W, Stewart FA. Retreatment tolerance of normal Tissues. In: *Basic Clinical Radiobiology*. Joiner M and van der Kogel A, editors. 4<sup>th</sup> Edition. London: Hodder Arnold; 2009. p. 259-90.
25. Marks LB, Yorke ED, Jackson A, Ten Haken RT, Comstine LS, Eisbruch A, et al. Use of normal tissue complication probability models in the clinic. *Int J Rad Oncol Biol Phys* 2010; **76(3 Suppl)**: S10-9.
26. Kupchak C, Battista J, Van Dyk J. Experience-driven dose-volume histogram maps of NTCP risk as an aid for radiation treatment plan selection and optimization. *Med Phys* 2008; **35**: 333-43.
27. Mendenhall WM, Amdur RJ, Palta JR. Intensity-modulated radiotherapy in the standard management of head and neck cancer: promises and pitfalls. *J Clin Oncol* 2006; **24**: 2618 -23.
28. Chen AM, Hall WH, Li B-Q, Guiou M, Wright C, Mathai M, et al. Intensity-modulated radiotherapy increases dose to the brachial plexus compared with conventional radiotherapy for head and neck cancer. *Br J Radiol* 2011; **84**: 58-63.
29. Longobardi B, De Martin E, Fiorino C, Delloca I, Broggi S, Cattaneo GM, et al. Comparing 3DCRT and inversely optimized IMRT planning for head and neck cancer: Equivalence between step-and-shoot and sliding window techniques. *Radiother Oncol* 2005; **77**: 148-56.
30. Winiiecki J, Zurawski Z, Drzewiecka B, Slosarek K. Anatomy-corresponding method of IMRT verification. *Rep Pract Oncol Radiother* 2011; **16**: 1-9.
31. Malicki J, Litoborski M, Kierzkowski J, Kosicka G. How the implementation of an in-vivo dosimetry protocol improved the dose delivery accuracy in head and neck radiotherapy. *Neoplasma* 2004; **51**: 155-8.
32. Knöös T, Kristensen I, Nilsson P. Volumetric and dosimetric evaluation of radiation treatment plans: radiation conformity index. *Int J Radiat Oncol Biol Phys* 1998; **42**:1169-76.
33. Clark CH, Miles EA, Urbano MTG, Bhide SA, Bidmead AM, Harrington KJ, et al. Pre-trial quality assurance processes for an intensity-modulated radiation therapy (IMRT) trial: PARSPOUR, a UK multicentre Phase III trial comparing conventional radiotherapy and parotid-sparing IMRT for locally advanced head and neck cancer. *Br J Radiol* 2009; **82**: 585-94.
34. Guerrero Urbano MT, Clark CH, Kong C, Miles E, Dearnaley DP, Harrington KJ, et al. Target volume definition for head and neck intensity modulated radiotherapy: Pre-clinical evaluation of PARSPOUR trial guidelines. *Clin Oncol* 2007; **19**: 604-13.
35. Gizynska M, Zawadzka A. IMRT versus 3D-CRT for thyroid cancer. *Pol J Med Phys Eng* 2008; **14**: 151-62.
36. Malicki J. The importance of accurate treatment planning, delivery, and dose verification. *Rep Pract Oncol Radiother* 2012; **17**: 63-5.



# Results of postoperative radiochemotherapy of the patients with resectable gastroesophageal junction adenocarcinoma in Slovenia

Ana Jeromen, Irena Oblak, Franc Anderluh, Vaneja Velenik, Marija Skoblar Vidmar, Ivica Ratoša

Department of Radiotherapy, Institute of Oncology Ljubljana, Slovenia

Radiol Oncol 2012; 46(4): 337-345.

Received 8 May 2012  
Accepted 27 July 2012

Correspondence to: Assist Prof Irena Oblak, MD, PhD, Department of Radiotherapy, Institute of Oncology Ljubljana, Zaloška 2, 1000 Ljubljana, Slovenia. Phone: +386 1 5879 515; Fax: +386 1 5879 304 407; E-mail: ioblak@onko-i.si

Disclosure: No potential conflicts of interest were disclosed.

**Background.** Although the incidence of adenocarcinomas of the gastroesophageal junction (GEJ) is sharply rising in the Western world, there are still some disagreements about the staging and the treatment of this disease. The aim of this retrospective study was to analyse the effectiveness and safety of postoperative radiochemotherapy in patients with a GEJ adenocarcinoma treated at the Institute of Oncology Ljubljana.

**Patients and methods.** Seventy patients with GEJ adenocarcinoma, who were treated with postoperative radiochemotherapy between January 2005 and June 2010, were included in the study. The treatment consisted of 6 cycles of chemotherapy with 5-FU and cisplatin and concomitant radiotherapy with the total dose of 45 Gy.

**Results.** Twenty-six patients (37.1%) completed the treatment according to the protocol. The median follow-up time was 17.7 months (range: 3.3-64 months). Acute toxicity grade 3 or more, such as stomatitis, dysphagia, nausea or vomiting, and infection, occurred in 2.9%, 34.3%, 38.6% and 41.5% of patients, respectively. At 3 years locoregional control (LRC), disease-free survival (DFS), disease-specific survival (DSS) and overall survival (OS) were 78.2%, 25.3%, 35.8%, and 33.9%, respectively. In the multivariate analysis of survival, splenectomy and level of Ca 19-9 >20 kU/L before the adjuvant treatment were identified as independent prognostic factors for lower DFS, DSS and OS. Age <60 years, higher number of involved lymph nodes and advanced disease stage were identified as independent prognostic factors for lower DSS and OS.

**Conclusions.** In patients with GEJ adenocarcinoma who first underwent surgery, postoperative radiochemotherapy is feasible, but we must be aware of a high risk of acute toxic side effects.

Key words: gastroesophageal junction adenocarcinoma; postoperative radiochemotherapy; toxicity

## Introduction

Adenocarcinomas of the gastroesophageal junction (GEJ) represent a heterogeneous group of tumours with poor prognosis. They are defined as tumours, which arise within 5 cm proximal or distal to the esophagogastric junction.<sup>1</sup> Despite a dramatic rise in the incidence of GEJ adenocarcinomas in the Western world<sup>2</sup>, there are still some uncertainties and disagreement about the staging and the treatment of this disease. In the past, GEJ adenocarcinomas were staged either as an oesophageal

or gastric cancers, depending on the centre of the tumour. According to the UICC 7<sup>th</sup> criteria, they are now classified along oesophageal adenocarcinoma<sup>3</sup>, although some investigators still consider them to be stomach carcinomas. Most of us agree that these tumours should be treated separately from other tumours of stomach and oesophagus, because they differ in terms of epidemiology, pathogenesis, surgical approach and in prognosis, as well. Based on the anatomic location of the tumour centre, GEJ adenocarcinomas are subclassified by Siewert into three types: type I are tumours of distal oesopha-

gus; type II tumours (also termed true carcinomas of the cardia) arise immediately at the gastroesophageal junction; type III tumours have subcardial centre with predominant involvement of the proximal stomach or gastric cardia.<sup>1</sup>

The principal treatment of nonmetastatic GEJ adenocarcinomas is the surgical resection like in others gastrointestinal tumours.<sup>4,6</sup> There exist several different surgical approaches, depending on the localization of tumour, but the common goal is en-bloc removal of the entire tumour with adequate lymphadenectomy. The locoregional disease recurrence is observed in 25-80% of patients operated on.<sup>7,8</sup> A number of studies were carried out in order to try to improve the survival of the patients with GEJ adenocarcinomas. Uncertainties still remain, because GEJ patients were included either in gastric or oesophageal cancer studies.<sup>9-14</sup> Therefore, the optimal multimodal treatment strategy is still to be determined. However, it is clear that the patients with T2, T3 and/or N+ disease need additional treatment to surgery alone.

Preoperative chemotherapy with epirubicine (E), cisplatin (C) and fluorouracile (FU), or CFU regimen improves the overall survival in some, but not in all trials.<sup>9,15-17</sup> Preoperative radiochemotherapy trials gave mixed results<sup>10,11</sup>, but meta-analysis comparing preoperative chemotherapy with chemoradiotherapy confirmed that the trimodal therapy has higher 2-years overall survival rate (13% vs. 7%).<sup>18</sup>

Randomized studies of adjuvant radiotherapy only did not report any benefit.<sup>19,20</sup> Benefit of adjuvant chemotherapy only is also questionable.<sup>12,21,22</sup> However, Intergroup 0116, a randomized phase III trial of adjuvant radiochemotherapy, showed benefit for adjuvant radiochemotherapy compared to observation only after the surgery. In the study, 556 patients with resected gastric cancer were included, 20% of them with the adenocarcinomas of GEJ. Higher 3-years disease free survival (48% vs. 31%;  $p=0.001$ ) and 3-years overall survival (50% vs. 41%;  $p=0.005$ ) were observed for patients treated with surgery and adjuvant radiochemotherapy compared to those treated with surgery only. Critic of this trial was the lack of optimal lymphadenectomy, since only 10% of patients had D2 lymphadenectomy and only 36% had D1 lymphadenectomy. The rest of patients underwent D0 lymphadenectomy. It has been postulated that adjuvant radiochemotherapy compensated for suboptimal surgical procedures thus resulting in an overestimation of the survival benefit.<sup>13</sup> Despite these doubts there has also been proved benefit of adjuvant chemoradiotherapy after D2 lymphadenectomy in the study of Kim *et al.* with 544 patients.<sup>14</sup>

However, no comparative data of all these multimodal approaches have been published so far.

In the Institute of Oncology Ljubljana, nowadays preoperative chemoradiotherapy is the treatment of choice. There are still some patients with locoregionally advanced disease in whom the surgical resection is performed as the first treatment, followed by postoperative radiochemotherapy. Some of these patients have tumours clinically staged as T1-2 N0, but at the time of the surgery more advanced disease is determined. Some other patients have advanced but technically resectable disease with profuse bleeding or other conditions that require an immediate surgical intervention.

The main endpoints of this retrospective study were to find locoregional control (LRC), disease-free survival (DFS), disease-specific survival (DSS), and overall survival (OS) in patients with resectable GEJ adenocarcinoma, who were treated with postoperative radiochemotherapy in Slovenia in the period 2005 -2010.

## Patients and methods

### Patients and tumour characteristics

In the period from January 2005 to June 2010, 70 patients (55 males and 15 females; aged 34-77 years, mean age 60 years) were treated for non-metastatic adenocarcinoma of GEJ with postoperative concomitant chemoradiation at the Institute of Oncology Ljubljana, Slovenia. As the Institute of Oncology is the only hospital in Slovenia with radiotherapy facilities, this number represents the total population of patients with operable GEJ adenocarcinomas treated with adjuvant radiochemotherapy in the country. All patients had locally or regionally advanced disease without distant metastases (stages IIa-IIIc) (Table 1).

### Surgical treatment

Of 70 patients, 63 (90%) were operated on in two major surgical centres in Slovenia, at the University Medical Centres in Maribor and Ljubljana, and the remaining 7 (10%) patients in one of the Slovenian regional hospitals. Proximal subtotal resection of the stomach was performed in 3 patients (4.3%), total resection of the stomach in 48 patients (68.5%), transhiatal esophagogastrectomy in 14 patients (20%), and transthoracic esophagogastrectomy in 5 patients (7.1%). As determined on the histopathological examination of surgical specimen, the radical resection (R0) was performed in 56 (80%)

TABLE 1. Patients and tumour characteristics

Characteristics		No.	%
Gender	Male	55	78.6
	Female	15	21.4
Tumour classification by Siewert	Type I	10	14.3
	Type II	14	20
	Type III	32	45.7
	Undetermined	14	20
pT – stage	1	0	0
	2	23	32.9
	3	41	58.5
	4	6	8.6
pN – stage	0	5	7.1
	1	26	37.1
	2	25	35.7
Overall stage	IIa	4	5.7
	IIb	11	15.7
	IIIa	25	35.7
	IIIb	13	18.6
Tumour differentiation	Well	5	7.1
	Moderately	20	28.6
	Poor	39	55.7
	Unknown	6	8.6
Surgical procedures	Transhiatal oesophagogastrectomy	14	20
	Trans thoracic oesophagogastrectomy	5	7.1
	Proximal subtotal gastrectomy	3	4.3
	Total gastrectomy	48	68.5
Surgical margins	Negative	56	80
	Positive	14	20
Perineurial invasion	Yes	39	55.7
	No	16	22.9
	Unknown	15	21.4
Lymphovascular invasion	Yes	40	57.1
	No	6	8.6
	Unknown	24	34.3
Angioinvasion	Yes	20	28.6
	No	23	32.9
	Unknown	27	38.6

pT = pathological T-stage; pN = pathological N-stage

patients and in the remaining 14 (20%) patients non-radical surgery was performed - R1 resection in 11 patients (15.7 %) and R2 in 3 patients (4.2%).

### Tumour characteristics

Most frequently (in 32 patients; 45.7%), the primary tumour originated in the subcardial stomach and infiltrated the GEJ (Siewert III). In 10 patients (14.3%) tumour originated in the distal oesophagus (Siewert I) and in 14 patients (20%) in the cardia (Siewert II). In 14 patients (20%) the tumours extended over large area and for this reason their classification was not possible. The tumour was staged as pT2 in 23 patients (32.8%), pT3 in 41 patients (58.6%) and as pT4 in 6 patients (8.6%). Sixty-five patients (92.9%) had N+ disease (Table 1).

### Investigations before and during therapy

After the surgery, all patients with the disease of pathological stage II or higher, were presented to a multidisciplinary advisory team, consisting of a surgeon, radiation oncologist and medical oncologist, in order to assess the prospects of the eventual adjuvant treatment. All patients underwent a general clinical examination and blood counts. The patients with heart, liver or renal diseases and those with poor performance status ( $\geq 2$  according to the World Health Organization - WHO) were assessed as non-eligible for the adjuvant therapy. The investigations performed before the surgery to define the extent of the disease and to rule out metastatic disease, such as esophagogastroduodenoscopy, endoscopic ultrasound (EUS) of tumour areas, computer tomography (CT) of the thorax or abdomen, and PET-CT, were repeated only in the patients in whom the progression of the disease was clinically suspected.

During the therapy, the patients were clinically examined and referred to haematology and biochemistry blood tests once a week. The therapy-related local and systemic toxicity was assessed according to National Cancer Institute Common Toxicity Criteria (NCI-CTC) version 2.0.<sup>23</sup> The performance status of patients was determined and their body weight was measured on the weekly basis. During the treatment all patients were monitored by the nutritionist as well.

### Postoperative radiochemotherapy

The adjuvant treatment was initiated six to eight weeks after the surgery. The treatment schedule

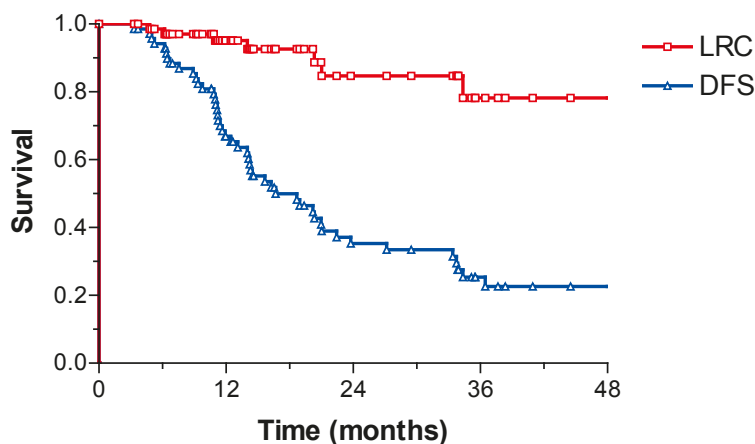


FIGURE 1. Locoregional control (LRC) and disease-free survival (DFS).

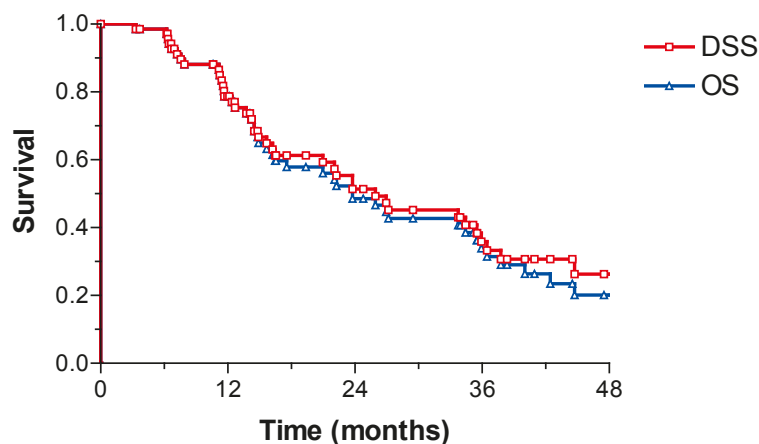


FIGURE 2. Disease-specific survival (DSS) and overall survival (OS).

included 6 cycles of chemotherapy with 5-FU (1000 mg/m<sup>2</sup>) in 96 hours continuous infusion and cisplatin (75 mg/m<sup>2</sup>) in a bolus on day 2 of each cycle. The treatment cycle was repeated every 28 days. Chemotherapy administration required hospitalization for appropriate monitoring, hydration, antiemetic therapy and other supportive treatment. Radiotherapy was supposed to start at the beginning of the second cycle. Three-dimensional conformal radiotherapy was performed using 15 MV photon beam linear accelerator. A prescribed dose was 45 Gy with daily fraction of 1.8 Gy, five times per week. The dose specification was based on the International Commission on Radiation Units (ICRU) Report 50 recommendations.<sup>21</sup> Treatment field borders were based on pretreatment investigations and imaging and postoperative anatomy, with tumour bed and regional lymph node areas

included. Dose-volume histograms were checked to verify that radiation plans were optimized regarding target coverage and normal tissue sparing. The position of individual irradiation fields was checked on the weekly basis.

In case of severe therapy-related toxicity, irradiation and/or chemotherapy doses were modified and adapted to the patient's physical condition or laboratory tests. When necessary, chemotherapy application was delayed, or radiotherapy was temporarily interrupted or terminated.

### Follow-up

After the completion of the treatment, patients performed regular follow-up visits. Physical examination and routine laboratory tests with tumour markers CEA, Ca 19-9 and Ca 72-4 were made every three months for the first two years after the treatment, every sixth months between two and five years after the treatment and thereafter once a year. Imaging investigations, CT of the thorax and abdomen and/or US of abdomen and chest X-ray, were performed two times per year for the first two years of the follow-up and then once a year. In case of suspected recurrence of the disease, other investigations such as endoscopy, EUS, magnetic resonance imaging of suspected area and PET-CT, were also performed.

### Statistical analysis and ethical consideration

The statistical analysis was performed using personal computer and software statistical package SPSS, version 18 (SPSS Inc., USA). LRC was defined as the period from the date of surgery till the local and/or regional recurrence, DFS till the local, regional or systemic recurrence, DSS till the death due to GEJ adenocarcinoma, and OS till the death from any cause, respectively. The survival of patients was computed from the date of surgery to the September 15, 2011 (close-out date). The survival probability was calculated using Kaplan-Meier estimate<sup>25</sup>, and the log rank test was used to evaluate the differences between individual groups of patients.<sup>26</sup> Independent prognostic values of variables that appeared as statistically significant on univariate analysis were tested by multivariate Cox regression analysis model.<sup>27</sup> Two-sided tests were used and the differences at  $p < 0.05$  were considered as statistically significant.

The retrospective study was carried out according to the Declaration of Helsinki.

TABLE 2. Toxicity of adjuvant radiochemotherapy

Toxicity	NCI grade (%)					total
	0	1	2	3	4	
Stomatitis	87.1	5.7	4.3	2.9	0	100
Radiodermatitis	97.1	1.4	1.4	0	0	100
Diarrhoea	74.3	21.4	4.3	0	0	100
Dysphagia	31.4	18.6	15.7	34.3	0	100
Nausea, vomiting	14.3	28.6	18.6	38.6	0	100
Infection	28.6	5.7	24.3	38.6	2.9	100
Leucocyte count	17.1	15.7	35.7	27.1	4.3	100
Haemoglobin level	8.6	57.1	31.4	2.9	0	100
Platelet count	60	28.6	7.1	2.9	1.4	100

## Results

### Outcome of disease

The median follow-up time of all 70 patients was 17.7 months (range: 3.3-64 months), whereas in survivors it was 27 months (range: 3.7-64 months). On the close-out date, 27 (38.6%) patients were still alive, 20 (28.6%) of them being with no signs of disease. Thirty-nine (55.7%) patients died from GEJ adenocarcinoma, and in 4 (5.7%) patients the cause of death could not be determined.

After adjuvant radiochemotherapy, the recurrence was observed in 46 (65.6%) patients. Local and/or regional recurrence developed in two (2.8%) patients at 20.3 and 33.4 months after the end of the treatment. Locoregional and systemic disease was observed in five (7.1%) patients in the median period of time of 11.4 months (range: 4.8-21 months), and distant metastases alone developed in 39 (55.7%) patients in the median period of time of 11.9 months (range: 3.3-36.5 months).

Median LRC was not reached. Median DFS, DSS and OS were 16.7 months (95% C.I.: 10-23.4), 25.9 (95% C.I.: 13.7-38.2) and 23.8 months (95% C.I.: 17-30.5), respectively. At 3 years LRC, DFS, DSS and OS were 78.2%, 25.3%, 35.8%, and 33.9%, respectively (Figures 1 and 2).

### Toxicity of adjuvant radiochemotherapy

Postoperative chemotherapy started in the median time of 6 weeks (range: 4.4-10.7 weeks) after the surgery. The total postoperative treatment time ranged from 0.5 to 25.6 weeks (median 14.6 weeks), whereas the duration of the radiotherapy part of

the protocol ranged from 1-5.6 weeks (median 5 weeks). Twenty-six patients (37.1%) completed the treatment according to the protocol. Sixty-seven patients (87.1%) reached the total radiation dose of 45 Gy, whereas in six patients (8.4%) the total delivered dose was lower (from 9-27 Gy). Three (4.3%) patients did not even start with the radiotherapy because of the side effects during the first cycle of chemotherapy. All six cycles of chemotherapy were administered in 26 patients (37.1%), 7 patients (10%) received five, 16 patients (22.9%) four, and 21 patients (30%) three cycles or less. No death occurred due to the therapy. Acute toxicity grade 3 or more, such as stomatitis, dysphagia, nausea and/or vomiting, and infection, occurred in 2.9%, 34.3%, 38.6% and 41.5% of patients, respectively (Table 2).

In 4 (5.7%) patients, an increase of body weight was recorded during the therapy, 5 (7.1%) patients maintained constant weight, whereas the remaining 61 (87.2%) patients lost their weight with respect to the weight they had at the beginning of the treatment. The maximum body weight loss was 20.5% (median 7.5%). Supplementary enteral nutrition was administered to 51 (72.9%) patients and for 20 (28.6%) patients parenteral nutrition was needed at least once during the treatment.

### Prognostic factors

In patients in whom splenectomy was performed as well, DFS ( $p=0.033$ ), DSS ( $p=0.032$ ) and OS ( $p=0.016$ ) were lower. Patients with the higher number of involved lymph nodes (stage N2 or N3) had lower DFS ( $p=0.022$ ) and OS ( $p=0.026$ ). Patients with weight loss >5 kg before the operation had lower DSS ( $p=0.032$ ) and OS ( $p=0.022$ ). Patients with advanced disease (stage IIIb, IIIc) and patients with perineurial invasion had lower OS ( $p=0.025$  and  $p=0.044$ , respectively). We did not find any differences in the survival regarding tumour localization classified by Siewert, tumour differentiation, type of the surgery and surgical specimen margins (R0 vs. R+). Older patients (aged 60 years or more) had higher DSS ( $p=0.045$ ) and OS ( $p=0.053$ ). Patients with levels of CEA more than 2 µg/L at the beginning of the postoperative treatment had lower DSS ( $p=0.023$ ) and OS ( $p=0.028$ ). Patients with levels of Ca 19-9 more than 20 kU/L at the beginning of the postoperative treatment had lower LRC, DFS, DSS and OS ( $p=0.018$ ,  $p=0.001$ ,  $p=0.007$  and  $p=0.017$ , respectively).

In the multivariate analysis of the survival, splenectomy and level of Ca 19-9 >20 kU/L before the

TABLE 3. Multivariate analysis of survival

Prognostic factors	n	Locoregional control	Disease free survival	Disease specific survival	Overall survival
		p	p	p	p
<i>pT- stage</i>					
pT 1+2	48			0.03	
pT 3+4	75				
<i>pN- stage</i>					
pN 0+1+2	98				
pN 3	25				
<i>Overall stage</i>					
Stage Ib-III	93	0.05			
Stage IV	30				
<i>Stomach involvement</i>					
Whole stomach	7				
Individual areas	116				
<i>Primary tumour site</i>					
Cardia	16				
Other sites	107				
<i>Perineurial invasion</i>					
Yes	45				
No	59				
<i>Angioinvasion</i>					
Yes	45		0.07		
No	23				
<i>Initial Hb level</i>					
Hb start ≤ 110 g/l	24	0.009	0.0001	0.02	0.01
Hb start > 110 g/l	99				
<i>5-FU total dose per cycle</i>					
≤ 4000 mg	109		0.03	0.07	
> 4000 mg	14				

pT = pathological T-stage; pN = pathological N-stage; Hb start = haemoglobin concentration at the start of the therapy

adjuvant treatment were identified as independent prognostic factors for the lower DFS ( $p=0.029$  and  $p=0.004$ ), DSS ( $p=0.012$  and  $p=0.001$ ) and OS ( $p=0.006$  and  $p<0.0001$ ). Age < 60 years, higher number of involved lymph nodes (stage N2 or N3) and advanced disease stage (stage IIIb or IIIc) were identified as independent prognostic factors for the lower DSS ( $p=0.009$ ,  $p=0.019$  and  $p=0.006$ , respectively) and OS ( $p=0.005$ ,  $p=0.014$  and  $p=0.003$ , respectively) (Table 3).

## Discussion

Patients with GEJ adenocarcinomas treated with surgery only have a very poor prognosis with a 5-year survival rate of approximately 20%.<sup>28,29</sup> Many authors proved that the combined radio-

therapy and chemotherapy, applied preoperatively, postoperatively or at inoperable patients might significantly improve the survival of these patients.<sup>10,11,13,14,18,30</sup> In our study the retrospective analysis of 70 patients with GEJ adenocarcinomas treated with postoperative radiochemotherapy was performed. The radical resection was performed in 80% of our patients, which could be comparable to results of other published studies.<sup>31-34</sup> In our study the 3-year LRC, DFS, DSS and OS results should not be compared with results of MacDonald *et al.*<sup>13</sup>, because the majority of patients in his study had stomach carcinoma and only 20% patients had GEJ carcinoma. The subanalysis for those patients was not performed. The other reason why the data are not comparable is the use of different cytostatics; in MacDonald's study chemotherapy included 5-FU and leucovorin and in our study 5-FU and cispl-

atin were administered. In MacDonald's study, patients treated with postoperative radiochemotherapy had 48% 3-years DFS and 50% 3-years OS. The study of Adelstein *et al.*<sup>31</sup> in which 50 patients with carcinomas of oesophagus and GEJ treated with postoperative radiochemotherapy with 5-FU and cisplatin were included, reported that 4-year LRC, DFS and OS were 86%, 50% and 51%. These results are better than ours, but in their study also patients with less advanced disease and, therefore, a better prognosis were included.

Although one of the critique of the American intergroup study<sup>13</sup> was referred to the high percentage of patients (36%), who did not complete the regimen, in our study only 37% finished the therapy according to the protocol. While most of our patients received full radiation therapy (87.1%), all six cycles of chemotherapy were applied in only 26 patients (37.1%). The most common toxic side effects classified as grade 3 or higher were, as in MacDonald's study<sup>13</sup>, gastrointestinal toxic effects, infections and leucopenia. In Adelstein's study<sup>31</sup> only 3 patients did not finished the treatment according to the protocol, but their schedule contained only 2 cycles while our schedule contained 6 cycles of chemotherapy with 5-FU and cisplatin. Therefore, greater toxicity and more treatment interruptions in our study were expected.

Our analysis demonstrated that patients with the involvement of numerous lymph nodes and more advanced stage of disease have a lower survival. These are well known factors that have an impact on the survival of patients with GEJ carcinoma.<sup>35-41</sup>

Tumour origin (tumour localization classified by Siewert), tumour differentiation, type of surgery and positive surgical margins did not have any impact on the outcome as in some other series as well.<sup>31,42</sup> On the other hand, some other authors reported that patients with GEJ adenocarcinomas Siewert type I have a better prognosis because they have an earlier onset of symptoms (like dysphagia) and are, therefore, diagnosed in earlier stages. They also argued that poor differentiation of tumours has negative effect on the survival due to the increased risk of lymphatic dissemination and that the presence of tumour cells in the resected margins could have a negative impact on the survival of operated patients.<sup>35</sup>

Weight loss is a common symptom of GEJ cancer. It is due to the mechanical effects of the tumour that causes dysphagia, early satiety, nausea and vomiting. Beside this, systemic influences like hypermetabolism, anorexia and altered protein me-

tabolism, have an important role in the nutritional status of these patients.<sup>43</sup> In our study, weight loss of more than 5 kg before the operation was associated with the lower DFS, DSS and OS. In several other studies – not only at patients with GEJ adenocarcinoma – weight loss before the treatment was a negative prognostic factor.<sup>42,44-47</sup> In a large study of patients with oesophageal cancer, weight loss greater than 10% of pre-morbid weight was the only significant predictor of early death in patients undergoing the surgical resection.<sup>45</sup>

Our analysis demonstrated the survival benefit for patients older than 60 years. Similar results were described in the study of Crumley *et al.* who found that patients older than 65 years had better 3-year survival than younger patients (32% vs. 29%;  $p=0.017$ ).<sup>42</sup> Some other studies did not find any prognostic significance between different groups of age.<sup>48-51</sup>

The multivariate analysis also identified splenectomy as a negative prognostic factor. In several published studies splenectomy had a negative impact on the survival,<sup>52-53</sup> while other studies did not demonstrate marked effect on the survival.<sup>33,34,54</sup> The need for splenectomy in patients with GEJ is still controversial. Compared with a gastric cancer, in GEJ cancer lymph node metastases in the splenic hilum are more frequent and that is why some surgeons consider splenectomy as necessary.<sup>55,56</sup> However, splenectomy is known to be associated with increased morbidity after the resection of proximal gastric and GEJ cancer, especially due to a higher risk of infections.

One of the independent prognostic factors in our study was also the level of Ca 19-9 more than 20 kU/L before the start of the postoperative treatment. Elevated tumour markers are known to be associated with the higher probability of lymph node metastases, lymphatic and blood vessel invasion, depth of invasion, higher stage and dissemination of the disease. Kočevar *et al.*<sup>57</sup> reported that translationally controlled tumour protein (TPT1) was shown to be differentially expressed only in patients GEJ cancer, but, it clinical have to be established.

## Conclusions

Postoperative radiochemotherapy for GEJ is an attractive approach for several reasons since the treatment decision is based on the true pathologic stage and hence a more accurate assessment of the disease extent. On the other hand, it also has some

disadvantages, such as difficult recovery of some patients after extensive resections and worse blood supply and oxygenation of tumour bed and, therefore, less effective treatment with radiochemotherapy. However, even if we consider that preoperative radiochemotherapy can improve resectability and, therefore, enables us the higher proportion of curative resections, postoperative radiochemotherapy is still reserved for the selected group of patients, who first underwent surgery due to different reasons.

## References

- Siewert JR, Stein HJ. Classification of adenocarcinoma of the oesophagogastric junction. *Br J Surg* 1998; **85**: 1457-9.
- Parkin DM, Bray F, Ferlay J, Pisani P. Global cancer statistic, 2002. *CA cancer J Clin* 2005; **55**: 74-108.
- American Joint Committee on Cancer. AJCC cancer staging manual, 7th edition. New York: Springer-Verlag; 2009.
- Wrnski M, Ziarkiewicz-Wroblewska B, Slodkowski M, Cebulski W, Gornicka B, Krasnodebski IW. Mesenteric fibromatosis with intestinal involvement mimicking a gastrointestinal stromal tumour. *Radiol Oncol* 2011; **45**: 59-63.
- Oblak I, Velenik V, Anderluh F, Strojanc P. Results of adjuvant radiochemotherapy for gastric adenocarcinoma in Slovenia. *Eur J Surg Oncol* 2007; **33**: 982-7.
- Oblak I, Anderluh Franc, Velenik V. Postoperative radiochemotherapy for gastric adenocarcinoma: long term results. *Radiol Oncol* 2009; **43**: 274-81.
- Power DG, Reynolds JV. Localized adenocarcinoma of the esophagogastric junction-is there a standard of care? *Cancer Treatm Rev* 2010; **36**: 400-9.
- Wayman J, Bennet MK, Rames SA, Griffin SM. The pattern of recurrence of adenocarcinoma of the oesophagogastric junction. *Br J Cancer* 2002; **86**: 1223-9.
- Schuhmacher C, Gretschel S, Lordick F, Reichardt P, Hohenberger W, Eisenberger CF, et al. Neoadjuvant chemotherapy compared with surgery alone for locally advanced cancer of the stomach and cardia: European Organisation for Research and Treatment of Cancer randomized trial 40954. *J Clin Oncol* 2010; **28**: 5210-8.
- Walsh TN, Noonan N, Hollywood D, Kelly A, Keeling N, Hennessy TP. A comparison of multimodal therapy and surgery for esophageal adenocarcinoma. *N Engl J Med* 1996; **335**: 462-7.
- Tepper J, Krasna MJ, Niedzwiecki D, Hollis D, Reed CE, Goldberg R, et al. Phase III trial of trimodality therapy with cisplatin, fluorouracil, radiotherapy and surgery compared with surgery alone for esophageal cancer: CALGB 9781. *J Clin Oncol* 2008; **26**: 1086-92.
- Ajani JA, Rodriguez W, Bodoky G, Moiseyenko V, Lichinitser M, Gorbunova V, et al. Multicenter phase III comparison of cisplatin/S-1 with cisplatin/infusional fluorouracil in advanced gastric or gastroesophageal adenocarcinoma study: the FLAGS trial. *J Clin Oncol* 2010; **28**: 1547-53.
- Macdonald JS, Smalley SR, Benedetti J, Hundahl SA, Estes NC, Stemmermann G, et al. Chemoradiotherapy after surgery compared with surgery alone for adenocarcinoma of the stomach or gastroesophageal junction. *N Engl J Med* 2001; **345**: 725-30.
- Kim S, Lim DH, Lee J, Kang WK, MacDonald S, Park CH, et al. An observational study suggesting clinical benefit for adjuvant postoperative chemoradiation in a population of over 500 cases after gastric resection with D2 nodal dissection for adenocarcinoma of the stomach. *Int J Radiat Oncol Biol Phys* 2005; **63**: 1279-85.
- Cunningham D, Allum WH, Stenning SP, Thompson JN, Van de Velde CJH, Nicolson M, et al. Perioperative chemotherapy versus surgery alone for resectable gastroesophageal cancer. *N Engl J Med* 2006; **335**: 11-20.
- Ychou M, Boige V, Pignon JP, Conroy T, Bouché O, Lebreton G, et al. Perioperative chemotherapy compared with surgery alone for resectable gastroesophageal adenocarcinoma: an FNCLCC and FFCD multicenter phase III trial. *J Clin Oncol* 2011; **29**: 1715-21.
- Stahl M, Walz MK, Stuschke M, Lehmann N, Meyer HJ, Riera-Knorrenschild J, et al. Phase III comparison of preoperative chemotherapy compared with chemoradiotherapy in patients with locally advanced adenocarcinoma of the esophagogastric junction. *J Clin Oncol* 2009; **27**: 851-6.
- Gebski V, Burmeister B, Smithers BM, Foo K, Zalberg J, Simes J; Australasian Gastro-Intestinal Trials Group. Survival benefits from neoadjuvant chemoradiotherapy or chemotherapy in oesophageal carcinoma: a meta-analysis. *Lancet Oncol* 2007; **8**: 226-34.
- Fok M, Sham JS, Choy D, Cheng SW, Wong J. Postoperative radiotherapy for carcinoma of the esophagus: a prospective, randomized controlled study. *Surgery* 1993; **173**: 138-47.
- Teniere P, Hay JM, Fingerhut A, Fagniez PL. Postoperative radiation therapy does not increase survival after curative resection for squamous cell carcinoma of the middle and lower esophagus as shown by a multicenter controlled trial. French university association for surgical research. *Surg Gynecol Obstet* 1991; **173**: 123-30.
- Sun P, Xiang JB, Chen ZY. Meta-analysis of adjuvant chemotherapy after radical surgery for advanced gastric cancer. *Br J Surg* 2009; **96**: 23-33.
- Liu TS, Wang Y, Chen SY, Sun YH. An updated meta-analysis of adjuvant chemotherapy after curative resection for gastric cancer. *Eur J Surg Oncol* 2008; **34**: 1208-16.
- Ajani JA, Welch SR, Raber MN, Fiels WS, Krakoff IM. Comprehensive criteria for assessing therapy-induced toxicity. *Cancer Invest* 1990; **8**: 147-59.
- ICRU 50: Prescribing, recording, and reporting photon beam therapy. Bethesda: International Commission on Radiation Units and Measurements Press; 1993.
- Kaplan EL, Meier P. Nonparametric estimation from incomplete observations. *J Am Stat Assoc* 1958; **53**: 457-81.
- Peto R, Pike MC, Armitage P. Design and analysis of randomized clinical trials requiring prolonged observation of each patient. II. Analysis and examples. *Br J Cancer* 1977; **35**: 1-39.
- Cox DR. Regression models and life-tables. *J R Stat Soc Bull* 1972; **34**: 187-220.
- Enzinger PC, Mayer RJ. Esophageal cancer. *N Engl J Med* 2003; **349**: 2241-52.
- Pisani P, Parkin DM, Ferlay J. Estimates of the worldwide mortality from 18 major cancers in 1985. *Int J Cancer* 1993; **55**: 891-903.
- Torrente S, Turri L, Deantonio L, Cena T, Gambaro G, Magnani C, et al. Concomitant chemo-radiotherapy for unresectable oesophageal cancer: A mono-institutional study on 40 patients. *Rep Pract Oncol Radiother* 2012; **17**: 226-32.
- Adelstein DJ, Rice TW, Rybicki LA, Saxton JP, Videtic GMM, Murthy SC, et al. Mature results from a phase II trial of postoperative concurrent chemoradiotherapy for poor prognosis cancer of the esophagus and gastroesophageal junction. *J Thorac Oncol* 2009; **4**: 1264-9.
- Feith M, Stein HJ, Siewert JR. Adenocarcinoma of the esophagogastric junction: surgical therapy based on 1602 consecutive resected patients. *Surg Oncol Clin N Am* 2006; **15**: 751-64.
- Weitz J, Jaques DP, Brennan M, Karpeh M. Association of splenectomy with postoperative complications in patients with proximal gastric and gastroesophageal junction cancer. *Ann Surg Oncol* 2004; **11**: 682-9.
- Pultrum BB, van Bastelaar J, Schreurs MA, van Dullemen HM, Groen H, Nijsten MWN, et al. Impact of splenectomy on surgical outcome in patients with cancer of the distal esophagus and gastro-esophageal junction. *Dis Esophagus* 2008; **21**: 334-9.
- Lagarde SM, ten Kate FJ, Reitsma JB, Busch OR, van Lanschot JJ. Prognostic factors in adenocarcinoma of the esophagus or gastroesophageal junction. *J Clin Oncol* 2006; **24**: 4347-55.
- Eloubeidi MA, Desmond R, Arguedas MR, Reed CE, Wilcox CM. Prognostic factors for the survival of patients with esophageal carcinoma in the US. *Cancer* 2002; **95**: 1434-43.



37. Steup WH, de Leyn P, Deneffe G, van Raemdonck D, Coosemans W, Lerut T. Tumors of the esophagogastric junction. Long-term survival in relation to the pattern of lymph node metastasis and a critical analysis of the accuracy or inaccuracy of pTNM classification. *J Thorac Cardiovasc Surg* 1996; **111**: 85-94.
38. Mariette C, Taillier G, van Seuning I, Triboulet JP. Factors affecting postoperative course and survival after en bloc resection for esophageal carcinoma. *Ann Thorac Surg* 2004; **78**: 177-83.
39. Lerut T, Coosemans W, Decker G, de Leyn P, Moons J, Naftoux P, et al. Extended surgery for cancer of the esophagus and gastroesophageal junction. *J Surg Res* 2004; **117**: 58-63.
40. Predrazzani C, de Manzoni G, Marrelli D, Giacomuzzi S, Corso G, Minicozzi AM, et al. Lymph node involvement in advanced gastroesophageal junction adenocarcinoma. *J Thorac Cardiovasc Surg* 2007; **134**: 378-85.
41. Siewert JR, Feith M, Werner M, Stein HJ. Adenocarcinoma of the esophagogastric junction: results of surgical therapy based on anatomical/topographic classification in 1002 consecutive patients. *Ann Surg* 2000; **232**: 353-61.
42. Crumley ABC, Stuart RC, McKernan M, Going JJ, Shearer CJ, McMillan DC. Comparison of the pre-treatment clinical prognostic factors in patients with gastro-oesophageal cancer and proposal of a new staging system. *J Gastrointest Surg* 2010; **14**: 781-7.
43. Deans DAC, Tan BH, Wigmore SJ, Ross JA, de Beaux AC, Paterson-Brown S, et al. The influence of systemic inflammation, dietary intake and stage of disease on rate of weight loss in patients with gastro-oesophageal cancer. *Br J Cancer* 2009; **100**: 63-9.
44. Stahl M, Wilke H, Stuschke M, Walz MK, Fink U, Molls M, et al. Clinical response to induction chemotherapy predicts local control and long-term survival in multimodal treatment of patients with locally advanced esophageal cancer. *J Cancer Res Clin Oncol* 2005; **131**: 67-72.
45. Kelsen DP, Ginsberg R, Pajak TF, Sheahan DB, Gunderson L, Mortimer J, et al. Chemotherapy followed by surgery compared with surgery alone for localized esophageal cancer. *N Engl J Med* 1998; **339**: 1979-84.
46. Plaisant N, Senesse P, Azria D, Lemanski C, Ychou M, Quenet F, et al. Surgery for esophageal cancer after concomitant radiochemotherapy: oncologic and functional results. *World J Surg* 2005; **29**: 32-8.
47. Kovac V, Zwitter M, Zagar T. Improved survival after introduction of chemotherapy for malignant pleural mesothelioma in Slovenia: Population-based survey of 444 patients. *Radiol Oncol* 2012; **46**: 136-44.
48. Leigh Y, Seagroatt V, Goldacre M, McCulloch P. Impact of socio-economic deprivation on death rates after surgery for upper gastrointestinal tract cancer. *Br J Cancer* 2006; **95**: 940-3.
49. Sabel MS, Smith JL, Nava HR, Mollen K, Douglass HO, Gibbs JF. Esophageal resection for carcinoma in patients older than 70 years. *Ann Surg Oncol* 2002; **9**: 210-4.
50. McKernan M, McMillan DC, Anderson JR, Angerson WJ, Stuart RC. The relationship between quality of life (EORTC QLQ-C30) and survival in patients with gastro-oesophageal cancer. *Br J Cancer* 2008; **98**: 888-93.
51. Sauvanet A, Mariette C, Thomas P, Lozac'h P, Segol P, Tiret E, et al. Mortality and morbidity after resection for adenocarcinoma of the gastroesophageal junction: predictive factors. *J Am Coll Surg* 2005; **201**: 253-62.
52. Cuschieri A, Weeden S, Fielding J, Bancewicz J, Craven J, Joypaul V, et al. Patient survival after D1 and D2 resections for gastric cancer: long-term results of the MRC randomized surgical trial. Surgical Co-operative Group. *Br J Cancer* 1999; **79**: 1522-30.
53. Schmid A, Thybusch A, Kremer B, Henne-Bruns D. Differential effects of radical D2-lymphadenectomy and splenectomy in surgically treated gastric cancer patients. *Hepatogastroenterology* 2000; **47**: 579-85.
54. Huang CM, Wang JB, Lu HS, Zheng CH, Li P, Xie JW, et al. Prognostic impact of splenectomy on advanced proximal gastric cancer with more than 10 lymph node metastasis. *Chin Med J* 2009; **122**: 2757-62.
55. Buyukasik O, Hasdemir AO, Gulnerman Y, Col1 C, Ikiz O. Second primary cancers in patients with gastric cancer. *Radiol Oncol* 2010; **44**: 239-43.
56. Ikequchi M, Kaibara N. Lymph node metastasis at the splenic hilum in proximal gastric cancer. *Am Surg* 2004; **70**: 645-8.
57. Kočevar N, Odreman F, Vindigni A, Grazio SF, Komel R. Proteomic analysis of gastric cancer and immunoblot validation of potential biomarkers. *World J Gastroenterol* 2012; **18**: 1216-28.

# Treatment outcomes and survival in patients with primary central nervous system lymphomas treated between 1995 and 2010 - a single centre report

Barbara Jezersek Novakovic

Department of Medical Oncology, Institute of Oncology Ljubljana, Ljubljana, Slovenia

Radiol Oncol 2012; 46(4): 346-353.

Received 9 June 2012

Accepted 1 September 2012

Correspondence to: Assoc. Prof. Barbara Jezeršek Novaković MD, PhD, Department of Medical Oncology, Institute of Oncology Ljubljana, Zaloška 2, SI-1000 Ljubljana, Slovenia. Phone: +386 1 5879 280, Fax: +386 1 5879 305, E-mail: bjezersek@onko-i.si

Disclosure: No potential conflicts of interest were disclosed.

**Background.** Primary central nervous system lymphomas (PCNSL) are rare variants of extranodal non-Hodgkin's lymphomas that are nowadays primarily treated with high-dose methotrexate or methotrexate-based chemotherapy with or without radiation therapy. The optimal treatment of PCNSL is still unknown and there are differences in clinical practice.

**Patients and methods.** With a retrospective research we evaluated our series of patients with PCNSL in regards to the patient's characteristics, treatment results, disease specific survival and overall survival. Fifty nine patients who attended the Institute of Oncology Ljubljana between 1995 and 2010 were treated according to the protocol that was valid at the time of the patient's admission. Between 1995 and 1999, the systemic treatment was classical CHOP (cyclophosphamide, doxorubicin, vincristine, steroids) chemotherapy, and later on high-dose methotrexate either alone or in combination with other agents. From 1999 onwards, radiation therapy was applied according to the patient's age and response to chemotherapy, prior to that all patients treated with CHOP were also irradiated. Patients ineligible for the systemic treatment were treated with sole radiation therapy.

**Results.** There was a strong female predominance in our series and the median age at diagnosis was 59.8 years. Patients had predominantly aggressive B cell lymphomas (69.5%), one patient had marginal cell lymphoma and two patients T cell lymphoma. In total, 20.3% of patients were treated just with chemotherapy, 33.9% with combined therapy and 42.4% with sole radiation therapy. The overall response rate to the primary treatment in patients treated with sole chemotherapy was 33.3%, in patients treated with combined therapy 65% and in patients treated only with radiation therapy 56%, respectively. In terms of response duration, significantly better results were achieved with combined therapy or radiation therapy alone compared to sole chemotherapy ( $p < 0.0006$ ). The median overall survival of the whole cohort was 11 months and the overall survival was significantly affected by the patient's age. The longest overall survival was observed in patients treated with combined therapy (median survival of 39 months). Patients treated just with radiation therapy had a median overall survival of 9 months and those treated with sole chemotherapy of 4.5 months, respectively.

**Conclusions.** The treatment outcomes in ordinary clinical practice are definitely inferior to the ones reported in clinical trials. The now standard treatment with high-dose methotrexate with or without radiation therapy is sometimes too aggressive and, therefore, a careful selection on the basis of patient's age, performance status and concomitant diseases of those eligible for such treatment is mandatory. According to our results from a retrospective study, radiation therapy should not be excluded from the primary treatment.

Key words: primary central nervous system lymphomas; treatment outcomes; survival

## Introduction

Primary central nervous system lymphomas (PCNSL) are quite rare variants of extranodal non-Hodgkin's lymphomas (NHL) that involve the brain, eyes, leptomeninges or spinal cord without evidence of systemic disease.<sup>1,2</sup> The largest part of cases of non-AIDS related PCNSL are diagnosed in patients between 45 and 70 years of age.<sup>3,4</sup> The incidence increases with advancing age and just a few cases have been reported in children where more frequently other tumors of the central nervous system are observed.<sup>5,6</sup> Men and women are reported to be equally affected.

The most important risk factor for the development of PCNSL is immunodeficiency (*e.g.* HIV infection, iatrogenic immune suppression, congenital immune deficiency) and this may play a role in the pathogenesis of disease.<sup>7,8</sup> Five distinct clinicopathological entities have been described – intracranial lesion (solitary or multiple); diffuse leptomeningeal or periventricular lesions; vitreous/uveal deposits; intradural spinal cord lesion and nerve seeking lymphoma (neurolymphomatosis).<sup>4,5,9</sup>

Presenting symptoms and signs of the disease vary, depending on the site of the involvement and they may include focal neurological deficits, neuropsychiatric symptoms, signs of raised intracranial pressure, seizures, and ocular symptoms – as they appear in other primary or secondary brain tumors.<sup>10-12</sup>

Untreated PCNSL have a rapidly fatal course, with a survival of approximately 1.5 months from the time of diagnosis. Survival after the whole brain radiation therapy ranges from 10 to 18 months, but was reported to rise to an average of 44 months following chemotherapy and radiation therapy, or chemotherapy alone.<sup>13-19</sup> Yet, radiation therapy is associated with a high incidence of neurotoxicity, which is however not seen after the radiation therapy of patients with brain metastases of solid tumors because of their shorter survival or lower tumor dose.<sup>20</sup> Although currently available therapeutic regimes prolong the survival, they are in contrast to therapies used to treat systemic lymphomas,<sup>21,22</sup> not curative in most patients.

The optimal treatment of PCNSL is unknown and there are differences in clinical practice. The PCNSL are primarily treated with a high-dose methotrexate or methotrexate-based chemotherapy with or without radiation therapy. The role of radiation therapy is controversial due to its late toxicity, especially in older adults.<sup>17-19, 23-27</sup> Treatment decisions should, therefore, take into consideration

both response rates and impact on the quality of life.

With this retrospective research we evaluated our series of patients with PCNSL in regards to the patient's characteristics, treatment results, disease specific survival and overall survival.

## Patients and methods

Fifty nine patients with PCNSL who attended the Institute of Oncology Ljubljana between 1995 and 2010 were identified from the database of the Cancer Registry of Slovenia. Patients who had any evidence of systemic disease (*i.e.* 10 patients from the primary database) were excluded from further evaluation. Patients with PCNSL were treated according to the protocol that was valid at the time of the patient's admission. Between 1995 and 1999, patients were treated with classical CHOP (cyclophosphamide, doxorubicin, vincristine, steroids) chemotherapy, intrathecal applications of methotrexate and cytarabine and radiation therapy (radiation to the whole brain with 30-36 Gy and 10 to 14 Gy boost on primary tumor localization). Those ineligible for systemic therapy were treated with radiation therapy only. From 1999 onwards, patients were treated with a high-dose methotrexate (3 to 5 g/m<sup>2</sup>) either alone or in combination with a high-dose cytarabine (2 to 3 g/m<sup>2</sup> twice daily for two consecutive days) or other blood-brain barrier passing agents (vincristine, procarbazine, carmustine). Radiation therapy was applied according to the patient's age and response to chemotherapy. The patients' characteristics, pathohistological diagnosis, disease stage, response to treatment and survival data were taken from patients' records. The treatment response was re-evaluated according to the International Primary CNS Lymphoma Collaborative Group Guidelines for Response Assessment<sup>28</sup> and the disease-free and overall survivals were assessed by means of Kaplan Meier survival curves. For the determination of statistical differences the log rank test and Chi-square test were applied.

## Results

### Patients' characteristics and treatment

The patients' characteristics are given in Table 1. None of the patients was HIV positive. Patients had predominantly aggressive B cell lymphomas (69.5%), one patient had marginal cell lymphoma and two patients T cell lymphoma (3.4%). Majority

**TABLE 1.** Characteristics of 59 patients with primary central nervous system lymphomas

Gender	Males 20; Females 39	F/M ratio: 1.95
<b>Age at diagnosis</b>	<b>14-85 years</b>	<b>Median: 59.8 years</b>
<b>Histology</b>		
Diffuse large B cell lymphoma (DLBCL)	39	66.1%
Immunoblastic lymphoma	1	1.7%
Burkitt's lymphoma	1	1.7%
Marginal cell lymphoma	1	1.7%
Unspecified B cell lymphoma	15	25.4%
T cell lymphoma	2	3.4%
<b>Site of disease</b>		
Cerebral hemisphere	20	33.9%
Deep structures	32	54.2%
Cerebellum	3	5.1%
Spinal cord	4	6.8%
<b>Multiple lesions</b>		
Yes	20	33.9%
<b>Positive cerebrospinal fluid cytology</b>		
Yes	6	10.2%
No	51	86.4%
Unknown	2	3.4%
<b>Leptomeningeal involvement (MRI or positive CSF cytology)</b>		
Yes	11	18.6%
No	47	79.7%
Unknown	1	1.7%
<b>Performance status (ECOG) prior to treatment</b>		
0	3	5.1%
1	13	22.0%
2	2	3.4%
3	10	16.9%
4	30	50.8%
Unknown	1	1.7%
<b>Serious concomitant diseases</b>		
Yes	13	22.0%
<b>IPI</b>		
0	3	5.1%
1	5	8.5%
2	18	30.5%
3	16	27.1%
4	8	13.6%
Undetermined	9	15.3%

MRI = magnetic resonance imaging; CSF = cerebrospinal fluid; ECOG = Eastern Cooperative Oncology Group; IPI = international prognostic index

**TABLE 2.** Primary treatment of primary central nervous system lymphomas

<b>Surgery</b>		
None	5	3.4%
Biopsy	22	37.3%
Radical	19	32.2%
Non radical	13	22.0%
<b>Chemotherapy (CHT)</b>		
None	27	45.8%
HD MTX	17	28.8%
Other	15	25.4%
<b>Radiation therapy (RT)</b>		
None	14	23.7%
Radical	37	62.7%
Non radical	8	13.6%
<b>Primary treatment</b>		
CHT	12	20.3%
CHT + radical RT	19	32.2%
CHT + palliative RT	1	1.7%
RT	25	42.4%
Radical surgery	2	3.4%

HD MTX – high dose methotrexate

of patients (93.2%) had intracranial lesions and in twenty (33.2%) these lesions were multiple. Deep brain structures were affected in 54.2% of patients. The leptomeningeal involvement was confirmed in 18.6% of the patients, cerebrospinal fluid cytology was positive in 10.2% of patients. Spinal cord lesions were detected in 6.8% of patients, while vitreous/uveal deposits and nerve seeking lymphoma have not been observed in our series.

Performance status prior to the treatment was poor, 71.1% of patients had the performance status of 2 or more. Thirteen patients also suffered from serious concomitant diseases. The international prognostic index (IPI) fell in the high intermediate or in the high risk group in 40.7% of patients. The prognostic factors reported by the International Extranodal Lymphoma study group were not followed systematically because the data on elevated cerebrospinal fluid (CSF) protein concentration were frequently not precise in patients' records.

Details on the primary treatment are given in Table 2. Just five patients had no surgery, while all the others had at least stereotactic biopsy to diagnose lymphoma. Chemotherapy was given to 54.2% of patients, slightly more than half of them received a high-dose methotrexate either as a sin-

gle agent (two patients) or in combination with a high-dose cytarabine (nine patients), CHOP (one patient) or with other blood-brain barrier passing agents (five patients). Fifteen patients received other regimens – eight patients from the beginning of our series (*i.e.* prior to 1999) were treated with CHOP and seven patients with either middle-dose (500 mg/m<sup>2</sup>) methotrexate (five patients) or just corticosteroids (two patients). Patients received median 4 cycles of CHOP chemotherapy (range 2 to 6), median 3 cycles of high-dose methotrexate (range 1 to 6) and median 3 cycles of high-dose methotrexate when combined with high-dose cytarabine (range 1 to 4). Twenty patients were treated after chemotherapy also with radiation therapy (one in a palliative setting) and in twenty-five patients radiation therapy was the only primary treatment. Two patients were treated just with radical surgery.

**Treatment outcomes**

The overall response rate to the primary treatment in patients treated with sole chemotherapy was 33.3%, in patients treated with chemotherapy followed by radiation therapy 65% and in patients treated only with radiation therapy 56%, respectively. In total, nineteen patients (57.6%) relapsed from the achieved complete or partial response. In fifteen patients, the relapse occurred in the central nervous system (CNS) (one of them had a concomitant systemic relapse) while five patients relapsed just outside the CNS. The disease-free survival for different treatment modalities is given in Figure 1. In terms of response duration, significantly better results were achieved with the combined therapy or radiation therapy alone compared to sole chemotherapy or radical surgery ( $p < 0.0006$ ).

When taking in account different chemotherapy regimens, the best outcomes were achieved with the combination of a high-dose methotrexate and a high-dose cytarabine since the overall response rate was 55.5%. In this group, three patients achieved complete remission and two patients partial remission all of them except one receiving a full course of treatment (4 cycles). In three patients, stable disease was observed after 2 cycles and another patient progressed after the first cycle. However, the disease-free survival was better in case of CHOP regimen (which was in all cases followed with radiation therapy) compared to regimens comprising a high-dose methotrexate, yet insignificantly ( $p = 0.29$ ) (Figure 2).

The median overall survival of the whole cohort was 11 months (95% CI: 0.71 – 21.29) The overall

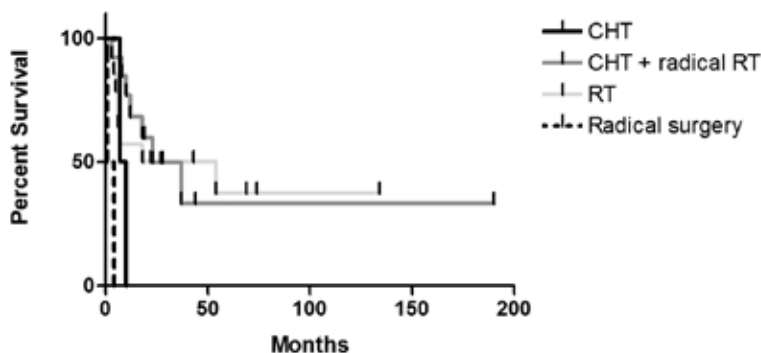


FIGURE 1. The disease-free survival for different treatment modalities.

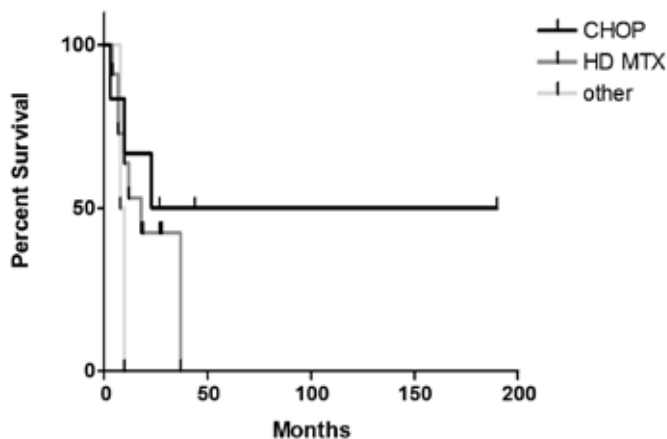


FIGURE 2. The disease-free survival after different chemotherapeutic regimens.

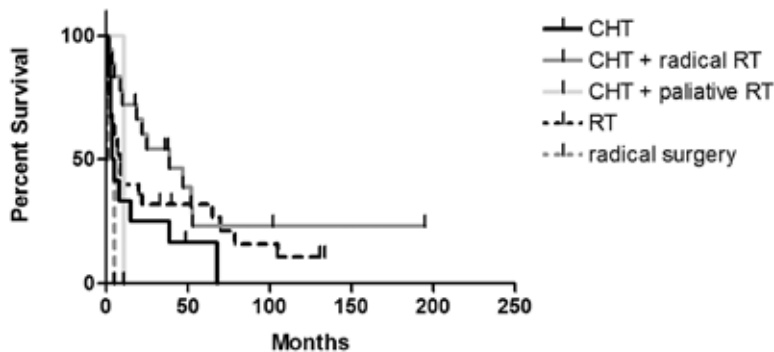


FIGURE 3. The overall survival for different treatment modalities.

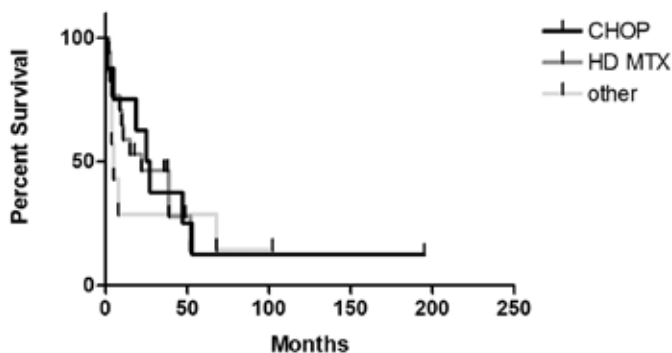


FIGURE 4. The overall survival after different chemotherapeutic regimens.

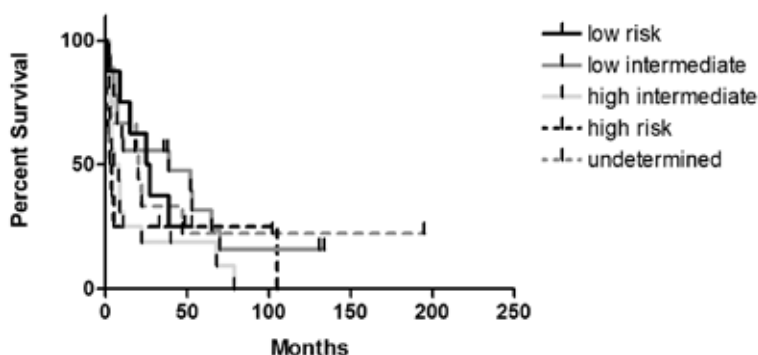


FIGURE 5. Overall survival according to different IPI categories.

survival was significantly affected by patient's age – the median overall survival in patients aged below 60 years was namely 27 months (95% CI: 0.00 – 71.96) while in patients aged over 60 years it was just 7 months (95% CI: 2.81 – 11.19) ( $p=0.006$ ). Six patients (10%) survived more than 105 months after the diagnosis of PCNSL has been made – all of them were aged below 60 years. Altogether, these patients had the diffuse large B cell histology and were treated as follows: three patients with radical radiotherapy, one with a high-dose methotrexate and radiation therapy, one with CHOP chemotherapy and radiation therapy and one with dexamethasone and radiation therapy.

The overall survival for different treatment modalities is presented in Figure 3. The longest overall survival was observed in patients treated with the combined treatment (median survival of 39 months, 95% CI: 10.41 – 67.59). This group comprised eight patients treated systemically with CHOP regimen, nine patients treated with a high-dose methotrexate (either as a single agent or in combination with other agents) and two patients treated with corticosteroids. Patients treated just with radiation therapy had a median overall survival of 9 months (95% CI: 4.14 – 13.87) and those treated with sole chemotherapy of 4.5 months (95% CI: 1.74 – 6.26), respectively. The group of patients treated with sole chemotherapy comprised eight patients treated with a high-dose methotrexate (either as a single agent or in combination with other agents) and four patients treated with a middle-dose methotrexate in combination with other blood-brain barrier passing agents. Just four of these patients achieved the complete remission with the primary systemic treatment while the others either progressed in the course of the systemic therapy (five patients) or died of treatment complications (three patients). The differences between the curves were not statistically significant ( $p=0.069$ ). All three toxic

deaths occurred in episodes of febrile neutropenia in patients suffering from severe mucositis following a high-dose methotrexate. Surprisingly, no toxic deaths were observed in the group of patients receiving a high-dose methotrexate in combination with a high-dose cytarabine.

As for different chemotherapeutic regimens, again the longest median overall survival was achieved with the CHOP regimen (median 26 months, 95% CI: 13.91 – 36.09). Yet, we have to take in account that all these patients were also treated with radiation therapy. The differences between the survival curves were statistically insignificant ( $p=0.93$ ) (Figure 4). On the other hand, the overall survival of the subgroup of patients treated with a high-dose methotrexate and a high-dose cytarabine was longer (yet insignificantly) compared to other patients treated with a high-dose methotrexate (33 months, 95% CI: 12.01 – 53.99, versus 22 months, 95% CI: 0.30 – 43.70).

Finally, we also determined the overall survival of patients in different international prognostic index (IPI) categories (Figure 5). The median overall survival of the low risk group was 26 months (95% CI: 8.37 – 41.63) and 39 months (95% CI: 0.00 – 101.98) in the low intermediate risk group, respectively. As expected, the median overall survival was shorter in the high intermediate risk group (6.5 months, 95% CI: 0.00 – 12.84) and in the high risk group (3.5 months, 95% CI: 0.23 – 5.77). The differences between the curves were insignificant ( $p=0.27$ ).

## Discussion

In the article, the PCNSL patients treated at the Institute of Oncology Ljubljana between 1995 and 2010 were analysed in regards to the patient's characteristics, treatment results, disease specific survival and overall survival.

Our series included almost twice as many females as males. This is different from the reports of Villano *et al.*<sup>2</sup> and Uhm *et al.*<sup>29</sup> who reported male predominance in their series. Only Lim *et al.*<sup>30</sup> reported female predominance but in PCNSL other than the diffuse large B cell lymphoma. The median age at diagnosis of PCNSL in immunocompetent patients was reported to be 55 years<sup>31</sup> which is slightly lower compared to the median age of 59.8 years in our patients. The diagnosis of PCNSL was made by the histological examination of a stereotactic biopsy in 22 patients and by the partial or radical resection in 32 patients. In 5 patients, the

diagnosis was due to their poor performance status established by the cytological examination of the cerebrospinal fluid. Patients had predominantly aggressive B cell lymphomas (69.5%), among which there were 39 cases (66%) of the diffuse large B cell lymphoma, one case of immunoblastic lymphoma and one case of Burkitt's lymphoma. One patient had marginal cell lymphoma (1.7%) and two patients T cell lymphoma (3.4%). In fifteen patients we diagnosed unspecified B cell lymphomas. The percentage of aggressive lymphomas is lower than the one reported by Miller *et al.* (89%)<sup>3</sup>, most probably on account of a large proportion of determined unspecified B cell lymphomas. We believe that with a more adequate surgical sampling and if the patients had not received corticosteroids prior to the procedure, the percentage of unspecified B cell lymphomas would have been lower, most probably on account of a higher proportion of the aggressive B cell lymphomas.

Multiple lesions were detected in 33.2% of patients which is substantially lower than 66% reported by Uhm *et al.*<sup>29</sup> Also the involvement of deep brain structures (54.2%) was in our series observed more rarely than in the study of Uhm *et al.*<sup>29</sup> where they found it in 78% of patients. Leptomeningeal involvement was identified in 18.6% of the patients and cerebrospinal fluid cytology was positive in 10.2% of patients while Uhm *et al.*<sup>29</sup> reported of 38% of patients with the diffuse large B cell PCNSL having positive cerebrospinal fluid cytology. The majority of our patients showed poor performance status since 67.7% had the performance status of 3 and 4. The series of Lim *et al.*<sup>30</sup> and Uhm *et al.*<sup>29</sup> on the other hand included just 13% and 38% of patients with performance status of 3 and 4, respectively. Moreover, 22% of our patients suffered from serious concomitant diseases.

Two patients were, because of their poor performance status, treated just with radical surgery, they survived one and five months from the diagnosis of PCNSL, respectively. Prior to 1999, all patients eligible for the systemic treatment were treated with CHOP chemotherapy and intrathecal applications of chemotherapy, which was in all cases combined with radical radiotherapy. Surprisingly, in these patients the overall response rate to chemotherapy was 25%, however, the complete response was achieved in six patients (75%) following primary chemotherapy and radiotherapy. The median overall survival in this group was 26 months which was longer than in patients treated with a high-dose methotrexate (22 months) but shorter than in the subgroup of patients treated

with a high-dose methotrexate in combination with a high-dose cytarabine (33 months). There was also one long term survivor (more than 105 months) in this group. These observations are discordant with the observations of O'Neill *et al.*, Schultz *et al.*, and Shibamoto *et al.*, who obtained unsatisfactory results with the anthracyclines and cyclophosphamide in combination with radiotherapy.<sup>23,24,32</sup> On the other hand, treatment results with a high-dose methotrexate (alone or in combinations) in our series were inferior to the ones reported in the literature. Namely, the overall response rate of 55.5% in case of combination of a high-dose methotrexate and a high-dose cytarabine was lower than the one reported for a high-dose methotrexate in monotherapy by Glass *et al.*<sup>33</sup> and other authors<sup>14,34</sup> and substantially lower than the 69% overall response rate reported by Ferreri *et al.* with the same combination in a randomized trial.<sup>35</sup> Also, the survival in the group receiving a high-dose methotrexate regimens (46.3% at two years) was inferior to the two year survival of 60-65% reported by the same authors.<sup>14,33,34</sup> We can only speculate about the underlying causes for such discrepant results between CHOP and high-dose methotrexate treatments. First of all, all patients treated with CHOP were also treated with radical radiotherapy while in the group of patients treated with a high-dose methotrexate only nine (52.9%) were irradiated. There were also three treatment related deaths in the group of patients who received methotrexate suggesting that this kind of treatment might possibly be too aggressive for some of them. Hypothetically, the fundamental shift in the biology of the PCNSLs between 1958 and 1989 described by Miller *et al.*<sup>3</sup> could be another explanation since our patients were treated with CHOP just until 1999.

Most consistent results in our series were obtained with radiation therapy – namely, the overall response rate was 56% in patients treated with sole radiotherapy and 65% in those treated with combined therapy. Also the median disease-free survival in our group of patients treated just with radiation therapy was longer compared to the data of Nelson *et al.*<sup>36</sup> and Laack *et al.*<sup>37</sup> who reported that the disease recurred in more than 90% of patients within one year of treatment. The median overall survival of this group, however, was just 9 months compared to a median survival time of 23 or 6 to 8 months for those less than or greater than 60 years of age, respectively, reported by the same authors.<sup>36,37</sup> Still, the five year overall survival was 32% which is higher than 3%-26% reported by Nelson *et al.*<sup>36</sup> and Laperriere *et al.*<sup>38</sup> Three out of six

long term survivors were treated just with the radical radiation therapy. The median disease-free survival of patients treated with chemotherapy combined with the radiation therapy was 23 months and the median overall survival 39 months, respectively. This strategy produced a five year survival of 23.2% falling in the range of 22%-40% reported by other authors.<sup>13,39,40</sup> Again, three out of six long term survivors were treated with the combined therapy.

The overall survival in our series was significantly affected by the patient's age – it was namely substantially shorter in patients aged over 60 years. This is in agreement with other reports of treatment results of central nervous system tumors.<sup>10,13,23,24,41</sup> On the other hand, the IPI that had been established as a good predictor of the survival in patients with systemic aggressive lymphomas, however, in case of PCNSL did not prove especially informative. Possibly this goes at least partially on account of a large proportion of patients in whom the IPI remained undetermined.

In conclusion, the treatment outcomes in ordinary clinical practice are definitely inferior to the ones reported in clinical trials. The now standard treatment with a high-dose methotrexate or methotrexate-based chemotherapy with or without radiation therapy is sometimes too aggressive and, therefore, a careful selection on the basis of the patient's age, performance status and concomitant diseases of those eligible for such treatment is mandatory. According to our results, the radiation therapy should not be excluded from the primary treatment. These recommendations are, however, based on a retrospective study.

## References

- Hoffman S, Propp JM, McCarthy BJ. Temporal trends in incidence of primary brain tumors in the United States, 1985-1999. *Neuro Oncol* 2006; **8**: 27-37.
- Villano JL, Koshy M, Shaikh H, Dolecek TA, McCarthy BJ. Age, gender, and racial differences in incidence and survival in primary CNS lymphoma. *Br J Cancer* 2011; **105**: 1414-8.
- Miller DC, Hochberg FH, Harris NL, Gruber ML, Louis DN, Cohen H. Pathology with clinical correlations of primary central nervous system non-Hodgkin's lymphoma. The Massachusetts General Hospital experience 1958-1989. *Cancer* 1994; **74**: 1383-97.
- Fine HA, Mayer RJ. Primary central nervous system lymphoma. *Ann Intern Med* 1993; **119**: 1093-104.
- Hochberg FH, Miller DC. Primary central nervous system lymphoma. *J Neurosurg* 1988; **68**: 835-53.
- Kachanov DY, Dobrenkov KV, Shamanskaya TV, Abdullaev RT, Savkova RF, et al. Solid tumors in young children in Moscow Region of Russian Federation. *Radiol Oncol* 2008; **42**: 39-44.
- Schabet M. Epidemiology of primary CNS lymphoma. *J Neurooncol* 1999; **43**: 199-201.
- Bhagavathi S, Wilson JD. Primary central nervous system lymphoma. *Arch Pathol Lab Med* 2008; **132**: 1830-44.
- Herrlinger U, Schabet M, Clemens M, Kortmann RD, Petersen D, Will BE, et al. Clinical presentation and therapeutic outcome in 26 patients with primary CNS lymphoma. *Acta Neurol Scand* 1998; **97**: 257-64.
- Bataille B, Delwail V, Menet E, Vandermarcq P, Ingrand P, Wager M, et al. Primary intracerebral malignant lymphoma: report of 248 cases. *J Neurosurg* 2000; **92**: 261-6.
- Linnert M, Iversen HK, Gehl J. Multiple brain metastases – current management and perspectives for treatment with electrochemotherapy. *Radiol Oncol* 2012; **46**: 271-8.
- Tezcan Y, Koc M. 3-D conformal radiotherapy with concomitant and adjuvant temozolomide for patients with glioblastoma multiforme and evaluation of prognostic factors. *Radiol Oncol* 2011; **45**: 213-9.
- Abrey LE, DeAngelis LM, Yahalom J. Long-term survival in primary CNS lymphoma. *J Clin Oncol* 1998; **16**: 859-63.
- Cher L, Glass J, Harsh GR, Hochberg FH. Therapy of primary CNS lymphoma with methotrexate-based chemotherapy and deferred radiation therapy: preliminary results. *Neurology* 1996; **46**: 1757-9.
- Dahlborg SA, Petrillo A, Crossen JR, Roman-Goldstein S, Doolittle ND, Fuller KH, et al. The potential for complete and durable response in nonglioma primary brain tumors in children and young adults with enhanced chemotherapy delivery. *Cancer J Sci Am* 1998; **4**: 110-24.
- Schlegel U, Pels H, Glasmacher A, Kleinschmidt R, Schmidt-Wolf I, Helmstaedter C, et al. Combined systemic and intraventricular chemotherapy in primary CNS lymphoma: a pilot study. *J Neurol Neurosurg Psychiatry* 2001; **71**: 118-22.
- Blay JY. Primary cerebral non-Hodgkin lymphoma in non-immunocompromised subjects. *Bull Cancer* 1997; **84**: 976-80.
- Pech IV, Peterson K, Cairncross JG. Chemotherapy for brain tumors. *Oncology (Williston Park)* 1998; **12**: 537-53.
- Ferreri AJ, Reni M, Villa E. Therapeutic management of primary central nervous system lymphoma: lessons from prospective trials. *Ann Oncol* 2000; **11**: 927-37.
- Stanic K, Kovac V. Prophylactic cranial irradiation in patients with small-cell lung cancer: the experience at the Institute of Oncology Ljubljana. *Radiol Oncol* 2010; **44**: 213-9.
- Horvat M, Jezersek Novakovic B. Effect of response quality and line of treatment with rituximab on overall and disease-free survival of patients with B-cell lymphoma. *Radiol Oncol* 2010; **44**: 232-8.
- Gregoric B, Zadnik V, Jezersek Novakovic B. The diffuse large B-cell lymphoma – where do we stand now in everyday clinical practice. *Radiol Oncol* 2012; **46**: 153-9.
- O'Neill BP, O'Fallon JR, Earle JD, Colgan JP, Brown LD, Krigel RL. Primary central nervous system non-Hodgkin's lymphoma: survival advantages with combined initial therapy. *Int J Radiat Oncol Biol Phys* 1995; **33**: 663-73.
- Schultz C, Scott C, Sherman W, Donahue B, Fields J, Murray K, et al. Preirradiation chemotherapy with cyclophosphamide, doxorubicin, vincristine, and dexamethasone for primary CNS lymphomas: initial report of radiation therapy oncology group protocol 88-06. *J Clin Oncol* 1996; **14**: 556-64.
- Ferreri AJ, Reni M, Pasini F, Calderoni A, Tirelli U, Pivnik A, et al. A multicenter study of treatment of primary CNS lymphoma. *Neurology* 2002; **58**: 1513-20.
- Shibamoto Y, Ogino H, Suzuki G, Takemoto M, Araki N, Isobe K, et al. Primary central nervous system lymphoma in Japan: changes in clinical features, treatment, and prognosis during 1985-2004. *Neuro Oncol* 2008; **10**: 560-8.
- Joergers M, Huitema AD, Krähenbühl S, Schellens JH, Cerny T, Reni M, et al. Methotrexate area under the curve is an important outcome predictor in patients with primary CNS lymphoma: A pharmacokinetic-pharmacodynamic analysis from the IELSG no. 20 trial. *Br J Cancer* 2010; **102**: 673-7.
- Abrey LE, Batchelor TT, Ferreri AJ, Gospodarowicz MJ, Pulczynski EJ, Zucca E, et al. Report of an international workshop to standardize baseline evaluation and response criteria for primary CNS lymphoma. *J Clin Oncol* 2005; **23**: 5034-43.



29. Uhm JE, Kim KH, Yi SY, Chang MH, Park KW, Kong DS, et al. A retrospective study to compare two methotrexate-based regimens for primary central nervous system lymphoma. *Leuk Lymphoma* 2009; **50**: 1110-8.
30. Lim T, Kim SJ, Kim K, Lee Ji, Lim do H, Lee DJ, et al. Primary CNS lymphoma other than DLBCL: a descriptive analysis of clinical features and treatment outcomes. *Ann Hematol* 2011; **90**: 1391-8.
31. Herrlinger U, Schabet M, Bitzer M, Petersen D, Krauseneck P. Primary central nervous system lymphoma: from clinical presentation to diagnosis. *J Neurooncol* 1999; **43**: 219-26.
32. Shibamoto Y, Sasai K, Oya N, Hiraoka M. Systemic chemotherapy with vincristine, cyclophosphamide, doxorubicin and prednisolone following radiotherapy for primary central nervous system lymphoma: a phase II study. *J Neurooncol* 1999; **42**: 161-7.
33. Glass J, Gruber ML, Cher L, Hochberg FH. Preirradiation methotrexate chemotherapy of primary central nervous system lymphoma: Long-term outcome. *J Neurosurg* 1994; **81**: 188-95.
34. O'Brien PC, Roos DE, Liew KH, Trotter GE, Barton MB, Walker QJ, et al. Preliminary results of combined chemotherapy and radiotherapy for non-AIDS primary central nervous system lymphoma. Trans-Tasman Radiation Oncology Group. *Med J Aust* 1996; **165**: 424-7.
35. Ferreri AJ, Reni M, Foppoli M, Martelli M, Pangalis GA, Frezzato M, et al. High-dose cytarabine plus high-dose methotrexate versus high-dose methotrexate alone in patients with primary CNS lymphoma: a randomised phase 2 trial. *Lancet* 2009; **374**: 1512-20.
36. Nelson DF, Martz KL, Bonner H, Nelson JS, Newall J, Kerman HD, et al. Non-Hodgkin's lymphoma of the brain: can high-dose, large volume radiation therapy improve survival? Report on a prospective trial by the Radiation Therapy Oncology Group (RTOG): RTOG 8315. *Int J Radiat Oncol Biol Phys* 1992; **23**: 9-17.
37. Laack NN, Ballman KV, Brown PB, O'Neill BP; North Central Cancer Treatment Group. Whole-brain radiotherapy and high-dose methylprednisolone for elderly patients with primary central nervous system lymphoma: Results of North Central Cancer Treatment Group (NCCTG) 96-73-51. *Int J Radiat Oncol Biol Phys* 2006; **65**: 1429-39.
38. Laperriere NJ, Cerezo L, Milosevic MF, Wong CS, Patterson B, Panzarella T. Primary lymphoma of brain: results of management of a modern cohort with radiation therapy. *Radiother Oncol* 1997; **43**: 247-52.
39. Brada M, Hjiyiannakis D, Hines F, Traish D, Ashley S. Short intensive primary chemotherapy and radiotherapy in sporadic primary CNS lymphoma (PCL). *Int J Radiat Oncol Biol Phys* 1998; **40**: 1157-62.
40. O'Brien P, Roos D, Pratt G, Liew K, Barton M, Poulsen M, et al. Phase II multicenter study of brief single-agent methotrexate followed by irradiation in primary CNS lymphoma. *J Clin Oncol* 2000; **18**: 519-26.
41. Niemiec M, Głogowski M, Tyc-Szczepaniak D, Wierchowski M, Kepka L. Characteristics of long-term survivors of brain metastases from lung cancer. *Rep Pract Oncol Radiother* 2011; **16**: 49-53.

# Angiogenin and vascular endothelial growth factor expression in lungs of lung cancer patients

Ales Rozman<sup>1,3</sup>, Mira Silar<sup>2</sup>, Mitja Kosnik<sup>3</sup>

<sup>1</sup> Department for Endoscopy, <sup>2</sup> Department for Immunology, <sup>3</sup> Department for Pulmonology, University Clinic Golnik, Slovenia

Radiol Oncol 2012; 46(4): 354-359.

Received 20 January 2012

Accepted 21 February 2012

Correspondence to: Aleš Rozman, MD, MSc, Department for Endoscopy and Department for Pulmonology, University Clinic Golnik, Golnik 36, 4204 Golnik, Slovenia. Phone: +386 41 313 811; Fax: +386 4 256 9117; E-mail: ales.rozman@klinika-golnik.si

Disclosure: No potential conflicts of interest were disclosed.

**Background.** Lung cancer is the leading cause of cancer deaths. Angiogenesis is crucial process in cancer growth and progression. This prospective study evaluated expression of two central regulatory molecules: angiogenin and vascular endothelial growth factor (VEGF) in patients with lung cancer.

**Patients and methods.** Clinical data, blood samples and broncho-alveolar lavage (BAL) from 23 patients with primary lung carcinoma were collected. BAL fluid was taken from part of the lung with malignancy, and from corresponding healthy side of the lung. VEGF and angiogenin concentrations were analysed by an enzyme-linked immunosorbent assay. Dilution of bronchial secretions in the BAL fluid was calculated from urea concentration ratio between serum and BAL fluid.

**Results.** We found no statistical correlation between angiogenin concentrations in serum and in bronchial secretions from both parts of the lung. VEGF concentrations were greater in bronchial secretions in the affected side of the lung than on healthy side. Both concentrations were greater than serum VEGF concentration. VEGF concentration in serum was in positive correlation with tumour size ( $p = 0,003$ ) and with metastatic stage of disease ( $p = 0,041$ ). There was correlation between VEGF and angiogenin concentrations in bronchial secretions from healthy side of the lung and between VEGF and angiogenin concentrations in bronchial secretions from part of the lung with malignancy.

**Conclusion.** Angiogenin and VEGF concentrations in systemic, background and local samples of patients with lung cancer are affected by different mechanisms. Pro-angiogenic activity of lung cancer has an important influence on the levels of angiogenin and VEGF.

Key words: angiogenin; BAL fluid; bronchoscopy; lung cancer; vascular endothelial growth factor

## Introduction

Lung cancer is one of the leading causes of morbidity and cancer-related mortality in Slovenia with 1216 new cases and 1125 deaths in 2007.<sup>1</sup> Five-year survival rate is around 10%, since most of the patients have advanced stage of disease at the time of diagnosis.<sup>2,3</sup> Tumour growth and progression is still poorly understood and in many cases doesn't follow currently accepted model of sequential multistep pathway.<sup>4-7</sup>

Beside transformation of normal cells into malignant, the cancer growth and progression re-

quires additional steps to transition from dormant to malignant state.<sup>8,9</sup> The role of angiogenesis – the growth of new vessels from preexisting – is probably fundamental in this process.<sup>10,11</sup> Angiogenesis is controlled by a delicate balance between pro- and anti-angiogenic factors which is disrupted by a malignant tumour in favour of forming its own blood vessel network.<sup>12,13</sup> Moreover, angiogenesis is involved also in the growth of distant metastases.<sup>14</sup>

The central roles in the process of neovascularisation have regulatory molecules with pro- and anti-angiogenic potential.<sup>15</sup> Vascular endothelial growth factor (VEGF) and angiogenin are two ma-

**TABLE 1.** Clinical and demographic characteristics of the lung cancer patients from the study

Variables	Data
No. of patients	23
Median age, years	66 (range 48-78)
Male, n (%)	22 (95.7%)
Female, n (%)	1 (4.3%)
Smoking status, n (%)	
Current and previous	22 (95.7%)
Never-smoker	1 (4.3%)
COPD, n (%)	14 (60.9%)
Cancer type	
Squamous cell carcinoma	13 (56.6%)
Small cell carcinoma	5 (21.7%)
Adenocarcinoma	3 (13.0%)
Others	2 (8.7%)
Stage, n (%)	
I	4 (17.4%)
II	1 (4.3%)
III	8 (34.8%)
IV	10 (43.5%)
Tumour size, cm	5.7 ± 3.0
Location, n (%)	
central	16 (69.6%)
peripheral	7 (30.4%)
CRP, mg/l	36.5 ± 32.8
WBC, x10 <sup>6</sup> /l	11.1 ± 9.6

COPD = chronic obstructive lung disease; CRP = C-reactive protein; WBC = white blood count

major positive regulators of blood vessel formation in physiological conditions and in pathological situations including lung cancer.<sup>16-20</sup>

The purpose of this study was to prospectively investigate the local concentrations of VEGF and angiogenin in the part of the lung, affected by a lung cancer and compare them by the healthy side of the lung and by the concentrations in the serum of patients with lung cancer.

## Patients and methods

### Patients

Thirty patients who underwent bronchoscopy with suspicion for lung malignancy were included. Exclusion criteria were: age under 18 years, malig-

nancy on both sides of the lung or additional malignoma elsewhere in the body, previous anticancer treatment or pneumonectomy. The procedure was explained to patients verbally and in writing, and signed informed consent was obtained prior to enrolment. The study was approved by the National Medical Ethics Committee. We subsequently excluded 7 patients where lung malignancy was not confirmed by invasive diagnostic procedures. Clinical and demographic characteristics of the included lung cancer patients are presented in Table 1. Ex-smokers were defined as former regular smokers, who stopped at least one year before enrolment.

### Broncho-alveolar lavage (BAL) and blood samples

Venous blood samples were collected before bronchoscopy into a vacutainer without anticoagulant or other additives. Serum was separated and centrifuged at 2500 revolutions per minute for 5 minutes, and supernatant was frozen at -40°C. During bronchoscopy BAL with 20 ml of saline was collected from segmental bronchus affected by lung cancer and from corresponding segmental bronchus on the healthy side of the lung. BAL was performed before biopsies, from the healthy side first to avoid contamination with blood and malignant cells. BAL fluid was centrifuged at 1600 revolutions per minute for 5 minutes after procedure and supernatant was frozen at -40°C for later analysis.

### VEGF, angiogenin and urea measurement

Enzyme-linked immunosorbent assay (ELISA) kits (Quantikine – R&D Systems, Minneapolis) were used for measurements of VEGF and angiogenin in plasma and BAL fluid. The limit of sensitivity of the VEGF assay was 5-9 pg/ml, the intra-assay coefficient of variation was 4.1-6.7% and the interassay coefficient of variation was 5.0-8.8%. The limit of sensitivity of the angiogenin assay was 6 pg/ml, the intra-assay coefficient of variation was 2.8-3.3% and the interassay coefficient of variation was 7.1 – 8.7%. Urea concentration in plasma and BAL fluid was measured by QuantiChrom urea assay kit Diur-500 (BioAssay Systems, Hayward) with linear detection range from 0.06 mg/l to 1000 mg/l.

### Data analysis

Concentrations of angiogenin and VEGF in bronchial samples were normalized to urea concentra-

**TABLE 2.** Concentrations of angiogenin in serum and in bronchial secretions from healthy side of the lung and from area, affected by lung cancer

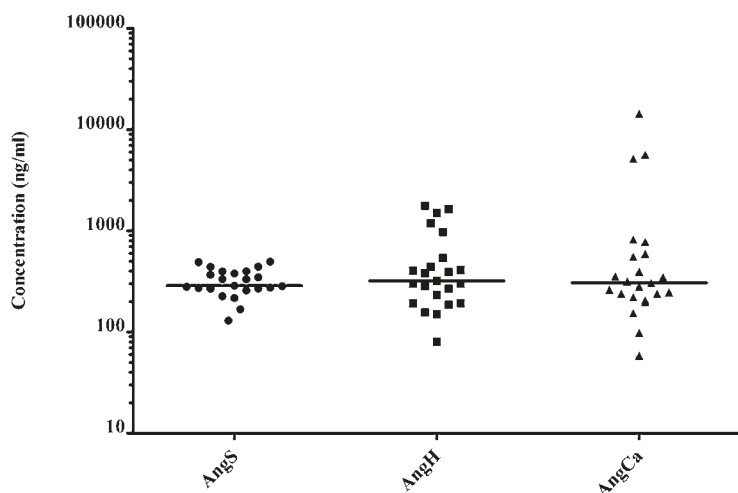
Angiogenin concentration	Me	Q1	Q3	95.centil
Serum (ng/ml)	286.94	267.88	397.08	495.88
Bronchial secretions – healthy side (ng/ml)	320.64	193.38	538.70	1746.17
Bronchial secretions – lung cancer (ng/ml)	306.11	221.19	592.69	12591.24

Me = median, Q1 = first quartile, Q3 = third quartile

**TABLE 3.** Concentrations of VEGF in serum and in bronchial secretions from healthy side of the lung and from area, affected by lung cancer. There was a significant difference between serum and bronchial concentrations ( $p < 0.05$ ), but no significant difference among VEGF concentrations between diseased and healthy side of the lung ( $p > 0.05$ )

VEGF concentration	Me	Q1	Q3	95.centil
Serum (ng/ml)	0.74	0.48	1.27	3.79
Bronchial secretions – healthy side (ng/ml)	14.52	8.59	26.59	111.05
Bronchial secretions – lung cancer (ng/ml)	17.89	8.64	84.30	565.49

Me – median, Q1 – first quartile, Q3 – third quartile

**FIGURE 1.** Distributions of angiogenin concentrations in serum (AngS), bronchial secretions from healthy side of the lung (AngH) and from area, affected by lung cancer (AngCa).

tion. Concentrations of VEGF and angiogenin in bronchial secretions were calculated using formula: bronchial secretions concentration = BAL fluid concentration  $\times$  (urea concentration in plasma / urea concentration in BAL fluid).

Data were analysed using the computer program Statistical Package for the Social Sciences version 14.0 (SPSS Inc., Chicago). Descriptive statistical methods were used (mean, standard deviation, range / median, percentiles). A Kolmogorov-

Smirnov (KS) test was used to check normal distribution. Associations between variables were tested by Pearson non-parametric test and by Wilcoxon matched-pairs test. Differences were analysed by Mann-Whitney U test. All tests were two-tailed;  $p < 0.05$  was considered to be statistical significant.

## Results

Median dilution of bronchial secretions in BAL fluid was 1:104 on the healthy side of the lung and 1:97 in the area of the lung affected by lung cancer, according to differences in urea concentrations.

Only serum concentrations of angiogenin followed Gaussian distribution (KS = 0.16,  $p > 0.05$ ).

Median angiogenin serum concentration in patients with lung cancer was 286.94 ng/ml (Table 2). We found no significant correlation among angiogenin concentrations in serum and bronchial secretions of both sides of the lung ( $p > 0.05$ ). No significant difference was found among angiogenin concentrations in serum and bronchial secretions of both sides of the lung ( $p > 0.05$ ) (Figure 1).

VEGF concentrations in bronchial secretions were higher than in the serum of patients with lung cancer (Table 3). VEGF concentrations in the bronchial secretions from lung cancer area show no statistical difference to VEGF concentrations in bronchial secretions from the healthy side of

the lung (Figure 2). There was no significant correlation among VEGF concentrations in serum and bronchial secretions found ( $p > 0.05$ ).

Concentrations of angiogenin and VEGF in bronchial secretions from the healthy side of the lung were in a correlation ( $p = 0.003$ ) as well as angiogenin and VEGF concentrations from area affected with lung cancer ( $p < 0.001$ ). Angiogenin and VEGF concentrations in the serum did not correlate.

Concentrations of serum VEGF were in a positive correlation with tumour size ( $p = 0.003$ ), plasma C-reactive protein (CRP) concentrations ( $p = 0.007$ ), white blood count (WBC) in peripheral blood sample ( $p < 0.001$ ) and metastatic stage of disease ( $p = 0.041$ ). Serum angiogenin concentrations were not in a correlation with any of tumour features or inflammatory markers.

## Discussion

The study showed that there is a strong local production of VEGF in lungs of patients with lung cancer and that VEGF serum concentration but not angiogenin concentration was in positive correlation with tumour size and with metastatic stage of disease. Concentrations of VEGF and angiogenin did not correlate for a particular molecule in any possible couple from three taken samples in patients with lung cancer. This is probably a consequence of different mechanisms, which regulate concentrations of these two molecules in any of these three settings.

Serum as a systemic sample has certain levels of VEGF and angiogenin present also in subjects without malignant disease and their concentration is therefore dependant on mechanisms other than malignancy, such are inflammation, hypoxemia, injury and tissue repair and maintenance.<sup>21,22</sup>

Angiogenin is normally present in the serum of healthy people and is produced in many tissues, among other in the liver as a constituent of acute phase response.<sup>23,24</sup> Its concentrations are higher in heart failure, abnormal pregnancy, blood malignancies and in some other conditions.<sup>25,26</sup> Higher expression of angiogenin was found in bronchial mucosa of asthmatics, especially during periods of exacerbation.<sup>27,28</sup> In this study serum angiogenin concentrations followed Gaussian distribution in contrast to angiogenin concentrations in bronchial secretions from both sides of the lung. Therefore we assume that serum angiogenin concentration was not significantly affected by local conditions in the lung and in the lung cancer. Moreover serum

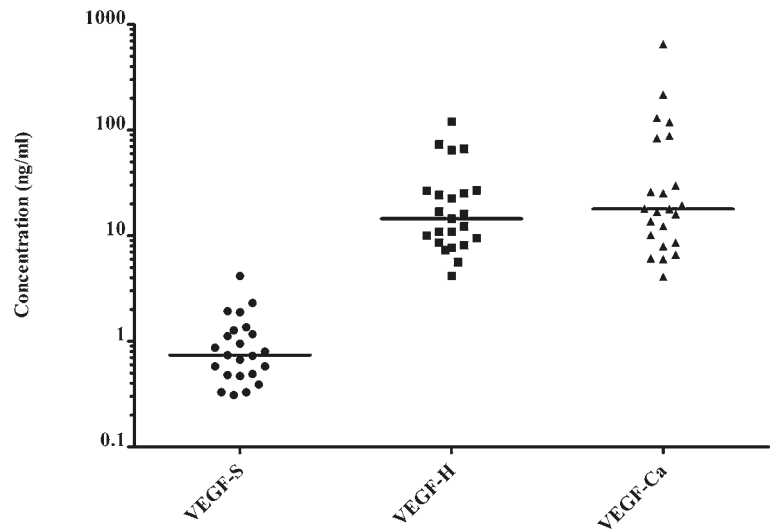


**FIGURE 2.** Distributions of VEGF concentrations in serum (VEGF-S), bronchial secretions from healthy side of the lung (VEGF-H) and from area, affected by lung cancer (VEGF-Ca).

angiogenin concentrations were not in correlation with any of the clinical variables as for example: CRP, WBC, tumour size, stage of the disease, chronic obstructive lung disease (COPD), etc.

In contrast, VEGF concentrations in the serum were much lower than in the samples from the lung, and were not in correlation with lung concentrations. Serum VEGF concentrations were strongly correlated with some clinical variables: CRP, WBC, tumour size and stage of the disease. This is in accordance with previously described higher serum VEGF expression in patients with advanced disease.<sup>29,30</sup> Serum concentrations of VEGF are normally very low and are probably the result of “washing” from tissues, where VEGF expression is higher.<sup>31,32</sup>

The measurements of exact concentrations of angiogenin and VEGF in bronchial secretions represented a certain challenge, since dilution rate of bronchial secretions in BAL was different from sample to sample. Angiogenin and VEGF concentrations in BAL fluid were dependant on their concentrations in bronchial secretions and on the amount of bronchial secretions captured in the retrieved BAL fluid. For defining of exact dilution rate of secretions in the BAL we used concentrations of urea molecules and two compartment model method. Urea freely diffuses between plasma and bronchial secretions and its concentration in both fluids is equal, since urea is neither degraded or produced in bronchi nor is volatile.<sup>33-35</sup>

Bronchial secretions from the healthy side of the lung were regarded as a “lung background”

sample. Correlation between angiogenin and VEGF concentrations in bronchial secretions from the healthy side of the lung is probably the consequence of the same stimulus. Bronchial inflammation in asthma and COPD can stimulate secretion of angiogenin and VEGF.<sup>27,28</sup> VEGF concentrations in bronchial secretions can rise even in asymptomatic smokers.<sup>36</sup> Almost all of the patients in this study were current or former smokers and 60.9% had diagnosis of COPD that could contribute especially to higher VEGF concentrations.

Bronchial secretions from the area of the lung, affected with lung cancer were "local" sample. Concentrations of angiogenin and VEGF were in correlation and we again assume that stimulus for secretion could be the same. VEGF concentrations were higher in bronchial washings from patients with lung cancer after treatment with chemotherapy and irradiation, but none of included patients in this study received such treatment before.<sup>37</sup> VEGF concentrations in bronchial secretions from affected side of the lung were not in correlation with any of the tumour features, what possibly reflects the effect of VEGF "washing" to the blood serum, which in contrast reflects such correlations. We were unable to confirm the findings that VEGF expression in the airways is inversely associated with tumour progression.<sup>38</sup>

Limitations of the study were small number of included patients, and inhomogeneity of the study group. Small sample size prevented subgroup analysis. In the study group were differences in gender and histological types of lung cancer with regard to general distribution in population of patients with lung cancer.

We summarize that angiogenin and VEGF expression in systemic, background and local samples of patients with lung cancer are affected by different mechanisms. The important role in serum angiogenin concentration has constitutional component in contrast to serum VEGF concentration, which is influenced by lung cancer. Angiogenin and VEGF concentrations in bronchial secretions from healthy and affected side of the lung show influence of lung cancer angiogenic activity and other conditions including co-morbidity.

## Acknowledgements

The authors would like to thank to Nadja Triller and to Viljem Kovač for support during clinical trial and preparation of the manuscript.

## References

1. *Cancer in Slovenia 2007*. Ljubljana: Institute of Oncology Ljubljana, Epidemiology and Cancer Registry, Cancer Registry of Republic of Slovenia; 2010.
2. Debevec L, Debeljak A, Eržen J, Kovač V, Kern I. Characterisation of lung cancer patients, their actual treatment and survival: experience in Slovenia. *Radiol Oncol* 2005; **39**: 115-21.
3. Lekic M, Kovac V, Triller N, Knez L, Sadikov A, Cufer T. Outcome of small cell lung cancer (SCLC) patients with brain metastases in a routine clinical setting. *Radiol Oncol* 2012; **46**: 54-9.
4. Bach PB. Is our natural – history model of lung cancer wrong? *Lancet Oncol* 2008; **9**: 693-7.
5. Park IW, Wistuba II, Maitra A, Milchgrub S, Virmani AK, Minna JD, et al. Multiple clonal abnormalities in the bronchial epithelium of patients with lung cancer. *J Natl Cancer Inst* 1999; **91**: 1863-8.
6. Venmans BJ, van Boxem TJ, Smit EF, Postmus PE, Sutedja G. Outcome of bronchial CIS. *Chest* 2000; **117**: 1472-6.
7. Bach PB, Jett JR, Pastorino U, Tockman MS, Swensen SJ, Begg CB. Computed tomography screening and lung cancer outcomes. *JAMA* 2007; **297**: 953-61.
8. Folkman J, Kalluri R. Cancer without disease. *Nature* 2004; **427**: 787.
9. McFarlane MJ, Feinstein AR, Wells CK. Clinical features of lung cancers discovered as a postmortem "surprise". *Chest* 1986; **90**: 520-3.
10. Naumov GN, Akslen LA, Folkman J. Role of angiogenesis in human tumor dormancy. Animal models of the angiogenic switch. *Cell Cycle* 2006; **5**: 1779-87.
11. Hanahan D, Folkman J. Patterns and emerging mechanisms of the angiogenic switch during tumorigenesis. *Cell* 1996; **86**: 353-64.
12. Kerbel RS. Tumor angiogenesis. *N Engl J Med* 2008; **358**: 2039-49.
13. Ciric E, Sersa G. Radiotherapy in combination with vascular-targeted therapies. *Radiol Oncol* 2010; **44**: 67-78.
14. Macchiarini P, Fontanini G, Dulmet E, de Montpreville V, Chapelier AR, Cerrina J, et al. Angiogenesis: an indicator of metastasis in non-small cell lung cancer invading the thoracic inlet. *Ann Thorac Surg* 1994; **57**: 1534-9.
15. Distler JH, Hirth A, Kurowska-Stolarska M, Gay RE, Gay S, Distler O. Angiogenic and angiostatic factors in the molecular control of angiogenesis. *Q J Nucl Med* 2003; **47**: 149-61.
16. Tello-Montoliu A, Patel JV, Lip GYH. Angiogenin: a review of the pathophysiology and potential clinical applications. *J Thromb Haemost* 2006; **4**: 1864-4.
17. Gao X, Xu Z. Mechanisms of action of angiogenin. *Acta Biochim Biophys Sin* 2008; **40**: 619-24.
18. Ferrara N, Davis-Smyth T. The biology of vascular endothelial growth factor. *Endocrine Rev* 1997; **18**: 4-25.
19. Veikkola T, Alitalo K. VEGFs, receptors and angiogenesis. *Semin Cancer Biol* 1999; **9**: 211-20.
20. Shibuya M. Vascular endothelial growth factor – dependent and – independent regulation of angiogenesis. *BMB reports* 2008; **41**: 278-86.
21. Shapiro R, Strydom DJ, Olson KA, Vallee BL. Isolation of angiogenin from normal human plasma. *Biochemistry* 1987; **26**: 5141-6.
22. Wasada T, Kawahara R, Katsumori K, Naruse M, Omori Y. Plasma concentration of immunoreactive vascular endothelial growth factor and its relation to smoking. *Metabolism* 1998; **47**: 27-30.
23. Olson KA, Verselis SJ, Fett JW. Angiogenin is regulated in vivo as an acute phase protein. *Biochem Biophys Res Commun* 1998; **242**: 480-3.
24. Patsulaia Ia, Trofimov S, Kobylansky E, Livshits G. Genetic and environmental determinants of circulating levels of angiogenin in community-based sample. *Clin Endocrinol* 2006; **64**: 271-9.
25. Kolben M, Bläser J, Ulm K, Schmitt M, Schneider KT, Tschesche H, et al. Angiogenin plasma levels during pregnancy. *Am J Obstet Gynecol* 1997; **176**: 37-41.

26. Patel JV, Sosin M, Gunarathne A, Hussain I, Davis RC, Hughes EA, et al. Elevated angiogenin levels in chronic heart failure. *Ann Med* 2008; **40**: 474-9.
27. Hoshino M, Takahashi M, Aoike N. Expression of vascular endothelial growth factor, basic fibroblast growth factor, and angiogenin immunoreactivity in asthmatic airways and its relationship to angiogenesis. *J Allergy Clin Immunol* 2001; **107**: 295-301.
28. Abdel-Rahman AMO, El-Sahrigy SAF, Bakr SI. A comparative study of two angiogenic factors: vascular endothelial growth factor and angiogenin in induced sputum from asthmatic children in acute attack. *Chest* 2006; **129**: 266-71.
29. Matsuyama W, Hashiguchi T, Mizoguchi A, Iwami F, Kawabata M, Arimura K, et al. Serum levels of vascular endothelial growth factor dependent on the stage progression of lung cancer. *Chest* 2000; **118**: 948-51.
30. Yuan A, Yu CJ, Chen WJ, Lin FY, Kuo SH, Luh KT et al. Correlation of total VEGF mRNA and protein expression with histologic type, tumor angiogenesis, patient survival and timing of relapse in non-small-cell lung cancer. *Int J Cancer* 2000; **89**: 475-83.
31. Berse B, Brown LF, Van de Water L, Dvorak HF, Senger DR. Vascular permeability factor (vascular endothelial growth factor) gene is expressed differentially in normal tissues, macrophages, and tumors. *Mol Biol Cell* 1992; **3**: 211-20.
32. Mura M, dos Santos CC, Stewart D, Liu M. Vascular endothelial growth factor and related molecules in acute lung injury. *J Appl Physiol* 2004; **97**: 1605-17.
33. Effros RM, Peterson B, Casaburi R, Su J, Dunning M, Torday J, et al. Epithelial lining fluid solute concentrations in chronic obstructive lung disease patients and normal subjects. *J Appl Physiol* 2005; **99**: 1286-92.
34. Rennard SI, Basset G, Lecossier D, O'Donnell KM, Pinkston P, Martin PG, et al. Estimation of volume of epithelial lining fluid recovered by lavage using urea as marker for dilution. *J Appl Physiol* 1986; **60**: 532-8.
35. Effros RM, Murphy C, Ozker K, Hacker A. Kinetics of urea exchange in air-filled and fluid-filled rat lungs. *Am J Physiol Lung Cell Mol Physiol* 1992; **263**: L619-26.
36. Rovina N, Papapetropoulos A, Kollintza A, Michailidou M, Simoes DC, Roussos C, et al. Vascular endothelial growth factor: an angiogenic factor reflecting airway inflammation in healthy smokers and in patients with bronchitis type of chronic obstructive pulmonary disease? *Respir Res* 2007; **8**: 53.
37. Beinert T, Binder D, Oehm C, Ziemer S, Priem F, Stuschke M, et al. Further evidence for oxidant-induced vascular endothelial growth factor up-regulation in the bronchoalveolar lavage fluid of lung cancer patients undergoing radio-chemotherapy. *J Cancer Res Clin Oncol* 2000; **126**: 352-6.
38. Ohta Y, Ohta N, Tamura M, Wu J, Tsunozuka Y, Oda M, et al. Vascular endothelial growth factor expression in airways of patients with lung cancer. A possible diagnostic tool of responsive angiogenic status on the host side. *Chest* 2002; **121**: 1624-7.

# Interstitial lung disease in a patient treated with oxaliplatin, 5-fluorouracil and leucovorin (FOLFOX) for metastatic colorectal cancer

Liam M Hannan<sup>1,3</sup>, Jaclyn Yoong<sup>2</sup>, Geoffrey Chong<sup>2</sup>, Christine F McDonald<sup>1,3</sup>

<sup>1</sup> Department of Respiratory and Sleep Medicine, Austin Health, Heidelberg, Victoria, Australia

<sup>2</sup> Ludwig Oncology Unit, Austin Health, Heidelberg, Victoria, Australia

<sup>3</sup> Institute for Breathing and Sleep, Austin Hospital, Heidelberg, Victoria, Australia

Radiol Oncol 2012; 46(4): 360-362.

Received 18 October 2011

Accepted 7 November 2011

Correspondence to: Dr Liam Hannan, C/o Department of Respiratory and Sleep Medicine, Austin Health, 145 Studley Road, Heidelberg, Victoria 3084, Australia. Phone: +61 394963688; Fax: +61 394965124; E-mail: liamhannan1@yahoo.com.au

Disclosure: No potential conflicts of interest were disclosed.

**Background.** Oxaliplatin in combination with 5-fluorouracil (5-FU) and leucovorin (FOLFOX) is a common chemotherapeutic regimen for advanced colorectal cancer. Here, we present a case of interstitial lung disease associated with FOLFOX therapy.

**Case report.** A 74-year-old man with a history of metastatic colorectal cancer was admitted with a four week history of progressive dyspnoea and evidence of severe respiratory failure. He had recently completed six cycles of FOLFOX chemotherapy in the months prior to presentation. Investigations did not reveal convincing evidence of infection or pulmonary embolism. CT chest demonstrated widespread pulmonary infiltrates and interlobular septal thickening. The patient was commenced on both broad spectrum antibiotic therapy and high dose corticosteroid treatment however his respiratory failure continued to progress. The patient died four days after admission due to progressive respiratory failure. Subsequent post-mortem examination demonstrated evidence of diffuse alveolar damage without evidence of tumour infiltration, infection or pulmonary embolism.

**Conclusions.** Although infrequent, pulmonary toxicity can occur in association with FOLFOX therapy. Cessation of therapy and prompt initiation of corticosteroids may improve outcomes.

Key words: oxaliplatin; interstitial lung disease; diffuse alveolar damage

## Introduction

Oxaliplatin in combination with 5-fluorouracil (5-FU) and leucovorin (FOLFOX) is an effective chemotherapeutic regimen for advanced colorectal cancer, improving survival with acceptable tolerability and side effect profile.<sup>1-3</sup> Common side effects from this regimen include neutropenia, sensory neuropathy and gastrointestinal symptoms.<sup>1,2</sup> There have been infrequent reports of pulmonary toxicity from this regimen.<sup>4-8</sup> Here we present a case of interstitial lung disease associated with FOLFOX therapy.

## Case report

A 74-year-old man with a history of metastatic colorectal cancer was admitted with a four week history of progressive dyspnoea and haemoptysis. He had undergone a right hemicolectomy three and a half years previously for a Duke's A colorectal cancer. Three years post resection, a large single liver metastasis was identified with no other evidence of metastatic disease on PET scanning. CT examination of the chest at the time demonstrated only mild emphysematous changes (Figure 1).



The patient was commenced on FOLFOX chemotherapy (oxaliplatin, 5-fluorouracil and leucovorin) and underwent six cycles from October to December 2008. A re-staging CT scan in January 2009 demonstrated progressive malignant disease with multiple new metastases within the liver. Chest imaging at this time revealed bilateral peripheral subpleural reticular changes and interlobular septal thickening without evidence of overt lung metastases (Figure 2). No changes to treatment occurred and the patient was planned for second line systemic chemotherapy.

The patient subsequently presented in early February 2009 with four weeks of worsening dyspnoea and haemoptysis. His C-reactive protein level was moderately elevated although white cell count and differential were normal. Arterial blood gases demonstrated severe type I respiratory failure. CT pulmonary angiogram excluded pulmonary embolism but demonstrated new patchy infiltrates with interlobular septal thickening (Figure 3). Sputum samples were unable to be obtained and the patient was considered to be too high risk to undergo bronchoscopy.

He was commenced on empirical broad spectrum antibiotics and high dose intravenous corticosteroid therapy. His respiratory failure worsened and after discussion with both the patient and his family, mechanical ventilation was not administered. The patient died four days after admission from progressive respiratory failure.

Post-mortem examination did not demonstrate evidence of an infective aetiology on staining and culture of fresh specimens. There was also no evidence of emboli, thrombus or malignant infiltration within the lungs. Histological examination demonstrated widespread generalised changes within both lungs, with oedema, intra-alveolar haemorrhage and fibrin deposition along with interstitial and intraluminal fibroblastic proliferation without mature fibrosis. These findings were consistent with diffuse alveolar damage.

## Discussion

Diffuse alveolar damage (DAD) is a common histopathological finding in patients with ARDS and is commonly associated with infections (both respiratory and systemic). It is more frequently seen in immunocompromised patients. Although drug reactions are a relatively uncommon cause of DAD, chemotherapeutic agents are overrepresented as potential precipitants. Mortality following histo-

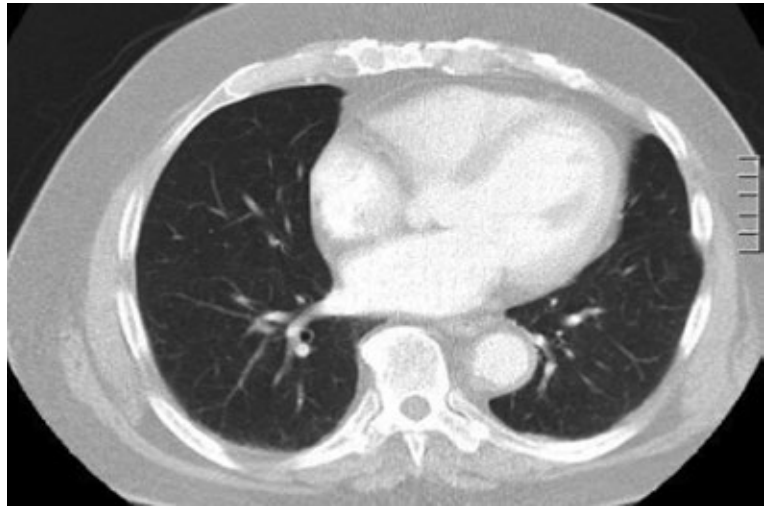


FIGURE 1. Representative image from initial staging CT; minor emphysematous changes



FIGURE 2. Representative image from re-staging CT January 2009; bilateral peripheral subpleural reticular changes and interlobular septal thickening without evidence of lung metastases.

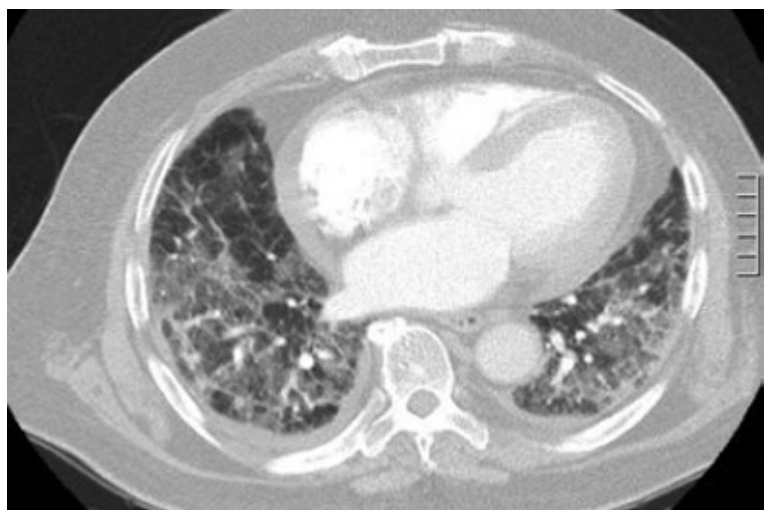


FIGURE 3. Representative image from CT pulmonary angiogram February 2009; diffuse infiltrates with interlobular septal thickening.

logically proven DAD obtained from surgical lung biopsy has been reported to be greater than 50%.<sup>7</sup>

Oxaliplatin, in combination with 5-fluorouracil and leucovorin (FOLFOX) has been shown to be an effective regimen for the treatment of advanced colorectal cancer.<sup>1,10-12</sup> Goldberg *et al.* demonstrated improved response rate, median time to progression and overall survival in patients with advanced colorectal cancer treated with FOLFOX in comparison to a regimen utilising Irinotecan instead of Oxaliplatin.<sup>1</sup> The most frequently reported side effects in this and other studies utilising FOLFOX have been cytopenias, peripheral neuropathy and diarrhoea.<sup>1,10</sup> Pulmonary toxicity associated with this regimen has been infrequently described in a small number of case reports.<sup>4-8,13-15</sup> In cases where a tissue diagnosis was obtained, DAD was the most frequent histopathological pattern obtained, although organising pneumonia has also been described.<sup>16</sup> Authors have suggested apparent clinical benefit with prompt cessation of FOLFOX therapy and the use of high dose systemic corticosteroids.<sup>8,14,17</sup>

Although pulmonary toxicity from FOLFOX appears to be an uncommon and apparently idiosyncratic effect of therapy, this case highlights the importance of clinicians being aware of this potentially fatal complication and the importance of regular follow-up.<sup>18</sup> Early changes consistent with acute interstitial lung disease were present on a routine re-staging CT chest over four weeks prior to this patient's acute presentation and it is possible that recognition of this problem may have altered the outcome.

## Conclusions

Given the temporal relationship between the use of FOLFOX and the onset of radiological changes and clinical symptoms, we believe that FOLFOX is the likely precipitant in this case. Whilst this appears to be an uncommon adverse effect, early recognition may allow prompt cessation of FOLFOX therapy and initiation of systemic corticosteroids, and this has the potential to improve outcomes for such patients.

## References

1. Goldberg RM, Sargent DJ, Morton RF, Fuchs CS, Ramanathan RK, Williamson SK, et al. A randomized controlled trial of fluorouracil plus leucovorin, irinotecan, and oxaliplatin combinations in patients with previously untreated metastatic colorectal cancer. *J Clin Oncol* 2004; **22**: 23-30.

2. Arevalo Lobera S, Sagastibelza Marinelarena N, Elejoste Echeberria I, Mele Olive M, Egana Otano L, Basterretxea Badiola L, et al. Fatal pneumonitis induced by oxaliplatin. *Clin Transl Oncol* 2008; **10**: 764-7.
3. Ocvirk J. Advances in the treatment of metastatic colorectal carcinoma. *Radiol Oncol* 2009; **43**: 1-8.
4. Rebersek M, Boc M, Cerkovnik P, Benedik J, Hlebanja Z, Volk N, et al. Efficacy of first-line systemic treatment in correlation with BRAF V600E and different KRAS mutations in metastatic colorectal cancer – a single institution retrospective analysis. *Radiol Oncol* 2011; **45**: 285-91.
5. Jung KH, Kil SY, Choi IK, Seo JH, Shin C, Kim YS, et al. Interstitial lung diseases in patients treated with oxaliplatin, 5-fluorouracil and leucovorin (FOLFOX). *Int J Tuberc Lung Dis* 2006; **10**: 1181-2.
6. Mundt P, Mochmann HC, Ebhardt H, Zeitz M, Duchmann R, Pauschinger M. Pulmonary fibrosis after chemotherapy with oxaliplatin and 5-fluorouracil for colorectal cancer. *Oncology* 2007; **73**: 270-2.
7. Park S, Jung JJ, Kim GB, Yoon HS, Ko SH, Ko JE, et al. Interstitial lung disease associated with combination chemotherapy of oxaliplatin, 5-fluorouracil, and leucovorin. *Korean J Gastroenterol* 2010; **55**: 340-3.
8. Trisolini R, Lazzari Agli L, Tassinari D, Rondelli D, Cancellieri A, Patelli M, et al. Acute lung injury associated with 5-fluorouracil and oxaliplatin combined chemotherapy. *Eur Respir J* 2001; **18**: 243-5.
9. Parambil JG, Myers JL, Aubry MC, Ryu JH. Causes and prognosis of diffuse alveolar damage diagnosed on surgical lung biopsy. *Chest* 2007; **132**: 50-7.
10. Goldstein D, Mitchell P, Michael M, Beale P, Friedlander M, Zalberg J, et al. Australian experience of a modified schedule of FOLFOX with high activity and tolerability and improved convenience in untreated metastatic colorectal cancer patients. *Br J Cancer* 2005; **92**: 832-7.
11. Lami L, Areces F, Lence JJ, Arbesu MA. FOLFOX-4 Regimen as a first-line therapy for cuban patients with metastatic colorectal cancer. *MEDICC Rev* 2009; **11**: 34-8.
12. Nagata N, Kondo K, Kato T, Shibata Y, Okuyama Y, Ikenaga M, et al. Multicenter phase II study of FOLFOX for metastatic colorectal cancer (mCRC) in Japan; SWIFT-1 and 2 study. *Hepatogastroenterology* 2009; **56**: 1346-53.
13. Lim JH, Kim H, Choi WG, Lee MH. Interstitial lung disease associated with FOLFOX chemotherapy. *J Cancer Res Ther* 2010; **6**: 546-8.
14. Muneoka K, Shirai Y, Sasaki M, Wakai T, Sakata J, Hatakeyama K. Interstitial pneumonia arising in a patient treated with oxaliplatin, 5-fluorouracil, and leucovorin (FOLFOX). *Int J Clin Oncol* 2009; **14**: 457-9.
15. Pena Alvarez C, Suh Oh HJ, Saenz de Miera Rodriguez A, Garcia Arroyo FR, Covela Rua M, Salgado Boquete L, et al. Interstitial lung disease associated with oxaliplatin: description of two cases. *Clin Transl Oncol* 2009; **11**: 332-3.
16. Dahlqvist C, Fremault A, Carrasco J, Colinet B. Obliterative bronchiolitis with organising pneumonia following FOLFOX 4 chemotherapy. *Rev Mal Respir* 2010; **27**: 84-7.
17. Shimura T, Fuse N, Yoshino T, Minashi K, Tahara M, Doi T, et al. Clinical features of interstitial lung disease induced by standard chemotherapy (FOLFOX or FOLFIRI) for colorectal cancer. *Ann Oncol* 2011; **21**: 2005-10.
18. Velenik V. Post-treatment surveillance in colorectal cancer. *Radiol Oncol* 2010; **44**: 135-41.

# Application of a color scanner for $^{60}\text{Co}$ high dose rate brachytherapy dosimetry with EBT radiochromic film

Mahdi Ghorbani<sup>1</sup>, Mohammad Taghi Bahreyni Toossi<sup>2</sup>, Ali Asghar Mowlavi<sup>3</sup>, Shahram Bayani Roodi<sup>2</sup> and Ali Soleimani Meigooni<sup>4</sup>

<sup>1</sup> North Khorasan University of Medical Sciences, Bojnurd, Iran

<sup>2</sup> Medical Physics Research Center, Medical Physics Department, Faculty of Medicine, Mashhad University of Medical Sciences, Mashhad, Iran

<sup>3</sup> Physics Department, School of Sciences, Hakim Sabzevari University, Sabzevar, Iran

<sup>4</sup> Comprehensive Cancer Center of Nevada, 3730 S. Eastern Avenue, Las Vegas, Nevada, USA

Radiol Oncol 2012; 46(4): 363-369.

Received 19 November 2011

Accepted 28 December 2011

Correspondence to: Mahdi Ghorbani, Vice Chancellery of Research and Technology, North Khorasan University of Medical Sciences, South Shariati No. 7, Bojnurd, North Khorasan, Iran. Phone: +98 584 2247124; Fax: +98 584 2247124; E-mail: mhdghorbani@gmail.com

Disclosure: No potential conflicts of interest were disclosed.

**Background.** The aim of this study is to evaluate the performance of a color scanner as a radiochromic film reader in two dimensional dosimetry around a high dose rate brachytherapy source.

**Materials and methods.** A Microtek ScanMaker 1000XL film scanner was utilized for the measurement of dose distribution around a high dose rate GZP6  $^{60}\text{Co}$  brachytherapy source with GafChromic® EBT radiochromic films. In these investigations, the non-uniformity of the film and scanner response, combined, as well as the films sensitivity to scanner's light source was evaluated using multiple samples of films, prior to the source dosimetry. The results of these measurements were compared with the Monte Carlo simulated data using MCNPX code. In addition, isodose curves acquired by radiochromic films and Monte Carlo simulation were compared with those provided by the GZP6 treatment planning system.

**Results.** Scanning of samples of uniformly irradiated films demonstrated approximately 2.85% and 4.97% non-uniformity of the response, respectively in the longitudinal and transverse directions of the film. Our findings have also indicated that the film response is not affected by the exposure to the scanner's light source, particularly in multiple scanning of film. The results of radiochromic film measurements are in good agreement with the Monte Carlo calculations (4%) and the corresponding dose values presented by the GZP6 treatment planning system (5%).

**Conclusions.** The results of these investigations indicate that the Microtek ScanMaker 1000XL color scanner in conjunction with GafChromic EBT film is a reliable system for dosimetric evaluation of a high dose rate brachytherapy source.

Key words: color scanner; GZP6 brachytherapy source;  $^{60}\text{Co}$  high dose rate source; HDR; EBT radiochromic film.

## Introduction

Radiation dosimetry is essential for quality assurance in diagnostic and therapeutic radiology.<sup>1,2</sup> One of the most frequent tools for dosimetry are radiochromic films (RCF) because (1) they have nearly a tissue equivalent base material, (2) their spatial resolution is high, (3) they have a minor en-

ergy and dose rate dependency, and (4) they do not require a darkroom and developing.<sup>3-5</sup> High spatial resolution is especially helpful in brachytherapy dosimetry in which there is a high dose gradient near the sources. They can also provide two dimensional dose distributions near these regions.<sup>4</sup>

The radiochromic films can be read with a number of devices such as film digitizers, micro-

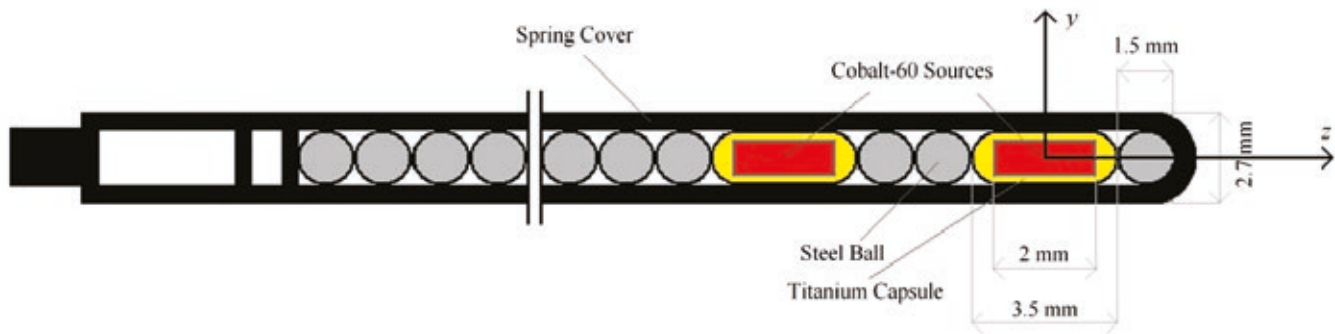


FIGURE 1. The GZP6 source braid (source number one) in the GZP6 afterloading brachytherapy unit.

densitometers, and laser based scanners.<sup>4</sup> Color/document scanners have also been used as a reader for radiochromic films. For example Agfa Arcus II, HP ScanJet II cx, Epson Pro 1680 Expression and some other different models of colour scanners have been evaluated for this purpose.<sup>6-10</sup> The advantage of such scanners is their lower price when compared with other radiochromic film densitometers.

However, with these scanners, it is possible to measure the film response in one of the three major wavelengths (red, green, and blue) and one must be careful to properly calibrate these devices for measurements of dose.<sup>11</sup> Commonly, the images are reduced to only the red color channel which is equivalent to using red filters.<sup>12</sup>

Recently, a new Microtek (ScanMaker 1000XL Pro: Microtek International Inc., Hsinchu, Taiwan) color scanner became commercially available. This scanner is a flatbed scanner with a cold cathode fluorescent lamp and a Tri-linear charge coupled device (CCD) array. Its maximum color depth is 48 bits per pixel (16 bits per each color channel). This scanner is capable to scan images of maximum 12×17 size with 3200×6400 dpi optical resolution and a maximum optical density of 4.0. Scanning may be performed either in reflection or transmission mode. Although there are reports on the application of different models of color/document scanners<sup>13-14</sup>, to our knowledge, this model of scanner has not yet been used as a RCF film reader.

The goal of this project is to investigate the application of the Microtek color scanner for dosimetric evaluation of a HDR GZP6 <sup>60</sup>Co source. In these evaluations the HDR source will be utilized to expose the Gafchromic EBT films in a PMMA equivalent phantom material. The results of these experimental data will be compared with the data from the GZP6 treatment planning system and the results of Monte Carlo (MC) simulations as well as the published MC results by Naseri *et al.*<sup>15</sup>

## Materials and methods

### Radioactive source and tandem applicator

GZP6 <sup>60</sup>Co afterloading HDR unit (Nuclear Power Institute of China) has 6 channels with non-stepping sources in channels 1-5 and a stepping source in channel 6. In this study, dose distribution around the source in channel 1 has been evaluated. This source is composed of two active cobalt-60 pellets placed in a nickel plating encapsulation with a number of non-active spherical pellets as spacers between and outside of the active pellets (Figure 1). Each active pellet is a 2 mm long and 1 mm diameter <sup>60</sup>Co source in a Titanium capsule. The active and non active pellets are fixed in a spring cover. The straight tandem applicator (UT0°) in GZP6 is normally used for the intracavitary brachytherapy treatment of cervical cancer patients. The applicator, which is made of stainless steel, has an inner diameter of 4.3 mm, wall thickness of 0.6 mm and a body length of 25.2 cm.

### Radiochromic film calibration

Characteristics of EBT radiochromic films: energy response, dose rate dependency, uniformity, post irradiation density growth etc. have been analyzed and discussed elsewhere.<sup>16-18</sup> In the present study, several sheets (20.3 cm × 25.4 cm) of EBT GafChromic® (lot number 34351-05, International Specialty Products, Wayne, NJ, USA) film were cut into 48 pieces of 2×3 cm<sup>2</sup> for irradiation. Care was taken to select the pieces from the same batch, for each measurement. Each piece was given an identity number, prior to the measurements.

The irradiated films were scanned by a Microtek ScanMaker 1000XL Pro color scanner. To obtain background optical density (OD) all 48 film pieces were scanned 24 hours prior to calibration. To minimize the warming up effect, the scanner was turned

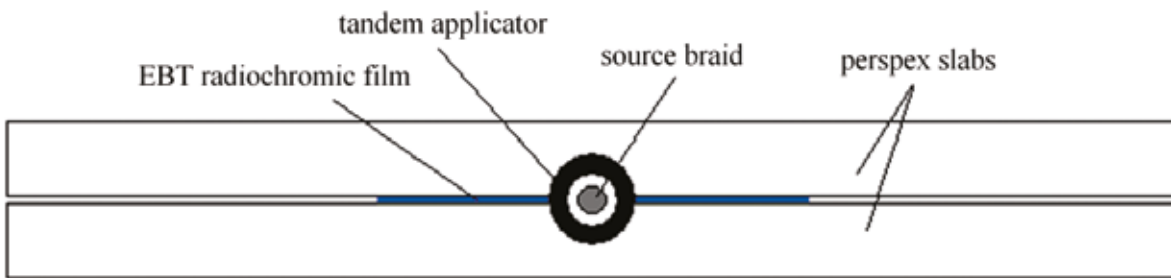


**FIGURE 2.** Schematic diagram showing the configuration of the EBT radiochromic film, GZP6 tandem applicator and the PMMA slabs during the film irradiation.

on at least 30 minutes before scanning. All film pieces were scanned by placing them at the center of the scanner bed and selecting 100 dpi resolutions. The films were scanned in 48-bit RGB color mode with the maximum OD range without applying any corrections or enhancements by the scanner's software. Since for EBT films the response is greatest in the red color channel<sup>16</sup>, the red components of RGB images were selected to derive the background OD of the films. All of images were saved as uncompressed tagged image file format (TIFF) files. To reduce noise effect, each film was scanned three times in transmission mode. As it has been recommended for EBT film, they were positioned in landscape orientation on the scanner bed. In addition, consecutive scanning of the films was avoided to minimize the film heating effects that could change the OD of the films. Appropriate care was taken to avoid dust particles and scratches on the films during film storage, scanning and calibrations.

Each group of films were calibrated using a Theratron 780C cobalt unit in the center of a 20×20 cm<sup>2</sup> field inside a dose range of 0.5-35 Gy inside a 32×32×31 cm<sup>3</sup> water phantom. The output of the cobalt unit was measured in the same conditions using a 0.6 cm<sup>3</sup> Farmer 2581 ionization chamber. The chamber reading was corrected for the ambient temperature and pressure. The films were scanned 24 hours after irradiation according to the aforementioned protocol. Net optical density (NOD) was calculated from equation [1] as the difference of averaged calibration and background optical density:

$$\text{NOD} = \text{OD}_{\text{cal}} - \text{OD}_{\text{back}} = -(\log_{10}(P_{\text{cal}}) - \log_{10}(P_{\text{back}})) \quad [1]$$

where:  $\text{OD}_{\text{cal}}$  is optical density of the calibration film,  $\text{OD}_{\text{back}}$  is background optical density (for unexposed film),  $P_{\text{cal}}$  is pixel value for calibration film and  $P_{\text{back}}$  is pixel value for the background film. The dose (Gy) was plotted versus the NOD and an exponential function was fitted to the curve.

Image manipulations such as: extraction of red component from the RGB images, calculation of mean pixel values (for a ROI on the whole film's surface except of the film edges), OD and dose mapping, dose contouring, etc were accomplished by means of appropriate scripts compiled accordingly in MATLAB (version 7.2.0.232, The Math Works, Inc., Natwick, MA) environment.

### In-phantom measurements

An EBT film sheet (from the same batch used for calibration) was cut in such a way that could house the GZP6 channel 1 applicator, the applicator tip was positioned symmetrically from the film edges. The film was scanned according to the protocol explained earlier in this section. The film was accommodated in a 50×50×50 cm<sup>3</sup> cubic PMMA phantom made from 1 cm thick slabs. Figure 2 shows the configuration of film, applicator and slabs during the irradiation.

To irradiate the film, a dose of 5 Gy was delivered to the point of 2 cm above and 2 cm lateral to the source position by GZP6 afterloading system. This was equal to a period of 671.3 s irradiation time in the date of measurements. According to the previous protocol, the film was scanned 24 hours after irradiation. The net optical densities in the measurement film's image then were correlated to the dose value by applying the calibration formula (equation [4]).

### EBT film sensitivity to the scanner's light source

Radiochromic films are sensitive to infra red (IR) light, therefore it is recommended to protect them against IR sources and avoid multiple consecutive scanning.<sup>19</sup> Radiochromic films are also sensitive to UV light.<sup>3</sup> UV source may include light bulbs, fluorescent lamps, sunlight and even light from the film scanner. The films sensitivity to the scanner's

light source was examined by the following manner: (1) Nine 20.3×12.7 cm<sup>2</sup> unexposed film pieces were scanned 15 times to assess whether this numbers of scanning would cause higher OD (or dose reading). (2) Mean optical density of individual film pieces in the red channel for the RGB image was obtained before and after the 15 times of scanning. This was accomplished by averaging the pixels values over the entire area of each film (except for the film edges).

### Uniformity checking

The combined effect of non-uniform response of EBT film and the Microtek scanner was examined. For this purpose nine 20.3×12.7 cm<sup>2</sup> pieces of films (from the same film batch already used) were irradiated in a clinically assumed uniform field. The films were scanned by the scanner before irradiation to obtain background pixels values for each film. The films were subjected to a wide range of absorbed dose 0.5-25 Gy, delivered in a 20×20 cm<sup>2</sup> 6 MV photon field of an ELEKTA linac (model SL75/25). To accomplish this protocol, films were positioned centrally at the depth of 10 cm in a solid water phantom (SP34, Wellhofer Scanditronix GmbH, Schwarzenbruck, Germany). Symmetry and flatness of the irradiation field were examined by an automated scanning water phantom system (RFA300plus; Scanditronix-Wellhofer, Nüremberg, Germany) before film irradiations. The films were scanned 48 hours following to irradiations.

The film pieces were positioned in the central part of the scanner's bed when scanning. The dose value represented by every film pixel was determined by the calibration fitted curve on the central area of 16×11 cm<sup>2</sup> size of each film. The images were saved as TIFF files and the red channel of RGB image was chosen to extract dose information. A wiener filter of 5 pixels×5 pixels was applied on the saved image of the films before image processing. Wiener filter is an adaptive filter predefined in MATLAB which is used to reduce the amount of noise present in an image. Film uniformities were evaluated in terms of coefficient of variation (in percentage) of dose for a region of interest (ROI) of 16×11 cm<sup>2</sup> on each film sheet. Coefficient of variation is defined as:

$$CV = \frac{100 \times \sigma}{\mu} \quad [2]$$

where  $\sigma$  is standard deviation and  $\mu$  is mean dose value. The peak-to-peak variation of optical density along longitudinal direction (the direction of scanning) and transverse direction (orthogonal to

the scanning direction) of the films were also evaluated for the 9 film pieces on the central area of 16×11 cm<sup>2</sup> size on each film piece:

$$\Delta OD_{\text{peak}} = \frac{OD_{\text{max}} - OD_{\text{min}}}{OD_{\text{central pixel}}} \quad [3]$$

where  $OD_{\text{central pixel}}$  is optical density value of central pixel of the film sheet in the longitudinal/transverse direction.

### Monte Carlo (MC) simulations

MCNPX version 2.4.0 MC code was used as the simulation tool in this study.<sup>20</sup> The loaded applicator including applicator body, active sources and inactive pellets were simulated. The applicator was positioned at the centre of a cylindrical PMMA phantom 25 cm in radius and 50 cm in length. A mesh (14 cm×14 cm×0.05 cm consisting of 0.5 mm<sup>3</sup> voxels) was used to score deposited dose, using MCNPX type 1 tally with pedep option.<sup>21</sup> This tally scores the average energy deposition per unit volume (MeV/(cm<sup>3</sup>.source-particle)). Then the dose value assigned to each voxel was determined by multiplying the tally value by a conversion factor; including the sources activity and source particles per disintegration, irradiation duration according to in-phantom irradiation and so on. A total number of 5×10<sup>8</sup> primary photon histories were simulated. The average uncertainty was 1.86% over the whole mesh voxels. Since the uncertainty on the source activity certified by the manufacturer is ±10%, the overall uncertainty of MC calculations will not be less than that.

### GZP6 treatment planning system

GZP6 afterloading unit, manufactured by Nuclear Power Institute of China (NPIC)<sup>22</sup>, incorporates an afterloader, a source container and a treatment planning system. The GZP6 treatment planning system uses Sievert integral to calculate dose distributions around the GZP6 sources.<sup>23</sup> The GZP6 treatment planning system produces 2D dose distributions in the transverse and longitudinal planes related to the selected source (or sources) configuration.

## Results

### Radiochromic film measurements

Figure 3 shows the calibration curve (dose versus NOD) obtained for the EBT films.

**TABLE 1.** Dose differences between MC, RCF and TPS dose distributions in this study (for dose contours of 2.5-7.5 Gy) and that by Naseri et al<sup>15</sup> (for dose contours 10-250%).

	This study		Naseri et al	
RCF-MC	MC-GZP6 TPS	RCF-GZP6 TPS	MC-GZP6 TPS	
4%	4%	5%	<2%	

Delivered dose  $D$  (in Gy) versus measured NOD can be obtained from the fitted formula using the following equation:

$$D = 0.7424e^{3.094\text{NOD}} - 0.8355e^{-4.848\text{NOD}} \quad [4]$$

The R-square value for the fitting is equal to 0.9995.

### EBT film sensitivity to the scanner's light sources UV component

The results of 15 times scanning with Microtek scanner have raised to an average change of 0.00157 in optical density of the nine scanned film pieces. This value equals to a net optical density of 0.000105 per scanning. With regard to our film calibrations, a dose of 0.5 Gy equals to a net optical density of 0.122. Thus, it can be concluded that scanning with Microtek scanner does not significantly change the optical density of EBT radiochromic film, due to the light source or the UV component of the light source.

### Uniformity checking

As it is mentioned in the materials and methods section, symmetry and flatness of the irradiation field were examined by an automated scanning water phantom. The resulted symmetry and flatness were 2% and 2.8% respectively. Mean value of coefficient of variation for represented absorbed dose by the 9 film pieces was 2.99%. Mean  $\Delta\text{OD}_{\text{peak}}$  averaged for 9 film pieces, in the longitudinal and transverse direction of the film were respectively 2.85% (1.59-4.06%) and 4.97% (2.47-8.50%).

### Comparisons of dose distributions

Dose distributions for the GZP6 source number one around the tandem applicator, obtained by radiochromic film measurement and MC simulation are presented in Figure 4. The curves are representing isodose lines of 1.25-7.5 Gy.

Calculated and measured dose values are only different by 4% on average. The difference is higher (nearly 20%) for the dose value of 1.25 Gy.

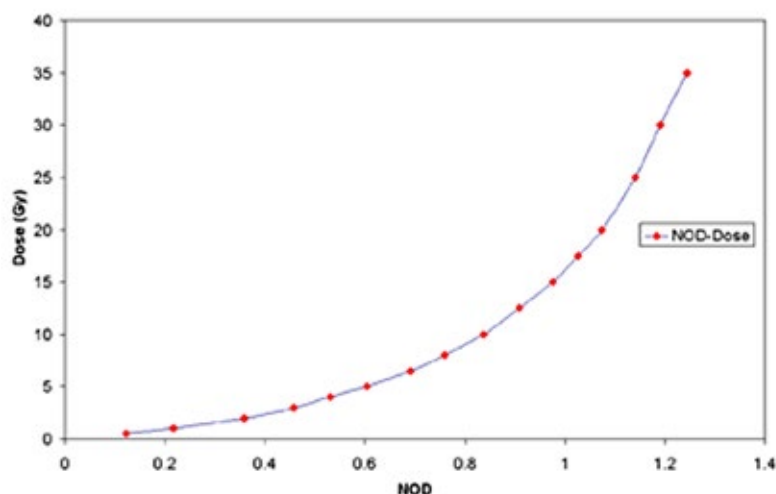


**FIGURE 3.** Calibration curves (dose versus net optical density (NOD)) obtained for EBT films for the red colour channel.

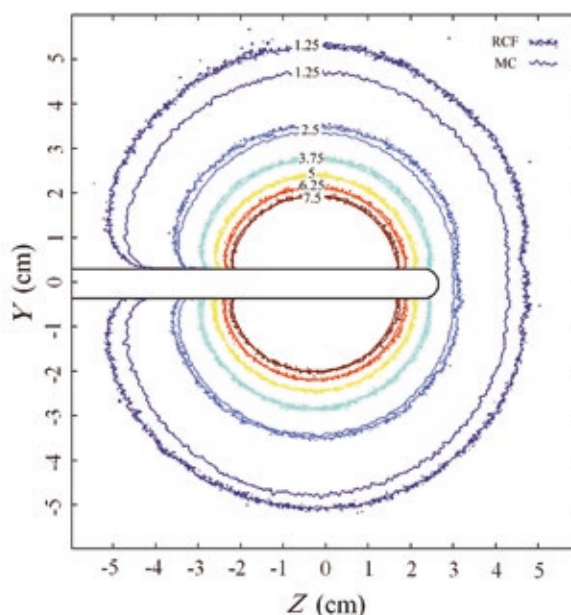


**FIGURE 4.** Dose distributions (in Gy) for the GZP6 source number one around the tandem applicator in a plane parallel to the long axis of the applicator as obtained by radiochromic films (RCF) measurements and Monte Carlo (MC) simulations.

Dose distribution around the tandem applicator as provided by the GZP6 treatment planning systems (TPS) versus calculated values by MC and

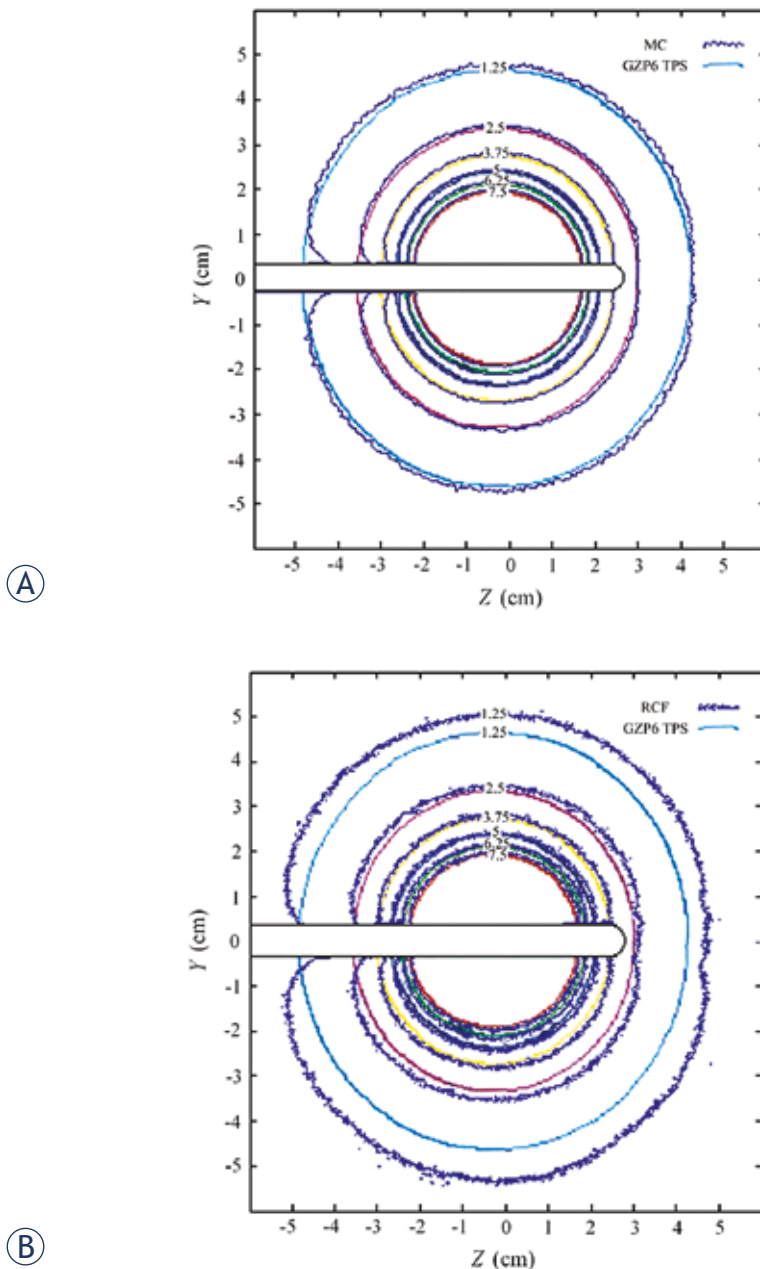


**FIGURE 5.** Dose distribution (in Gy) for the GZP6 source number one around the tandem applicator in a plane parallel to the long axis of the applicator (A) GZP6 treatment planning systems (TPS) versus Monte Carlo (MC) calculations (B) GZP6 TPS versus radiochromic films (RCF) measurement.

radiochromic film measurements are shown in Figure 5.

When calculated, an average dose difference of 4% was observed between the dose contours representing MC simulation and TPS. The difference between dose values obtained from radiochromic film measurement and those provided by TPS is in order of 5%. The difference is more pronounced

for lower doses (18% for 1.25 Gy). A summary of dose distribution differences related to MC, RCF and GZP6 TPS are presented in Table 1. The Table also presents the difference between MC versus GZP6 TPS isodose lines (in percent) for the study by Naseri *et al.*<sup>15</sup>

## Discussion

We have used a Microtek ScanMaker 1000XL Pro scanner as a radiochromic film reader. Different features of the scanner were examined for this purpose. Scanning of uniformly irradiated EBT film pieces on ROIs of 16×11 cm<sup>2</sup> size have demonstrated acceptable nonuniformity levels in both longitudinal and transverse directions. This is particularly true when compared to the study of Lynch *et al.*, in which 7% and 17% and variations in optical density for an Epson scanner and 12% and 8% for a Microtek scanner was reported respectively in the longitudinal and transverse directions.<sup>19</sup> Our results of examining EBT sensitivity to UV component of the scanner's light source has showed that multiple scanning of a film does not considerably change its optical density.

We have obtained isodose curves around a GZP6 tandem applicator first by MC simulations and then by film dosimetry by EBT radiochromic films. Generally the results are indicating there is a good agreement between radiochromic film measurement, MC simulations and GZP6 TPS. However the differences between the radiochromic film-MC, and radiochromic film-TPS for the dose contour of 1.25 Gy are 20% and 18% respectively. This implies that for dose values of equal to or less than 1.25 Gy the noise contribution of the scanner is high, giving rise to a high error.<sup>21</sup> The deviation could be attributed to our fitting curve to the calibration data, so that it has a deviation of 15.7% for the dose of 1 Gy.

By taking into account our MC uncertainty, it can be concluded that the difference between MC calculation versus the GZP6 TPS and radiochromic film measured dose distributions are within the uncertainties expected for MC calculations and radiochromic film measurements. Compared to our study, the less difference between MC calculations and GZP6 treatment planning system in the study of Naseri *et al.*<sup>15</sup> can be related to the fact that in that study there were a comparison between the relative isodose contours (in percent) but in this study the isodose curves were compared in terms of Gy. There is also a minor difference between the types of applicators simulated in two studies.



As it is evident from Figure 5, there are also some attenuation effects near the tip and base of the applicator which is not taken into account by the GZP6 planning system while it is considered by the radiochromic film measurement and MC calculations.

A rigorous scanning protocol was employed for film scanning. The protocol includes: avoiding multiple consecutive scanning; films were scanned always in landscape orientation; images were saved as uncompressed TIFF files; they were handled in a relatively stable temperature; noise effects were eliminated by pixel averaging of multiple scanning of film pieces in different steps of reading. It is concluded that by using a standard protocol, the Microtek ScanMaker 1000XL Pro can be used as a radiochromic film reader in combination with EBT radiochromic film. The combination can be used as a practical tool for HDR brachytherapy dose measurements. Since a color scanner has not appropriate software for reading RC films, designing appropriate MATLAB functions is necessary in the different steps of film reading; for example to extract pixel values, film calibration and correlation of pixel values to dose values on the RCF images.

## Acknowledgments

The authors would like to thank Dr. Abdol-Reza Hashemian for his assistance by providing the radiochromic film sheets. We also would like to acknowledge Dr. Ghorban Safaeian for film calibrations. This work was funded by office of vice president for research of Mashhad University of Medical Sciences.

## References

- de Denaro M, Bregant P. Dosimetric evaluation of a 320 detector row CT scanner unit. *Radiol Oncol* 2011; **45**: 64-7.
- Tran TA, Wu V, Malhotra H, Steinman, JP, Prasad D, Podgorsak MB. Target and peripheral dose from radiation sector motions accompanying couch repositioning of patient coordinates with the Gamma Knife (R) Perfexion (TM). *Radiol Oncol* 2011; **45**: 132-42.
- Butson MJ, Yu PKN, Cheung T, Metcalfe P. Radiochromic film for medical radiation dosimetry. *Mater Sci Eng R* 2003; **41**: 61-120.
- Niroomand-Rad A, Blackwell C.R, Coursey BM, Gall KP, Galvin JM, McLaughlin WL, et al. Radiochromic film dosimetry: Recommendations of AAPM Radiation Therapy Committee Task Group 55. *Med Phys* 1998; **25**: 2093-115.
- Jurkovic S, Zauhar G, Faj D, Radojicic DS, Svabic M, Kasabasic M, et al. Dosimetric verification of compensated beams using radiographic film. *Radiol Oncol* 2011; **45**: 310-4.
- Devic S, Seuntjens J, Sham E, Podgorsak EB, Schmidtlein CR, Kirov AS, et al. Precise radiochromic film dosimetry using a flat-bed document scanner. *Med Phys* 2005; **32**: 2245-53.
- Ferreira BC, Lopes MC, Capela M. Evaluation of an Epson flatbed scanner to read Gafchromic EBT films for radiation dosimetry. *Phys Med Biol* 2009; **54**: 1073-85.
- Chung H, Lynch B, Samant S. High-precision GAFCHROMIC EBT film-based absolute clinical dosimetry using a standard flatbed scanner without the use of a scanner non-uniformity correction. *J Appl Clin Med Phys* 2010; **11**: 101-5.
- Paelinck L, De Neve W, De Wagter C. Precautions and strategies in using a commercial flatbed scanner for radiochromic film dosimetry. *Phys Med Biol* 2007; **52**: 231-42.
- Matney JE, Parker BC, Neck DW, Henkelmann G, Rosen II. Evaluation of a commercial flatbed document scanner and radiographic film scanner for radiochromic EBT film dosimetry. *J Appl Clin Med Phys* 2010; **11**: 198-208.
- Hupe O, Brunzendorf J. A novel method of radiochromic film dosimetry using a color scanner. *Med Phys* 2006; **33**: 4085-94.
- Odero DO, Gluckman GR, Welsh K, Wlodarczyk RA, Reinstein LE. The use of an inexpensive red acetate filter to improve the sensitivity of GAFChromic dosimetry. *Med Phys* 2001; **28**: 1446-8.
- Alva H, Mercado-Uribe H, Rodríguez-Villafuerte M, Brandon ME. The use of a reflective scanner to study radiochromic film response. *Phys Med Biol* 2002; **47**: 2925-33.
- Menegotti L, Delana A, Martignano A. Radiochromic film dosimetry with flatbed scanners: a fast and accurate method for dose calibration and uniformity correction with single film exposure. *Med Phys* 2008; **35**: 3078-85.
- Naseri A, Mesbahi A. Application of Monte Carlo calculations for validation of a treatment planning system in high dose rate brachytherapy. *Rep Pract Oncol Radiother* 2009; **14**: 200-4.
- International Speciality Products (ISP). GAFCHROMIC EBT: Self-developing film for radiotherapy dosimetry (white paper). Wayne, NJ: ISP, 2009. Available from: [http://online1.ispcorp.com/\\_layouts/Gafchromic/content/products/ebt/pdfs/EBTwhitepaper.pdf](http://online1.ispcorp.com/_layouts/Gafchromic/content/products/ebt/pdfs/EBTwhitepaper.pdf) [accessed December 6 2010].
- Butson MJ, Cheung T, Yu PKN. Weak energy dependence of EBT gafchromic film dose response in the 50 kVp-10 MVp X-ray range. *Appl Radiat Isot* 2006; **64**: 60-2.
- Chiu-Tsao ST, Ho Y, Shankar R, Wang L, Harrison LB. Energy dependence of response of new high sensitivity radiochromic films for megavoltage and kilovoltage radiation energies. *Med Phys* 2005; **32**: 3350-4.
- Lynch BD, Kozelka J, Ranade MK, Li JG, Simon WE, Dempsey JF. Important considerations for radiochromic film dosimetry with flatbed CCD scanners and EBT GAFCHROMIC® film. *Med Phys* 2006; **33**: 4551-6.
- Waters LS. MCNPX User's Manual, Version 2.4.0. Report LA-CP-02-408 2002; Los Alamos National Laboratory.
- Gifford KA, Mourtada F, Cho SH, Lawyer A, Horton Jr JL. Monte Carlo calculations of the dose distribution around a commercial gynecologic tandem applicator. *Radiother Oncol* 2005; **77**: 210-5.
- Nuclear Power Institute of China (NPIC), 2010. Available at: [www.npic.ac.cn/](http://www.npic.ac.cn/) [accessed December 6, 2010].
- Mesbahi A. Radial dose functions of GZP6 intracavitary brachytherapy <sup>60</sup>Co sources: treatment planning system versus Monte Carlo calculations. *Iran J Radiat Res* 2008; **5**: 181-6.

*errata*

## What sampling device is the most appropriate for vaginal vault cytology in gynaecological cancer follow up?

Del Pup Lino<sup>1</sup>, Canzonieri Vincenzo<sup>2</sup>, Serraino Diego<sup>3</sup>, Campagnutta Elio<sup>1</sup>

<sup>1</sup> Gynaecology Oncology Department,

<sup>2</sup> Pathology Department and

<sup>3</sup> Epidemiology Unit, National Cancer Institute CRO, Aviano, PN, Italy

Radiol Oncol 2012; 46(2): 166-169.  
doi:10.2478/v10019-012-0019-x

---

The first and family names of the authors were not quoted adequately. The correct author's first and given names are: Lino Del Pup, Vincenzo Canzonieri, Diego Serraino, Elio Campagnutta.

---

Radiol Oncol 2012; 46(4): 271-278.  
doi:10.2478/v10019-012-0042-y

## Multipli možganski zasevki - sodobno zdravljenje in možnosti uporabe elektrokemoterapije

Linnert M, Iversen HK, Gehl J

**Izhodišča.** Število bolnikov z možganskimi zasevki je v stalnem porastu. Glavni razlogi so vse bolj učinkovito onkološko zdravljenje z daljšim preživetjem bolnikov, povečana incidenca raka in boljši diagnostični postopki. V članku predstavljamo sodobne načine zdravljenja multiplih možganskih zasevkov in možnost uporabe elektrokemoterapije, ki je novo eksperimentalno zdravljenje teh bolnikov.

**Zaključki.** Nevro- in stereotaktična kirurgija ter obsevanje celotnih možgan so priznani načini zdravljenja multiplih možganskih zasevkov. Uporabljamo tudi kemoterapijo in molekularna tarčna zdravila. Pojavljajo pa se tudi novi eksperimentalni načini, eden od njih je elektrokemoterapija. Pri tem zdravljenju apliciramo električne pulze na tumor zaradi učinkovitejšega vnosa citostatikov v tumorske celice. S takim načinom zdravljenja lahko n. pr. povečamo citotoksičnost bleomicina za 300 krat. Predklinični podatki so spodbudni in na ta način so v kliničnem poskusu že zdravili prvega bolnika z možganskimi zasevki. Pričakujemo, da bomo lahko na takšen način zdravili primarne tumorje in zasevke v možganih, kot tudi tumorje v mehkih tkivih.

Radiol Oncol 2012; 46(4): 279-283.  
doi:10.2478/v10019-012-0017-z

## Uporabnost F-18 FDG PET/CT pri podkožnem panikulitičnem T-celičnem limfomu za oceno razširjenosti bolezni in odgovora na zdravljenje

Kim JS, Jeong YJ, Sohn MH, Jeong HJ, Lim ST, Kim DW, Kwak JY, Yim CY

**Izhodišča.** Podkožni panikulitični T-celični limfom je redka oblika kožnega limfoma, predstavlja manj kot 1% primerov ne-Hodkin-ovega limfoma. Do sedaj je bilo malo poročil o uporabi fluor-18 fluorodeoksiglukoze (F-18 FDG) s pozitronsko emisijsko tomografijo in računalniško tomografijo (PET/CT) pri panikulitičnem T celičnem limfomu.

**Prikaz primera.** Prestavljamo bolnika s podkožnim panikulitičnim T-celičnim limfomom, pri katerem je preiskava F-18 FDG PET/CT pokazala povečano kopičenje FDG v številnih podkožnih vozličih, drugje pa kopičenja nismo ugotovili. Med preiskavo F-18 FDG PET/CT smo naredili tudi CT slikanje s kontrastom in videli minimalno povečano kopičenje kontrasta v tumorskih vozličih, ki so infiltrirali podkožno tkivo po celem telesu. Po treh krogih kemoterapije CHOP smo naredili ponovno preiskavo s F-18 FDG PET/CT, ki je pokazala popoln metabolni odgovor na zdravljenje pri vseh podkožnih spremembah.

**Zaključki.** F-18 FDG PET/CT je lahko primerna metoda za oceno aktivnosti podkožnega panikulitičnega T-celičnega limfoma, kot tudi razširjenosti bolezni in odgovora na zdravljenje.

Radiol Oncol 2012; 46(4): 284-295.

doi:10.2478/v10019-012-0033-z

## Ultrazvočna elastografija kot objektivna meritvena metoda za diagnozo limfedema pri bolnicah z rakom dojke po operaciji in obsevanju

Adriaenssens N, Belsackm D, Buyl R, Ruggiero L, Breucq C, De Mey J, Lievens P, Lamote J

**Izhodišča.** Limfedem po operaciji in obsevanju je pogost zaplet zdravljenja zgodnjega raka dojke. Soglasja o objektivnih diagnostičnih kriterijih in standardnih postopkih zdravljenja ni. Klinične raziskave proučujejo uporabo ultrazvočne elastografije kot objektivne kvantitativne meritvene metode za diagnozo parenhimskega edema dojke.

**Bolnice in metode.** Razmerje elastičnosti podkožja, izmerjeno z ultrazvočno elastografijo, smo primerjali s parametri visokofrekvenčnega ultrazvoka in subjektivnimi simptomi pri dvajsetih bolnicah; bilateralno, pred in po ohranitveni operaciji dojke ter po obsevanju dojke.

**Rezultati.** Elastično razmerje podkožja operiranih dojke po obsevanju je naraslo pri 88,9% bolnic in je bilo značilno višje kot pred operacijo in kot pri neoperiranih dojkah. Ti rezultati so bili značilno povezani z vidljivostjo ehogene linije, izmerjene z visokofrekvenčnim ultrazvokom. Značilen dejavnik tveganja za razvoj edema dojke je bila velika preoperativna velikost košarice.

**Zaključki.** Ultrazvočna elastografija je objektivna kvantitativna meritvena metoda za diagnozo parenhimskega edema dojke v kombinaciji z ostalimi objektivnimi diagnostičnimi kriteriji. Za potrditev teh rezultatov so potrebne nadaljnje raziskave z daljšim časom sledenja in večjim številom vključenih bolnic.

Radiol Oncol 2012; 46(4): 296-301

doi:10.2478/v10019-012-0038-7

## Zanesljivost določanja lokacije karcinoma rektuma glede na višino duplikature peritoneja s pomočjo MR rektuma

Eun Joo Jung EJ, Ryu CG, Gangmi Kim G, Kim SR, Nam SE, Park HS, KimYJ, Hwang DY

**Izhodišča.** Objektivna metoda za določanje lokacije karcinoma z oziroma na duplikaturo peritoneja bi bistveno pripomogla k boljši odločitvi o ustrezni obliki zdravljenja rektalnega karcinoma. Namen raziskave je bil ugotoviti natančnost in uporabnost MR rektuma za ugotavljanje odnosa med višino duplikature peritoneja in rektalnim karcinomom ter primerjati le-to z operativnim izvidom.

**Bolniki in metode.** V raziskavo so bili vključeni bolniki, ki so bili med novembrom 2008 in junijem 2010 operirani zaradi rektalnega karcinoma po MR preiskavi rektuma. Bolniki, ki so predhodno dobili preoperativno kemo-radioterapijo ali pa so imeli transanalno lokalno ekscizijo so bili iz raziskave izključeni.

**Rezultati.** V raziskavo je bilo vključenih 54 bolnikov. Primerjava operativnih in radioloških izvidov je pokazala, da je bila natančnost napovedi tumorske lokacije v odvisnosti od duplikature peritoneja z rektalno MR 90,7 %. Pri tem je bila natančnost 93,5% pri karcinomih nad peritonealno duplikaturo, 90,0 % pri bolnikih s tumorjem na peritonealni duplikaturi in 84,6 % pri bolnikih s tumorjem pod peritonealno duplikaturo ( $P=0.061$ ). Razdelitev bolnikov glede spola, indeksa telesne mase, operativnega izvida in velikosti tumorja ni pokazala statistično značilnih razlik med podskupinami.

**Zaključki.** Rektalna MR bi bila lahko uporabna pri ugotavljanju razmerja med rektalnim karcinomom in peritonealno duplikaturo, zlasti, če je tumor manjši od 8 cm. MR rektuma lahko da pomembne informacije glede lokacije karcinoma v odvisnosti od peritonealne duplikature, s tem pa pomaga pri odločitvi o ustreznem zdravljenju.

Radiol Oncol 2012; 46(4): 302-311.  
doi:10.2478/v10019-012-0044-9

## Potenciacija elektrokemoterapije z elektrogensko terapijo z IL-12 v mišico na različno imunogenih tumorjih mišjega sarkoma in karcinoma

Sedlar A, Dolinšek T, Markelc B, Prosen L, Kranjc S, Bošnjak M, Blagus T, Čemažar M, Serša G

**Izhodišča.** Z elektrokemoterapijo učinkovito dosežemo lokalni nadzor rasti tumorjev, vendar za povečan lokalni odziv in delovanje na oddaljene metastaze, potrebujemo adjuvantno zdravljenje. Lokalni elektrokemoterapiji s cisplatinom smo zato dodali elektrogensko terapijo z interlevkinom 12 (IL-12) v mišico, ki zagotavlja sistemsko sproščanje IL-12. Ovrednotili smo vpliv imunogenosti tumorjev in imunokompetence gostitelja na učinek kombinirane terapije.

**Materiali in metode.** *In vitro* smo testirali občutljivost celic sarkoma SA-1 in karcinoma TS/A na elektrokemoterapijo s cisplatinom. *In vivo* smo elektrokemoterapijo s cisplatinom v tumorje (dan 1) kombinirali z enkratno (dan: 0) ali večkratno (dnevi: 0, 2, 4) elektrogensko terapijo z mišjim IL-12 (mIL-12) v mišico. Protitumorsko učinkovitost kombinacijskega zdravljenja smo določili na imunogenem mišjem sarkomu SA-1 na miših A/J in zmerno imunogenem mišjem karcinomu TS/A na imunokompetentnih miših BALB/c in imunsko oslabljenih miših SCID.

**Rezultati.** Po elektrokemoterapiji *in vitro* smo na celičnih linijah sarkoma in karcinoma dobili podobni vrednosti IC<sub>50</sub>. *In vivo* je bila elektrokemoterapija bolj učinkovita na sarkomu, bolj imunogenem izmed obeh tumorjev, z višjim deležem ubitih celic, specifičnim zaostankom v rasti in 17 % ozdravitvijo v primerjavi s karcinomom, kjer nismo opazili nobenih ozdravitvev. Adjuvantna elektrogenska terapija z mIL-12 je povečala delež ubitih celic v obeh tumorskih modelih, in potenciala specifični zaostanek v rasti tumorjev za faktor 1.8 - 2 ter ozdravljivost za 20 %. Pri tumorjih sarkoma je bila potenciacija odziva z elektrogensko terapijo z mIL-12 dozno odvisna in se je odražala tudi v hitrejšem pojavu ozdravitve. Primerjava odziva na kombinirano terapijo pri karcinomu na imunokompetentnih in imunsko oslabljenih miših je pokazala, da je imunski sistem potreben tako za povečanje ubijanja celic kot tudi za doseganje ozdravitve.

**Zaključki.** Glede na primerjavo protitumorske učinkovitosti elektrokemoterapije s cisplatinom v tumorje lahko zaključimo, da je delež ubitih celic in ozdravitve večji pri imunogenih tumorjih sarkoma kot pri zmerno imunogenih tumorjih karcinoma. Delež ubitih celic in odstotek ozdravitve sta odvisna od imunskega odziva, ki ga sprožijo mrtve tumorske celice, le-ta pa bi lahko bil, kot nakazuje naša raziskava, odvisen tudi od imunogenosti tumorjev. Učinek adjuvantne elektrogenske terapije z mIL-12 je odvisen od sistemkega sproščanja IL-12 in imunokompetence gostitelja kot smo pokazali z dozno odvisnim povečanjem odstotka ozdravitve tumorjev SA-1 po večkratni elektrogenski terapiji z mIL-12 in z različno ozdravljivostjo tumorjev TS/A, rastočih na imuno kompetentnih in imunsko oslabljenih miših.

Radiol Oncol 2012; 46(4): 312-320  
doi:10.2478/v10019-012-0036-9

## Stavrosporin sproži v kulturah podganjih astrocitov različni obliki celične smrti

Šimenc J, Lipnik-Štangelj M

**Izhodišča.** Astroцитi pogosto maligno transformirajo. Kaže, da je poleg apoptoze tudi nekroptoza kot druga oblika programirane celične smrti povezana s tumorigenezo, proliferacijo glioblastomov, angiogenezo in invazijo. V raziskavi smo proučevali molekularne mehanizme nekroptoze in jih primerjali z apoptozo, povzročeno s stavrosporinom.

**Materiali in metode.** Uporabili smo kulture podganjih astrocitov. Za proučevanje celične smrti smo uporabili stavrosporin ter inhibitorje apoptoze (z-vad-fmk) in nekroptoze (nekrostatin-1). Različne oblike celične smrti smo opazovali s pomočjo pretočne citometrije.

**Rezultati.** Stavrosporin lahko, odvisno od koncentracije, sproži tako apoptozo kot tudi nekroptozo. Apoptoza je odvisna od kaspaz in jo lahko zavremo s pan-kaspaznim inhibitorjem, nekroptoza pa je od kaspaz neodvisna. Nekroptoza je odvisna od RIP1 kinaz, lahko jo zavremo z nekrostatinom-1 in je povezana s tvorbo kisikovih radikalov. Prisotnost antioksidanta (BHA) zmanjša pojav nekroptoze.

**Zaključek.** Stavrosporin lahko v kulturah astrocitov sproži apoptozo in/ali nekroptozo, in sicer po različnih signalnih poteh. Razlikovanje med različnimi oblikami celične smrti je ključno pri proučevanju terapevtsko sprožene nekroptoze.

Radiol Oncol 2012; 46(4): 321-327.

doi:10.2478/v10019-012-0024-0

## Polimorfizmi 5-HTTLPR in anksioznost pri bolnicah z zgodnjim rakom dojke

Schillani G, Era D, Cristante T, Mustacchi G, Richiardi M, Grassi L, Giraldi T

**Izhodišča.** Doživljanje rakave bolezni večkrat spremljata anksioznost in depresija, kar vpliva na kvaliteto življenja bolnic z zgodnjim rakom dojke. 5-HTTLPR (*5-Hydroxytryptamine Transporter Gene-linked Polymorphic Region*) je funkcionalni polimorfizem serotoninskega transporterja, za katerega so ugotovili, da vpliva na adaptacijo na stres. Namen raziskave je bil proučiti povezavo med 5-HTTLPR polimorfizmi ter prilagoditev na diagnozo in zdravljenje raka.

**Bolniki in metode.** V raziskavo smo vključili 48 zaporednih bolnic z diagnozo raka dojke in jih sledili po enem in treh mesecih. Bolnice smo psihometrično ocenjevali s bolnišnično lestvico anksioznosti in depresije (*Hospital Anxiety and Depression Scale*) ter z lestvico, ki je prilagojena rakavim bolnikom (*Mini-Mental Adjustment to Cancer Scale – Mini-MAC*). Alelne variante 5-HTTLPR smo določevali z metodo PCR.

**Rezultati.** Psihometrična analiza bolnic je pokazala visoko stopnjo izogibanja in anksioznosti po lestvici Mini-MAC, kar se je s časom zmanjševalo. Zmanjševanje anksioznosti je bilo manjše pri bolnicah s S/S in S/L genetsko varianto 5-HTTLPR kot pri tistih, ki so bile nosilke L/L ( $p=0.023$ ), kar nakazuje na genetsko in okoljsko povezanost.

**Zaključki.** Rezultati raziskave nakazujejo, da bi lahko z določanjem polimorfizmov 5-HTTLPR pri bolnicah z zgodnjim rakom dojke odkrivali tiste, ki težje sprejemajo bolezen ter jih moramo zato dodatno obravnavati in ustrezneje zdraviti.

Radiol Oncol 2012; 46(4): 328-336.

doi:10.2478/raon-2013-0001

## Sevalne doze na občutljive organe pri obsevanju tumorjev glave in vratu ob uporabi intenzitetno modulirane radioterapije (IMRT) in 3-dimenzionalne conformalne radioterapije (3D-CRT)

Peszyńska-Piorun M, Malicki J, Golusiński W

**Izhodišča.** Načrtovanje obsevanja pri tumorjih glave in vratu je zahtevno zaradi številnih občutljivih organov, ki so v bližini načrtovanega volumna obsevanja (PTV). Upoštevati moramo tudi občutljive organe, ki so nekoliko oddaljeni. IMRT in 3D-CRT sta pogosta, a tudi zelo različna načina obsevanja pri zdravljenju tumorjev glave in vratu. Čeprav IMRT omogoča bolj prilagojeno dozo sevanja v PTV, še niso natančno ugotovili, pri katerem načinu zdravljenja občutljivi organi prejmejo manjšo dozo sevanja. Tako je bil namen raziskave primerjati zdravljenje z IMRT in 3D-CRT pri tumorjih glave in vratu glede na razporeditev sevalne doze na občutljive organe.

**Bolniki in metode.** V prospektivno raziskavo smo vključili 25 bolnikov z rakom grla in bolezenskim stadijem cT3-4N0-2. Pri vseh bolnikih je bila narejena totalna laringektomija in obojestranska selektivna odstranitev vratnih bezgavk. Vse bolnike smo zdravili z IMRT, primerjalno pa smo naredili tudi načrt zdravljenja s 3D-CRT. Za primerjavo sevalnih doz na občutljive organe smo naredili nov primerjalni indeks.

**Rezultati.** Največkrat smo z IMRT obsevali občutljive organe s primerljivo ali večjo dozo sevanja. Statistično značilna razlika se je pokazala le v malih možganih, ki bi s 3D-CRT zdravljenjem prejeli znatno manjšo dozo sevanja.

**Zaključki.** Organi, ki ležijo izven žarkovnih snopov IMRT (oddaljeni organi) so zelo zaščiteni pred sevanjem. Rezultate raziskave pa kažejo, da to ne velja za male možgane. Potrebujemo večje raziskave, da bi boljše določili učinek IMRT na oddaljena tkiva. Raziskave na antropomorfnem fantomu bi lahko potrdile izračunane rezultate.

Radiol Oncol 2012; 46(4): 337-345.  
doi:10.2478/v10019-012-0049-4

## Kombinirano zdravljenje raka gastroezofagealnega prehoda

Jeromen A, Oblak I, Anderluh F, Velenik V, Skoblar Vidmar M, Ratoša I

**Izhodišča.** Čeprav incidenca adenokarcinomov gastroezofagealnega prehoda v zahodnem svetu strmo narašča, še vedno obstajajo nesoglasja pri določevanju stadija in zdravljenju te bolezni. Namen retrospektivne raziskave je bil opredeliti učinkovitost in varnost pooperativne radiokemoterapije pri bolnikih s karcinomom gastroezofagealnega prehoda, ki so bili zdravljeni na Onkološkem inštitutu v Ljubljani.

**Bolniki in metode.** V raziskavo smo vključili 70 bolnikov s karcinomom gastroezofagealnega prehoda, ki so bili v obdobju med januarjem 2005 in junijem 2010 zdravljeni s pooperativno radiokemoterapijo. Bolnikom smo predpisali 6 krogov kemoterapije s 5-FU in cisplatinom in sočasno obsevanje z dozo 45 Gy.

**Rezultati.** Celotno zdravljenje je po protokolu zaključilo 26 bolnikov (37,1%). Srednje opazovalno obdobje je bilo 17,7 mesecev (3,3-64 mesecev). Akutne toksične sopojeve stopnje 3 ali več, kot so stomatitis, disfagija, slabost ali bruhanje in okužbe, smo ugotovili pri 2,9%, 34,3%, 38,6% in 41,5% bolnikih. Triletno preživetje brez ponovitve bolezni lokalno in področno (LRC) je bilo 78,2%, triletno preživetje brez ponovitve bolezni (DFS) 25,3%, triletno bolezensko specifično preživetje (DSS) 35,8% in triletno celokupno preživetje 33,9%. V multivariatni analizi preživetja sta bila splenektomija in vrednost Ca 19-9 >20 kU/L pred pričetkom pooperativnega zdravljenja neodvisna napovedna dejavnika za nižje DFS, DSS in celokupno preživetje. Starost pod 60 let, večje število prizadetih bezgavk in višji stadij bolezni pa so bili neodvisni napovedni dejavniki za nižje DSS in celokupno preživetje.

**Zaključki.** Pri bolnikih z adenokarcinomom gastroezofagealnega prehoda, ki so bili najprej operirani, je pooperativna radiokemoterapija primerna metoda zdravljenja, vendar moramo biti pozorni na pogoste akutne toksične sopojeve.

Radiol Oncol 2012; 46(4): 346-353.  
doi:10.2478/v10019-012-0048-5

## Rezultati zdravljenja in preživetje bolnikov s primarnimi limfomi centralnega živčevja zdravljenimi v obdobju od 1995 do 2010 na Onkološkem inštitutu Ljubljana

Barbara Jezeršek Novaković

**Izhodišča.** Primarni limfomi centralnega živčevja (PLCŽ) so redke oblike ektranodalnih ne-Hodgkinovih limfomov, ki jih največkrat zdravimo z visokimi odmerki metotreksata ali drugimi shemami na osnovi metotreksata, čemur lahko sledi obsevalno zdravljenje. Optimalnega zdravljenja PLCŽ še ne poznamo in v klinični praksi uporabljamo različne oblike zdravljenja. Z retrospektivno raziskavo smo proučevali bolnike s PLCŽ glede na njihove značilnosti, rezultate zdravljenja, preživetje brez bolezni in glede na celokupno preživetje.

**Bolniki in metode.** Devetinpetdeset bolnikov, ki so bili napoteni na Onkološki inštitut Ljubljana v letih 1995 do 2010, smo zdravili v skladu s tedaj veljavnimi smernicami. V letih od 1995 do 1999 so bili sistemsko zdravljeni s kemoterapijo CHOP (ciklofosfamid, doksorubicin, vinkristin, steroidi) in kasneje z visokimi odmerki metotreksata v monoterapiji ali v kombinaciji z drugimi učinkovinami. Od leta 1999 dalje so bili bolniki obsevani glede na njihovo starost in odgovor na sistemsko zdravljenje, pred tem so bili vsi bolniki, ki so prejeli CHOP kemoterapijo, zdravljeni tudi z obsevanjem. Bolniki, ki niso bili primerni za sistemsko zdravljenje, so bili zdravljeni samo z obsevanjem.

**Rezultati.** V naši skupini bolnikov so prevladovala ženske, srednja starost ob diagnozi je bila 59,8 let. Bolniki so imeli večinoma agresivne variante ne-Hodgkinovih B limfomov (69,5%), en bolnik je imel marginalnocelični limfom in dva bolnika T-celični limfom. V celoti je bilo 20,3% bolnikov zdravljenih samo s kemoterapijo, 33,9% s kombinirano terapijo in 42,4% samo z obsevanjem. Celokupni odgovor na primarno zdravljenje je bil 33,3% v primeru same kemoterapije, 65% v primeru kombiniranega zdravljenja in 56% v primeru samega obsevanja. Statistično značilno daljše trajanje odgovora na zdravljenje smo dosegli s kombiniranim zdravljenjem ali samim obsevanjem v primerjavi s samo kemoterapijo ( $p < 0,0006$ ). Srednje celokupno preživetje celotne skupine je bilo 11 mesecev, na celokupno preživetje pa je statistično značilno vplivala starost bolnikov. Najdaljše celokupno preživetje smo dosegli pri bolnikih, ki so bili zdravljeni s kombiniranim zdravljenjem, s srednjim preživetjem 39 mesecev. Bolniki zdravljeni samo z obsevanjem so imeli srednje celokupno preživetje 9 mesecev in tisti zdravljeni samo s kemoterapijo 4,5 mesecev.

**Zaključki.** Rezultati zdravljenja v rutinski klinični praksi so slabši od rezultatov kliničnih raziskav. Danes standardno zdravljenje z visokimi odmerki metotreksata z ali brez obsevanja je za nekatere bolnike preveč agresivno. Zato je potreben skrben izbor bolnikov, ki so primerni za takšno zdravljenje, na osnovi njihove starosti, stanja zmogljivosti in morebitnih spremljajočih bolezni. Glede na rezultate naše retrospektivne raziskave izključitev obsevalnega zdravljenja iz primarnega zdravljenja precej poslabša izhod bolezni, zato priporočamo obsevanje v kombiniranem zdravljenju.



Radiol Oncol 2012; 46(4): 354-359.  
doi:10.2478/v10019-012-0031-1

## Izražanje angiogenina in rastnega dejavnika žilnega endotela (VEGF) v pljučih bolnikov s pljučnim rakom

Rozman A, Šilar M, Košnik M

**Izhodišča.** Med umrlimi zaradi raka ima vodilno mesto pljučni rak. Pri rasti in napredovanju raka ima ključno vlogo angiogeneza. V prospektivni klinični raziskavi smo vrednotili izražanje dveh osrednjih regulatornih mediatorjev: angiogenina in rastnega dejavnika žilnega endotela (VEGF) pri bolnikih s pljučnim rakom.

**Bolniki in metode.** Zbrali smo klinične podatke, vzorce periferne venske krvi in bronho-alveolarne izpirke (BAL) 23-ih bolnikov s primarnim pljučnim rakom. BAL smo pridobili iz dela pljuč, ki je bil prizadet s pljučnim rakom in iz zrcalnega segmenta zdrave strani pljuč. Koncentracije VEGF in angiogenina smo izmerili z encimskoimunskim testom. Razredčitev bronhialnih izločkov v BAL smo izračunali iz razmerij koncentracij sečnine v serumu in BAL.

**Rezultati.** Med koncentracijami angiogenina v serumu in bronhialnih izločkih obeh strani pljuč nismo našli statistično pomembne povezave. Koncentracije VEGF so bile višje v bronhialnih izločkih dela pljuč, prizadetega s pljučnim rakom, kot v zdravi strani pljuč. Koncentracije VEGF so bile višje v bronhialnih izločkih obeh strani pljuč glede na serumske koncentracije. Serumske koncentracije VEGF so bile statistično značilno povezane z velikostjo tumorja ( $p = 0,003$ ) in z metastatskim stadijem bolezni ( $p = 0,041$ ). Koncentracije angiogenina in VEGF v bronhialnih izločkih zdrave strani pljuč so bile statistično povezane, prav tako kot njune koncentracije v bronhialnih izločkih delov pljuč, prizadetih s pljučnim rakom.

**Zaključki.** Na koncentraciji angiogenina in VEGF v sistemskih vzorcih, vzorcih ozadja in v lokalnih vzorcih bolnikov s pljučnim rakom vplivajo različni mehanizmi. Proangiogena aktivnost pljučnega raka ima pomemben vpliv na velikost koncentracij angiogenina in VEGF.

Radiol Oncol 2012; 46(4): 360-362.  
doi:10.2478/v10019-012-0006-2

## Intersticielna pljučna bolezen pri bolniku z metastatskim rakom debelega črevesa in danke, zdravljenega z oksaliplatinom, 5-fluorouracilom in leukovorinom (FOLFOX)

Hannan LM, Yoong J, Chong G, McDonald CF

**Izhodišče.** Standardna kemoterapevtska shema za zdravljenje napredovelega raka debelega črevesa in danke je kombinacija oksaliplatina, 5-fluorouracila in leukovorina (FOLFOX). Predstavljamo primer bolnika ki je razvil intersticielno pljučno bolezen, ob zdravljenju po shemi FOLFOX.

**Prikaz primera.** Moški, star 74 let z anamnezo metastatskega raka debelega črevesa in danke, je bil sprejet v bolnico zaradi 4 tedne trajajočih resnih težav z dihanjem, zlasti napredovale dispneje. Pred mesecem dni je zaključil šest krogov zdravljenja s kemoterapijo po shemi FOLFOX. Preiskave niso pokazale pljučne infekcije ali embolij. Računalniška tomografija pa je pokazala številne pljučne infiltrate in interlobarne zadebelitve septumov. Bolnik je takoj pričel zdravljenje s širokospektralnimi antibiotiki in kortikosteroidi, vendar se je dihalna stiska nadaljevala. Bolnik je štiri tedne po sprejemu v bolnišnico umrl zaradi respiratorne odpovedi. Obdukcija je pokazala difuzne alveolarne poškodbe, brez znakov tumorskih infiltracij, infekcije ali pljučnih embolij.

**Zaključek.** Čeprav redko, lahko zdravljenje s kemoterapijo po shemi FOLFOX povzroči resen zaplet s pljučno toksičnostjo. Takojšnja prekinitev kemoterapevtskega zdravljenja in aplikacija kortikosteroidov lahko izboljša potek bolezni.

Radiol Oncol 2012; 46(4): 363-369.

doi:10.2478/v10019-012-0015-1

## Uporaba barvnega čitalca za $^{60}\text{Co}$ z visoko hitrostjo doze pri brahiterapijski filmski dozimetriji z EBT radiokromskim filmom

Ghorbani M, Toossi MTB, Mowlavi AA, Roodi SB, Meigooni AS

**Izhodišča.** Namen raziskave je bil z radiokromskim filmom ovrednotiti delovanje barvnega čitalca pri dvodimenzionalni dozimetriji okrog brahiterapijskega izvira visoke hitrosti.

**Materiali in metode.** Uporabili smo Microtecov filmski čitalec ScanMaker 1000XL za izmero doznih porazdelitev okoli brahiterapijskega izvira  $^{60}\text{Co}$  GZP6 z radiokromskimi filmi GafChromic EBT. V preiskavah smo ocenili ne-uniformnost filma in čitalskega odziva kot tudi filmsko občutljivost na čitalski vir svetlobe. Pred samo dozimetrijo smo uporabili več filmskih vzorcev. Rezultate meritev smo primerjali s simuliranimi podatki MCNPX Monte Carlo. Izodozne krivulje pridobljene z radiokromskimi filmi in simulacijami Monte Carlo smo primerjali s tistimi iz planirnega sistema GZP6.

**Rezultati.** Skeniranje vzorcev enakomerno obsevanih filmov je pokazalo približno 2,85% in 4,97% neenakomernosti odziva v vzdolžni in prečni smeri filma. Ugotovitve so pokazale, da filmski odziv ni bil odvisen od izpostavljenosti čitalskemu viru svetlobe, zlasti pri večkratnem skeniranju. Rezultati merjenja z radiokromskim filmom so se dobro ujemali z izračuni Monte Carlo (4%) in z dozami, dobljenimi iz planirnega sistema GZP6 (5%).

**Zaključki.** Rezultati raziskave kažejo, da je barvni čitalec Microtek ScanMaker 1000XL v povezavi s filmom GafChromic EBT zanesljiv sistem za dozimetrično oceno brahiterapijskega izvira visoke hitrosti.



# Authors Index 2012

- Adeyanju OO: **2/126-135**  
 Adriaenssens N: **4/284-295**  
 Ahmad S: 3/265-270  
 Akansel G: 2/106-113  
 Al - Angari HA: 2/126-135  
 Aliakbarian M: 1/75-80  
 Anderluh F: 2/145-152;  
 3/252-257; 4/337-345  
 Arıkkök A: 1/28-31  
 Aryana K: **1/75-80**
- Bandi A: 3/226-232  
 Barden B: 3/189-197  
 Belsack D: 4/284-295  
 Bešić N: 2/160-165  
 Bešlić Š: **1/19-22**  
 Blagus T: 4/302-311  
 Blas M: 3/242-251  
 Bostancı H: 1/28-31  
 Bošnjak M: 4/302-311  
 Botros M: **1/23-27**  
 Breucq C: 4/284-295  
 Bruegel M: 1/8-18  
 Buyl R: 4/284-295
- Campagnutta E: 2/166-169  
 Canzonieri V: 2/166-169  
 Chang K: 1/23-27  
 Chen J: **3/179-188**  
 Chong G: 4/360-362  
 Christensen IJ: 3/207-212  
 Çiftçi E: 2/106-113  
 Cristante T: 4/321-327
- Čavlek M: 2/97-105  
 Čemažar M: 1/31-45; 4/302-311  
 Čufer T: 1/54-59
- De Mey J: 4/284-295  
 Debeljak N: 3/213-225  
 Del Pup L: **2/166-169**  
 Demirci A: 2/106-113
- Dilli A: 1/28-31  
 Dimopoulos J: 3/242-251  
 Ding Y: 3/189-197  
 Dolinšek T: 4/302-311  
 Dolžan V: 1/46-53
- Engels HP: 1/8-18  
 Era D: 4/321-327  
 Erčulj N: 1/46-53
- Fang L: **3/233-241**  
 Firoozabadi SM: 2/119-125;  
 3/226-232  
 Fras PA: 2/145-152  
 Fu N: 3/198-206  
 Fu Y: 3/233-241
- Gaberšček S: 1/81-88  
 Gehl J: 4/271-278  
 Gholizadeh M: 1/75-80  
 Ghorbani M: 2/170-178;  
**4/363-369**  
 Giraldi T: 4/321-327  
 Glavač D: 1/31-45  
 Glumac N: **3/258-264**  
 Golusiński W: 4/328-336  
 Goričar K: **1/46-53**  
 Grassi L: 4/321-327  
 Gregorič B: **2/153-159**  
 Gültekin S: **1/28-31**  
 Gümüştas S: **2/106-113**
- Hannan LM: **4/360-362**  
 Hasdemir A: 1/28-31  
 Herman T: 3/265-270  
 Hertl K: 2/97-105  
 Hočevar M: 1/60-68; 3/258-264  
 Hu J: 1/69-74  
 Hudej R: 3/242-251  
 Hwang DY: 4/296-301
- Inan N: 2/106-113  
 Iott M: 1/23-27  
 Iversen HK: 4/271-278
- Jeong HJ: 4/279-283  
 Jeong YJ: 4/279-283  
 Jeromel M: 2/89-96  
 Jeromen A: **4/337-345**  
 Jezeršek Novaković B:  
 2/153-159; **4/346-353**  
 Ji P: 1/69-74; 2/114-118  
 Jin X: 3/179-188  
 Jung EJ: **4/296-301**  
 Juvan P: 3/213-225
- Kadivec M: 2/97-105  
 Kafi-abad SA: 3/226-232  
 Kehl V: 1/8-18  
 Keller FS: 2/89-96  
 Kim DW: 4/279-283  
 Kim G: 4/296-301  
 Kim JS: **4/279-283**  
 Kim SR: 4/296-301  
 Kim YJ: 4/296-301  
 Knez L: 1/54-59  
 Kos J: 3/207-212  
 Košnik M: 4/354-359  
 Kovač V: 1/54-59; **2/136-144**  
 Kranjc S: 4/302-311  
 Krhin B: **2/160-165**  
 Krishnan S: 1/23-27  
 Kwak JY: 4/279-283
- Lamote J: 4/284-295  
 Lekić M: **1/54-59**  
 Li CH: 3/189-197  
 Li H: 3/233-241  
 Li X: 3/179-188  
 Lievens P: 4/284-295  
 Lim ST: 4/279-283  
 Linnert M: **4/271-278**  
 Lipnik-Štangelj M: 4/312-320

- Lu G: 3/198-206  
Luo ZH: 2/89-96  
Lv L: 3/198-206
- Ma RF: 3/189-197  
Malicki J: 4/328-336  
Mao H: 1/69-74; 2/114-118  
Markelc B: 4/302-311  
Matthiesen C: **3/265-270**  
McDonald CF: 4/360-362  
Meigooni AS: 2/170-178;  
4/363-369  
Meng Q: **3/198-206**  
Metz S: 1/8-18  
Miklavčič D: 2/119-125  
Milišić S: 1/19-22  
Miller R: 1/23-27  
Mir LM: 3/226-232  
Mlakar V: 1/31-45  
Momennezhad M: 1/75-80  
Mowlavi AA: 2/170-178;  
4/363-369  
Mozdarani H: 2/119-125  
Muenzel D: **1/8-18**  
Mustacchi G: 4/321-327  
Mušič M: 1/60-68
- Naji M: 1/75-80  
Nam SE: 4/296-301  
Naser Forghani M: 1/75-80  
Nielsen HJ: 3/207-212
- Oblak I: **2/145-152**; 3/252-257;  
4/337-345  
Ocvirk J: 3/252-257  
Özkara KS: 2/106-113
- Park HS: 4/296-301  
Pavčnik D: **2/89-96**  
Peszyńska-Piorun M: **4/328-336**  
Petrič P: 2/145-152; **3/242-251**  
Pilko G: **1/60-68**
- Podobnik G: 2/97-105  
Prosen L: 4/302-311
- Raeisi E: **3/226-232**  
Rahmatpour N: 3/226-232  
Ramgopol R: 3/265-270  
Ratoša I: 4/337-345  
Reza Aghamiri SM: 3/226-232  
Richiardi M: 4/321-327  
Rogelj P: 3/242-251  
Roodi SB: 4/363-369  
Rösch J: 2/89-96  
Rozman A: **4/354-359**  
Ruggiero L: 4/284-295  
Rummeny EJ: 1/8-18  
Ryu CG: 4/296-301
- Sadeghi R: 1/75-80  
Sadikov A: 1/54-59  
Sahakian AV: 2/126-135  
Schillani G: **4/321-327**  
Seavey J: 3/265-270  
Sedlar A: **4/302-311**  
Serraino D: 2/166-169  
Serša I: 1/1-7  
Serša G: 1/31-45; 3/213-225;  
4/302-311  
Shen HY: 3/189-197  
Shen J: 3/189-197  
Skoblar Vidmar M: 4/337-345  
Slavec K: 1/81-88  
Snoj M: 2/97-105; 3/258-264  
Sohn MH: 4/279-283  
Sun P: 3/179-188
- Šegedin B: 3/242-251  
Šilar M: 4/354-359  
Šimenc J: 4/312-320  
Šušterčič D: **1/1-7**
- Tekulve K: 2/89-96  
Todorović V: **1/31-45**
- Toossi MTB: **2/170-178**;  
4/363-369  
Towhidi L: **2/119-125**  
Triller N: 1/54-59  
Trošt N: **3/213-225**
- Uchida BT: 2/89-96
- Van Alstine WG: 2/89-96  
Velenik V: 2/145-152;  
**3/252-257**; 4/337-345  
Vižin T: **3/207-212**
- Wang M: 3/179-188  
Wang R: 3/179-188  
Wu J: 2/114-118
- Xu J: **3/189-197**
- Yang B: 3/198-206  
Yang GS: 3/233-241  
Yim CY: 4/279-283  
Yoong J: 4/360-362
- Zadel M: 1/46-53  
Zadnik V: 2/153-159  
Zebič-Šinkovec M: **2/97-105**  
Zeng ZP: 3/189-197  
Zhang HB: 3/233-241  
Zhao Y: 3/179-188  
Zheng X: **1/69-74**; **2/114-118**  
Zobec Logar HB: 3/242-251  
Zukić F: 1/19-22  
Zupanič Slavec Z: **1/81-88**  
Zwitter M: 2/136-144
- Žagar T: 2/136-144  
Žgajnar J: 1/60-68

# Subject Index 2012

- 3D visualization: 1/1-7  
 3D-CRT: 4/328-336  
 5-HTTLPR polymorphism: 4/321-327  
<sup>60</sup>Co high dose rate source: 4/363-369
- aggressiveness: 3/179-188  
 anal cancer: 2/145-152  
 angiogenin: 4/354-359  
 anxiety: 4/321-327  
 apoptosis: 3/233-241; 4/312-320;  
 apparent diffusion coefficient: 2/106-113  
 arterioportal fistula: 3/198-206  
 astrocytes: 4/312-320  
 atrial septal defect: 2/89-96  
 axial and radial rigidity: 2/114-118  
 Ayre's spatula: 2/166-169
- BAL fluid: 4/354-359  
 benign prostatic hyperplasia: 1/69-74  
 biomaterial: 2/89-96  
 bleomycin: 4/271-278; 1/31-45  
 blood-brain barrier: 4/271-278  
 brachytherapy: 2/170-178; 3/242-251  
 brain metastases: 1/54-59; 4/271-278  
 breast cancer: 1/23-27; 2/97-105; 3/213-225; 4/321-327  
 breast conserving surgery: 4/284-295  
 breast implant: 1/23-27  
 breast irradiation: 4/284-295  
 breast oedema: 4/284-295  
 bronchoscopy: 4/354-359
- carcinoma: 4/302-311  
 cardiogenic trans-sinusoidal shunting: 3/198-206  
 Castleman's disease: 3/265-270  
 cathepsin X: 3/207-212  
 cervix cancer: 3/242-251  
 cetuximab: 3/252-257  
 chemotherapy: 2/136-144  
 choline: 3/179-188  
 cisplatin: 3/213-225; 3/226-232; 4/302-311  
 Clinic for Nuclear Medicine: 1/81-88  
 collimator: 1/75-80  
 color scanner: 4/363-369  
 colorectal cancer: 3/207-212  
 colour Doppler ultrasonography: 1/28-31  
 comet assay: 1/46-53  
 computed tomography (CT): 3/189-197  
 contouring: 3/242-251  
 core biopsy: 1/19-22  
 CT: 1/19-22  
 cysteine cathepsins: 3/207-212  
 cytobrush: 2/166-169  
 cytotoxicity: 3/213-225
- dental pupil anatomy: 1/1-7  
 depression: 4/321-327  
 diffuse alveolar damage: 4/360-362  
 diffuse large B-cell lymphoma: 2/153-159  
 diffusion-weighted imaging: 2/106-113  
 digital rectal examination: 1/69-74  
 DNA repair: 1/46-53  
 early breast cancer: 4/284-295
- EBT radiochromic film: 4/363-369  
 electrochemotherapy: 1/31-45; 4/271-278; 4/302-311  
 electrode configuration: 2/126-135  
 electrode device: 4/271-278  
 electro-endocytosis: 2/119-125  
 electroporation: 1/31-45; 2/119-125; 3/226-232; 4/271-278  
 embolism: 2/89-96  
 endodontic treatment: 1/1-7  
 erection: 2/114-118  
 erythropoietin: 3/213-225
- F-18 FDG: 4/279-283  
 false positive radioiodine: 1/28-31  
 female cancer: 2/166-169  
 flow cytometry: 4/312-320  
 FNAB: 1/19-22
- gastroesophageal junction adenocarcinoma: 4/337-345  
 gemcitabine in prolonged infusion: 2/136-144  
 gene electrotransfer: 4/302-311  
 genetic polymorphism: 1/46-53  
 GZP6: 2/170-178  
 GZP6 brachytherapy source: 4/363-369
- HDR: 4/363-369  
 head and neck cancer: 4/328-336  
 HEAP: 1/75-80  
 heart septal defects: 2/89-96  
 hepatocellular carcinoma: 2/126-135  
 high energy all purpose: 1/75-80  
 history: 1/81-88  
 homologous recombination: 1/46-53
- IL-12: 4/302-311  
 IMRT: 3/265-270; 4/328-336  
 incidence: 2/136-144  
 inguinal: 3/258-264  
 interstitial lung disease: 4/360-362

- invasive ductal carcinoma: 3/226-232  
 invasive lobular carcinoma: 1/23-27  
 irradiation: 3/226-232  
 irreversible electroporation: 2/126-135  
  
 LEHR: 1/75-80  
 limb salvage surgery: 3/189-197  
 liver cancer stem cells: 3/233-241  
 Ljubljana: 1/81-88  
 LMS: 1/8-18  
 low energy high resolution: 1/75-80  
 L-thyroxine: 2/160-165  
 lung cancer: 4/354-359  
 lung lesions: 1/19-22  
 lymphadenectomy: 3/258-264  
 lymphoedema of the breast: 4/284-295  
 lymphoscintigraphy: 1/75-80  
  
 magnetic resonance imaging: 1/28-31; 2/106-113  
 magnetic resonance imaging (MRI): 3/189-197; 4/296-301  
 malignant pleural mesothelioma: 2/136-144  
 melanoma: 1/31-45; 1/60-68; 3/258-264  
 mental adjustment to cancer: 4/321-327  
 metastatic potential: 1/31-45  
 mice: 4/302-311  
 microarray analysis: 1/31-45  
 micrometastases: 3/258-264  
 miR-548c-5p: 3/233-241  
 Monte Carlo simulation: 2/170-178  
 MR microscopy: 1/1-7  
 MRI: 2/97-105; 3/242-251  
 MRI guided vacuum assisted biopsy: 2/97-105  
 multimodalities: 3/226-232  
  
 necroptosis: 4/312-320  
 NF- $\kappa$ B,  $\beta$ -catenin: 3/233-241  
 nuclear medicine: 1/81-88  
  
 optimization: 2/126-135  
 outcome: 2/145-152  
 overall survival: 1/60-68  
 oxaliplatin: 4/360-362  
  
 PACS: 1/8-18  
 peritoneal reflection: 4/296-301  
 PET/CT: 4/279-283; 3/179-188  
 portal hypertension: 3/198-206  
 postoperative radiochemotherapy: 4/337-345  
 post-therapy I-131 whole body scan: 1/28-31  
 pregnancy: 2/160-165  
 primary central nervous system lymphomas: 4/346-353  
 prognosis: 3/207-212  
 prophylactic cranial irradiation: 1/54-59  
 prostate cancer: 3/179-188; 1/69-74  
 pulmonary lesions: 2/106-113  
  
 radiochemotherapy: 2/145-152  
 radio-chemotherapy: 3/252-257  
 radiotherapy: 4/328-336  
 R-CHOP: 2/153-159  
 reactive oxygen species: 4/312-320  
 RECIST: 1/8-18  
 rectal cancer: 3/252-257; 4/296-301  
 routine treatments: 2/153-159  
 rupture: 1/23-27  
  
 salvage surgery: 2/145-152  
 sarcoma: 4/302-311  
 sentinel lymph node biopsy: 3/258-264  
  
 sentinel node: 1/75-80  
 serum biomarker: 3/207-212  
 shear wave velocity: 2/114-118  
 shear wave velocity: 1/69-74  
 Slovenia: 1/81-88  
 small intestinal submucosa: 2/89-96  
 small-cell lung cancer: 1/54-59  
 staurosporine: 4/312-320  
 subcutaneous panniculitis-like T-cell lymphoma: 4/279-283  
 superimposition method: 2/170-178  
 survival: 2/136-144; 4/346-353  
  
 TG-43: 2/170-178  
 thyroid cancer: 1/28-31  
 thyroid carcinoma: 2/160-165  
 time-varying magnetic field: 2/119-125  
 toxicity: 4/337-345  
 transcatheter closure: 2/89-96  
 transmembrane molecular transport: 2/119-125  
 transthoracic biopsy: 1/19-22  
 treatment outcomes: 4/346-353  
 treatment result: 2/153-159  
 tricuspid regurgitation: 3/198-206  
 TSH suppression: 2/160-165  
 tumour burden: 1/60-68  
 tumour measurement: 1/8-18  
  
 ultrasound: 1/60-68  
 ultrasound elastography: 4/284-295  
  
 vaginal cytology: 2/166-169  
 vascular endothelial growth factor: 4/354-359  
 velocity tracing: 3/198-206  
 virtual touch tissue quantification: 1/69-74; 2/114-118

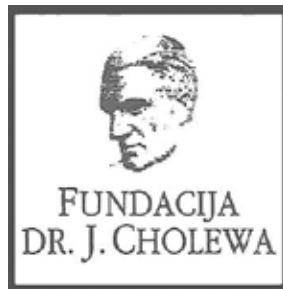


FUNDACIJA "DOCENT DR. J. CHOLEWA"  
JE NEPROFITNO, NEINSTITUCIONALNO IN NESTRANKARSKO  
ZDRUŽENJE POSAMEZNIKOV, USTANOV IN ORGANIZACIJ, KI ŽELIJO  
MATERIALNO SPODBUJATI IN POGLABLJATI RAZISKOVALNO  
DEJAVNOST V ONKOLOGIJI.

DUNAJSKA 106  
1000 LJUBLJANA

ŽR: 02033-0017879431





## **Activity of "Dr. J. Cholewa" Foundation for Cancer Research and Education - a report for the third quarter of 2012**

The Dr. J. Cholewa Foundation for Cancer Research and Education is a non-profit, non-government and non-political association of experts, institutions and organisations associated with cancer research, cancer education, cancer treatment and prevention. Its principal aim is to search for and support new ideas, initiatives and forward thinking in all of the activities associated with cancer.

The Foundation plans to broaden its sphere of activity with the establishment of a number of boards of commissioners that are to further advance the planning, execution and evaluation of research and publishing projects in the future. A new program for the Foundation's activities is to be discussed in the near future. Among other activities, the Foundation continues to support the publication of "Radiology and Oncology", an international scientific journal that is edited, published and printed in Ljubljana, Slovenia. "Radiology and Oncology" publishes scientific articles, reviews, case reports, short reports and letters to the editor about research and studies in experimental and clinical oncology, supportive therapy, experimental and clinical research in radiology, radiophysics, and prevention and early diagnostics of different types of cancer. "Radiology and Oncology" is an open access journal available in pdf format and with a Science Citation Index impact factor. Throughout the year 2012 the Foundation continued to support a number of lay associations and organizations that are involved in education and spread of information to professionals and lay people about cancer in Slovenia.

The Dr. J. Cholewa Foundation for Cancer Research and Education continues to assist and oncological, radiological and other professional associations in Slovenia to organise scientific and other meetings of specific interest in different fields of cancer research and education. The Foundation is also firmly committed to support all non-professional organisations that are involved in cancer education of groups interested in problems associated with oncology and population in general in Slovenia.

Tomaž Benulič, MD  
Borut Štabuc, MD, PhD  
Andrej Plesničar, MD

# TANTUM® VERDE

Benzidamin



Lajšanje bolečine in oteklina pri vnetju v ustni votlini in žrelu, ki nastanejo zaradi okužb in stanj po operaciji in kot posledica radioterapije (t.i. radiomukozitis).



Imetnik dovoljenja za promet  
CSC Pharma d.o.o.  
Jana Husa 1a  
1000 Ljubljana



www.tantum-verde.si

## Tantum Verde 1,5 mg/ml oralno pršilo, raztopina

### **Kakovostna in količinska sestava**

1 ml raztopine vsebuje 1,5 mg benzidaminijevega klorida, kar ustreza 1,34 mg benzidamina. V enem razpršku je 0,17 ml raztopine. En razpršek vsebuje 0,255 mg benzidaminijevega klorida, kar ustreza 0,2278 mg benzidamina. En razpršek vsebuje 13,6 mg 96 odstotnega etanola, kar ustreza 12,728 mg 100 odstotnega etanola, in 0,17 mg metilparahidroksibenzoata (E218).

### **Terapevtske indikacije**

Samozdravljenje: lajšanje bolečine in oteklina pri vnetju v ustni votlini in žrelu, ki so lahko posledica okužb in stanj po operaciji. Po nasvetu in navodilu zdravnika: lajšanje bolečine in oteklina v ustni votlini in žrelu, ki so posledica radiomukozitisa.

### **Odmerjanje in način uporabe**

Uporaba 2- do 6-krat na dan (vsake 1,5 do 3 ure). Odrasli: 4 do 8 razprškov 2- do 6-krat na dan. Otroci od 6 do 12 let: 4 razprški 2- do 6-krat na dan. Otroci, mlajši od 6 let: 1 razpršek na 4 kg telesne mase; do največ 4 razprške 2 do 6-krat na dan.

### **Kontraindikacije**

Znana preobčutljivost za zdravilno učinkovino ali katerokoli pomožno snov.

### **Posebna opozorila in previdnostni ukrepi**

Pri manjšini bolnikov lahko resne bolezni povzročijo ustne/žrelne ulceracije. Če se simptomi v treh dneh ne izboljšajo, se mora bolnik posvetovati z zdravnikom ali zobozdravnikom, kot je primerno. Zdravilo vsebuje aspartam (E951) (vir fenilalanina), ki je lahko škodljiv za bolnike s fenilketonurijo. Zdravilo vsebuje izomalt (E953) (sinonim: izomaltitol (E953)). Bolniki z redko dedno intoleranco za fruktozo ne smejo jemati tega zdravila. Uporaba benzidamina ni priporočljiva za bolnike s preobčutljivostjo za salicilno kislino ali druga nesteroidna protivnetna zdravila. Pri bolnikih, ki imajo ali so imeli bronhialno astmo, lahko pride do bronhospazma. Pri takih bolnikih je potrebna previdnost.

### **Medsebojno delovanje z drugimi zdravili in druge oblike interakcij**

Pri ljudeh raziskav o interakcijah niso opravljali.

### **Nosečnost in dojenje**

Tantum Verde z okusom mentola 3 mg pastile se med nosečnostjo in dojenjem ne smejo uporabljati.

### **Vpliv na sposobnost vožnje in upravljanja s stroji**

Uporaba benzidamina lokalno v priporočenem odmerku ne vpliva na sposobnost vožnje in upravljanja s stroji.

### **Neželeni učinki**

**Bolezni prebavil** Redki: pekoč občutek v ustih, suha usta.

**Bolezni imunskega sistema** Redki: preobčutljivostna reakcija.

**Bolezni dihal, prsnega koša in mediastinalnega prostora** Zelo redki: laringospazem.

**Bolezni kože in podkožja** Občasni: fotosenzitivnost. Zelo redki: angioedem.

### **Rok uporabnosti**

4 leta. Zdravila ne smejo uporabljati po datumu izteka roka uporabnosti, ki je naveden na ovojnjini. Posebna navodila za shranjevanje Za shranjevanje pastil niso potrebna posebna navodila. Platenko z raztopino shranjujte v zunanji ovojnjini za zagotovitev zaščite pred svetlobo. Shranjujte pri temperaturi do 25°C. Shranjujte v originalni ovojnjini in nedosegljivo otrokom.



*Iščete rešitve na področju znanosti o življenju?  
Potrebujete ustrezna orodja za analitiko?*

***Mi vam jih ponujamo!***

- Reagenti za diagnostiko in biomedicino
- Instrumenti in tehnična podpora
- Potrošni material
- Aplikativna pomoč
- Pipetni program in akreditirane kalibracije
- Plastika

*Kakovost • Izbira • Zadovoljstvo*

T H E

*Natrelle*<sup>TM</sup>

C O L L E C T I O N

*Prsni vsadki in ekspanderji tkiv*

*I*ndividualne ženske  
*I*ndividualen izbor



 **ALLERGAN**

**DISTRIBUCIJA IN PRODAJA:**

SANOLABOR, d.d.,  
Leskoškova 4, 1000 Ljubljana, Slovenija  
Tel: +386 (0)1 585-42-11  
Fax: +386 (0)1 585-42-98  
www.sanolabor.si

 **Sanolabor**

**PROMOCIJA, MARKETING IN STROKOVNA PODPORA:**

EWOPHARMA d.o.o., Cesta 24. junija 23, 1000 Ljubljana, Slovenija  
Jurij Pivka, vodja poslovne enote - Medicinska estetika  
Tel: +386 (0) 59 084 845, mobilnik: +386 (0) 51 326 058  
Fax: +386 (0) 59 084 849

**ERBITUX<sup>®</sup>**  
CETUXIMAB

See the difference

This is what  
tumor shrinkage  
looks like



Merck Serono Oncology | *Combination is key™*

**Erbix 5 mg/ml raztopina za infundiranje**  
Skrajšan povzetek glavnih značilnosti zdravila

**Sestava:** En ml raztopine za infundiranje vsebuje 5 mg cetuximaba in pomožne snovi. Cetuximab je himerno monoklonsko IgG<sub>1</sub> protitelo. **Terapevtske indikacije:** Zdravilo Erbitux je indicirano za zdravljenje bolnikov z metastatskim kolorektalnim rakom z ekspresijo receptorjev EGFR in nemutiranim tipom KRAS v kombinaciji s kemoterapijo na osnovi irinotekana, kot primarno zdravljenje v kombinaciji s FOLFOX in kot samostojno zdravilo pri bolnikih, pri katerih zdravljenje z oksaliplatinom in irinotekanom ni bilo uspešno ter pri bolnikih, ki ne prenašajo irinotekana. Zdravilo Erbitux je indicirano za zdravljenje bolnikov z rakom skvamoznih celic glave in vratu v kombinaciji z radioterapijo za lokalno napredovalo bolezen in v kombinaciji s kemoterapijo na osnovi platine za ponavljajočo se in/ali metastatsko bolezen. **Odmerjanje in način uporabe:** Zdravilo Erbitux pri vseh indikacijah infundirajte enkrat na teden. Pred prvo infuzijo mora bolnik prejeti premedikacijo z antihistaminikom in kortikosteroidom. Začetni odmerek je 400 mg cetuximaba na m<sup>2</sup> telesne površine. Vsi naslednji tedenski odmerki so vsak po 250 mg/m<sup>2</sup>. **Kontraindikacije:** Zdravilo Erbitux je kontraindicirano pri bolnikih z znano hudo preobčutljivostno reakcijo (3. ali 4. stopnje) na cetuximab. Kombinacija zdravila Erbitux s kemoterapijo, ki vsebuje oksaliplatin, je kontraindicirana pri bolnikih z metastatskim kolorektalnim rakom z mutiranim tipom KRAS ali kadar status KRAS ni znan. **Posebna opozorila in previdnostni ukrepi:** Če pri bolniku nastopi blaga ali zmerna reakcija, povezana z infundiranjem, lahko zmanjšate hitrost infundiranja. Priporočljivo je, da ostane hitrost infundiranja na nižji vrednosti tudi pri vseh naslednjih infuzijah. Če se pri bolniku pojavi huda kožna reakcija (≥ 3. stopnje po kriterijih US NCI-CTC), morate prekiniti terapijo s cetuximabom. Z zdravljenjem smete nadaljevati le, če se je reak-

cija izboljšala do 2. stopnje. Zaradi možnosti pojava znižanja nivoja magnezija v serumu se pred in periodično med zdravljenjem priporoča določanje koncentracije elektrolitov. Če se pojavi sum na nevtropenijo, je potrebno bolnika skrbno nadzorovati. Potrebno je upoštevati kardiovaskularno stanje bolnika in sočasno dajanje kardiotskičnih učinkovin kot so fluoropirimidini. Cetuximab je treba uporabljati previdno pri bolnikih z anamnezo keratitisa, ulcerativnega keratitisa ali zelo suhih oči. **Interakcije:** Farmakokinetične značilnosti cetuximaba ostanejo nespremenjene po sočasni uporabi enkratnega odmerka irinotekana, tudi farmakokinetika irinotekana je nespremenjena pri sočasni uporabi cetuximaba. Pri kombinaciji s fluoropirimidini se je povečala pogostnost srčne ishemije, vključno z miokardnim infarktom in kongestivno srčno odpovedjo ter pogostnost sindroma dlani in stopal. V kombinaciji s kemoterapijo na osnovi platine se lahko poveča pogostnost hude levkopenije ali hude nevtropenije. **Neželeni učinki:** Zelo pogosti (≥ 1/10): hipomagneziemija, povečanje ravnih jetrnih encimov, kožne reakcije, blage ali zmerne reakcije povezane z infundiranjem, blag do zmeren mukozitis. Pogosti (≥ 1/100, < 1/10): dehidracija, hipokalciemija, anoreksija, glavobol, konjunktivitis, driska, navzeja, bruhanje, hude reakcije povezane z infundiranjem, utrujenost. **Posebna navodila za shranjevanje:** Shranjujte v hladilniku (2 °C - 8 °C). **Pakiranje:** 1 viala z 20 ml ali 100 ml raztopine. **Način in režim izdaje:** H. Imetnik dovoljenja za promet: Merck KGaA, 64271 Darmstadt, Nemčija. **Datum zadnje revizije besedila:** Avgust 2012. Pred predpisovanjem zdravila natančno preberite celoten Povzetek glavnih značilnosti zdravila. **Podrobnejše informacije so na voljo pri predstavniku imetnika dovoljenja za promet z zdravilom:** Merck d.o.o., Ameriška ulica 8, 1000 Ljubljana, tel.: 01 560 3810, faks: 01 560 3830, el. pošta: info@merck.si



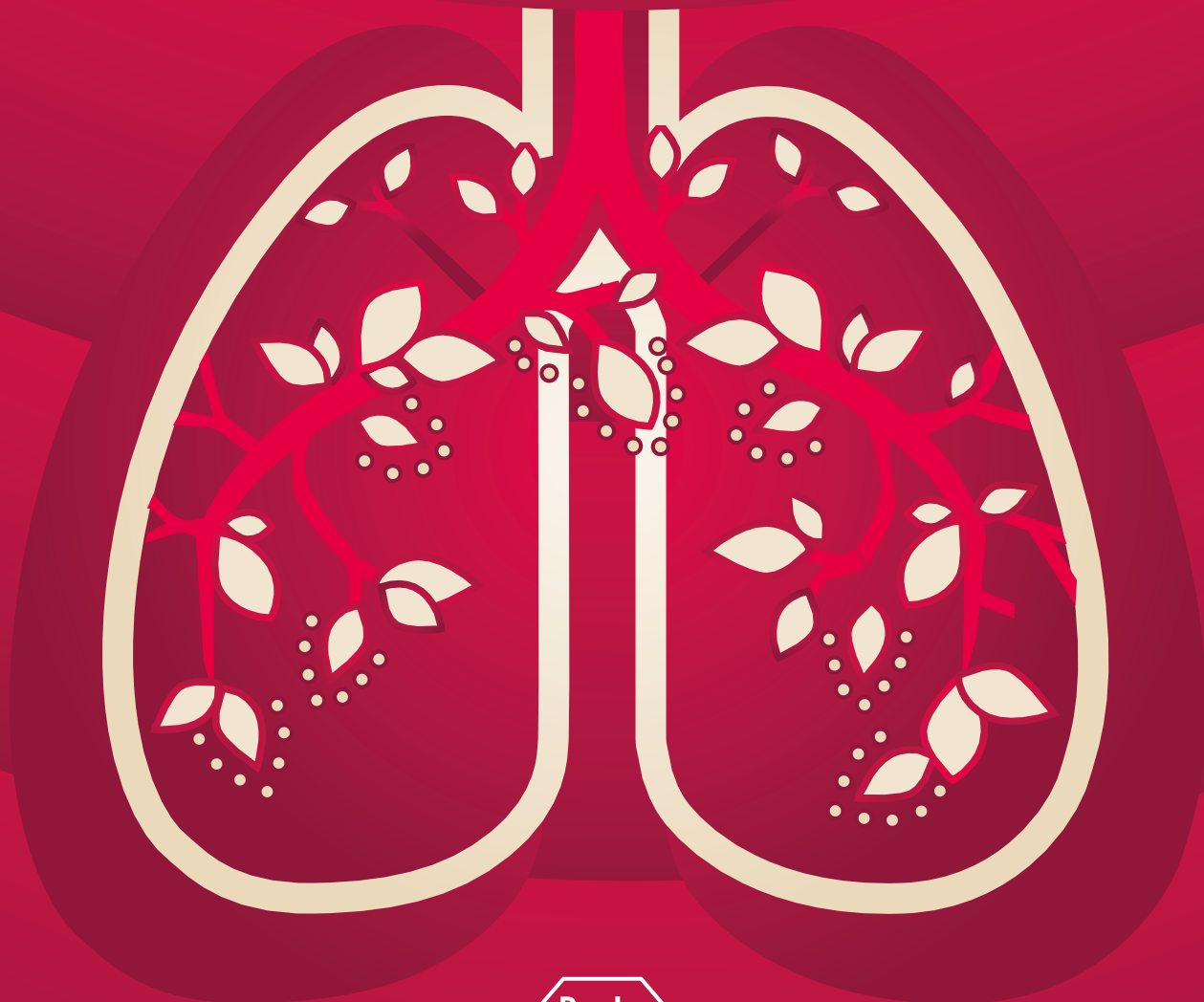


# ČAS ZA ŽIVLJENJE.

## DOKAZANO PODALJŠA PREŽIVETJE PRI BOLNIKI<sup>1</sup>:

- z lokalno napredovalim ali metastatskim nedrobnoceličnim rakom pljuč<sup>1</sup>
- z metastatskim rakom trebušne slinavke<sup>1</sup>

<sup>1</sup> Povzetek glavnih značilnosti zdravila TARCEVA, [www.ema.europa.eu](http://www.ema.europa.eu)





# odprto

Vir  
Sodelovanje  
Izobraževanje  
Jasnost  
Zavezanost

Novartis Oncology prinaša spekter inovativnih zdravil, s katerimi poskuša spremeniti življenje bolnikov z rakavimi in hematološkimi obolenji.

Ta vključuje zdravila kot so Glivec® (imatinib), Tassigna® (nilotinib), Afinitor® (everolimus), Zometa® (zoledronska kislina), Femara® (letrozol), Sandostatin® LAR® (oktreetid/i.m. injekcije) in Exjade® (deferasiroks).

Novartis Oncology ima tudi obširen razvojni program, ki izkorišča najnovejša spoznanja molekularne genomike, razumskega načrtovanja in tehnologij za odkrivanje novih učinkovin.

 **glivec**  
imatinib

 **Tassigna**  
(nilotinib)

 **AFINITOR**  
(everolimus) tablete

**ZOMETA**  
zoledronska kislina

 **Femara**  
(letrozol)

 **Sandostatin LAR**  
oktreetid / i.m. injekcija

 **EXJADE**  
deferasiroks



# Instructions for authors

## The editorial policy

Radiology and Oncology is a multidisciplinary journal devoted to the publishing original and high quality scientific papers, professional papers, review articles, case reports and varia (editorials, short communications, professional information, book reviews, letters, etc.) pertinent to diagnostic and interventional radiology, computerized tomography, magnetic resonance, ultrasound, nuclear medicine, radiotherapy, clinical and experimental oncology, radiobiology, radiophysics and radiation protection. Therefore, the scope of the journal is to cover beside radiology the diagnostic and therapeutic aspects in oncology, which distinguishes it from other journals in the field.

The Editorial Board requires that the paper has not been published or submitted for publication elsewhere; the authors are responsible for all statements in their papers. Accepted articles become the property of the journal and, therefore cannot be published elsewhere without the written permission of the editors.

## Submission of the manuscript

The manuscript written in English should be submitted to the journal via online submission system Editorial Manager available for this journal at: [www.radioloncol.com](http://www.radioloncol.com).

In case of problems, please contact Sašo Trupej at [saso.trupej@computing.si](mailto:saso.trupej@computing.si) or the Editor of this journal at [gsera@onko-i.si](mailto:gsera@onko-i.si)

All articles are subjected to the editorial review and the review by independent referees.

Authors are requested to suggest persons competent to review their manuscript. However, please note that this will be treated only as a suggestion, the final selection of reviewers is exclusively the Editor's decision. The authors' names are revealed to the referees, but not vice versa.

Manuscripts which do not comply with the technical requirements stated herein will be returned to the authors for the correction before peer-review. The editorial board reserves the right to ask authors to make appropriate changes of the contents as well as grammatical and stylistic corrections when necessary. Page charges will be charged for manuscripts exceeding the recommended page number, as well as additional editorial work and requests for printed reprints.

All articles are published printed and on-line as the open access. To support the open access policy of the journal, the authors are encouraged to pay the open access charge of 500 EUR.

Manuscripts submitted under multiple authorship are reviewed on the assumption that all listed authors concur in the submission and are responsible for its content; they must have agreed to its publication and have given the corresponding author the authority to act on their behalf in all matters pertaining to publication. The corresponding author is responsible for informing the coauthors of the manuscript status throughout the submission, review, and production process.

## Preparation of manuscripts

Radiology and Oncology will consider manuscripts prepared according to the Uniform Requirements for Manuscripts Submitted to Biomedical Journals by International Committee of Medical Journal Editors ([www.icmje.org](http://www.icmje.org)). The manuscript should be typed double-spaced with a 3-cm margin at the top and left-hand side of the sheet. The manuscript should be written in grammatically and stylistically correct language. Abbreviations should be avoided. If their use is necessary, they should be explained at the first time mentioned. The technical data should conform to the SI system. The manuscript, including the references, must not exceed 15 typewritten pages, and the number of figures and tables is limited to 8. If appropriate, organize the text so that it includes: Introduction, Materials and methods, Results and Discussion. Exceptionally, the results and discussion can be combined in a single section. Start each section on a new page, and number each page consecutively with Arabic numerals.

**The Title page** should include a concise and informative title, followed by the full name(s) of the author(s); the institutional affiliation of each author; the name and address of the corresponding author (including telephone, fax and E-mail), and an abbreviated title. This should be followed by the abstract page, summarizing in less than 250 words the reasons for the study, experimental approach, the major findings (with specific data if possible), and the principal conclusions, and providing 3-6 key words for indexing purposes. Structured abstracts are preferred. Slovene authors are requested to provide title and the abstract in Slovene language in a separate file. The text of the research article should then proceed as follows:

Introduction should summarize the rationale for the study or observation, citing only the essential references and stating the aim of the study.

**Materials and methods** should provide enough information to enable experiments to be repeated. New methods should be described in detail.

**Results** should be presented clearly and concisely without repeating the data in the figures and tables. Emphasis should be on clear and precise presentation of results and their significance in relation to the aim of the investigation.

**Discussion** should explain the results rather than simply repeating them and interpret their significance and draw conclusions. It should discuss the results of the study in the light of previously published work.

**Charts, Illustrations, Photographs and Tables** must be numbered and referred to in the text, with the appropriate location indicated. Charts, illustrations and photographs, provided electronically, should be of appropriate quality for good reproduction. Illustrations and charts must be vector image, created in CMYK colour space, used font families are encouraged "Century Gothic" and saved as .AI, .EPS or .PDF format. Color charts, illustrations and photographs are encouraged. Picture (image) size must be 2,000 pixels on the longer side and saved as .JPG (maximum quality) format. In photographs, mask the identities of the patients. Tables should be typed double-spaced, with a descriptive title and, if appropriate, units of numerical measurements included in the column heading. The files with the figures can be uploaded as separate files.

**References** must be numbered in the order in which they appear in the text and their corresponding numbers quoted in the text. Authors are responsible for the accuracy of their references. References to the Abstracts and Letters to the Editor must be identified as such. Citation of papers in preparation or submitted for publication, unpublished observations, and personal communications should not be included in the reference list. If essential, such material may be incorporated in the appropriate place in the text. References follow the style of Index Medicus. All authors should be listed when their number does not exceed six; when there are seven or more authors, the first six listed are followed by "et al.". The following are some examples of references from articles, books and book chapters:

Dent RAG, Cole P. *In vitro* maturation of monocytes in squamous carcinoma of the lung. *Br J Cancer* 1981; **43**: 486-95.

Chapman S, Nakielny R. *A guide to radiological procedures*. London: Bailliere Tindall; 1986.

Evans R, Alexander P. Mechanisms of extracellular killing of nucleated mammalian cells by macrophages. In: Nelson DS, editor. *Immunobiology of macrophage*. New York: Academic Press; 1976. p. 45-74.

### Authorization for the use of human subjects or experimental animals

Manuscripts containing information related to human or animal use should clearly state that the research has complied with all relevant national regulations and institutional policies and has been approved by the authors' institutional review board or equivalent committee. These statements should appear in the Materials and methods section (or for contributions without this section, within the main text or in the captions of relevant figures or tables).

When reporting experiments on human subjects, authors should indicate whether the procedures followed were in accordance with the Helsinki Declaration. Patients have the right to privacy; therefore the identifying information (patient's names, hospital unit numbers) should not be published unless it is essential. In such cases the patient's informed consent for publication is needed, and should appear as an appropriate statement in the article.

The research using animal subjects should be conducted according to the EU Directive 2010/63/EU and following the Guidelines for the welfare and use of animals in cancer research (*Br J Cancer* 2010; **102**: 1555 – 77). Authors must identify the committee approving the experiments, and must confirm that all experiments were performed in accordance with relevant regulations.

### Transfer of copyright agreement

For the publication of accepted articles, authors are required to send the Transfer of Copyright Agreement to the publisher on the address of the editorial office. A properly completed Transfer of Copyright Agreement, signed by the Corresponding Author on behalf of all the authors, must be provided for each submitted manuscript. The non-commercial use of each article will be governed by the Creative Commons Attribution-NonCommercial-NoDerivs license.

### Conflict of interest

When the manuscript is submitted for publication, the authors are expected to disclose any relationship that might pose real, apparent or potential conflict of interest with respect to the results reported in that manuscript. Potential conflicts of interest include not only financial relationships but also other, non-financial relationships. In the Acknowledgement section the source of funding support should be mentioned. The Editors will make effort to ensure that conflicts of interest will not compromise the evaluation process of the submitted manuscripts; potential editors and reviewers will exempt themselves from review process when such conflict of interest exists. The statement of disclosure must be in the Cover letter accompanying the manuscript or submitted on the form available on [www.icmje.org/coi\\_disclosure.pdf](http://www.icmje.org/coi_disclosure.pdf)

**Page proofs** will be sent by E-mail or faxed to the corresponding author. It is their responsibility to check the proofs carefully and return a list of essential corrections to the editorial office within three days of receipt. Only grammatical corrections are acceptable at this time.

**Reprints:** The electronic version of the published papers will be available on [www.versitaopen.com/ro](http://www.versitaopen.com/ro) free of charge.



# Zdravljenje metastatskega raka ledvičnih celic (mRCC), gastrointestinalnega stromalnega tumorja (GIST) in neuroendokrinih tumorjev trebušne slinavke (pNET)

## BISTVENE INFORMACIJE IZ POVZETKA GLAVNIH ZNAČILNOSTI ZDRAVILA

### SUTENT 12,5 mg, 25 mg, 37,5 mg, 50 mg trde kapsule

**Sestava in oblika zdravila:** Ena kapsula vsebuje 12,5 mg, 25 mg, 37,5 mg ali 50 mg sunitiniba (v obliki sunitinibijevega malata). **Indikacije:** Zdravljenje neizrežljivega in/ali metastatskega malignega gastrointestinalnega stromalnega tumorja (GIST) pri odraslih, če zdravljenje z imatinibom zaradi odpornosti ali neprenašanja ni bilo uspešno. Zdravljenje napredovalnega in/ali metastatskega karcinoma ledvičnih celic (MRCC) pri odraslih. Zdravljenje neizrežljivih ali metastatskih, dobro diferenciranih neuroendokrinih tumorjev trebušne slinavke (pNET), kadar gre za napredujoče obolenje pri odraslih (izkušnje z zdravilom Sutent kot zdravilom prve izbire so omejene). **Odmerjanje in način uporabe:** Terapijo mora uesti zdravnik, ki ima izkušnje z uporabo zdravil za zdravljenje rakavih obolenj. *GIST in MRCC:* Priporočeni odmerek je 50 mg peroralno enkrat na dan, 4 tedne zapored; temu sledi 2-tedenski premor (Shema 4/2), tako da celotni ciklus traja 6 tednov. *pNET:* Priporočeni odmerek je 37,5 mg peroralno enkrat na dan, brez načrtovanega premora. *Prilaganje odmerka:* Odmerek je mogoče prilagajati v povečanjih po 12,5 mg, upoštevaje individualno varnost in prenašanje. Pri GIST in MRCC dnevni odmerek ne sme preseči 75 mg in ne sme biti manjši od 25 mg; pri pNET je največji odmerek 50 mg na dan, z možnimi prekinitivami zdravljenja. Pri sočasni uporabi z močnimi zaviralci ali induktorji CYP3A4 je treba odmerek ustrezno prilagoditi. *Pediatrična populacija:* Uporaba sunitiniba ni priporočljiva. *Starejši bolniki (≥ 65 let):* Med starejšimi in mlajšimi bolniki niso opazili pomembnih razlik v varnosti in učinkovitosti. *Okvara jeter:* Pri bolnikih z jetno okvaro razreda A in B po Child-Pughu prilagoditev odmerka ni potrebna; pri bolnikih z okvaro razreda C sunitinib ni bil preizkušen, zato njegova uporaba ni priporočljiva. *Okvara ledvic:* Prilaganje začetnega odmerka ni potrebno, nadaljnje prilaganje odmerka naj temelji na varnosti in prenašanju pri posameznem bolniku. *Način uporabe:* Sutent se uporablja peroralno, bolnik ga lahko vzame s hrano ali brez nje. Če pozabi vzeti odmerek, ne sme dobiti dodatnega, temveč naj vzame običajni predpisani odmerek naslednji dan. **Kontraindikacije:** Preobčutljivost na zdravilno učinkovino ali katero koli pomožno snov. **Posebna opozorila in previdnostni ukrepi:** *Bolezni kože in tkiv:* obarvanje kože, bolečine/draženje v ustih. *Krvavitve* v prebavilih, dihalih, sečilih, možganih; najpogosteje epistaksa; krvavitve tumorja, včasih s smrtnim izidom. Pri bolnikih, ki se sočasno zdravijo z antikoagulantni, se lahko redno spremlja celotna krvna slika (trombociti), koagulacijski faktorji (PT / INR) in opravi telesni pregled. *Bolezni prebavil:* poleg navzee, diareje, stomatitisa, dispepsije in bruhanja tudi resni zapleti (včasih s smrtnim izidom), vključno s perforacijo prebavil. *Hipertenzija,* povezana z zdravljenjem; pri bolnikih s hudo hipertenzijo, ki je ni mogoče urediti z zdravili, je priporočljivo začasno prenehanje zdravljenja. *Hematološke bolezni:* zmanjšanje števila nevtrofilcev, trombocitov, anemija. *Bolezni srca in ožilja:* srčno-žilni dogodki, vključno s srčnim popuščanjem, kardiomiopatijo in motnjami v delovanju miokarda, v nekaterih primerih s smrtnim izidom. Sunitinib povečuje tveganje za pojav kardiomiopatije. *Podaljšanje intervala QT:* previdna uporaba pri bolnikih z znano anamnezo podaljšanja intervala QT, tistih, ki jemljejo antiaritmike, in tistih z relevantno, že obstoječo srčno boleznijo, bradikardijo ali elektrolitskimi motnjami. *Venski in arterijski tromboembolični dogodki;* arterijski včasih s smrtnim izidom. *Dogodki na dihalih:* dispneja, plevralni izliv, pljučna embolija ali pljučni edem; redki primeri s smrtnim izidom. *Moteno delovanje ščitnice:* bolnike je treba med zdravljenjem rutinsko spremljati glede delovanja ščitnice vsake 3 mesece. *Pankreatitis,* tudi resni primeri s smrtnim izidom. *Hepatotoksičnost,* nekateri primeri s smrtnim izidom. *Delovanje ledvic:* primeri zmanjšane delovanja ledvic, odpovedi ledvic in/ali akutne odpovedi ledvic, v nekaterih primerih s smrtnim izidom. *Fistula:* če nastane fistula, je treba zdravljenje s sunitinibom prekiniti. *Oteženo celjenje ran:* pri bolnikih, pri katerih naj bi bil opravljen večji kirurški poseg, je priporočljiva začasna prekinitev zdravljenja s sunitinibom. *Osteonekroza čeljustnic:* pri sočasnem ali zaporednem dajanju zdravila Sutent in intravenskih difosfonatov je potrebna previdnost; invazivni zobozdravstveni posegi predstavljajo dodatni dejavnik tveganja. *Preobčutljivost/angioedem.* *Motnje okušanja.* *Konvulzije.* *Sindrom lize tumorja,* v nekaterih primerih s smrtnim izidom. *Okužbe:* hude okužbe z ali brez nevtropenije (okužbe dihal, sečil, kože in sepsa), vključno z nekaterimi s smrtnim izidom. **Medsebojno delovanje z drugimi zdravili:** (Študije so izvedli le pri odraslih.) Zdravila, ki lahko zvišajo koncentracijo sunitiniba v plazmi (ketokonazol, ritonavir, itrakonazol, eritromicin, klaritromicin ali sok grenivke). Zdravila, ki lahko znižajo koncentracijo sunitiniba v plazmi (deksametazon, fenitoin, karbamazepin, rifampin, fenobarbital, *Hypericum perforatum* oz. šentjanževka). **Plodnost, nosečnost in dojenje:** Sutenta ne smemo uporabljati med nosečnostjo in tudi ne pri ženskah, ki ne uporabljajo ustrezne kontracepcije, razen če možna korist odtehta možno tveganje za plod. Ženske v rodni dobi naj med zdravljenjem s Sutentom ne zanosijo. Ženske, ki jemljejo Sutent, ne smejo dojeti. Neklinični izsledki kažejo, da lahko zdravljenje s sunitinibom poslabša plodnost samecev in samic. **Vpliv na sposobnost vožnje in upravljanja s stroji:** Sutent lahko povzroči omotico. **Neželeni učinki:** Najbolj resni neželeni učinki so odpoved ledvic, srčno popuščanje, pljučna embolija, predrtrje črevesja in krvavitve (npr. dihal, prebavil, krvavitve tumorja). Najpogostejši neželeni učinki so: zmanjšan apetit, motnje okusa, hipertenzija, utrujenost, prebavne motnje (npr. driska, slabost, stomatitis, dispepsija in bruhanje), sprememba barve kože/motnje pigmentacije in sindrom palmarno-plantarne eritrodisezestije. Med najbolj pogostimi neželenimi učinki so hematološke motnje (nevtropenija, trombocitopenija in anemija). Ostali zelo pogosti neželeni učinki so: glavobol, epistaksa, bolečina v trebuhu/napihnjenost, zaprtje, glasodimnija, izpuščaj, spremembe barve las, suha koža, bolečine v udih, vnetje sluznice, edemi. **Način in režim izdaje:** Predpisovanje in zdaja zdravila je le na recept, zdravilo pa se uporablja samo v bolnišnicah. Izjemoma se lahko uporablja pri nadaljevanju zdravljenja na domu ob odpuštu iz bolnišnice in nadaljnjem zdravljenju. **Imetnik dovoljenja za promet:** Pfizer Limited, Ramsgate Road, Sandwich, Kent, CT13 9NJ, Velika Britanija. **Datum zadnje revizije besedila:** 16.3.2012  
Pred predpisovanjem se seznanite s celotnim povzetkom glavnih značilnosti zdravila.

